TECHNISCHE UNIVERSITÄT MÜNCHEN

Lehrstuhl für Bioverfahrenstechnik

One-step expression and enzyme immobilisation in cellular envelopes of *Escherichia coli*

Ilka Sührer

Vollständiger Abdruck der von der Fakultät für Maschinenwesen der Technischen Universität München zur Erlangung des akademischen Grades eines Doktors der Naturwissenschaften genehmigten Dissertation.

Vorsitzender: Univ.-Prof. Dr. med., Dr.-Ing. habil. Erich Wintermantel

Prüfer der Dissertation: 1. Univ.-Prof. Dr.-Ing. Dirk Weuster-Botz

2. Univ.-Prof. Dr. rer. nat. habil. Dieter Langosch

Die Dissertation wurde am 24.09.2015 bei der Technischen Universität München eingereicht und durch die Fakultät für Maschinenwesen am 02.12.2015 angenommen.

Acknowledgements

This thesis was completed during my work at the Institute of Biochemical Engineering at the Technische Universität München under the supervision of Prof. Dr.-Ing Dirk Weuster-Botz. Numerous people supported me during this work, for which I would like to express my gratitude.

Foremost, I would like to thank Prof. Dr.-Ing. Weuster-Botz for the possibility to realize this thesis and I am very grateful for his excellent supervision, help and guidance during my time at the institute.
Additionally, I would like to thank Prof. Dr. rer. nat. habil. Dieter Langosch for accepting to be the co-examiner and Prof. Dr. med., Dr.-Ing.habil. Erich Wintermantel for being the chairman of my jury.

I owe deepest gratitude to Dr. Kathrin Castiglione for her invaluable support, guidance and encouragement during the last four years. I am very thankful for her readiness to share her time for inspiring discussions and contributing valuable ideas to this work.

I would like to thank the project partner Bird-C, especially Prof. Dr. rer. nat. Werner Lubitz and Dr. rer. nat. Timo Langemann, for providing the sequences and plasmids of different lysis genes as well as technical expertise for setting up the cellular envelope technology at the Institute of Biochemical Engineering.

The funding of this research project was provided by the Deutsche Forschungsgemeinschaft, for which I would like to express my gratitude.

For their great support in the lab, I would like to thankfully acknowledge the students Andreas Schmiededer, Caroline Hauser, Diana Kreitmayer, Carolin Flessner, Sabine Helmrath, Nadine Steinberger, Susanne Pettinger, Tobias Schirmer, Claudia Schuler, Michael Birkner, Pius Benz, Kristin Schoppel, Bettina Langer and Tobias Bierig.

Special thanks goes to Dr. Kathrin Castiglione, Dr. Jakob Franke and Ludwig Klermund for carefully proofreading the manuscript.

I would like to thank all my colleagues and former colleagues at the Institute of Biochemical Engineering for the great time and the help whenever it was needed, with special acknowledgement of Michael Weiner, Florian Sedlmaier and Tom Schwarzer.

Finally, I would like to thank my family for everlasting support, my partner for his encouraging words and my little son for putting a smile on my face even after the most exhausting day.

Table of contents

1 Introduction

The use of enzymes as biocatalysts in organic catalysis is not new. For more than 100 years enzymes have been employed for the transformation of non-natural and natural substrates. In the early stages, whole cell biocatalysts were used to elucidate metabolic pathways. The intention to employ the catalytic properties for industrial purposes did not begin until somewhat later (Faber 2011). With the developments in life science a wide variety of biotechnological processes was introduced for the production of a multitude of products (Hatti-Kaul et al. 2007). Using enzymes as biocatalysts, synthesis of organic compounds can be expanded to products and reactions which are difficult to obtain with classical chemical catalysis. Especially side directed chemo-, regio- and stereo-selective modification reactions can be challenging (Schmid et al. 2001). Enzymes provide the catalytic ability and offer mild working conditions. Enzymatic catalysis can therefore be conducted causing less pollution and posing less danger potential than the chemically catalysed equivalent (Hatti-Kaul et al. 2007; Schmid et al. 2001; Liese & Hilterhaus 2013).

Nowadays, biotransformations can be performed using whole cell biocatalysts, isolated enzymes or cell organelles. The portfolio of reactions and catalysts was enlarged and new technologies were developed. Today, biotransformations often comprise not one, but multiple reactions. Additionally, different methods such as multiphase reactions, biocatalyst production in large scale and techniques for catalyst immobilisation are available. (Faber 2011)

However, even though many possible applications for biotransformations exist, feasibility of enzymatic catalysis is frequently limited by process costs (Schmid et al. 2001). Expansion of the classical toolboxes for enzyme catalysis is therefore desirable. More economic application of enzymes as biocatalysts would enhance the shift from classic chemistry to the “green” synthesis with enzymatic catalysis (Bommarius & Paye 2013).

2 Motivation and objectives

The application of whole cells and isolated enzymes are state-of-the-art techniques for industrial biocatalytic processes. However, both methods have disadvantages. Whole cell biocatalysts are cheap in production, can easily be reused, and have internal cofactor regeneration (Schrewe et al. 2013). However, they can produce undesired by-products due to the cellular metabolism, which complicate downstream processing (León et al. 1998). Moreover, the cell wall can cause mass transfer limitation, and toxic substrates or by-products can be greatly damaging to the whole cell biocatalyst (Schrewe et al. 2013; León et al. 1998; Schmid et al. 2001; Smith et al. 2015). Therefore, enzymes are frequently purified. This does, of course, prevent the formation of undesired by-products and thereby greatly facilitates the downstream processing (DiCosimo et al. 2013). However, the purification of enzymes is expensive in time and costs, causes losses during the purification and possibly a reduction in the catalytic activity (Secundo 2013; Rodrigues et al. 2013). Immobilisation of enzymes after purification increases preparation costs for biocatalysts, but allows for the efficient reuse of the enzymes in the biocatalytic process (Secundo 2013; Rodrigues et al. 2013). The majority of immobilisation techniques either use artificial surfaces to attach or encapsulate the catalyst in artificial particles (Hanefeld et al. 2013; DiCosimo et al. 2013). Furthermore, purification is required prior to the immobilisation, which is time consuming and cost intensive.

Immobilisation techniques, which offer one-step expression and immobilisation are desirable. The “outer surface- or auto-display” of enzymes on the outer membrane of the microorganisms is one option, which has been studied before (Smith et al. 2015; Schüürmann et al. 2014; Jose 2006). Here, the enzymes are attached to the outer membrane by fusing them to outer membrane proteins or so called autotransporters, to ensure sufficient translocation of the enzymes to the outer membrane (Schüürmann et al. 2014; Jose 2006; Jose et al. 2012). Such whole cell biocatalysts displaying enzymes on their surface retain their complete metabolism, which can again cause the formation of undesired by-products. Therefore, a new approach for one-step expression and immobilisation was aimed for.

A new option for one-step expression and immobilisation was to be studied in this work. The desired enzyme or enzyme system was to be immobilised on the inner membrane of *Escherichia*

coli (*E. coli*). Biocatalysts were then to be created as cellular envelopes which contain afore immobilised enzymes by the removal of the cytosol. The cytosol can be removed by the formation of a pore by the lytic protein E from phage PhiX174 (Lubitz et al. 1984). It inserts into the inner membrane of growing Gram-negative cells. Subsequently, a conformational change takes place which eventually leads to fusion of inner and outer membrane due to protein E. A lysis pore (40−200 nm) is formed, the cytosol is released due to the osmotic pressure and a cellular envelope is retained (Schön et al. 1995). If proteins with membrane anchors were expressed prior to lysis, the cellular envelope will contain afore immobilised enzymes (Lubitz et al. 1999). Generally, the lytic phage protein E can be used to create cellular envelopes from growing Gram-negative bacteria and has a wide variety of applications (Eko et al. 1999; Langemann et al. 2010). So far, most studies focused on the generation of vaccines from pathogens. First experiments on immobilisation within the cellular envelopes regarded additional heterologous antigens to enhance immune response, which were expressed in low amounts (Eko et al. 1999; Lubitz et al. 1999).

In this work the cellular envelope technology was to be transferred from production of vaccines to biocatalysis by immobilising large amounts of synthesis enzymes at the inner surface of the cytosolic membrane of *Escherichia coli* (*E. coli*). Immobilisation of the the β-galactosidase from *E. coli* and co-immobilisation the of 3-ketoacyl-[acyl-carrier-protein]-reductase from *Synechoccocus* PCC7942 and the formate dehydrogenase from *Mycobacterium vaccae* N10 oxidoreductases were to be analysed.

Oxidoreductases have an advantage in stereoselective synthesis of chiral compounds from prochiral molecules (Schmid et al. 2001). Among them enzymes of the dehydrogenase and ketoreductase family have been studied for asymmetric reductions, which offer a wide area of applications (Kataoka et al. 2003). The 3-ketoacyl-[acyl-carrier-protein]-reductase from *Synechoccocus* PCC7942, was used for the reduction of prochiral molecules to chiral alcohols, which provide building blocks in the synthesis of industrially important compounds (Wichmann et al. 1981; Zhao & Van Der Donk 2003). However, the cofactor NADPH is required for catalysis, which is expensive. Thus, a coupled reaction system for cofactor recycling is needed. The formate dehydrogenase from *Mycobacterium vaccae* N10 can be used for regeneration of nicotinamide adenine dinucleotide cofactors (Hölsch & Weuster-Botz 2010a). Co-immobilisation of an enzyme system is challenging and was to be analysed in this project.

The following issues were to be addressed in this project:

- Design and expression of fusion proteins of the synthesis enzymes with different membrane anchors, verification of membrane immobilisation and identification of the best anchoring system
- Application of the cellular envelope technology for protein E-mediated lysis along with the required analytics
- Combination of expression and immobilisation of different enzyme systems with subsequent protein E-mediated lysis
- Establishing a production process in stirred-tank bioreactors to prove feasibility in industrial application
- Characterisation of the new biocatalysts regarding the number of immobilised enzyme molecules, catalytic properties and performance in comparison to whole cell biocatalysts and isolated enzymes.

The following study is therefore important to provide a basis for later industrial applications of the cellular envelope technique as biocatalyst preparations.

3 Theoretical background

3.1 Enzymes for biocatalytic applications

With the development of life sciences, new technologies have arisen for the use of enzymes and microorganisms. The field of applications is very diverse, ranging from the application of microorganisms for drug- and food production to bulk enzymes added to washing agents (Sutton et al. 2012; Faber 2011; Gröger & Asano 2012). This project focused on the use of enzymes as an alternative catalyst in organic reactions. The following chapter will cover an introduction to enzyme catalysis. Compared to classic organic synthesis, enzymes have advantages and disadvantages, which are discussed in the following section.

3.1.1 Chemical versus enzymatic catalysis

The use of enzymes instead of classic organic synthesis has become more prominent in recent years (Faber 2011; Sutton et al. 2012; Gröger & Asano 2012). In comparison to the classical chemical approach, application of enzymes has several advantages. Enzymes derive from organisms and are consequently able to catalyse reactions under mild conditions. “Eco friendly” production is highly desirable. The use of aqueous reactions conditions in mild pH (5.0-8.0) and moderate temperatures as well as atmospheric pressure can be energy-saving during production processes (Faber 2011). As proteins, enzymes are biodegradable, whereas the chemically catalysed equivalent often requires heavy metal ion catalysts, which are toxic and need special treatment for removal (Rozzell 1999). Additionally, harsher reaction conditions, such as increased pressure or temperatures are less environmentally friendly and can lead to reduced yields by undesired by-product formation and destruction of substrates when damageable substances are used (Panke et al. 2004; Panke & Wubbolts 2005; Pollard & Woodley 2007).

Depending on the catalysed reaction, enzymes can have up to $10^8 – 10^{10}$ fold higher reaction rates and are thus more efficient than chemical catalysts (Wolfenden & Snider 2001). Additionally, enzymes are able to perform almost any organic reaction and they also accept non-natural substrates, which broadens the potential range of applications (Faber 2011; Gröger & Asano 2012).

Most importantly, enzymes are able to catalyse regio- and stereo-selectively whereas the

chemically catalysed equivalents are often less selective and efficient (Stewart 2001; Matsuda et al. 2009). Undesired formation of by-products enhances costs and complicates down-stream processing (Schmid et al. 2001; Matsuda et al. 2009). Especially in production of biopharmaceuticals undesired by-products can be potentially toxic if they are administered alongside (Margolin 1993; Caner et al. 2004; Faber 2011; Gröger & Asano 2012).

On the other hand, catalysis with enzymes can also have drawbacks. Like any other catalyst, enzymes need to be produced. Thus, expression and purification from microorganisms is required. Enzyme expression especially in heterologous host organisms can be challenging. Depending on the enzyme, such catalysts can be very expensive, and recycling of the catalysts may be required to obtain a profitable process (DiCosimo et al. 2013; Faber 2011).

In classical catalysis, energy for the reaction is provided by heat and pressure or inorganic catalysts (Clayden et al. 2001). Enzymes work under mild reaction conditions, which is generally desirable (Sheldon & van Pelt 2013), however, increase in temperature or alteration of salinity or the pH can quickly render an enzyme inoperable (Faber 2011). Additionally, enzymes require aqueous buffer systems in which many substrates are hardly soluble. It may be necessary to use biphasic reaction systems to enhance yields (Rogers & Seddon 2003; León et al. 1998; Faber 2011).

Some enzymes require transport metabolites to catalyse the desired reaction. To use such enzymes for the catalytic formation of organic molecules, it is necessary to provide them with the respective transport metabolite source they require for the reaction (Faber 2011; Gröger & Asano 2012).

Much research has been done to eliminate drawbacks of enzymes as catalysts. Recycling of enzymes or whole cells by immobilisation is analysed (Liese & Hilterhaus 2013; Katchalski-Katzir 1993; DiCosimo et al. 2013; Hanefeld et al. 2013; Faber 2011). New techniques are developed for enzyme immobilisation and substrate supply (León et al. 1998; Hanefeld et al. 2013; Sheldon & van Pelt 2013; Faber 2011). There is an ever ongoing search for new enzymes to enlarge the repertoire of enzymatic catalysis. Protein engineering is used and modifications are introduced to existing enzymes to alter catalytic stability, broaden substrate acceptance and enhance catalytic performance (Faber 2011; Gröger & Asano 2012).

3.1.2 Enzymes in organic synthesis

Enzymes catalyse a wide variety of chemical reactions. According to their catalytic properties, they are divided into enzyme classes. A basic division is made between oxidoreductases, transferases, hydrolases, lyases, isomerases and ligases (see Figure 3-1). Each group comprises a multitude of subdivisions to define the catalysed reaction. The variety of reactions to each subdivision provides the opportunity for manifold applications (Faber 2011; Gröger & Asano 2012; Sutton et al. 2012).

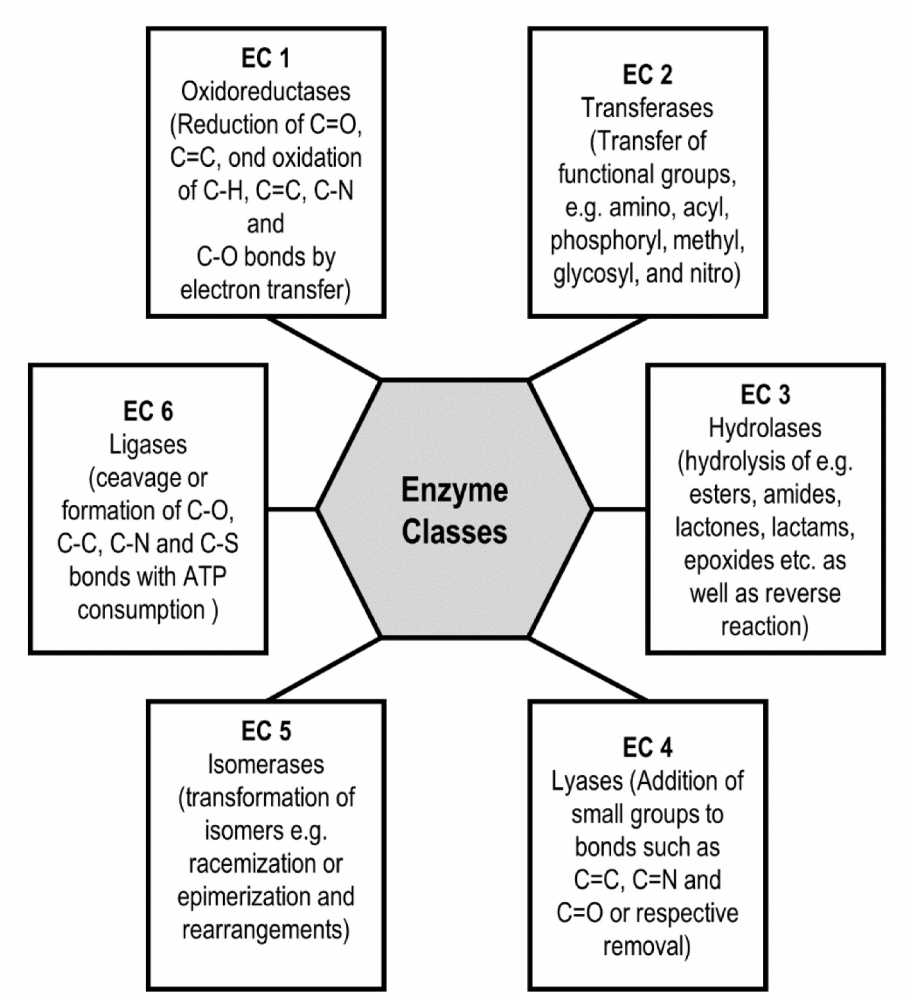

Figure 3-1 Classification of enzymes according to the International Union of Biochemistry and Molecular Biology (1992)
Subdivison of enzyme classes according to the Enzyme Commission (EC) numbers in allusion to Gröger & Asano (2012).

Application of enzymes is state of the art, mainly hydrolases are used e.g. for additives in washing agents (Hollmann et al. 2011; Faber 2011; Gröger & Asano 2012). Hydrolases are highly desirable because they are independent from transport metabolites (Hollmann et al. 2011). However, application of enzymes from other catalytic classes is becoming more

prominent. Especially, the use in organic synthesis for the production of fine chemicals and pharmaceuticals is frequently studied (Katchalski-Katzir 1993; Panke et al. 2004; Schmid et al. 2001). Enzymes offer a wide variety of catalysed reactions and many are able to accept and convert non-natural substrates in addition to their natural ones. Thus, enzymes provide a natural catalytic portfolio, which can be applied as an alternative to the classic organic synthesis (Faber 2011; Gröger & Asano 2012; Sutton et al. 2012).

Stereo- and regio-selective catalysis is challenging with classic chemical synthesis up until now (Schmid et al. 2001; Matsuda et al. 2009). The selective production of enantiomerically pure material with the methods used in organic chemistry is so far difficult, often requires complex handling and special separation techniques (Schmid et al. 2001; Matsuda et al. 2009). Many pharmaceuticals were administered as a racemic mixture till 1990 (Faber 2011; Sutton et al. 2012), which is undesirable. In cases where the other enantiomer has no effect, the effectiveness of the drug is reduced by the presence of the other enantiomer. In other cases, the other enantiomer can cause sometimes severe and undesired side effects and therefore needs to be removed (Faber 2011).

Nature has developed enzymes as catalysts, which are able to produce molecules with high enantiomeric excess (Caner et al. 2004; Faber 2011). Chiral L-amino acids are the building blocks of all natural enzymes. Consequently, enzymes themselves are chiral macromolecules (Clayden et al. 2001). The active site of enzymes is composed of amino acid moieties, which provide a chiral environment for catalysis. Thus, the steoreospecific binding and conversion of one enantiomer (regarding chiral conversion) or conversion mode of the prochiral (regarding asymmetric synthesis) molecule is highly preferred over the other (Clayden et al. 2001; Faber 2011). In 1992 the U.S. Food and Drug Administration (FDA) released a decree that all drugs should be administered as single enantiomers if possible, or otherwise proof stringently that a racemic mixture had no negative effects. Since 2002 the number of drug approvals for racemic mixtures has almost disappeared, while more than half of all drug candidates comprise at least one chiral center (Margolin 1993; Caner et al. 2004; Faber 2011).

For the conversion of some substrates it can be necessary to use harsher reaction conditions or alternatively enzymes capable of accepting these special substances. Nature's diversity provides manifold enzymes from diverse sources. Microorganisms living in extreme habitats

with high or low temperature, high pressure, extreme pH or salinity are of interest, as they might also provide enzymes which are active under such conditions (Chartrain et al. 2001; Faber 2011). On the other hand, many enzymes also derive from eukaryotes such as mushrooms or algae, which feature unique metabolisms with the respective enzymes for catalysis (Gröger & Asano 2012; Faber 2011).

3.1.3 Whole cell biotransformation versus isolated enzymes

In whole cell biotransformations, the (host-)organism comprises the catalytic enzymes, which are then used for the conversion of chemical substances to a product (Schmid et al. 2001; Schoemaker et al. 2003; Faber 2011). At the beginning of the 20th century, first attempts were made to produce other products e.g. L-ephedrine using whole cell biocatalysts (Gröger & Asano 2012). Initially, whole cell biocatalysts featuring unmodified wild type organisms were used. Back then, results suffered from e.g. low cell amounts and low enzyme concentrations. With the development of recombinant microorganisms and high cell density processes, whole cell biotransformations evolved as a competing option to the classic chemical synthesis (Faber 2011; Schrewe et al. 2013; Schoemaker et al. 2003). Nowadays, there are numerous new biotransformation approaches featuring whole cells, such as the generation of drugs or the production of chemical compounds as building blocks for chemical synthesis (Schmid et al. 2001; Matsuda et al. 2009; Margolin 1993). The vast majority of all white biotechnological applications are performed using traditional microorganisms belonging to bacteria, yeasts or filamentous fungi.

With the development of life sciences, purification techniques for enzymes were developed and improved. Today, production of purified enzymes in large scale is state of the art in industrial processes. Thus, there exist two basic strategies for the application of enzymes in industrial processes: the use of whole cell biocatalysts or isolated enzymes. Both options have advantages and disadvantages regarding different criteria. The most important factors in choosing either whole cells or purified enzymes as production platforms are: i) the type of reaction, ii) whether cofactors are required, and iii) the intended scale of the biotransformation. The main criteria are summarised in Table 3-1 (Schmid et al. 2001; Faber 2011; Gröger & Asano 2012; Schrewe et al. 2013).

Table 3-1 Comparison of whole cell biocatalysts and isolated enzymes for industrial processes (Schmid et al. 2001; Faber 2011; Sutton et al. 2012; Drauz et al. 2012; Schrewe et al. 2013)

Criterion	Whole cells	Isolated enzymes
Catalyst price	Low	Medium – high (down-stream processing required)
Competing enzymes	Yes (intact metabolism and cytoplasm)	None
Stereo-selectivity	Medium – high (competing enzymes from host cell)	High
Formation of by-products	In many cases (competing enzymes from host cell)	Less or none (only by-products from synthesis enzyme)
Mass transfer limitation	Yes (intact cell wall)	No
Cofactor regeneration	Internal	Required
Downstream processing	More complex (removal of host cell and undesired by-products)	Simple

Whether whole cells or purified enzymes are best suitable needs to be evaluated for each individual process. Whole cell biocatalysts are desirable for production in large scale as the production is cheap, easy and internal cofactor regeneration is provided. Isolated enzymes on the other hand are preferably used in conversion of expensive materials, where by-product formation is highly undesirable, easy down-stream processing is needed or high mass transfer limitation of the substrates occurs due to the cell wall (Bisswanger 2008; Faber 2011; Drauz et al. 2012; Sutton et al. 2012).

3.1.4 Enzyme characterisation

Enzymes are characterised according to their performance in catalysis by describing the rate at which they convert the substrate(s) to the respective product(s). The most commonly used model to describe enzyme kinetics was introduced by Leonor Michaelis and Maud Menten (Bisswanger 2008). The most simplified description of an enzymatic reaction is the one-substrate one-product reaction shown in Figure 3-2.

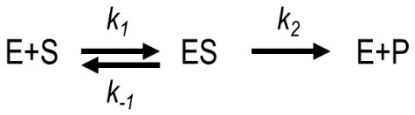

Figure 3-2 Irreversible one enzyme one-substrate one-product reaction
Enzyme (E) and substrate (S) form the substrate-enzyme complex (ES), the substrate is then converted to the product (P). $k_{1/-1/2}$ are the respective rate constants. (Bisswanger 2008)

In the Michaelis-Menten model several assumptions are made, which simplify the mathematical description of the process:

- The model describes a single substrate molecule (S) to bind one on one to an enzyme (E) in order to form an enzyme-substrate-complex (ES).
- A steady-state equilibrium of the complex ES is assumed, its concentration is defined to be constant ($\frac{dES}{dt} = 0$). The enzyme is not converted during the process, so the total enzyme concentration (E) is assumed constant.
- The reaction elapses far off the thermodynamic equilibrium, a reverse reaction can therefore be neglected

Using these assumptions the classic Michaelis-Menten kinetic is described using equation 3-1 (Wolf 1991).

$$v_0 = v_{max} \frac{[S]}{[S] + K_m} \qquad \textbf{3-1}$$

v_0	current reaction rate, mol/s
v_{max}	maximum possible reaction rate when all enzyme molecules are in the enzyme-substrate-complex mol/s
K_m	Michaelis-Menten-constant, mol/L
[S]	substrate concentration, mol/L

The Michaelis-Menten constant is calculated from the ratio of on- and off-rate constants from formation of the Michaelis-Menten-complex ES (equation **3-2**).

$$K_m = \frac{k_{-1} + k_2}{k_1} \qquad \textbf{3-2}$$

$k_{x/-x/y}$	on- and off-rate constants (see Figure 3-2), 1/s

The turnover number is another important enzyme parameter, which is calculated as k_{cat} (3-4) and therefore an equivalent to v_{max} if the substrate is present in great surplus to the K_m:

$$S \gg K_m$$

k_{cat} then is equivalent to the dissociation constant k_2. Thus, the maximum rate constant

consequently depends on the initial enzyme concentration and the turnover number.

$$k_{cat} = k_2 \qquad \textbf{3-3}$$

$$v_{max} = k_{cat} \cdot [E]_0 \qquad \textbf{3-4}$$

k_{cat}	turnover number, 1/s
$[E]_0$	initial enzyme amount t=0, mol

Using the initial rate constants determined at varying initial substrate concentrations, the kinetic constants of the enzyme can be determined in batch experiments. Mostly non-linear regression is applied where equation 3-1 is fitted to the raw data and the kinetic constants are thus estimated. Notably, the Michaelis-Menten kinetic describes a model which is only valid for ideal irreversible one-substrate-one-product reactions, which are rather rare. This very simple model does not incorporate effects such as substrate or product inhibition or allosteric inhibition by other substances. Thus, it can be employed for simplified calculations only. Incorporation of reversible reactions greatly complicates the calculation of the kinetic constants (Bisswanger 2008; Cornish-Bowden 2012).

The vast majority of enzymatic reactions require a more complex description, as their mechanisms differ from the simplified Michaelis-Menten kinetics. Frequently, enzymes convert more than one substrate at a time, which greatly complicates the mathematical description of the reaction. In two-substrate conversions the on- and off- rate constants of both substrates and product(s) need to be taken into account. The mode of substrate binding becomes more complicated. Some enzymes feature just one binding site where the substrates have to bind in a defined order. Other enzymes have two binding sites within the catalytic center, which allow for independent binding of the substrates. If all substrates have to be bound to the enzyme before a product is released, the reaction type is referred to as *sequential*. Some enzymes release one product before all substrates are bound, which is referred to as *ping-pong*-mechanism. The mode of substrate binding is crucial for the mathematical description. Generally, substrate binding may either be *ordered* or *random*. (Segel 1993; Bisswanger 2008)

Reactions which feature two substrates, of which one has to bind before the other are referred

to as *ordered bi-bi*-mechanisms (Figure 3-3). The 3-ketoreductase employed in this work follows this mechanisms (Hölsch & Weuster-Botz 2011). If the substrate binding of the two-substrates is *random*, the mechanisms is referred to as *random bi-bi* (Figure 3-3). The formate dehydrogenase used in this project is described using such a model (Segel 1993; Tishkov & Popov 2004; Bisswanger 2008).

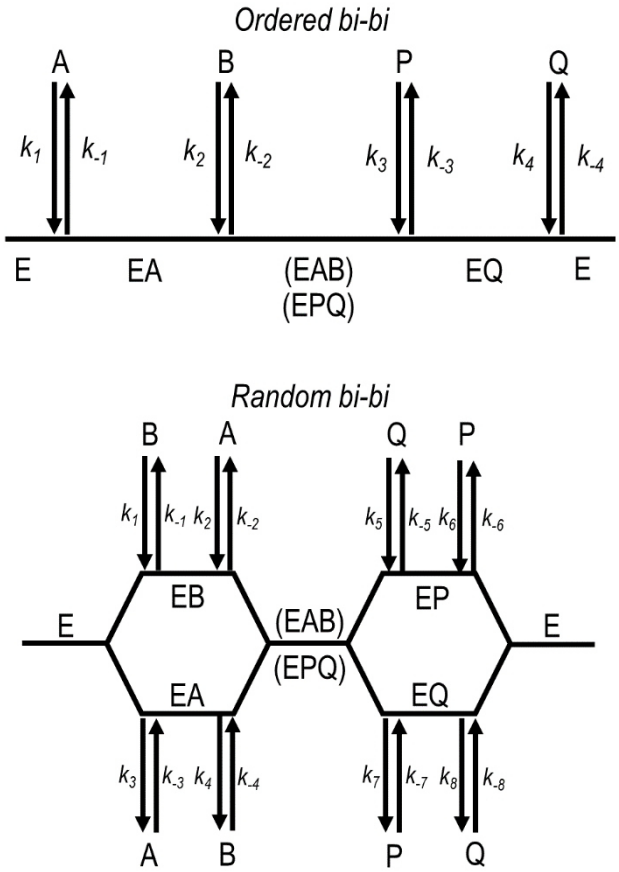

Figure 3-3 *Ordered bi-bi*- and *random bi-bi*-mechanism
A schematic description is given for the *ordered bi-bi* and *random bi-bi* mechanisms. The substrates (A,B) are bound to the enzyme (E) and form the substrate-enzyme complex (EAB). The enzyme produces the products (PQ) and releases them. k_x are the on-and off-rate constants.

3.1.5 Enzyme stability

The stability of enzymes is a crucial factor for their application. Enzyme performance changes depending on conditions such as pH, temperature and salinity. Some enzymes require prosthetic groups or metal ions, and their activity is dependent on the respective concentrations. Each enzyme has characteristic conditions required for optimal activity and a range of condition changes in which the enzyme remains active, though not with the highest possible performance. Outside of that condition range but also within, enzymes suffer from inactivation. Working conditions must therefore be chosen to allow for an optimal compromise of enzyme activity

and stability. For instance, an enzyme may work best at high temperatures, but may simultaneously also suffer from strong temperature-induced inactivation at that condition. Enzymes are expensive, the reaction temperature must therefore be chosen outside of a temperature range of considerable inactivation and at the same time allow for the best activity (Bisswanger 2008; Faber 2011; Gröger & Asano 2012; Zhao 2005).

Inactivation of enzymes can have multiple reasons. Next to denaturation at high temperatures, too high or low pH and salt concentrations can change the charge of amino acid groups and alter the hydration status in the protein environment, which causes conformational change and inactivation (Zhao 2005; Faber 2011). Additives such as chaotropic salts and detergents can be necessary, but they can also denature the enzyme structure and consequently cause inactivation (Zhao 2005). In industrial applications enzymes are frequently used to convert non-natural products. If the substrate or product is damaging to the enzyme, this can be problematic (Hoelsch et al. 2013). Inactivation of enzymes is described by a pseudo-first-order reaction, if the substance causing the inactivation can be assumed in great excess in comparison to the enzyme concentration (Bisswanger 2008). Inactivation is then described by equation 3-5.

$$\frac{dE_A}{dt} = -k_i \cdot E_A \qquad \textbf{3-5}$$

E_A	enzyme activity, U
t	time, s
k_i	apparent inactivation constant, 1/s

The half life of the enzyme ($t_{½}$) is then calculated by integration of equation 3-5 as the time point at which half the enzyme activity remains according to equation 3-6

$$t_{1/2} = \frac{\ln(2)}{k_i} \qquad \textbf{3-6}$$

To prolong the lifetime of the enzymes special care is required, not only during the reaction, but also during purification and storage. Enzymes can either be stored solved in liquids or as a solid. In liquid form enzymes should be stored at or below 4 °C to avoid temperature degradation and microbial contaminations. Additives such as glycerol may be added for stabilization during storage below 0 °C. Most commercial enzymes are stored as solid formulations, where many enzymes are much more stable even without a stabilizer. Formulation via freeze drying, spray drying or precipitation is state of the art. Thus gained

enzyme preparations may be stored without cooling for years without substantial activity losses (Gröger & Asano 2012).

3.2 Asymmetric biosynthesis

Asymmetric synthesis describes the conversion of prochiral substrates, where the product is composed mostly of one enantiomer. The purity of the product is described by the enantiomeric excess (ee), which gives the ratio of one enantiomer in comparison to the other. It is calculated using equation 3-7. An ee of 100% means that only one enantiomer is produced, an ee of 0% indicates a racemic mixture of both enantiomers with no excess of either.

$$ee_S\% = \frac{(n_S - n_R)}{(n_S + n_R)} \cdot 100\% \qquad \textbf{3-7}$$

ee_s	enantiomeric excess of the (*S*)-enantiomer, %
n_S	amount of (*S*)-enantiomer, mol
n_R	amount of (*R*)-enantiomer, mol

In asymmetric synthesis different reaction types can be distinguished. Prochiral moieties may be sp^3-hybridized carbon atoms with two identical substituents. Substitution of either atom or group creates a chiral center. The substituents are thereby referred to as pro-*S* and pro-*R*, depending on which chirality is gained by replacement of the respective atom or group. Prochirality is also found in sp^2-hybridized carbon atoms such as ketones and double-bonds, where double-bonds take a special role as their reduction can create two chiral centers simultaneously. Addition of a group or atom to the sp^2-hybridized carbon atom changes it to a chiral sp^3-atom, if the added group or atom is not identical to any other attached. Direction of the nucleophilic attack thereby defines the chirality of the product. In biocatalysis the reduction of prochiral ketones to alcohols is an important field. This work focused on asymmetric synthesis of chiral alcohols, which is therefore discussed in the following chapter (Faber 2011; Garcia-Urdiales et al. 2012).

3.2.1 Chiral alcohols from asymmetric reductions

Enantiomerically pure chiral alcohols as building blocks for flavours, fine chemicals and pharmaceuticals are frequently demanded in industrial productions. Thus, the asymmetric production of such alcohols from prochiral substrates is important. For this purpose chiral

alcohols are frequently gained from asymmetric reduction of prochiral ketones (Kataoka et al. 2003; Matsuda et al. 2009).

A schematic description of ketone reduction is displayed in Figure 3-4. If no chiral environment is provided, the nucleophilic attack on the ketone occurs randomly from either side, which is referred to as *si* or *re.* The product is then composed of a racemic mixture of both enantiomers. If the substrate is bound in a chiral environment, the nucleophilic attack on the substrate from one side is preferred and the corresponding chiral alcohol is preferably produced. Enzymes and some chemical catalysts are able to provide such a chiral environment and thus enable asymmetric synthesis of one enantiomer (Faber 2011; Garcia-Urdiales et al. 2012).

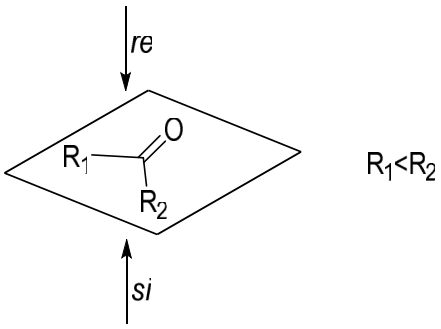

Figure 3-4 Prochirality of ketones
The prochirality of ketones is displayed with R_1 and R_2 being two substituents with defined priority according to the rule of Cahn-Ingold-Prelog (Clayden et al. 2001).

A prominent and Nobel Prize awarded classical chemical method of asymmetric ketone reduction was developed by Noyori (Noyori & Ohkuma 2001; Noyori et al. 2001). For this a molecular scaffold containing a ruthenium catalyst is used, which provides a chiral environment. Depending on the substrate, the method offers moderate to high enantiomeric purity and good yields (Etayo & Vidal-Ferran 2013). This chemical method for ketone reduction is used e.g. in menthol synthesis with an overall amount of 1000 t product per annum (Noyori 2001). However, the catalyst requires the rare and expensive element ruthenium and a complicated production along with a high amount of toxic chemical waste. Catalysis with enzymes offers often better stereo-selectivity along with mild reaction conditions and without toxic elements (Rozzell 1999; Panke et al. 2004).

Enzymes used for the asymmetric reduction of ketones usually belong to the group of oxidoreductases. Prominent among them are alcohol dehydrogenases from various organisms,

which are frequently employed. The first applications used whole cell biotransformations featuring baker's yeast for the asymmetric reductions of ketones. With the development of cloning techniques, recombinant microorganisms, gene sequencing, data mining and genome annotation, the portfolio of enzymes capable of asymmetric reduction was expanded. It now also comprises enzymes originating from organisms not found in everyday life, which can be used in purified form or expressed in recombinant microorganisms in whole cell biotransformations (Chartrain et al. 2001). Exemplary are ketoreductases from cyanobacteria, which are found in the organisms fatty acid and synthesis metabolisms (Kataoka et al. 2003; Hölsch & Weuster-Botz 2010b).

One major drawback regarding the application of oxidoreductases such as ketoreductases and alcohol dehydrogenases is their dependence on cofactors such as nicotinamide adenine dinucleotides (NAD(P)H), flavines or pyrroloquinoline quinone, which is discussed in more detail in the following section (Faber 2011; Gröger & Asano 2012; Sutton et al. 2012).

3.2.2 Cofactor regeneration

In many enzymatic reactions, cofactors are required as transport metabolites. Some of these cofactors are bound to the enzyme as prosthetic groups and are self-regenerating such as biotin. If such enzymes are used in purified form, it may be necessary to add the prosthetic group to the buffer, to ensure catalytic activity. On the other hand there are cofactors which remain free and unbound to the enzyme. Prominent among them are nucleoside triphosphates (NTPs) such as adenosine triphosphate (ATP) and pyridine nucleoside-based cofactors (e.g. NAD(P)H). (Zhao & Van Der Donk 2003; Wang et al. 2013).

Cofactors are very expensive and cannot be added stoichometrically in production processes. Replacement of natural cofactors with artificial equivalents is challenging and mostly the original substance needs to be added. In nature, cofactors are either self-regenerating or regenerated by co-enzymes which oxidize a co-substrate. Thus, *in situ* cofactor regeneration can be applied in industrial processes and the cofactor only needs to be provided in catalytic and not in stoichiometric amounts (Faber 2011).

For the synthesis of chiral alcohols by enzymatic catalysis oxidoreductases are frequently used, which require nicotinamid adenine dinucleotide based cofactors for the transport of a hydride anion. NAD(P)H is the most often used cofactor and $NAD(P)^+$ regeneration is a frequently

studied topic (Faber 2011). Some enzymes are able to perform both, substrate conversion and cofactor regeneration, simultaneously (e.g. alcohol dehydrogenases) and reduce their cofactor in a reverse reaction by oxidizing a cheap co-substrate. To shift the reaction to the product side and enable the reverse reaction, the co-substrate needs to be provided in great excess (Zhao & Van Der Donk 2003; Goldberg et al. 2006). However, not all enzymes are able to regenerate their own cofactor and are dependent on external cofactor regeneration. For $NAD(P)^+$ reduction, enzymes of the oxidoreductase family are most commonly used, which oxidize a cheap co-substrate to reduce the cofactor. A schematic description of enzyme-coupled cofactor regeneration in asymmetric reductions of prochiral ketones is displayed in Figure 3-5.

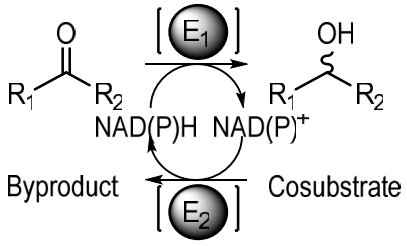

Figure 3-5 Schematic display of coupled enzymatic catalysis for chiral synthesis
An oxidoreductase (E_1) catalyses the enantioselective reduction of the ketone, which is coupled to NAD(P)H consumption. A cofactor regenerating enzyme (E_2) reduces $NAD(P)^+$ to NAD(P)H by oxidizing a co-substrate to a by-product.

In industrial applications nicotinamide adenine dinucleotide based cofactors are frequently regenerated by enzymes of the dehydrogenase family, a subdivision of the oxidoreductases (Zhao & Van Der Donk 2003; Wang et al. 2013). Prominent among them are glucose dehydrogenase and formate dehydrogenase, which require glucose and formate as co-substrates, respectively (Zhao & Van Der Donk 2003). Notably, dehydrogenases originate from catabolic pathways in metabolism and consequently have a high preference for the non-phosphorylated NAD^+ and low activities for $NADP^+$ (Tishkov & Popov 2004). Contrary to this, many enzymes employed in asymmetric synthesis are naturally found in anabolic pathways and thus require NADPH (Kataoka et al. 2003; Zhao & Van Der Donk 2003; Chenault & Whitesides 2007). In coupled enzyme synthesis, the choice of enzyme system is crucial, as the enzyme with the lowest catalytic speed determines the catalytic efficiency of the whole system. One possible option to overcome this problem would be to use the enzymes in a ratio equivalent to their corresponding activity.

Coupled enzymatic catalysis with internal cofactor regeneration is mostly required if purified enzymes or cell-free expression systems are used. In whole cell biotransformations cofactor

regeneration is provided by the cell metabolism. However, it may also be necessary to supply whole cell biocatalysts with additional enzymes for cofactor regeneration if the cell's own metabolism is insufficient to provide enough reductive energy. To increase product yields additional enzymes may be co-expressed and the respective co-substrate added. (Hölsch & Weuster-Botz 2010a; Sun et al. 2013; Fu 2013)

In this work coupled enzymatic catalysis with internal cofactor regeneration was used featuring a ketoreductase for asymmetric synthesis and a formate dehydrogenase for cofactor recycling. Both enzymes are described in more detail in the following sections.

3.2.3 3-Ketoacyl-[acyl-carrier-protein]-reductase from *Synechococcus elongatus* PCC7942

The 3-ketoacyl-[acyl-carrier-protein]-reductase (KR) belongs to the group of oxidoreductases (EC 1.1.1.100) and originates from the bacterial fatty acid biosynthesis. It is found in the fatty acid synthase II (FAS II) multifunctional macromolecular complex of plants and bacteria. The KR originally catalyses the reduction of 3-keto-acids, which are activated by connection to the acyl carrier protein (Wakil 1989; Magnuson et al. 1993; Rock & Jackowski 2002). In asymmetric reductions the KR can be used in whole cell biotransformations in wild type and recombinant host cells, but also in purified form. Enzymes of the ketoreductase family are able to reduce alien substrates, which are structurally related to the natural ones as (Bali et al. 2006). Because of this ability, KR were targeted in the research for new enzymes in asymmetric reductions. Several KR enzymes from different organisms such as *Saccharomyces cerevisiae* were characterised and compared by scientists (Kataoka et al. 2003; Yasohara et al. 2001). In this work the KR from *Synechococcus elongatus* PCC7942 was used. *Synechococcus* PCC7942 is a frequently studied freshwater cyanobacterium (Rippka et al. 1979).

The 25 kDa KR from *Synechococcus* PCC7942 was first identified in 2006 by Havel and has since then been used to for asymmetric reductions of various ketones such as pentafluoroacetophenone (Havel 2006; Hölsch et al. 2008). It forms multimers and requires at least dimeric structure to be catalytically active (Hölsch 2009). Belonging to the oxidoreductase family, the KR requires nicotinamide adenine dinucleotide based cofactors for reduction of substrates. Fatty acid synthesis belongs to anabolic metabolism, consequently the KR has an absolute requirement for NADPH and thus needs supply with the cofactor for catalysis (Hölsch et al. 2008).

Depending on the substrate, the KR features good to excellent enantiomeric excess with ee >99% (Hölsch & Weuster-Botz 2011). In this work reduction of ethyl 4-chloroacetoacetate (ECAA) to the corresponding (*S*)-alcohol ethyl (*S*)-4-chloro-3-hydroxybutyrate ((*S*)-ECHB) was aimed for. A schematic description of the reaction is given in Figure 3-6. The KR is able to convert this substrate with a specific activity of 38.29 ± 2.15 U/mg and an ee_s of 99.8 ± 0.4% (Hölsch et al. 2008). The chiral alcohol gained from ECAA reduction is a building block used in the synthesis of atorvastatin (see Figure 3-6). Atorvastatin is a drug belonging to the statin group, which comprises substances used to lower blood cholesterol. It is frequently listed among the world's top selling pharmaceuticals (Pfizer Worldwide 2015). Cofactor regeneration was to be provided by a formate dehydrogenase in a coupled enzymatic reaction, which is discussed in more detail in the next section.

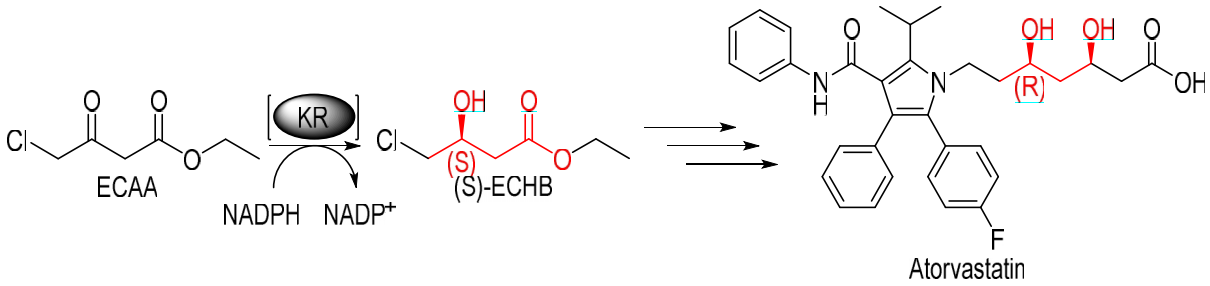

Figure 3-6 Schematic conversion of ECAA to the corresponding product
Schematic display of the asymmetric reduction of ECAA by a ketoreductase (KR) with coupled NADPH oxidation to the corresponding alcohol ethyl (*S*)-4-hydroxybutanoate ((*S*)-ECHB) and the product of the industrial application atorvastatin. The final product parts originating from the chiral alcohol are highlighted.

3.2.4 Formate dehydrogenase from *Mycobacterium vaccae* N10

Formate dehydrogenases (FDH) are ubiquitously found in plants, fungi, yeasts and bacteria. The term is used for a group of enzymes belonging to the superfamily of D-specific 2-hydroxy acid dehydrogenases [EC 1.2.1.2]. They catalyse the oxidization of formate to CO_2, which is connected to the reduction of $NAD(P)^+$ (see schematic display in Figure 3-7). Mainly methylotrophic organisms contain the enzyme as a crucial part of their metabolism (Tishkov et al. 1993; Tishkov & Popov 2004). All enzyme family members feature structural and catalytic similarities. They form homodimers and most members of this enzyme family have a metal-free enzymatic mechanism, generally using a limited group of conserved catalytic amino acids (Popov & Lamzin 1994; Lamzin et al. 1994). In most FDH the reaction is catalysed by using the electrostatic effects of amino acid side chains. Conserved amino acids within the active center polarise the substrates to enable the hydride anion transfer from formate to the positively

charged nicotinamide moiety of NAD^+ or $NADP^+$, respectively (Tishkov et al. 1993; Popov & Lamzin 1994). FDH use the cheap substrate formate and are frequently used for cofactor regeneration in bisubstrate reactions (Tishkov & Popov 2006).

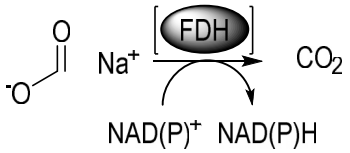

Figure 3-7 Cofactor regeneration by formate dehydrogenases
The FDH catalyses the reduction of $NAD(P)^+$ to NAD(P)H coupled to the oxidization of formate (displayed as the sodium salt) to CO_2.

This work focused on the FDH from *Mycobacterium vaccae* N10, which is a soil-living, non-pathogenic member of the Mycobacteriaceae family. The organism is methylotrophic and lives on methanol (Karzanov et al. 1991). It was therefore a target for the search of a new FDH. The enzyme was first discovered and cloned in 1995 and was found to possess high sequence homology with the FDH from *Pseudomonas* sp.101, showing an almost identical sequence except for two amino acids (Galkin et al. 1995) (see structure in Figure 3-8). Each subunit of the FDH homodimer has a molecular mass of about 44 kDa and consists of 400 amino acids which form a separate active site for each subunit. The stability as well as the catalytic activity are of interest for the application of FDH. Much research has been performed to enhance the characteristic of the enzyme regarding both factors (Tishkov & Popov 2006).

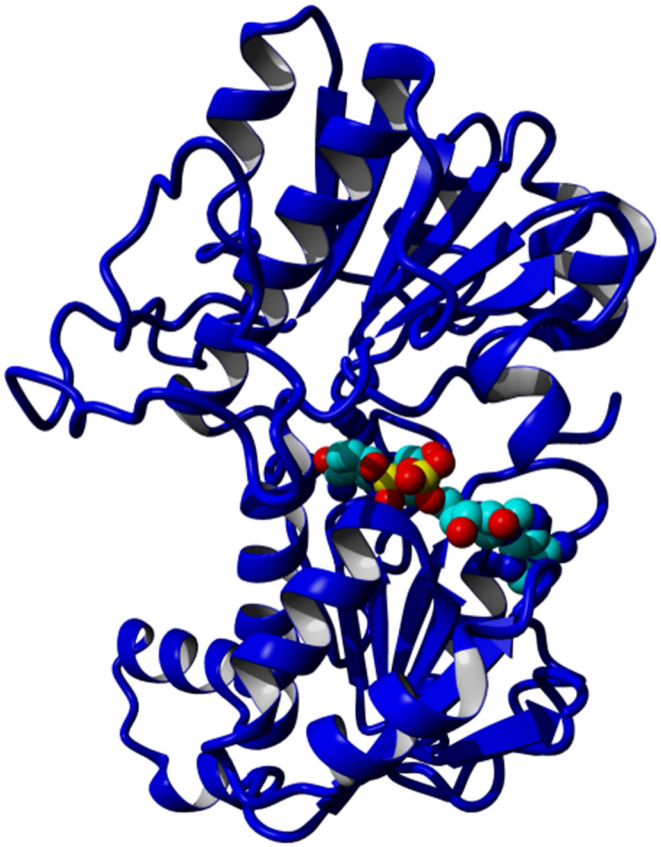

Figure 3-8 Model of the tertiary structure of formate dehydrogenase from *Pseudomonas* sp. 101
The structure of one formate dehydrogenase subunit from *Pseudomonas* sp. 101 [PDB ident. 2NAD (Lamzin et al. 1994)] is displayed with a co-crystallized NAD^+ molecule in the active site. The model is shown in backbone-ribbon-style with NAD^+ as a ball-model bound to the active site.

The prochiral ketones, such as the α-haloketone ECAA used in asymmetric reductions are highly reactive and cause inactivation to enzymes such as the FDH (Yamamoto et al. 2005). Therefore, the search for stable enzymes (Nanba et al 2003) or mechanisms to stabilize the already present ones is of interest (Tishkov and Popov 2006). Solvent accessible cysteines have been assumed responsible for the major effects of inactivation by α-haloketones. They are considered to be involved in the general catalytic mechanism for the mediation of substrate interaction, but not irreplaceable, as they are not highly conserved throughout the various FDH from different organisms (Hatrongjit & Packdibamrung 2010; Yamamoto et al. 2005; Tishkov & Popov 2006). Replacement of cysteine residues on the 145th and 255th position prolonged the half life in the presence of ECAA. The mutation of these cysteines was observed to cause losses in enzymatic activity, which is unfavourable (Yamamoto et al. 2005; Tishkov & Popov 2006).

Similar to the vast majority of FDH enzymes, the FDH from *M. vaccae* N10 has a preference

for the non-phosphorylated nicotinamide adenine dinucleotide NAD^+ (Tishkov & Popov 2004; Tishkov & Popov 2006). The FDH was intended for cofactor recycling in asymmetric reductions with the KR (see Figure 3-5), which requires NADPH. The native FDH from *M. vaccae* has a $K_m > 40$ mM for $NADP^+$. Engineering in cofactor preference revealed mutant FDH, which comprise a mutation in position 221 to either glycine, serine, alanine or glutamine, which reduced the K_m to < 0.44 mM and caused a change in cofactor preference to the phosphorylated nicotinamide nucleotide with a catalytic efficiency of up to 2.67 ± 0.21 1/(s*mM) for the D221Q variant (Hoelsch et al. 2013). Notably, combination of mutations for a change in cofactor preference and enzyme stability towards α-haloketones caused a synergistic effect, with enhanced activity and improved cofactor acceptance for $NADP^+$. The resulting FDH comprises three mutations C145S/D221Q/C225V, leading to a specific activity of 10.25 ± 1.63 U/mg and a cofactor preference of 1.14 for $NADP^+$ (Hoelsch et al. 2013).

3.2.5 Fusion proteins

In nature, enzymes frequently work in catalytic cascades. Large synthetase complexes like the fatty acid synthase or polyketide synthase comprise different catalytic subunits for the production of a multitude of goods (Bülow 1987; Conrado et al. 2008). In the course of evolution, the modification of the enzymes within such sequential reactions lead to new molecules such as antibiotics, which are of tremendous importance in today's health care (Magnuson et al. 1993). In biotechnological research such multi-enzyme reactions are thus of high interest. Here, enzyme and cascade reactions provided by an individual organism can be combined with enzymes from different organisms. This opportunity greatly expands the possibilities in multi-enzyme synthesis.

Sometimes, enzymes for cascade reactions are not only co-expressed, but also adjoined to new fusion proteins, which comprise the catalytic abilities of the distinct catalytic subunits. Fatty acid synthesis complex I (FAS I) is a common example for a natural fusion protein. It is the equivalent of FAS II and can be found in eukaryotes and fungi. Whereas the bacterial FAS II is built up of separate enzymatic subunits, the FAS I comprises the same catalytic sites, but expresses them fused into dimeric protein subunits (Stoops et al. 1975). In nature, this principle is found for enzymes, which are sequentially employed in biosynthesis. Fusion proteins permit easy adjoining of functionally related reactions, thereby offering entropic advantage due to locally enhanced substrate concentrations (Huang et al. 2001; Simmel 2012).

Production processes in industrial applications can be improved by the use of fusion proteins, if better availability of the substrates enhances the catalytic activity. Additionally, expression of just one polypeptide chain instead of many simplifies the enzymatic production, as reduced expression levels in co-expressions and multiple plasmids with corresponding selection factors are avoided. Fusion proteins are frequently studied and find application in biosynthesis (Conrado et al. 2008), e.g. in a fusion protein of the β-galactosidase and the galactose dehydrogenase (Pettersson & Pettersson 2001).

Another example is the fusion protein of FDH from *M. vaccae* N10 and KR from *Synechococcus*. Fusion proteins comprising both enzymes within one polypeptide chain have been studied and described in different publications. For example by adjoining the FDH at the N-terminus and the KR at the C-terminus with a serine-glycine linker sequence in between, a multifunctional fusion protein FDH-SG-KR for asymmetric reduction with internal cofactor regeneration was created (see Figure 3-9). (Hölsch & Weuster-Botz 2010a; Sührer et al. 2014)

Figure 3-9 Schematic display of FDH-SG-KR fusion protein

During design of the fusion protein FDH-SG-KR, it was discovered to be prone to proteolytic degradation. Amino acid sequences at the C-terminus of the FDH were revealed as the cleavage site. Four site-directed mutations at the respective positions (K395G/F396S/K397S/K398S) were introduced and resulted in a proteolytically stable FDH within the fusion protein. Mutations for proteolytic stability of the FDH subunit were combined with mutations for enhanced stability towards α-haloketones and increased preference for $NADP^+$. Eventually, the FDH within the fusion protein comprised a total of seven mutations (C145S/D221Q/C255V/K395G/F396S/K397S/K398S). The introduction of the C-terminal mutations reduced the catalytic speed of the enzyme compared to the FDH containing only the mutations C145S/D221Q/C255V and increased the K_m to 0.70 mM. This indicated a negative effect of C-terminal modifications on the catalytic properties of the FDH. In asymmetric reductions with the FDH-SG-KR containing the modified FDH, the fusion protein was advantageous compared to the separate enzymes in the asymmetric reduction of the prochiral ketone ethyl benzoylacetate. This was possibly due to locally enhanced substrate concentration caused by a close proximity of both enzymes (Sührer et al. 2014).

C-terminal proteolytic degradation is also highly unfavourable if membrane anchors are attached, since proteolytic loss of the anchor could reduce the amount of immobilised enzyme molecules. The proteolytically stable FDH comprising all seven mutations for enhanced cofactor preference and α-haloketone resistance was used in this work

3.2.6 Ionic Liquids

Ionic liquids, which are also referred to as liquid salts, are salts with organic and/or inorganic components with a melting temperature below 100 °C. They are attractive for various industrial applications, because they feature very unique characteristics. Ionic liquids:

- Are largely chemically inert, which makes them interesting for numerous organic chemical applications.
- Have a scarcely detectable vapour pressure and are thermally stable.
- Show good solubility for many substrates, which are hardly soluble in aqueous buffers.

Generally thermal stability is of interest for organic synthesis and less important for biotransformations, which are performed at moderate temperatures. However, high boiling points enable easy product work-up, as separation by distillation is possible (Rogers & Seddon 2003; Zhao 2005; De Maria 2012).

Ionic liquids are often referred to as “designer solvents”, as properties such as the melting point or the solubility are highly dependent on the choice of the cation and anion. They may be used as the single solvent or in two-phase approaches. For biotransformations biphasic systems are of interest, in which ionic liquid and aqueous phase are not miscible (Rogers & Seddon 2003; Pfruender et al. 2006; De Maria 2012). Contrary to organic solvents, ionic liquids are described to be often better biocompatible and are therefore frequently investigated (León et al. 1998; Bräutigam 2008).

In biotranformations using biphasic systems with ionic liquids, the amount of substrate and product in the aqueous phase is highly dependent on the respective distribution coefficient. It defines the ratio of concentrations of a substance in both phases in biphasic systems. The distribution coefficient is characteristic for each ionic liquid and organic molecule, respectively (De Maria 2012) and calculated using equation 3-8. Generally, a distribution coefficient of > 2 is desired, which means that the majority of the substance is dissolved in the ionic liquid (Pfruender et al. 2006).

$$D_{1/2} = \frac{c_{i,phase\ 1}}{c_{i,phase\ 2}} \qquad \textbf{3-8}$$

$D_{1/2}$ distribution coefficient between phases 1 and 2, -

c_i concentration of substance *i* in each phase, mol/L

A schematic description of a two-phase system using an ionic liquid for biotransformation is displayed in Figure 3-10. Within the two-phase system the substrate is dissolved in the ionic liquid phase. Subsequently, equilibrium concentrations are generated between the ionic liquid and the aqueous phase. The substrate is converted by the biocatalyst, which may be whole cells or purified enzymes. Then product is retransferred into the ionic liquid, in which it preferably has superior solubility. The products can finally be extracted from the ionic liquid using organic solvents or distillation (Bräutigam 2008; De Maria 2012). Due to the partition coefficient, exposure of the organic material to the aqueous phase is reduced. If the substrate or products are highly susceptible to hydrolysis in aqueous buffers, losses can be reduced if the majority of the material is not dissolved in the aqueous phase. If the substrate or products are toxic to the biocatalyst (general effects on whole cells or inactivation of the synthesis enzyme), reduced concentration of the toxic material can reduce inactivation, and the life of the catalyst is thereby prolonged. (Rogers & Seddon 2003; Bräutigam 2008; Bräutigam et al. 2009; Dennewald 2011; De Maria 2012)

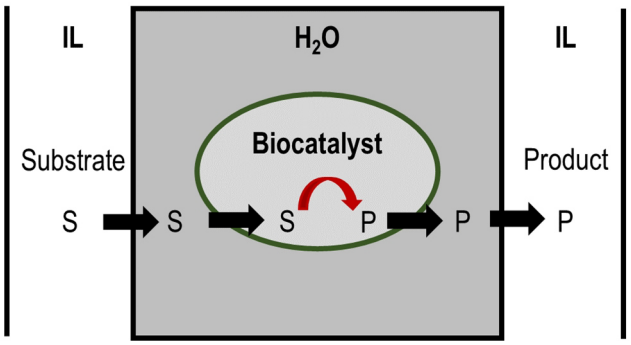

Figure 3-10 Biotransformation in biphasic reaction systems with ionic liquids
The substrate is transferred from the ionic liquid (IL) to the aqueous (aq.) phase in an equilibrium. It is converted to the product by the biocatalyst (whole cell or isolated enzyme or other preparation). The products are then retransferred into the ionic liquid.

The ionic liquid employed in this work is [HMPL][NTF] (see Figure 3-11). It consists of the organic anion bis(trifluoromethanesulfonyl)amide $[NTF]^-$ and the organic cation 1-hexyl-1-methylpyrrolidinium $[HMPL]^+$. The applicability of this ionic liquid for biotransformations has been the subject of several studies (Bräutigam 2008; Dennewald 2011).

The ketone ECAA and corresponding alcohols analysed in this work have higher solubility in the ionic liquid compared to aqueous buffers (Bräutigam 2008), with a distribution coefficient of 1.88 for ECAA and 1.25 for (*S*)-ECHB, respectively (unpublished data). In asymmetric reductions of ECAA, biphasic reaction systems with [HMPL][NTF] were proved to be preferable to the single-phase ones (Bräutigam 2008; Dennewald 2011).

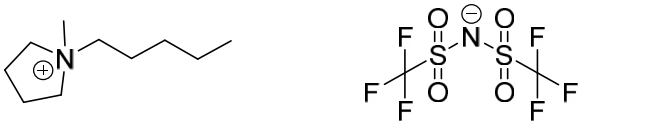

1-hexyl-1-methylpyrrolidinium $[HMPL]^+$ bis(trifluoromethylsulfonyl)amide $[NTF]^-$

Figure 3-11 Ionic liquid used in this research project
The structure of the organic cation and anion of [HMPL][NTF] are displayed.

3.3 β-Galactosidase from *Escherichia coli* K12

The β-galactosidase is a hydrolase (EC 3.2.1.23), which is ubiquitously found in prokaryotes and eukaryotes such as mammalians, plants and fungi. More specifically, it is an exoglycosidase, as it cleaves the *O*-glycosidic bond between a β-D-galactose and an *O*-glycosidic bound organic moiety. The enzyme is encoded by a gene called *lacZ*. Its most prominent representative is the β-galactosidase found in *E. coli* K12. The gene encodes for a 1023 amino acid long polypeptide (117 kDa). The monomers are not catalytically active and the single polypeptide chains form a tertiary structure composed of four subunits, which form the active tetramer, being a dimer of two dimers. The contact surfaces in the multimer are referred to as "activating interface" and "long interface" (see Figure 3-12). Within the tertiary structure, amino acids from one monomer contribute to the active site of another and each active site is composed of the amino acids from two monomers. Additionally, the β-galactosidase requires thiols, Mg^{2+} and Na^+ to prevent dissociation of the monomer (Fowler & Zabin 1977; Jacobson et al. 1994; Juers et al. 2012).

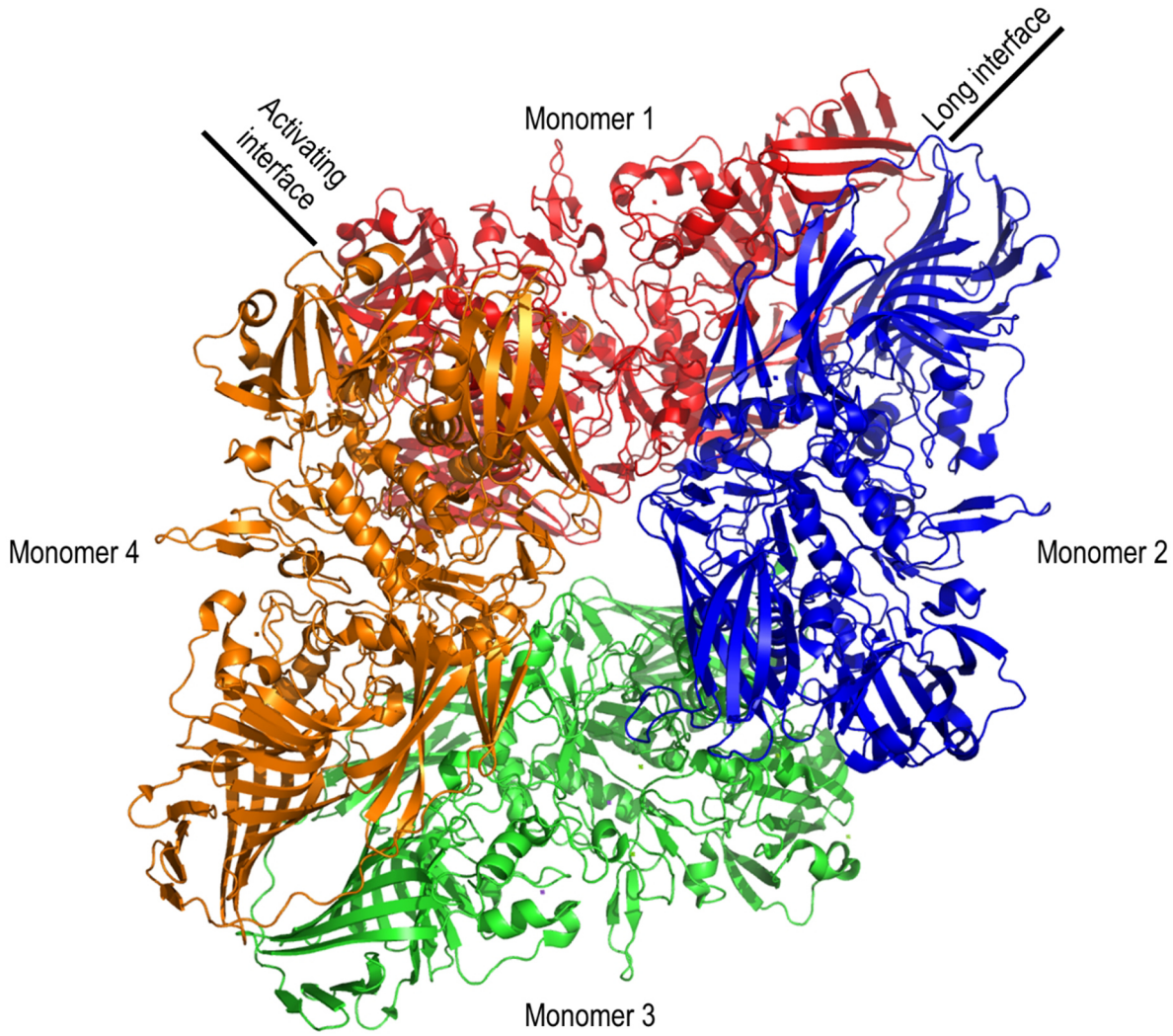

Figure 3-12 Crystal structure of β-galactosidase from *E. coli*
Cartoon display of β-galactosidase from *E. coli* showing all four monomers with each one highlighted [PDB ident. 1JYV (Juers et al. 2001)].

The β-galactosidase is able to accept non-natural products. Generally, a β-D-galactose subunit is required, to which a second moiety is bound via an *O*-glycosidic bond. The catalytic mechanism is divided into two modes. The first is the "shallow mode", in which the substrate is bound. The second is the "deep mode", where the substrate is shifted from the binding position to the catalytic site. Substrate conversion is only possible in the deep-mode. The first step in substrate conversion is the cleavage of the *O*-glycosidic bond and release *O*-glycosidic bound moiety. The second is addition of water to the bound β-D-galactose molecule and release of the monosaccharide. Notably, all reactions can also be performed in reverse direction if high concentrations of the products are present. Moreover, a transgalactosylation is possible. In hydrolysis of lactose, the cleaved D-glucose is not always released after cleavage from lactose. It is then used as the acceptor for D-galactose instead of water and the *O*-glycosidic bond is

formed at the oxygen at the carbon atom 6, thus forming allolactose (Cupples et al. 1990; Juers et al. 2003; Juers et al. 2012).

The natural function of the β-galactosidase consists of three enzymatic activities. The first is hydrolysis of lactose to glucose and galactose. The second is transgalactosylation of lactose to allolactose and the third is hydrolysis of allolactose to the monosaccharides. Allolactose is required for the regulation of the *lacZ*-operon, which encodes for the β-galactosidase and two other enzymes. The function of the *lacZ*-operon is schematically displayed in Figure 3-13. It comprises a promotor binding site for RNA polymerase binding, a repressor binding site called the operator and the structural genes. Activation and repression of transcription are regulated by the following factors:

- Lactose needs to be present, which is converted to allolactose by a low basal expression level of β-galactosidase. Allolactose binds to a repressor and causes a conformational change. The repressor is constitutively bound to the operator sequence, where it blocks transcription by the RNA polymerase. Conformational change in the repressor due to allolactose binding causes its release from the operator.
- A low level of free β-D-glucose is required, which is the preferred carbon source. Low levels in β-D-glucose cause high cAMP concentrations. cAMP binds to an activator protein, which itself then binds to the promotor. Activator binding at the promotor binding site is required for the RNA polymerase to begin with transcription.
- Transcription by the polymerase is only possible of the repressor is removed and the activator protein bound at the same time, meaning that there is lactose in the absence of glucose(Juers et al. 2012).

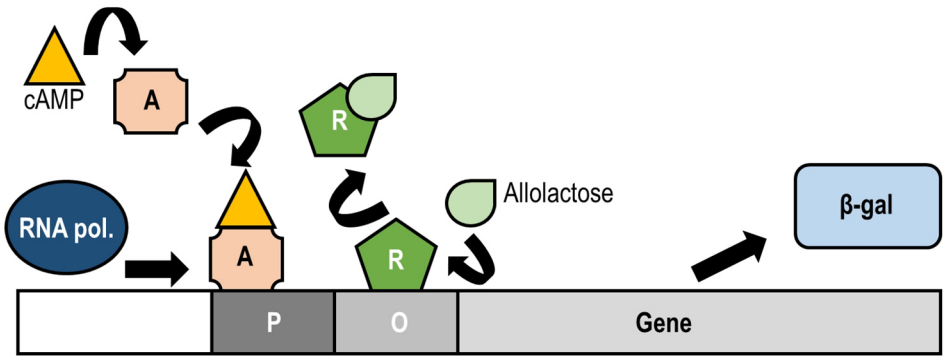

Figure 3-13 Schematic display of β-galactosidase expression regulation by the *lacZ*-operon
cAMP binds to the activator protein (A), which then binds to the promotor binding site (P) to activate expression. Allolactose binds to the repressor protein (R), which is constitutively bound to the operator sequence (O). Allolactose binding to the repressor causes a conformational change and the release of the repressor from the operator. The RNA polymerase (RNA pol.) can now transcribe the gene(s) encoded downstream of promotor and operator.

The β-galactosidase is frequently used in manifold experiments in life science. The different features of the β-galactosidase and the *lacZ*-operon have been used for many decades in many applications, because of which the β-galactosidase has become very important and very well characterised:

- The *lacZ*-operon of *E. coli* is frequently used for the regulation of gene expression for production of recombinant proteins. The desired protein sequence is added down-stream of the operator, thus addition of lactose or an artificial inductor will cause transcription of the recombinant protein.
- Induction of the operon is also possible by artificial inductors such as isopropyl β-D-1-thiogalactopyranoside (IPTG), which binds better and is not degraded and therefore frequently used in expression of recombinant proteins (Baneyx 1999).
- The ability to convert non-natural products is used as a reporter. Co-expression of the β-galactosidase can be connected to a shift in fluorescence, chemiluminescence or colouring, which is used as a reporter. Most prominent are the dyes are X-Gal (or BCIG for 5-bromo-4-chloro-3-indolyl-β-D-galactopyranoside) and *o*NPG (*ortho*-nitrophenyl-β-galactoside, see Figure 3-14).
- N-terminal sequence parts, which are crucial for enzyme activity can be expressed separately from the remaining polypeptide chain. The shorter, separate polypeptide is still able to form the secondary structure and can thus inserts into the tetramer, activating the enzyme. This phenomenon is called "α-complementation" and used in reporter experiments.

(Langley et al. 1975; Lottspeich & Zorbas 1998; Juers et al. 2012; Hannig & Makrides 1998)

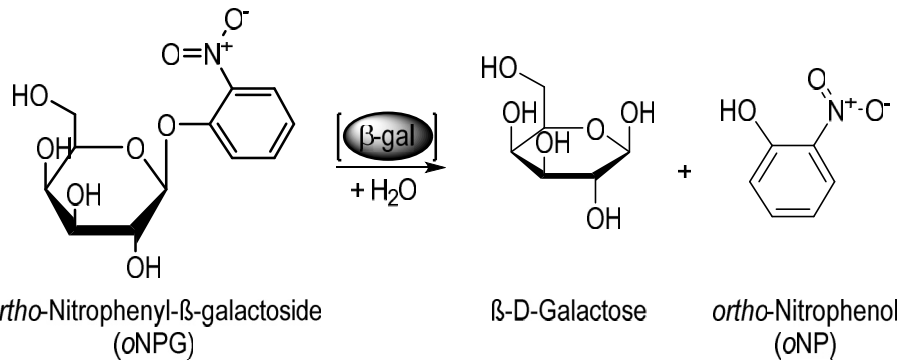

Figure 3-14 Schematic display of *o*NPG hydrolysis by the β-galactosidase
The hydrolysis of colourless *o*NPG by the β-galactosidase (β-gal) to β-D-galactose and the dye *o*NP, which can be photometrically detected at 436 nm.

3.4 Enzyme immobilisation

This project focused on the development of a new immobilisation method. The subsequent chapter will give an overview on the state of the art in immobilisation techniques.

3.4.1 Methods

Immobilisation of biocatalysts is state of the art in industrial applications. A summarising overview on the different methods is given in Figure 3-15. As discussed in section 3.1.3, enzymes can be applied purified or expressed within whole cells. Both types of biocatalysts are frequently immobilised to:

- Enable recycling of enzymes or whole cells, as the biocatalyst can be expensive (depending on the application).
- Enable continuous processes.
- Simplify down-stream processing, as the catalyst can be separated more easily by e.g. filtration or centrifugation if provided in coarse-particles. A different approach is to immobilise the substrate instead of the biocatalyst.
- Stabilize the catalyst (especially purified enzymes), by preventing enzyme degradation (León et al. 1998; Hanefeld et al. 2013; Gray et al. 2013; Sheldon & van Pelt 2013; Rupp 2013).

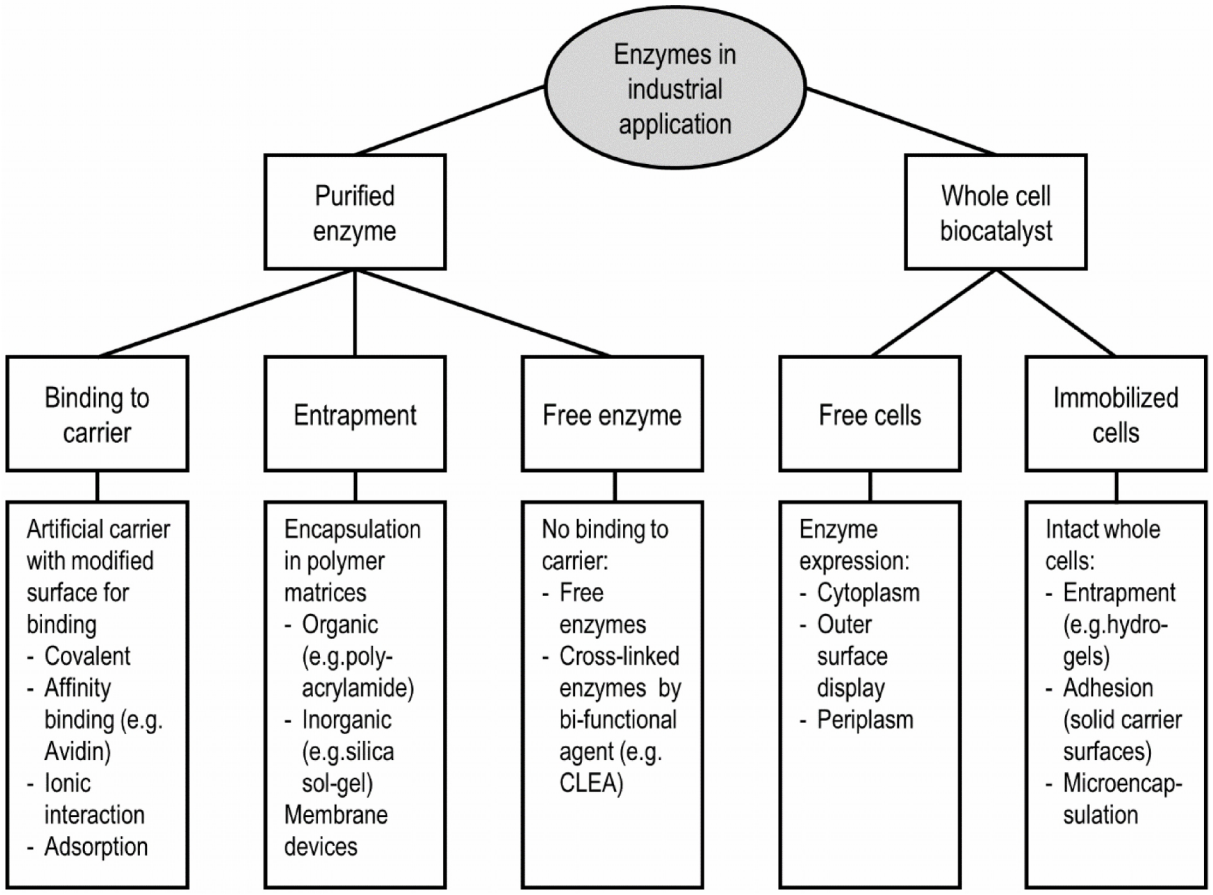

Figure 3-15 Summary immobilisation methods
(León et al. 1998; Sheldon & van Pelt 2013; Hanefeld et al. 2013; Jia et al. 2014)

As summarised in Figure 3-15, there are a multitude of approaches to the immobilisation of biocatalysts. Each of the options has advantages and disadvantages. A comparison between purified enzymes and whole cell biocatalysts is described in section 3.1.3. Generally, whole cells or purified enzymes can be used free, entrapped or fixed onto surfaces.

- Entrapment into artificial or natural polymers does not require modifications to the enzyme or cell. However, entrapment systems frequently suffer from leaking of encapsulated enzymes and mass transfer limitation of the substrates, which have to diffuse into the material to reach the fixed enzymes. Catalyst activities are consequently reduced, the further away the enzyme or cell is fixed from the particle surface. Microencapsulation is an alternative, where enzymes or whole cells are immobilised within an artificial capsule. Within that capsule they can diffuse freely. Problems due to mass transfer limitation are then only caused by the transfer through the membrane of the capsule (León et al. 1998; Hanefeld et al. 2013; Liese & Hilterhaus 2013).
- In fixation usually highly porous carriers are used, which provide large surface areas for immobilisation. Thus problems due to mass transfer arise similar to entrapment, because

the substrate needs to diffuse into the pores to reach the innermost fixed enzymes. Purified enzymes can generally be fixed either covalently, with affinity binding, with adsorption or physical interaction. Thereby, the nature of fixation can have a strong impact on enzyme activity e.g. some enzymes are rendered inactive by covalent fixation or suffer activity changes by the addition of affinity tags. On the other hand, some enzymes are stabilized by covalent binding to surface carriers. Generally, strong fixation is aimed for, because losses of enzymes from the carrier are to be reduced. Whole cells on the other hand can be fixed by van der Waals like physical interactions, where losses of cells from the carrier become more likely (León et al. 1998; Liese & Hilterhaus 2013; Jia et al. 2014; Hanefeld et al. 2013; Sheldon & van Pelt 2013; Secundo 2013; Bommarius & Paye 2013).

- Free enzymes or cells are generally used, when effects by fixation are highly undesirable or fixation cost are not economic in contrast to the production of new biocatalysts. Cross-linked enzyme particles (as aggregates or crystals) are an exception. Here, an additive is added, which causes the agglomeration of enzyme particles to one multimeric complex by crosslinking of the polypeptides. The resulting multimer allows for easier handling and stabilization of multimeric proteins, while being cheap as no external carrier is required. Notably, mass transfer limitation can occur in such multimeric complexes (depending on the particle size) as the substrates have to penetrate the complex to reach the innermost enzymes. Additionally, linking of the polypeptides to a somewhat more rigid structure reduces the flexibility of the enzymes, which can cause a reduction of activity (Bommarius & Paye 2013; Fernandez-Lafuente 2009; Sheldon & van Pelt 2013).

All immobilisation methods have advantages and disadvantages and the immobilisation method needs to be chosen specifically for each application. Economic features thereby have to be considered alongside other factor such as the practicability or influence on enzyme activity.

All methods described above feature mostly artificial carriers or material for entrapment. However, whole cell biocatalysts as such are, in a way, a method for enzyme immobilisation, since the synthesis enzymes are entrapped within the cell. The use of cells is a special field in enzyme immobilisation, which was studied in this work. Immobilisation via anchoring in membranes is one option in whole cell biocatalysis, which is discussed in more detail in the following section.

3.4.2 Membrane anchoring

This work focused on expression with *E. coli*, which is a frequently used and studied

microorganism for expression of various recombinant proteins. These Gram negative prokaryotic cells provide different compartments for expression:

- The cytoplasm, which is most often used
- The periplasm, which offers a reducing environment and thus enables formation of tertiary structure elements of eukaryotic proteins e.g. disulfide bonds
- The inner- or cytoplasmic membrane
- The outer membrane
- Secretion of enzymes via the complete cell wall (rare cases)

(Cornelis 2000)

In this study, membrane immobilisation was of interest, which will therefore be focused on. Membrane binding of enzymes can occur via complete insertion as transmembrane helical structures (e.g. heptahelical membrane proteins), via short anchoring sequences (N-or C-terminal) or posttranslationally added lipid- or glycosyl-chains, which interact with the lipid or peptidoglycan and thus provide immobilisation (Kutay et al. 1993). To immobilise soluble enzymes to membranes, they consequently need to be fused to integral membrane proteins or equipped with anchoring sequences.

One problem of (*E. coli*) whole cell biocatalysts is mass transfer limitation due to low permeability of the cell wall for many substrates used in biotransformations (see section 3.1.3). One frequently studied option as a solution to this issue is expression of the enzymes on the surface of the cells, commonly referred to as “surface display” (Lee et al. 2003; Schüürmann et al. 2014). The method was originally developed for the screening and preparation of e.g. peptide libraries, bio-adsorbents or bio-detectors using display on various organisms such as yeast or *E. coli* (Lee et al. 2003). Recently, the method has gained interest in the development of biocatalysts (Schüürmann et al. 2014). For surface display in *E. coli*, the enzymes are expressed in the cytoplasm and subsequently transported via the cytoplasmic membrane, the periplasm and outer membrane to the surface of the cell (Lee et al. 2003). Therefore, secretion and transporter systems are required. Generally, a transporter protein is used, which mediates the trans-membrane secretion. The desired peptide is anchored to the transporter as a passenger and thus carried along (van Bloois et al. 2011; Jose et al. 2012). There are several different methods for enzyme secretion and transport in surface display which are summarised in Table 3-2.

Table 3-2 Overview on typical surface-display methods for *E. coli*
(van Bloois et al. 2011; Lee et al. 2003)

System	Characteristics
Outer membrane proteins	Attachment to proteins which are naturally displayed on the surface (e.g. proteins of the outer membrane protein family).
Surface appendages	Attachment to surface protrusions such as flagellum or pili, the passenger is inserted at exposed sequences.
Lipoproteins	Attachment to proteins which are membrane-anchored by lipid modified termini (e.g. Lpp-OmpA).
Virulence factors	Virulence factors from pathogenic bacteria, which express on the membrane are used as transporter (e.g. adhesin). Many virulence factors are so called "autotransporters", e.g. AIDA-I.

Each of the methods described above has advantages and disadvantages regarding the application and not all of them are suitable for biocatalysts. The type of anchoring (N-,C-terminal or insertional), if multimerization of subunits is required and the number of copies immobilised per cell vary greatly depending on the anchoring method (van Bloois et al. 2011; Lee et al. 2003). The number of copies per cell varies from about 10^3 to 10^5. The systems with the highest number of enzyme copies per cell use autodisplay with "autotransporters". The term refers to a family of proteins, which contain sufficient information on a single gene to direct secretion out of the cell (where most insert into the outer membrane), most autotransporters are virulence factors (see Table 3-2). Depending on the enzyme and the autotransporter used, 15,000 to 180,000 molecules per cell are reported fixed to the surface (Jose & Meyer 2007; Jose et al. 2012).

Another option for membrane anchoring in *E. coli* analysed in this work is immobilisation to the cytoplasmic membrane. In comparison to surface display, anchoring to the cytoplasmic membrane is advantageous, as no translocation of the enzyme through the cell wall is required. There are different options for the anchoring of proteins to the cytoplasmic membrane, which are summarised in Figure 3-16. Similar to surface display, the recombinant protein requires anchoring, which can be provided by fusion to integral membrane proteins or anchoring sequences.

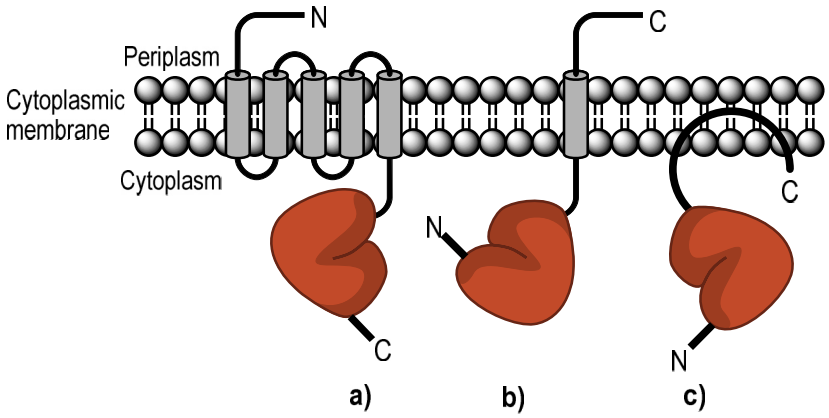

Figure 3-16 Most frequently used membrane anchoring options for immobilisation in the cytoplasmic membrane
Options for membrane anchoring are summarised for a) N-terminal anchoring with integral membrane protein, b) C-terminal anchoring with membrane spanning anchor and c) C-terminal membrane anchoring with short "dip-in" of C-terminal sequence.

Similar to surface display, there are different options for attachment (C- or N-terminal) and anchors (short anchoring sequences vs. integral membrane proteins). Many N-terminal anchoring options feature integral membrane proteins where the desired protein is linked C-terminally to the integral protein, which inserts into the membrane and thus fixes the appendix to the cytoplasmic membrane (Wagner et al. 2006). Most prominent among them is the integral membrane protein Mistic from *Bacillus subtilis* (Roosild et al. 2005; Roosild et al. 2006; Wagner et al. 2006). Often, insertion of the N-terminal integral membrane anchor is dependent on signalling sequences and secretory pathways (Wagner et al. 2006). So immobilisation amounts are limited by the capacity of the translocation mechanisms. Notably, N-terminal integral membrane anchoring proteins have been described to prevent inclusion body formation such as the glycerol-conducting channel (GlpF) from *E. coli* (Neophytou et al. 2007).

C-terminal anchoring is an alternative, which is not much described in the literature as it is assumed a peculiarity among membrane-bound enzymes. Contrary to N-terminal membrane anchors, C-terminal anchoring features short C-terminal sequences mainly composed of hydrophobic amino acids. C-terminal membrane immobilisation is described for eukaryotic and phage proteins, which use such C-terminal sequences to immobilise to cell membrane. These sequences form short C-terminal anchor structures that insert post-translationally into the membrane and are therefore independent from secretory pathways. Insertion can be a complete span or just a partial "dip-in" of hydrophobic amino acids (see Figure 3-16 b) and c)). Among

this group of membrane anchors the C-terminal sequence of cytochrome b_5 is considered the archetype of C-terminally anchored proteins. This particular membrane anchor is 43 amino acids long and proposed to form a defined secondary structure for membrane insertion, which spans the complete membrane (Ahuja et al. 2013). However, there are also very short C-terminal anchoring sequences e.g. the anchoring sequences of soluble *N*-ethylmaleimide-sensitive-factor attachment receptor (SNARE)-proteins and the ubiquitin-conjugating-enzyme 6 (UBC6), which is anchored using a mere 17 amino acids (Yang et al. 1997). There is little understood about C-terminal anchoring and few experiments have so far been conducted on the use of such anchoring sequences. Prominent among such experiments is the anchoring of β-galactosidase from *E. coli* K12 to the cytoplasmic membrane using the anchoring motif of cytochrome b_5 from rabbit liver. In these experiments described by George et al. (1989) it was demonstrated that multimerization despite C-terminal anchoring is possible and that such anchoring is incomplete. Some proportion of the protein containing a membrane anchor was found soluble in the cytoplasm. Notably, some C-terminally anchored proteins have been discovered to insert spontaneously to artificial membranes such as liposomes (George et al. 1989; Kutay et al. 1993).

3.4.3 *Escherichia coli* strains for membrane protein expression

E. coli is the most frequently used microorganism for biotechnological applications in research and industry. It is a Gram negative, rod shaped, non-sporulating bacterium, which is commonly found in the lower intestine of warm-blooded organisms. Its frequent use in life sciences originates from its completely sequenced genome, its easy handling, high growth rates and many existing systems for genetic modification and recombinant protein expression. However, there are also draw-backs in the use of *E. coli*. The lipopolysaccharides (LPS) found on the outer membrane are referred to as endotoxins and can cause immunological response. Thus, LPS need to be removed, which is complex and time-and cost-intensive. Additionally, not all proteins can be expressed and folded correctly in *E. coli*. Formation of disulfide bonds and posttranslational modifications such as the addition of glycosyl groups are still a challenge when expressing in *E. coli* (Sharma 1990; Weickert et al. 1996; Baneyx 1999).

Likewise, the (over)expression of membrane proteins in *E. coli* is challenging as expression of membrane proteins with membrane insertion is toxic to the cells (Miroux & Walker 1996; Wagner et al. 2006; Wagner et al. 2008). Therefore, Miroux and Walker developed special *E. coli* strains, which are more resistant towards membrane protein over-expression (Miroux &

Walker 1996). These special strains are commonly referred to as "*Walker*"-strains and are commercially available as C41 (DE3) and C43 (DE3). Both strains are derivatives from *E. coli* BL21 (DE3), a frequently used strain for expression of recombinant proteins (Miroux & Walker 1996; Wagner et al. 2008). The "*Walker*"-strains have mutations in the *lacUV5* promotor of the genomic T7-*lac* operon (see Figure 3-13) (Wagner et al. 2008). These mutations are assumed to cause a reduced expression of the T7-polymerase, which in consequence reduces the expression rates of the recombinant membrane protein and thereby enhances cellular vitality (about 4-6-fold) (Miroux & Walker 1996; Wagner et al. 2006; Wagner et al. 2008). However, these mutations were gained by unspecific treatment with mutagens. The complete nature of the strains resistance towards membrane protein expression and other probable effects on the strain performance are unknown (Wagner et al. 2008).

3.5 Protein E-mediated lysis

In this work, new biocatalysts were to be gained as cellular envelopes of *E. coli*. Cellular envelopes comprise the cell wall and membranes of the cell without the cytoplasm. Therefore, the cytoplasm needs to be removed. This removal can be realised by a special type of lysis, which will be described and discussed in detail in the following section.

3.5.1 Theory

During the infective cycle in phage and virus reproduction, the newly assembled phage or virus particles need to be released from the host cells, a mechanism for which many different strategies exist. The phage PhiX174 uses a lysis protein called protein E, which is encoded in the phage genome and expressed for the lysis of the cells. In 1966 protein E expression by phage PhiX174 for lysis was first described by Hutchinson and Sinsheimer. Cloning and expression of the recombinant protein E in *E. coli* was performed, which caused lysis of the cells (Hutchison & Sinsheimer 1966). Protein E was analysed closer and discovered to be a 91 amino acid long polypeptide (10 kDa), which contrary to many other viral lysis protein lacks any catalytic properties (Bläsi et al. 1985).

Since, protein E has no apparent catalytic properties the mechanism of lysis remained a mystery for some time, which was tackled in many scientific studies. On analysis of the different cellular fractions after lysis for the presence of protein E, it was found in oligomerized state and attached

to the inner- and outer-membrane fractions. Consequently it became clear that expression of the protein must somehow cause the formation of a tunnel in the cell membrane (Bläsi et al. 1989). A more detailed mechanism of protein E lysis was not elucidated until the mid-1990s'. Experiments using electron microscopy were performed featuring immuno-gold labelled protein E molecules to visualize protein E-mediated lysis (Schön et al. 1995). Based on the results and previous data a mechanism was proposed, which is shown in Figure 3-17.

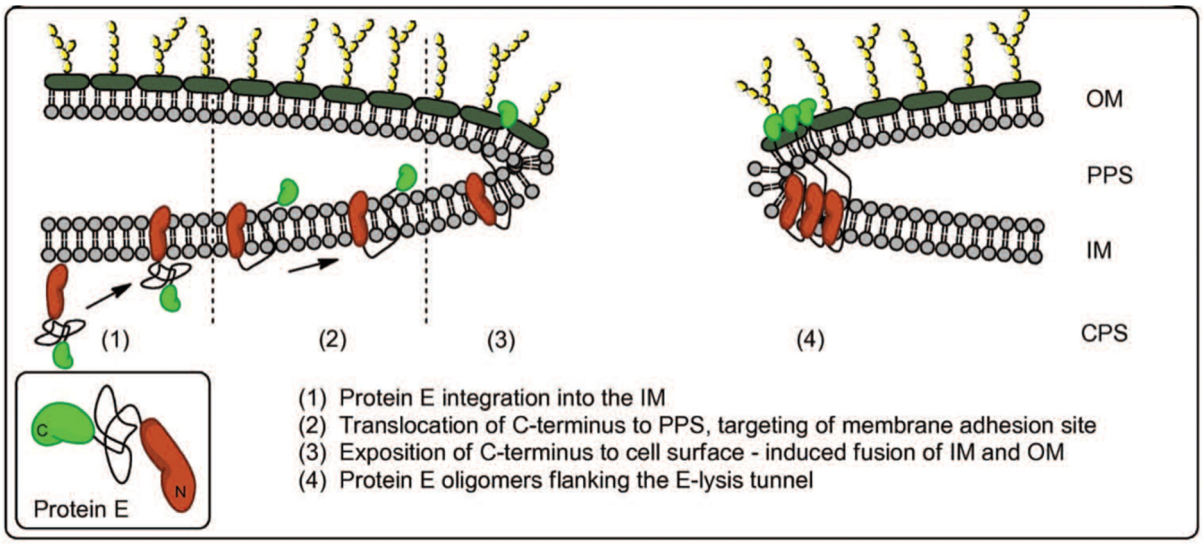

Figure 3-17 Schematic display of protein E insertion and pore formation
Stepwise display of protein E insertion from the cytoplasm (CPS) into the inner membrane (IM), through the periplasmic space (PPS) into the outer membrane (OM) (source: Langemann et al. 2010)

Protein E-mediated lysis is divided into the following steps:

1. Insertion of the N-terminus of protein E to the inner membrane.
2. Translocation of the C-terminus to the periplasm.
3. Translocation of the C-terminus through the peptidoglycan and outer membrane to the surface and fusion of inner and outer membrane.
4. Tunnel formation by oligomerization of protein E, with closing of the periplasmatic space.
5. Release of the cytoplasm driven by osmotic pressure through the lysis pore.

The formed lysis tunnel has a diameter of 40−200 nm and is composed of about 100-300 protein E molecules (Bläsi et al. 1985; Schön et al. 1995). Protein E inserts preferentially at the division zone of the cells, as it seems to require the characteristic lipid structure. The reason for this observation is not entirely understood but in consequence growing cells, able to perform cell division, are required for protein E-mediated lysis (Bläsi et al. 1985). After protein E-mediated lysis, the cellular envelope is retained. It consists of the cell wall, everything attached to it and

the periplasm while the native peptidoglycan remains intact (Langemann et al. 2010). Because of the loss of the cytoplasm, cellular envelopes are somewhat more transparent than whole cells. Due to this, cellular envelope particles cause reduced scattering of light in photometric measurements. Protein E-mediated lysis and loss of the cytoplasm can therefore be detected by a decline in the optical density of a cell culture (Langemann et al. 2010).

In the past decades, many applications for protein E-mediated lysis were analysed, which are summarised in the following section.

3.5.2 Applications

Not only *E. coli*, but Gram negative cells in general can be lysed by protein E-mediated lysis. Cellular envelopes have been gained from several Gram negative microorganisms such as *Salmonella typhimurium, Vibrio cholerae, Klebsiella pneumoniae*, and *Actinobacillus pleuropneumoniae* (Szostak et al. 1996).

Most research regarding the cellular envelope technology focuses on vaccine development (Szostak et al. 1996; Eko et al. 1999). In this context cellular envelopes are commonly referred to as "*bacterial ghosts*". Lysis and removal of the cytoplasm are used for pathogen inactivation, the cellular envelopes from pathogens are then intended as antigens (Mayr et al. 2005; Tabrizi et al. 2004). Additionally, non-pathogenic hosts can be used, which contain heterologous expressed antigens from a pathogen immobilised to their membranes or within the periplasm (Lubitz et al. 1999; Tabrizi et al. 2004). In such experiments, antigens were expressed and immobilised in low amounts (Eko et al. 1999; Lubitz et al. 1999). The non-pathogenic host (mostly *E. coli*) contains structural elements such as LPS, flagella or peptidoglycan, which enhance the immunologic response and thus function as adjuvants (Tabrizi et al. 2004; Mayr et al. 2005; Ebensen et al. 2004; Lubitz et al. 1999). Research for vaccines based on the "*bacterial ghost*" technology is diverse and focusing on medications for humans as well as veterinary applications (Szostak et al. 1996; Jalava et al. 2002). Exemplary is the production of a vaccine against streptococcal disease in olive flounder using *E. coli* as the non-pathogenic host. Cellular envelopes from *E. coli* were produced, which contained antigens against *Streptococcus iniae* and were successfully used to immunize olive flounder (Ra et al. 2009).

Next to antigens the application of cellular envelopes as carrier for biologically active substances in drug delivery is proposed. One cellular envelope offers the volume of about

250 femtoliters, which could be filled with the desired substance (Tabrizi et al. 2004; Langemann et al. 2010). One example is delivery of DNA as an antigen, which is challenging as DNA immunogenicity is poor. It was demonstrated that cellular envelopes containing desired DNA sequences were able to cause a better immune response in mice than pure DNA by acting as adjuvants (Ebensen et al. 2004).

Protein E is not the only lysis protein which is based on membrane insertion. Protein L is another member of this lysis protein family, which originates from phage MS2. This lysis protein uses the perforation of the host membrane. However, unlike protein E, protein L causes an undefined perforation of the cell wall due to which the cytoplasm is released (Witte et al. 1998). Both proteins have been extensively studied and another application was developed which employs the use of the hydrophobic membrane insertion sequences of protein E and L as membrane anchor sequences. The resulting membrane anchors are referred to as E' and L', mediate C- and N-terminal immobilisation, respectively and were cloned to recombinant proteins, realizing their membrane attachment in *E. coli* (Lubitz et al. 1999; Szostak et al. 1996).

3.5.3 Process for the production of cellular envelopes from *Escherichia coli*

Frequently, cellular envelopes are produced for use in research and mostly production of low amounts in shaking flasks is sufficient. Production of cellular envelopes from microorganisms such as *Vibrio cholera* and *Klebsiella pneumonia* has so far been restricted to laboratory scale shaking flask experiments. However, for application as vaccines, larger scale production is of interest and production of cellular envelopes from *E. coli* as vaccines in stirred tank bioreactors has been described in the literature.

In experiments performed by Ra et al., cellular envelopes from *E. coli* were produced as vaccines carrying heterologous antigens from streptococcal pathogens. Therefore, process characterisation of different cultivation and lysis conditions were analysed. Ra et al. describe the production of 5.2 g/L product in batch processes and up to 22 g/L product in fed-batch processes using intermitted feeding in 2.5 L working volume. Whether the product concentration refers to unlysed cells prior to lysis or cellular envelopes is not stated clearly. Lysis yields were described to be 99.7%. The gained vaccines were successfully used for immunization of fish. However, the exact amount and method of immobilisation of the streptococcal antigens is not described in this work (Ra et al. 2009; Ra et al. 2010).
Another batch-production process for cellular envelopes from *E. coli* is described by

Langemann et al. (2010), who produced cellular envelopes from the probiotic strain *E. coli* Nissle without membrane-anchored proteins in up to 20 L-scale with lysis yields ≥ 99.9%.
The general procedure in all these processes is very similar and uses roughly the following steps:

1. Preculture and generation of biomass
2. Lysis of cells
3. Harvest of cells and application

Production processes of cellular envelopes from *E. coli* described for stirred tank bioreactors use the phage promotor λ p_R for repression of protein E expression during biomass formation. The promotor incorporates the temperature sensitive repressor cI857, which can be inactivated by shifts to increased temperatures. The wild type repressor is inactivated at 30 °C, which is not suitable for *E. coli* production. Therefore the repressor was modified to allow for stringent repression of protein E expression up to 36 °C and inactivation by a temperature shift to 42 °C (Jechlinger et al. 1999).

4 Material and methods

4.1 Material

All materials, equipment and chemicals used in this work are summarised in the appendix, only special modifications, treatments and calculations are described in the following paragraphs.

4.1.1 General material

All consumables and equipment used for this work are listed in the appendix 12.1.

4.1.2 Chemicals

All chemicals are listed in the appendix Table 12-8.

4.1.3 *Escherichia coli* strains

E. coli DH5α was used for cloning, *E. coli* XL Gold were used for site-directed mutations, *E. coli* Bl21 (DE3), *E. coli* C41 (DE3) and *E. coli* C43 (DE3) were used for protein expression and protein E-mediated lysis. All *E. coli* strains are summarised in Table 12-11 in the appendix.

4.1.4 Primers and plasmids

Primers for cloning were purchased at MWG Eurofins (Ebersberg, Germany) and biomers.net. (Ulm, Germany) and are listed in the appendix Table 12-12. A list of all vectors used in this study is given in the appendix in Table 12-13. All primers for site-directed mutagenesis were designed using the QuickChange® Primer Design program.

4.1.5 Antibodies and enzymes

Enzymes and kits for cloning are listed in the appendix in Table 12-10 and Table 12-9. All antibodies used for sandwich ELISA are summarised in Table 12-10 in the appendix.

4.2 Media and buffers

All materials and media used for cell culture were either purchased sterile, sterilized by autoclave treatment for 20 min at 121 °C and 2.1 bar or sterilized by filtration using a 0.22 µm filter. All media and buffers were made with distilled water (dH_2O). For selection 50 µg/mL ampicillin sulfate, 30 µg/mL kanamycin sulfate and 20 µg/mL gentamycin were added to the media as required.

4.2.1 Media

The following paragraph lists all media and respective modifications used in this work

LB medium and its derivative NZY$^+$

LB medium and derivate were used in cloning and in 4 mL precultures.

Table 4-1 LB medium and its derivative NZY$^+$
All components were added and the medium was adjusted to pH 7.2. LB medium was sterilized by autoclave treatment.

Medium	Components/concentrations	pH
LB-medium	10 g/L peptone from casein, 5 g/L NaCl, 5 g/L yeast extract	7.2 (NaOH/HCl)
NZY$^+$	LB-medium with 20 mM glucose, 12.5 mM $MgCl_2$, 12.5 mM $MgSO_4$	7.5

Defined medium for cultivation in stirred-tank bioreactors

A defined medium was used in all cultivations and respective precultures in the stirred-tank bioreactor. The composition of the trace element stock solution and the concentrated feeding medium used in fed-batch processes are listed separately.

Table 4-2 Composition of the defined medium for shaking flask and stirred-tank bioreactor cultivation
The medium was composed according to DeLisa et al. (1999). A stock from KH_2PO_4, $(NH_4)_2HPO_4$ and citric acid was prepared and adjusted to pH 7.2 using 5 M KOH and sterilized in an autoclave. Glucose, $MgSO_4$ and ethylenediaminetetraacetic acid (EDTA) were sterilized by autoclave treatment, all other components were sterilized by filtration through a 0.22 µm filter. The remaining components were added prior to use from sterile stock solutions. The final concentrations and concentrations of the stock are given below. The antifoam was prepared as a 1:10 dilution in dH_2O and sterilized in an autoclave prior to use.

Component	Final concentration, g/L	Conc. stock solution, g/L
KH_2PO_4	13.3	–
$(NH_4)_2HPO_4$	4.00	–
Citric acid	1.70	–
Glucose	8.0[a]/5.0[b]/20[c]	22 0
$MgSO_4$ x 7 H_2O	1.20	600
Fe(III) citrate	0.100	10.0
EDTA	0.00840	0.840
$Zn(CH_3COO)_2$ x 2 H_2O	0.0130	2.60
Trace elements (see Table 4-3)	see Table 4-3	200 x
Thiamine hydrochloride	0.00450	4.50
Gentamycin sulfate	0.0200	2.00
Kanamycin sulfate	0.0300	–
Antifoam *	0.300	4.50

*) in fermentation only

a) shaking flasks

b) fed-batch cultivation

c) batch cultivation

Table 4-3 Composition of the trace element stock solution
The trace element stock was prepared as a 200x stock solution and sterilized by filtration through a 0.22 µm filter.

Component	Final concentration, g/L	Conc. stock solution, g/L
$CoCl_2$ x 6 H_2O	0.0025	0.5000
$MnCl_2$ x 4 H_2O	0.0150	3.0000
$CuCl_2$ x 2 H_2O	0.0012	0.2400
H_3BO_3	0.0030	0.6000
Na_2MoO_4 x 2 H_2O	0.0025	0.5000

Table 4-4 Composition of the feed medium
Feeding medium was used for substrate limited feeding in fed-batch processes. Glucose, $MgSO_4$ and EDTA were sterilized by autoclave treatment, all other components were sterilized by filtration through a 0.22 µm filter. The remaining components were added prior to use from sterile stock solutions, the final concentration and concentration of the stock are given below. The antifoam was prepared as a 1:10 dilution in dH_2O and sterilized in an autoclave prior to use.

Component	Final concentration, g/L	Conc. stock solution, g/L
Glucose	See Table 4-5	-
$MgSO_4$ x 7 H_2O	2.50	600
Fe(III) citrate	0.00500	10.0
EDTA	0.00163	0.840
$Zn(CH_3COO)_2$ x 2 H_2O	0.00200	2.60
Trace elements	-	-
Antifoam	5.00	-

Table 4-5 Summary growth rate and corresponding glucose concentration in feeding medium

Growth rate, 1/s		Glucose concentration of feeding medium, g/L	
Expression	Lysis	Expression	Lysis
0.075	0.3	50	100
0.09	0.3	100	200
0.12	0.3	200	400

4.2.2 Buffers

The following paragraph lists all buffers and respective modifications, which were not purchased ready to use from or were treated other than instructed by the manufacturer.

Table 4-6 Summary of buffer compositions
All buffers used in this work are summarised in alphabetical order.

Buffer	Components/concentrations	pH
5 x Laemmli buffer	300 mM Tris-HCl, 50% (w/v) glycerol, 10% (w/v) sodium dodecyl sulfate (SDS), 5% (v/v) 2-mercaptoethanol, 0.05% (w/v) bromophenol blue	6.8
6 x loading buffer	0.25% (w/v) bromophenol blue, 40% (w/v) sucrose	-
Blocking buffer	5% (w/v) milk powder in phosphate buffered saline (PBS)	7.4
Coating buffer	0.1 M sodium carbonate	9.6
Fairbanks buffer A	25% (v/v) isopropanol, 10% (v/v) acetic acid, 0.05% (w/v) Coomassie blue R	-
Fairbanks buffer B	10% (v/v) isopropanol, 10% (v/v) acetic acid, 0.005% (w/v) Coomassie blue R	-
Fairbanks buffer C	10% (v/v) acetic acid	-
FDH binding buffer	20 mM sodium phosphate, 500 mM NaCl, 40 mM imidazole	7.4 (HCl/NaOH)
FDH elution buffer	20 mM sodium phosphate, 500 mM NaCl, 500 mM imidazole	7.4
Phosphate buffered saline (PBS)	8 g/L NaCl, 0.2 g/L KCl, 1.42 g/L Na_2HPO_4, 0.27 g/L KH_2PO_4	7.4
Reaction buffer	0.1 M sodium phosphate	7.0
Separating gel	0.2% (w/v) SDS, 0.375 M Tris-HCl, 1 ‰ (v/v) TEMED, 1 ‰ (v/v) APS	8.8
Sodium formate buffer	2 M sodium formate in 0.1 M sodium phosphate	7.0
Stacking gel	0.2% (w/v) SDS, 0.125 M Tris-HCl, 2 ‰ (v/v) TEMED, 2 ‰ (v/v) APS	6.8

TAE buffer	1% (w/v) Tris, 1 mM EDTA, 20 mM acetic acid	8.5
TEV binding buffer	20 mM sodium phosphate, 100 mM NaCl, 25 mM imidazole, 10% (v/v) glycerol	8.0
TEV elution buffer	20 mM sodium phosphate, 100 mM NaCl, 500 mM imidazole, 10% (v/v) glycerol	8.0
β-galactosidase buffer	0.1 M potassium phosphate buffer, 0.124 M 2-mercaptoethanol, 1 mM $MgCl_2$	7.0

4.2.3 Special treatments

The following paragraph lists all special treatments and solutions used in this work

Ethyl acetate

The ethyl acetate (EtOAc) used for sample preparation in gas chromatography was dried with 20% (v/v) potassium carbonate for 24 h prior to use and is further referred to as EtOAc dry.

$NADP^+$/NADPH

$NADP^+$ and NADPH were prepared as stock solutions in dH_2O prior to use.

4.3 Molecular cloning

4.3.1 DNA sequencing

DNA sequencing was performed by MWG Eurofins Operon (Ebersberg, Germany).

4.3.2 Plasmid purification

Plasmid purification was performed using the GenElute™ HP Plasmid Miniprep Kit according to the manufacturer's instructions.

4.3.3 Polymerase chain reaction

Amplification of cloning fragments

Cloning fragments were amplified using the Phusion™ High Fidelity DNA polymerase in a three-step polymerase chain reaction (PCR) cycling. The reaction volume was 50 µL with 4 µM primers, all other item concentrations and cycling parameters were chosen according to the manufacturer's instructions.

Colony PCR

After insertion and ligation, cloning experiments were verified using colony PCR. A swab of the colony was suspended in 10 µL dH_2O, heated at 95 °C for 5 min and subsequently used as template in a PCR. Taq DNA polymerase was used in a three-step cycling with 4 µM primers in 25 µL total volume according to the manufacturer's instructions.

4.3.4 Agarose gel electrophoresis

Agarose gel electrophoresis was used to analyse PCR. Samples were diluted with 6x loading buffer. Gels were run in TAE buffer at 120 V. Roti® Stain Safe was used for staining according to the manufacturer's instructions. For identification of fragment sizes the 100 bp-extended standard was run along.

4.3.5 DNA purification

The GenElute™ PCR Clean-Up Kit was used for DNA clean-up after PCR, after DNA restriction or desalination of plasmids. For fragments with less than 100 bp length the GenElute™ Gel Extraction Kit was used.

4.3.6 Site-directed mutagenesis

Site-directed mutations were introduced using the QuickChange Lightnin Site-Directed Mutagenesis Kit according to the manufacturer's instructions.

4.3.7 Restriction and ligation of DNA

10 µL PCR product or 500-900 ng DNA were digested with 10 U restriction enzyme according to the manufacturer's instructions. If the enzyme NotI was used for plasmid digestion 50 U were employed to ensure sufficient digestion of supercoiled DNA. 5 U Antarctic phosphatase were used for dephosphorylation of restriction fragments for 1 h at 37 °C. All fragments were purified using the GenElute™ PCR Clean-Up Kit prior to ligation with 20 U T4 ligase according to the manufacturer's instructions.

4.3.8 Sequence-directed alignment of DNA

Sequence-directed alignment was used for the cloning of short membrane anchor fragments. First, the fragments were accordingly digested using restriction enzymes as described in 4.3.7. Subsequently, the fragments were aligned using the Cold Phusion Cloning Kit according to the manufacturer's instructions.

4.3.9 Preparation of chemically competent cells

$CaCl_2$ chemically competent cells were generated using the Roti®-Transform Kit according to the manufacturer's instructions.

4.3.10 Transformation of chemically competent cells

Chemically competent cells were thawed on ice, then 1 µL of plasmid preparation or 10 µL ligation reaction were added. The cells were incubated for 30 min on ice and then treated with a heat shock at 42 °C, or 37 °C if cells were transformed with the lysis plasmid pGlysivb. 500 µL NZY^+ medium were added and the cells were incubated for 1 h at 37 °C or 35 °C for transformations with pGlysivb, respectively. After incubation the cells were concentrated for 10 min at 1000 rpm in a benchtop centrifuge and spread onto LB plates containing the respective antibiotics for selection.

4.3.11 Preparation of electrocompetent cells

A swab of a cryoculture was used to inoculate 200 mL LB medium. Respective antibiotics for selection were used if cells containing the lysis plasmid pGlysivb were prepared for a co-transformation. The cells were grown at 30 °C, 200 rpm until the optical density at 600 nm (OD_{600}) was 0.4-0.6, then the cells were harvested (4000 x g, 4 °C, 15 min). The supernatant was discarded and the pellet was incubated on ice for 20 min. Then, the cell pellet was washed and subsequently harvested using 200 mL, 100 mL and 8 mL 10% (v/v) glycerol in dH_2O to remove salt from the surrounding media. After the last washing step the pellet was suspended in 1.2 mL 10% (v/v) glycerol and stored in 40 µL aliquots at −80 °C.

4.3.12 Transformations via electroporation

40 µL electrocompetent cells were thawed on ice and 0.5 µL desalinated plasmid or 2 µL desalinated ligation reaction were added, respectively. The cells were transformed in 2 mm cuvettes with 25 µF at 2.5 kV and 200 Ω. Then, 800 µL LB medium (pre warmed to 35 °C) were added and the cells were incubated with gentle shaking for 1 h at 37 °C or 35 °C if cells were transformed or co-transformed containing the pGlysivb plasmid. Then, cells were concentrated (1000 rpm, 10 min) and spread onto LB plates containing the respective antibiotics.

4.4 Microbiological methods

4.4.1 Strain maintenance

Cells were stored as $CaCl_2$ competent or electrocompetent cells at −80 °C for long-term storage (see 4.3.9). For storage of up to 3 weeks, cells were kept on LB agar plates using Plate Count Agar which were prepared according to the manufacturer's instructions. Antibiotics for selection were applied as required.

4.4.2 Precultures of *Escherichia coli* in 4 mL

For plasmid propagation and as first precultures, *E. coli* cells were grown in 4 mL LB medium containing the respective antibiotics either over night at 30 °C, 200 rpm or for 3 d at room temperature (RT), 200 rpm.

4.4.3 Cultivation of *Escherichia coli* in shaking flasks

Protein expression

For the expression of soluble and membrane-bound protein 1000 mL or 500 mL unbaffled shaking flasks were filled with LB-medium containing the respective antibiotics at 20% of the nominal volume. Cells from a preculture grown in 4 mL LB-medium were used at a ratio of 1:200 for inoculation. Cells were grown at 200 rpm, 37 °C. Cells were induced at an OD_{600} of 0.4-0.6 with 1 mM isopropyl β-D-1-thiogalactopyranoside (IPTG). Expression of the KR lasted for 3 h, 37 °C at 250 rpm. Expression of the FDH and the fusion protein of FDH and KR lasted for 18 - 20 h, 20 °C at 250 rpm. Expression of the β-galactosidase lasted for 3 h at 35 °C, 250 rpm. Then, cells were harvested at 4,500 x g, 4 °C for 10 min and stored at −20 °C.

Protein E-mediated lysis

The inoculation procedure as well as type and amount of medium used for protein E-mediated lysis were equivalent to protein expression in shaking flasks. Cells were grown at 35 °C, 250 rpm until the OD_{600} was 0.6-0.8. Then, expression was induced with 1 mM IPTG. Expression lasted for 18 h at 20 °C, 25 °C or 30 °C at 250 rpm. Then, lysis was induced by a temperature shift to 42 °C. If no expression was performed, direct lysis in shaking flasks was induced at an OD_{600} of 0.6 to 0.8. Experiments inn shaking flasks were terminated when no more change in optical density was observed.

Precultures for cultivation in stirred-tank bioreactor

Precultures were grown in 1000 mL or 500 mL unbaffled shaking flasks filled with defined medium containing the respective antibiotics at 20% of the nominal volume. Cells from a

preculture grown in 4 mL LB medium were used at a ratio of 1:200 for inoculation. Cells were incubated over night at 30 °C and 200 rpm. Then, cells were concentrated to 1/10 of the initial volume at 4,500 x g, 4 °C for 10 min and used for inoculation.

4.4.4 Cultivation of *Escherichia coli* in 3.6 L and 7.5 L stirred-tank bioreactors

Cultivation in a 3.6 L stirred-tank bioreactor

Cultivations in a 3.6 L stirred-tank bioreactor were used for combined expression and lysis experiments. The stirred-tank bioreactor was equipped with two Rushton turbine impellers. Cells from precultures in shaking flasks were used to inoculate 1.5 L defined medium to an initial OD_{600} of 0.5. The pH was adjusted to 7.2 using 12.5% (v/v) NH_4OH and 1 M H_3PO_4. The dissolved oxygen (DO) was set to >20% air saturation by adjusting the aeration up to 8 L/min, the stirrer was set to 1,000 rpm. The permittivity was observed using a permittivity biomass probe. Samples were taken successively and analysed for glucose concentration, OD_{600} and cell dry weight concentration (CDW). Glucose consumption was observed using the AccuCheck™ device (see section 4.7.6). During lysis the samples were additionally analysed using colony forming units. In batch processes the temperature was 35 °C during biomass formation and expression. In fed-batch processes the temperature was 35 °C during biomass formation and 20 °C, 25 °C or 30 °C during expression. In batch and fed-batch processes expression was induced using 0.1 mM to 1 mM IPTG. For batch processes the cells were induced at OD_{600} ~1.5 (β-galactosidase) or ~3.0 (KR and FDH). The expression in batch processes lasted 3 h at 35 °C. In fed-batch cultivations, the expression was induced upon glucose depletion and lasted 18 h. Substrate limited feeding was initiated in fed-batch cultivations upon glucose depletion. An exponential growth was adjusted during expression with μ_{set} = 0.075 1/h to μ_{set} = 1.2 1/h using equation 4-1 according to (Jenzsch et al. 2006) and a $Y_{XS.,\mu}$ of 0.4 $g_{CDw}/g_{glucose}$. During lysis in fed-batch processes the growth rate was increased to μ_{set} = 0.3 1/h and samples were taken in intervals of 30 min until glucose accumulation was detected using the AccuCheck™ device. At this point the feeding was stopped. The process was terminated in both batch and fed-batch mode by initiating protein E-mediated lysis using a temperature shift to 42 °C, as described by Langemann et al. 2010. When the decline in OD_{600} and increase in dissolved oxygen indicated lysis, 50 µg/mL ampicillin were added.

$$F(t) = \frac{\mu_{Set} \cdot V_0 \cdot c_{x0}}{Y_{X,S} \cdot c_s} \qquad \textbf{4-1}$$

F(t) feeding rate, L/h

μ_{set} adjusted specific growth rate, 1/h

V_0	initial volume, L
c_{x0}	initial biomass concentration, g/L
$Y_{X,S}$	biomass to substrate yield coefficient, g_{CDW}/g_s; $Y_{XS} = 0.4$ was used for the calculation of feed medium inflow
c_s	concentration of the limiting substrate in the feed medium, g/L

Cultivation in 7.5 L stirred-tank bioreactor

Experiments on the production of cellular envelopes without immobilised enzymes were performed in a 7.5 L stirred-tank bioreactor equipped with three Rushton impellers in 4.0 L total volume. 20 g/L glucose were prepared as the carbon source in defined medium. The medium was inoculated with cells to an initial OD_{600} of ~0.5 and cultivated at 35 °C and 1000 rpm. The pH was adjusted to 7.2 with an aeration of up to 8 L/min to maintain a DO of > 20%. On-line measurements, parameter regulation, sample treatment and fermentation conditions were similar to batch fermentation in the 3.6 L stirred-tank bioreactor. Cells were grown until 50% of the initial glucose were consumed, then the temperature was increased to 42 °C and lysis was induced.

4.4.5 Cross-flow filtration

Cross-flow filtration was used to concentrate and wash cellular envelopes and whole cells prior to lysis. A picture of the experimental setup and a schematic description is given in Figure 4-1.

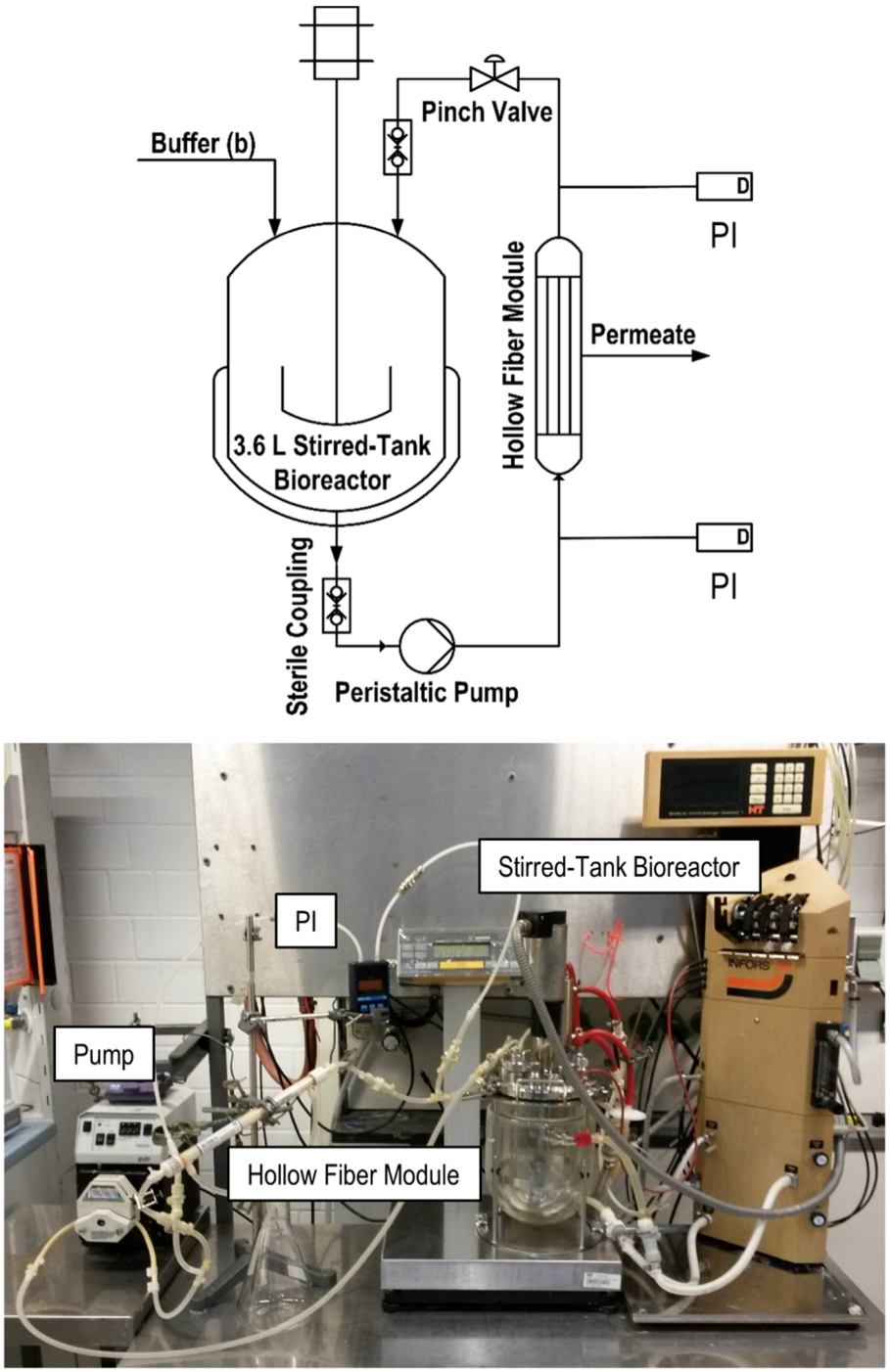

Figure 4-1 Experimental set up for cross-flow filtration in a bypass
The experimental set-up for the concentration of cellular envelopes directly after lysis is displayed. The different equipment is highlighted, with PI being the pressure indicator. For washing of cellular envelopes the stirred-tank bioreactor was replaced by a cooled bottle with respective in- and outlet and buffer was added through inlet (b).

A 0.22 µm hollow fiber module with 4.2 m^2 surface was used with a transmembrane pressure of 1-1.2 bar and a flowrate of 27.5 L/h (determined using water). Directly after lysis, the fermentation broth was concentrated to ~1/3 of the initial amount (see Figure 4-1a)). Between concentration of the cellular envelopes and washing, a freezing step was used in order to

perforate remaining unlysed cells. Subsequently, the concentrated cellular envelopes were harvested and frozen at −20 °C at least over night until further use. Then, the frozen and concentrated cellular envelopes were thawed and washed (see Figure 4-1). Cellular envelopes were washed using the final buffer system applied in enzymatic reactions and about 4-10 mL/min (depending on the viscosity of the fermentation broth) permeate were achieved. The flow was maintained at maximum value throughout the process to avoid sediment formation of the filter surface and the cellular envelopes were cooled during the process by placing the bottle onto ice. Each diafiltration step was performed using reaction buffer for cellular envelopes containing the KR and FDH, or PBS for cellular envelopes containing the β-galactosidase, respectively. 500 mL reaction buffer/PBS were used to wash either 250 mL or 100 mL whole cellular envelopes with either 2-fold or 5-fold volume of cellular envelopes/whole cells, respectively. Contrary to cellular envelopes, whole cells were not concentrated and stored at 4 °C after sampling until work-up using cross-flow filtration. For experiments on the comparison of whole cells and cellular envelopes with immobilised KR and FDH, the whole cells were washed in similar fashion to the cellular envelopes.

4.4.6 Optical density

To adjust samples for membrane preparation and observe cellular growth, the optical density at 600 nm (OD_{600}) was measured. The OD_{600} was determined in 10 mm cuvettes, the samples were adjusted to measure in the linear range of the photometer and analysed in triplicates.

4.4.7 Colony forming units

For the determination of colony forming units (CFU), the samples were diluted using sterile 0.85% (w/v) NaCl. Subsequently the cells were spread onto agar plates and incubated over night at 30 °C. The dilution was adjusted to result in 50-400 counts per plate.

4.4.8 Cell dry weight/ Cellular envelope dry weight

The cell dry weight (CDW) was determined using gravimetry. 2 mL sample were harvested at 13,000 rpm in a benchtop centrifuge for 10 min in pre-weighed reaction tubes. The supernatant was discarded and the cell pellet was dried at 80 °C for at least 24 h. The CDW was then determined from the weight difference between empty and filled reaction tube.

The cellular envelope dry weight was determined using gravimetry of lyophilised samples. The Cellular envelopes were lyophilised without prior centrifugation at −60 °C, 0.1 mbar, subsequently, the samples were weighed out.

4.4.9 Storage of cellular envelopes

For long term storage cellular envelopes were frozen at −20 °C. Comparison of storage properties of cellular envelopes was performed at 4 °C and −20 °C. For the determination of cellular envelope weight-to-count correlation, the cellular envelopes were lyophilised for 24 h at −60 °C and 0.25 mbar.

4.4.10 Calculation of specific growth rates

The growth rate μ is defined as the increase of biomass concentration within time relative to the actual biomass concentration (equation 4-2).

$$\mu \equiv \frac{1}{c_x} \cdot \frac{dc_x}{dt} \qquad \textbf{4-2}$$

μ	specific growth rate, 1/h
c_x	CDW, g/L
t	time, h

During exponential growth and substrate limitation, the growth rate can be described using the kinetic model introduced by Monod (1942). This model assumes constant pH, temperature and oxygen supply and determines growth with one limiting substrate (equation 4-3).

$$\mu = \mu_{max} \cdot \frac{c_S}{K_S + c_S} \qquad \textbf{4-3}$$

μ_{max}	specific growth rate under non-limiting conditions, 1/h
c_S	concentration of the limiting substrate, mol/L
K_S	half saturation constant of the limiting substrate, mol/L

Growth rates were determined using equation 4-2 using half logarithmic display of the CDW in time during exponential growth of the cells. If CDW determination was not possible due to low cell concentrations, the OD_{600} was measured and the corresponding CDW calculated using an OD_{600} to CDW correlation coefficient.

4.5 Protein biochemistry

4.5.1 Protein expression

For a description of protein expression see 4.4.3.

4.5.2 Protein purification using metal affinity chromatography

For protein expression the enzymes were equipped with N- or C-terminal His_6-tag. The cell pellets from protein expression (see 4.4.3) were suspended in 5 mL pre-cooled FDH binding buffer containing 1 mM phenylmethanesulfonyl flouride (PMSF) per g wet pellet weight. Then, the cells were disrupted in a rocker bar mill using 50% (v/v) silica beads (d = 0.25-0.5 mm) at 30 1/s for 3 min. The lysate was cleared at 50,000 x g for 30 min at 4 °C. Subsequently, fast protein liquid chromatography (FPLC) was performed using a 1 mL Ni^{2+}-charged sepharose HisTrap crude column. The column was equilibrated with binding buffer and cleared lysate was applied at a flow of 1 mL/min. Then, the bound protein was eluted from the column using a linear gradient of FDH elution buffer from 0 to 100% over 20 column volumes. Loading and elution of protein was monitored online at 280 nm. Fractions correlating with the elution peak were collected and pooled. Protein concentrations and buffer change was performed with Viva spin columns with 5 kDa molecular weight cut off (MWCO).

The purification of tobacco etch virus (TEV) protease was similar to the procedure described above, however TEV binding buffer and elution buffer were used for FPLC.

For the production of enzymes without an affinity tag, the enzymes were designed with a TEV cleaving site between the His_6-tag and the enzyme. Then, the enzyme was expressed and purified as described above and dialyzed against binding buffer. 0.5 mM ethylenediaminetetraacetic acid (ETDA) and 1 mM dithiothreitol (DTT) were added to the purified enzyme and TEV protease was applied in 1:10 ratio (regarding protein concentration determined with absorption at 280 nm) for 1 h at 37 °C or over night at 4 °C. Then, the cleaved enzyme without His_6-tag was separated using FPLC as the flow-through from protein application to the Ni^{2+}-charged column.

After purification, the protein was stored at 4 °C for short term or −80 °C for long term storage.

4.5.3 Sodium dodecyl sulfate polyacrylamide gelelectrophoresis

Sodium dodecyl sulfate polyacrylamide gel electrophoresis (SDS-PAGE) was performed using discontinuous acrylamide/bis-acrylamide gels with a 5% (w/v) stacking and a 12.5 or 10% (w/v) separating gel. Prior to application the samples were diluted in 5 x Laemmli buffer and denatured for 5 min at 95 °C. Rotiphorese® SDS-PAGE buffer was used for the separation,

which was perfomed at 30 mA per gel. Roti®-Mark standard and Just Blue standard were used for protein size identification. Gels were stained in analogy to (Fairbanks et al. 1968) using coomassie blue R. The gel was heated to boil in the microwave in Fairbanks buffer A and afterwards incubated with shaking at room temperature (RT) for 5 min. The same procedure was repeated at first in Fairbanks-buffer B and subsequently in Fairbanks buffer C. The gels were scanned to preserve the results.

4.5.4 Determination of protein concentration

The protein concentration was determined using the Pierce® bicinchoninic acid (BCA) protein assay kit according to the manufacturer's instructions.

4.5.5 Enzyme linked immunosorbent assay

Enzyme linked immunosorbent assay (ELISA) was applied for the determination of β-galactosidase concentrations. Prior to application, samples were treated with Popculture® detergent according to manufacturer's instructions. Cellular envelopes were additionally disrupted with a 2 mm tip sonicator for 10 min with an amplitude of 126.5 µm. Subsequently the lysate was cleared for 30 min at 50,000 x g, 4 °C. Then, the protein concentration was determined in samples from cellular envelopes and diluted to 20 µg/mL. Liposomes were treated with detergent only and applied without centrifugation using dilutions of 1:20 to 1:60. All samples were diluted in PBS. A standard sandwich ELISA protocol was used according to http://www.abcam.com/ (accessed in November 2014). Sandwich ELISA was performed using 96 well Maxisorp® Plates. The capture antibody was applied at a 1:2,000 dilution in coating buffer for 2 h, at RT. Blocking buffer was used for blocking for 2 h at RT. Then, 100 µL of the diluted samples in PBS were applied in duplicates and incubated for 1.5 h at 37 °C. The detection antibody was applied at a 1:8,000 dilution (in blocking buffer) over night at 4 °C. Then, the secondary antibody-horseraddish peroxidase (HRP) construct was applied (1:20,000 dilution in blocking buffer) for 2 h, at RT. Detection was achieved by application of 3,3',5,5'-tetramethylbenzidine (TMB) Substrate Solution according to manufacturer's instructions. The colorimetric change was detected at 450 nm and a standard with purified β-galactosidase was run along at concentrations of 0.05-1.0 µg/mL for quantification. The samples were diluted to be within range of the calibration.

4.5.6 Cell membrane isolation

For membrane preparation, cells were disrupted using a rocker bar mill. Therefore the cells

were adjusted to OD_{600} 2.0 using PBS. 3 mL PBS containing 1 mM PMSF and 1 mM EDTA were added to a cell pellet from 50 mL culture with an optical density of 2.0 to ensure an equivalent cell concentration for comparability of different expressions. Then the cells were disrupted in a rocker bar mill using 50% (v/v) silica beads (d = 0.25-0.5 mm) at 30 1/s for 5 min. The lysate was cleared at 20,000 x g for 30 min at 4 °C. Then, the membranes were harvested at 125,000 x g for 1 h at 4 °C from 1 mL cleared lysate. The supernatant was discarded and the membrane pellet from 1 mL cleared lysate was washed with 1 mL 0.1 M sodium phosphate buffer (pH 7.0) and again harvested using 125,000 x g for 1 h, 4 °C. The supernatant was again discarded and the membranes suspended in 1 mL fresh 0.1 M sodium phosphate buffer. The membranes were stored at 4 °C until further use.

4.5.7 Liposome preparation

Thin layer rehydration was used to generate liposomes as small unilamellar vesicles (SUV). 2 mg/mL 1-palmitoyl-2-oleoylphosphatidylcholine (POPC) were diluted in ethanol (99.5%) in a 5 mL round bottom flask and a thin layer was formed using a rotary evaporator (50 °C, 50 mbar). The lipid was further dried using a vacuum desiccator for 30 min. Then, 2 mL PBS were added and film rehydration was achieved by rotation for 30 min at RT. The liposomes were cleared from not incorporated lipid by centrifugation for 6 min at 13,000 rpm using a benchtop centrifuge and sonicated using a 2 mm tip sonicator for 3 min with an amplitude of 25.3 µm.

For the incorporation of β-galactosidase onto the liposome surface, the enzyme was expressed with a C-terminal membrane anchor as described in section 4.4.3. PBS containing 1 mM PMSF was added at a ratio of 5 mL per g wet pellet weight. Then, the cells were disrupted using a 2 mm tip sonicator for 10 min with an amplitude of 126.5 µm and the lysate was cleared for 30 min at 50,000 x g. Soluble membranes were removed from the clear supernatant by ultracentrifugation for 1 h, 125,000 x g at 4 °C. Subsequently, the soluble protein was concentrated to 1/5 of the initial volume using 3 kDa MWCO spin columns at 4,500 x g.
The concentrated soluble protein was then added at a ratio of 1:3 and 1:5 to the liposomes. The liposomes were incubated for 1 h at 30 °C at 250 rpm in a thermal shaker and subsequently washed twice by ultracentrifugation at 125,000 x g for 1 h, 4 °C.

4.5.8 Determination of enzyme activity

FDH

For purified FDH, the kinetic parameters K_m and v_{max} were determined for the substrates $NADP^+$ and sodium formate. The assays were based on the detection of NADPH formation at 340 nm using a molar extinction coefficient of 6.22 1/(mM*cm). 96-well plates were used and the total reaction volume was 200 µL (path length 0.59 cm). The enzyme concentration was adjusted to ensure a linear concentration-to-signal ratio (20 µg/mL). The concentration of the analysed substrate was varied between 0.2 to 5-fold K_m, where each concentration was measured at least in triplicates. The second substrate was applied in about 5 to 10-fold K_m to start the reaction. Reactions were measured at 30 °C, where all components were pre-heated before the assay. Reaction buffer was used and the data was detected in intervals of 10 s. The obtained data was used to calculate the initial rate constants at different initial substrate concentrations using equation 4-4. SigmaPlot 8.0 was used for non-linear regression to estimate the kinetic parameters K_m and v_{max}.

$$EA_x = \frac{\Delta c_{Substrate/Product} \cdot V_R}{\Delta t \cdot V_x \cdot c_p} = \frac{\Delta A_\lambda \cdot V_R \cdot 10^3}{\Delta t \cdot \varepsilon_{Substrate/Product} \cdot d \cdot V_x \cdot c_p} \qquad \textbf{4-4}$$

EA_x	specific activity, U/mg
$\Delta c_{Substrate/Product}/\Delta t$	change of substrate or product concentration over time, µM/min
V_R	reaction volume, µL
V_x	sample volume, µL
c_p	protein concentration, mg/L
$\Delta A_\lambda/\Delta t$	change of absorption at specific wavelength over time, 1/min
$\varepsilon_{Substrate/Product}$	molar extinction coefficient of substrate or product at specific wavelength, 1/(mM*cm)
d	path length, cm

For the characterisation of cellular envelopes with membrane-bound FDH, the cellular envelopes were employed in activity assays at unlimited conditions. The assays were performed as described in 200 µL at 30 °C as described above and both substrate concentrations were adjusted to at least 5-fold of the expected K_m with 5 mM $NADP^+$ and 0.5 M sodium formate. The cellular envelope concentration was adjusted using flow cytometry (see section 4.7.4) to ensure measurement of linear initial reaction rates to be 0.75 x 10^9 particles in 200 µL total

volume. The obtained data was used to calculate the activity per defined number of cellular envelopes using equation 4-4. The obtained data was then used to calculate the corresponding amount of enzyme molecules per cellular envelope from equation 4-5.

$$EA_{ce} = \frac{\Delta c_{Substrate/Product} \cdot V_R}{\Delta t \cdot V_x \cdot c_{ce}} = \frac{\Delta A_\lambda \cdot V_R \cdot 10^3}{\Delta t \cdot \varepsilon_{Substrate/Product} \cdot d \cdot V_x \cdot c_{ce}} \quad \textbf{4-5}$$

EA_{ce} Activity of defined number of cellular envelopes, U

c_{ce} concentration of cellular envelopes, 1/L

$$N_{Enzymes} = \frac{EA_{ce}}{EA_{ref}} \quad \textbf{4-6}$$

$N_{Enzymes}$ number of enzymes per cellular envelope, -

EA_{ref} reference activity of the free enzyme, U

For the characterisation of membrane preparations regarding enzyme activity, the membrane suspension (see section 4.5.6) or the corresponding amount of soluble protein after membrane removal in ultracentrifugation were analysed in activity assays at RT and unlimited conditions. The total reaction volume was 200 µL and 5 mM $NADP^+$ and 0.5 M sodium formate were used. The assays were measured in triplicates at 340 nm as described above. The amount of membrane suspension or soluble protein was chosen for a linear signal-to-concentration ratio. The detected slope was used to calculate the corresponding activity according to equation 4-4 in the membrane suspension or corresponding amount of soluble protein, respectively. The resulting activities were compared as relative amounts of the total activity using equation 4-7

$$EA_{rel.} = \frac{EA_{membrane}}{(EA_{membrane} + EA_{soluble})} \cdot 100\% \quad \textbf{4-7}$$

$EA_{rel.}$ relative amount of activity in the membrane fraction, %

KR

For the characterisation of cellular envelopes with membrane-bound KR, the cellular envelopes were employed in activity assays at unlimited conditions. NADPH and ECAA were chosen as substrates. The assays were performed in 200 µL at 30 °C using 20 mM ECAA and 10 mM NADPH to ensure unlimited conditions. The cellular envelope concentration was adjusted using flow cytometry (see section 4.7.4) to ensure measurement of linear initial reaction rates. The assay was based on the amount of produced (*S*)-ECHB, which was detected using gas chromatography (see section 4.7.2). Reactions were initiated simultaneously and then

terminated by addition of ethyl acetate (EtOAc) and subsequent extraction after different time intervals. Samples were prepared for gas chromatographic analysis as described in section 4.7.1. Each sample was measured in triplicates. The obtained amount of product was detected and used to calculate the corresponding activity of the cellular envelopes using equation 4-4. The obtained data was then used to calculate the corresponding amount of enzyme molecules per cellular envelope from equation 4-6 using a reference activity from the literature (Hölsch et al. 2008; Hölsch & Weuster-Botz 2011).

For the characterisation of membrane preparations (see section 4.5.6) with immobilised KR, the membranes were purified and used in activity assays similar to the biotransformations described in section 4.5.8. The total reaction volume was 300 µL with 5 mM NADPH and 20 mM ECAA containing 60 µL membrane suspension or a corresponding amount of a soluble protein sample after removal of the membranes. The batches were incubated at 30 °C for 5 h and then terminated, prepared as described in section 4.7.1 and analysed using gas chromatography. The resulting amounts of obtained (*S*)-ECHB were compared and used to calculate the relative activity of the membrane preparation according to equation 4-8, where the amount of product was equivalent to the activity.

$$EA_{KR} = \frac{\Delta n_{product}}{\Delta t} \qquad \textbf{4-8}$$

EA_{KR}	activity of KR, µmol/min
$\Delta n_{product}$	change in product amounts, µmol
Δt	change in time, min

β-Galactosidase

The maximum initial reaction rate v_{max} of the purified β-galactosidase was determined for the substrate *o*NPG at unlimited conditions. The assay was based on the hydrolysis of *o*NPG to *o*NP, which can be detected photometrically at 436 nm. 1 mL cuvettes with 1 cm path length were used and 50 µL of diluted sample were analysed in a total reaction volume of 1 mL. The enzyme concentration was adjusted to ensure a linear concentration-to-signal ratio. The concentration of the analysed substrate was 1 mM, which is the 10-fold K_m of *o*NPG given in (Lo et al. 2010) to ensure unlimited conditions. Reactions were measured at RT, where all components were adjusted to RT before the assay. β-Galactosidase buffer was used and the data was collected in intervals of 30 s. The obtained data was used to calculate the maximum initial reaction rate v_{max} using a molar extinction coefficient of 3.5 1/(mM*cm) and equation 4-4. For the characterisation of cellular envelopes with membrane-bound β-galactosidase, the cellular

envelopes were employed in activity assays at unlimited conditions similar to the purified enzyme. The cellular envelope concentration was adjusted using flow cytometry (see 4.7.4) to 10^8 1/mL to ensure measurement of linear initial reaction rates. All samples were analysed at least in triplicates. The obtained data was used to calculate the activity per defined number of cellular envelopes using equation 4-4. Then, the reference activity measured using purified enzyme was used to calculate the corresponding amount of enzyme molecules per cellular envelope from equation 4-6.

4.5.9 Determination of enzyme stability

FDH

The enzyme stability of purified and membrane-bound FDH was determined by analysing enzyme activity after exposure to ECAA. Therefore, the purified enzyme or the cellular envelopes containing the immobilised enzymes were incubated at 30 °C, 250 rpm in reaction buffer containing different amounts of ECAA. Assays containing no additives were treated along for comparison. Samples were taken at different time intervals and analysed for enzyme activity. Activity assays were performed at unlimited conditions using at least 5-fold of the expected K_m of both $NADP^+$ and sodium formate, respectively. 200 µL total volume with 0.5 M sodium formate and 5 mM $NADP^+$ were used and samples were analysed in a 96-well plate at 340 nm, 30 °C in intervals of 10 s. The concentration of the purified protein or cellular envelopes was chosen to ensure a linear concentration to signal ratio of the produced NADPH. The slope was then used to calculate the activity EA_x using equation 4-4. The inactivation constant k_i and the half life $t_{1/2}$ were then obtained by linear regression from a natural logarithmic display of the activity EA_x in the course of time according to equation 3-5 and 3-6.

4.6 Biotransformations with whole cells and cellular envelopes

Asymmetric synthesis of (*S*)-ECHB from ECAA was conducted with whole cells and cellular envelopes containing the afore-immobilised enzymes FDH and KR. A schematic description of the reaction is given in Figure 3-6 and Figure 3-5.

4.6.1 Biotransformations in monophasic systems

Multi-enzyme reactions in monophase were conducted in 0.1 M sodium phosphate buffer (pH 7.0) at 30 °C. Reactions were conducted in volumes from 0.2 to 1.12 mL. Stirred 4 mL glass

reaction vessels were employed for volumes of ≥ 500 µL at 500 rpm as described in Bräutigam (2008), reactions in < 500 µL were performed in 1.5 mL reaction tubes at 250 rpm in a thermal shaker. The concentration of cellular envelopes and whole cells was adjusted using flow cytometry (see 4.7.4) to the same particle concentrations. The concentrations of ECAA, $NADP^+$ and sodium formate were varied. Samples were either taken by terminating the reaction of a whole preparation or by taking 200 µL samples at different time intervals and prepared for analysis in gas chromatography (see 4.7.2).

4.6.2 Biotransformations in biphasic systems

Biotransformations in biphasic systems were performed using the ionic liquid (IL) [HMPL][NFT] at 20% (v/v). The total volume was 1.4 mL and reactions were conducted in 4 mL stirred glass vessels (according to (Bräutigam 2008)) at 30 °C and 500 rpm. The aqueous phase contained whole cells or cellular envelopes as catalysts, $NADP^+$ and sodium formate in 0.1 M sodium phosphate buffer (pH 7.0). All concentrations were adjusted using the volume of the aqueous phase. The IL phase contained ECAA, and the ECAA concentration was adjusted to the volume of the IL only. The concentration of the substrates, cofactors and catalysts was varied. Samples were taken in different time intervals by terminating a whole preparation as described in 4.7.1. The concentration of product and substrates in the ionic liquid phase were determined using equation 4-9. The total amount of substrate or product in both phases was determined using equation 4-10.

$$c_{i,IL} = c_{i,buffer} \cdot 10^{logD_{IL/buffer}} \quad \textbf{4-9}$$

$c_{i,IL}$ concentration of *i* in the ionic liquid phase, mol/L

$c_{i,buffer}$ concentration of *i* in the reaction buffer, mol/L

$logD_{IL/buffer}$ decadic logarithm of the distribution coefficient (determined using equation 3-8), -

$$c_{i,total} = c_{i,IL} + c_{i,buffer} \quad \textbf{4-10}$$

$c_{i,total}$ total concentration of *i*, mol/L

4.6.3 Determination of substrate or cofactor degradation

ECAA/(*S*)-ECHB

The stability of ECAA and (*S*)-ECHB in the reaction buffer system was determined at 30 °C. The α-haloketones were diluted in 0.1 M sodium phosphate buffer (pH 7.0) containing 0.5 M sodium formate to a final concentration of 20 mM and 40 mM, respectively. 4 mL glass

reaction vessels were used and the preparations were stirred at 500 rpm. 200 µL samples were taken at different time intervals, prepared as described in 4.7.1 and analysed using gas chromatography (see 4.7.2). The degradation of ECAA and (S)-ECHB is assumed to be a hydrolytic process, therefore a first order reaction was assumed. The logarithmic display of the decrease in ECAA/(*S*)-ECHB concentration against time was used to calculate the decay constant and the corresponding half life according to equation 3-5 and 3-6.

NADPH

The stability of NADPH was determined in 0.1 M sodium phosphate buffer in 200 µL total volume in 96-well plates. 0.5 mM and 0.25 mM NADPH were incubated at 30 °C and the absorption at 340 nm was measured. A first order reaction was assumed for the degradation of NADPH. Therefore, the natural logarithmic display of the absorption at different time intervals was used to calculate the corresponding decay constant according to equation 3-5 and 3-6.

4.7 Analytical methods

4.7.1 Sample preparation for gas chromatography

For analysis by gas chromatography, samples were extracted using dry EtOAc at RT. Samples were either taken as 200 µL volume from the reaction batch or as a whole preparation. If a whole batch was terminated, the catalyst was first removed by centrifugation at 13,000 rpm for 3 min in a benchtop centrifuge. Then the cleared supernatant was extracted 1:1 with dry EtOAc containing 36 mM acetophenone as internal standard. If 200 µL were sampled from the reaction, samples were extracted directly by adding 1:1 dry EtOAc with internal standard. All samples were extracted in a rocker bar mill for 10 min at 30 1/s. Subsequently, the samples were spun down in a benchtop centrifuge for 2 min at 13,000 rpm and the organic phase of the extraction was diluted 1:5 in dry EtOAc.

4.7.2 Gas chromatography

Gas chromatographic spectra were recorded with a CP-3800 gas chromatograph with a 1079 Programmable Temperature Vaporizing (PTV) injector. Samples were separated on a Lipodex E capillary column (25 m x 0.25 mm inner diameter, covered with 0.25 µm liquid layer). 5 µL sample were injected with an inlet-split of 50. Helium was used as carrier gas. Detector and injector were adjusted to 250 °C. A flame ionization detector (FID) was used with hydrogen as fuel and room air as the oxidant. The column flow was 4 mL/min. Standard curves of ECAA

and the corresponding alcohols were used for the quantification along with an internal standard of 7.2 mM acetophenone. If two-phase reactions with IL were analysed, the distribution coefficient of substrate or product was used to calculate the corresponding total amount of substrate or product using equations 4-9 and 4-10. The retention times were: 2.8 min acetophenone, 5.0 min ECAA, 6.8 min (*R*)-ECHB and 7.3 min (*S*)-ECHB.

4.7.3 UV-Vis spectroscopy

Kinetic and absorbance UV-Vis measurements were recorded using the Infinite M200, Multiscan and Genesys 20 spectrometers.

4.7.4 Flow cytometry

Flow cytometry was performed using the CyFlow® SL. It was used for the analysis of protein E-mediated lysis as well as the adjustment of particle concentrations for biotransformations and activity assays. Bidistilled water, filtered through a 0.22 µm filter was used as carrier fluid. Samples were diluted prior to analysis in 0.85% (w/v) NaCl (filtered through a 0.22 µm filter) and were measured at a flow of 0.8-1.2 µL/s with 800-1200 counts/s, the dilutions were chosen accordingly. For visualization of the different sub-populations the samples were stained with 0.75 µM bis-(1,3-dibarbituric acid) trimethine oxonol ($DiBAC_{[4]}(3)$) and 3 µM *N*-(3-triethylammoniumpropyl)-4-(4-(4-(diethylamino)phenyl)butadienyl)pyridinium dibromide (RH414) prior to analysis. The determination of populations was performed according to Haidinger et al. (2003) and Langemann et al. (2010). Notably, positions of the polygons had to be adjusted specifically for each measurement. The parameter settings of the flow cytometer are listed in Table 4-7.

Table 4-7 Parameter settings in flow cytometry
The signal amplification (gain) and upper- and lower-level threshold values are summarised. The detection channels for fluorescene 3 and 4 were not used.

Parameter	Gain, -	Lower level, -	Upper level, -
Forward Scatter	200	30	999.9
Side Scatter*	300	10	999.9
Fluorescene 1	500	10	999.9
Fluorescene 2	560	10	999.9

*) the side scatter was used as the trigger factor

The particle concentration from populations with positive RH414 staining was used to adjust particle concentrations of whole cells and cellular envelopes for activity assays, SDS-PAGE, biotransformations and ELISA. In screening experiments in shaking flasks, flow cytometry was used for the quantification of protein E-mediated lysis according to equation 4-11.

$$Y_{Lysis} = \frac{c_{cellular\ envelopes}}{c_{total\ particles}} \quad \textbf{4-11}$$

Y_{Lysis}	Lysis yield, %
$c_{cellular\ envelopes}$	concentration of cellular envelopes, positive population in 2-parameter dot plot, count/mL
$c_{total\ particles}$	total particle concentration, positive population in RH414 staining, count/mL

4.7.5 Densitometry

Densitometry was used to analyse scans from SDS-PAGE for the determination of protein concentrations, amounts of immobilised membrane protein and the amounts of residual host cell protein from protein purification. Purified protein or the Perfect Protein marker were used as internal standard for the quantification. Scans were analysed using the ImageJ Software .

4.7.6 Determination of glucose concentration

Determination of glucose concentration using the AccuCheck™ device

During experiments in stirred-tank bioreactors the glucose concentration in the samples was analysed using AccuCheck™ quick tests. 10 µL sample were applied to the testing strip. If the glucose concentration exceeded the detection range, the samples were diluted accordingly in 0.85 (w/v) NaCl.

Determination of glucose concentration using an enzymatic kit

The glucose concentration was determined using the D-Glucose Assay Kit assay in a modified protocol. The assay is based on the photometric detection of NADPH at 340 nm, which is produced in stoichiometric amounts relative to the glucose concentration. All solutions were prepared according to the manufacturer's instructions. Samples from cultivations were harvested at 50,000 x g for 30 min at 4 °C. The cleared supernatant was used for analysis in 96 multiwell plates. The total volume was 200 µL. Solution 1 was used undiluted, solution 2 was diluted 1:20 in solution 1 prior to use. 80 µL solution1, 80 µL dH_2O and 20 µL sample were mixed in each well and incubated for 3 min at RT. Then, the initial absorption was determined. Subsequently, 20 µL solution 2 were added and the reactions were incubated for 15 min at RT. Then, the final absorption was measured. The difference between initial and final absorption was calculated. An internal standard of glucose from 0.025 g/L to 1.125 g/L was run along for quantification, the samples were diluted appropriately to be within range of the standard.

4.7.7 Determination of acetate concentration

The acetate concentration was determined using the Acetic Acid Assay Kit assay in a modified protocol. The assay is based on the photometric detection of NADH at 340 nm. The assay comprised subsequent reactions, in which the cofactor is produced in amounts proportional to the acetate concentration. All solutions were prepared according to the manufacturer's instructions. Samples from cultivations were harvested at 50.000 x g for 30 min at 4 °C. The cleared supernatant was used for analysis in 96 multiwell plates. The total volume was 200 µL. Solutions 1 and 2 were used undiluted, solution 3 was diluted 1:33.3 and solution 4 was diluted 1:16.7 in dH_2O prior to application, respectively. 70 µL solution 1, 12 µL solution 2, 20 µL sample and 58 µL dH_2O were mixed in each well and the initial absorption was determined. 20 µL diluted solution 3 were added, the reactions were incubated for 3 min at RT and the absorption was determined a second time. Finally, 20 µL diluted solution 4 were added, the reactions were incubated at RT for 15 min and the final absorption value was measured. The resulting absorption was converted to the NADH concentration according to manufacturer's instructions. An internal standard from 0.04 g/L to 0.15 g/L acetate was run along for quantification. The samples were diluted appropriately to be within range of the internal standard.

.

5 Membrane anchoring of a multi-enzyme system

The first step in the development of cellular envelopes with membrane-bound enzymes was the membrane anchoring of these enzymes to the cytosolic membrane. The following chapter describes the results on the membrane anchoring of the formate dehydrogenase (FDH) from *M. vaccae* N10, 3-ketoacyl-[acyl-carrier-protein]-reductase (KR) from *Synechococcus* PCC7942 and a fusion protein of FDH and KR (FDH-SG-KR). To compare a wide range of anchoring options of the enzymes, different possibilities were chosen, which are summarised in Table 5-1.

Table 5-1 Membrane anchors used in this research project

Anchor	N-/C-terminal	Reference	Origin	Length of anchor, aa
Cyt b_5	C	(George et al. 1989)	Cytochrome b_5 from rabbit liver	43
GlpF	N	(Neophytou et al. 2007)	Glycerol-conducting channel protein (GlpF) from *E. coli* K12	952
UBC6	C	(Kutay et al. 1993)	C-Terminal hydrophobic sequence of the Ubiquitin-conjugating enzyme 6 from *S. cerevisiae*	17
E'	N	(Szostak et al. 1996)	N-terminal sequence of lysis protein E from Phage PhiX174	54
L'	C	(Szostak et al. 1996)	C-Terminal hydrophobic sequence of lysis protein from phage MS2	55
E'/L'	N/C	(Szostak et al. 1996)	Combination of E' and L'	Sum of E' and L'

C-terminal and N-terminal anchoring were analysed and compared. C-terminal anchoring was independent from the secretory pathway and analysed using the Cyt b_5 and L'-anchors, which are 43 amino acids (aa) and 55 aa long, respectively. These were compared with the 17 aa short C-terminal UBC6-anchoring motif. N-terminal anchoring was analysed with the E' sequence, which is 54 aa short and also independent from the secretory pathway. As an example for N-terminal anchoring via the secretory path, the GlpF protein was chosen, which is described to prevent inclusion body formation during membrane immobilisation. Except for the UBC6 membrane anchor, all other anchoring motifs have already been demonstrated for the attachment of heterologous proteins to the cytoplasmic membrane of *E. coli* (see section 3.4.2 and 3.5.2).

5.1 Anchoring of the formate dehydrogenase

All experiments featured the modified FDH from *M. vaccae* N10, described in section 3.2.4, which contains a total of seven mutations for increased $NADP^+$ preference, stability towards α-haloketones and stability towards proteolytic degradation at the C-terminus. The FDH was fused to the membrane anchors described in Table 5-1, and it was possible to obtain FDH fusion protein constructs for all membrane anchor motifs. All experiments on membrane immobilisation were performed using *E. coli* BL21 and shaking flasks for better comparability. The FDH-constructs were expressed using vectors of the pET vector series for high expression levels at 20 °C for 18 h at which the FDH expresses in high amounts (Hölsch et. al. 2013). A schematic description and summary of all FDH fusion proteins produced is given in Figure 5-1.

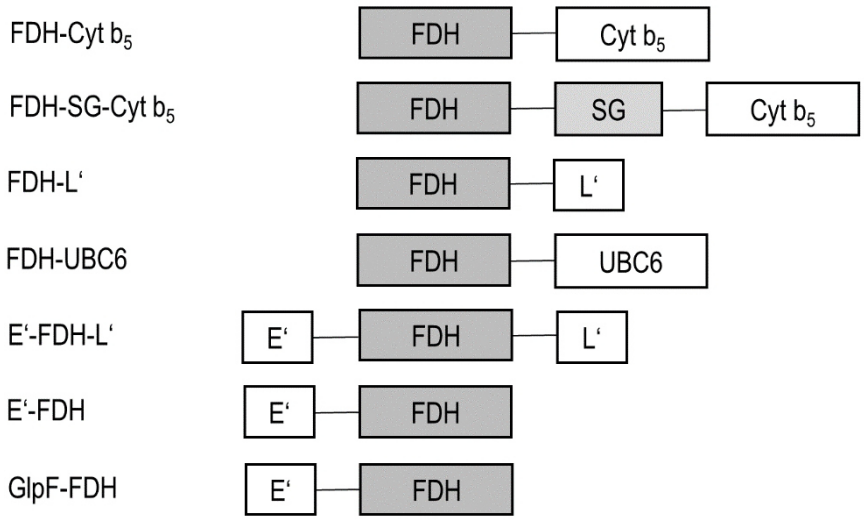

Figure 5-1 Schematic display of different membrane anchors cloned to the FDH
All different membrane anchors analysed for FDH immobilisation are summarised schematically.

After expression, the membranes were purified and analysed for enzyme activity using photometric assays. Data from literature indicate that membrane insertion can be incomplete and non-immobilised proteins can be found in the cytoplasm. Therefore, the soluble protein after removal of the membranes was collected to characterise membrane insertion, and activity from not inserted enzymes were compared in activity assays to the cellular membranes. In this context non-immobilised enzymes in the cytoplasm are further referred to as “soluble protein”. All FDH membrane anchor constructs were expressed and compared for membrane insertion. The results are summarised in Table 5-2.

Table 5-2 Summary of results of FDH membrane anchoring
The anchor motif chosen for further work is highlighted.

Anchor	N-/C-terminal	Result
Cyt b_5	C	Inclusion body formation only
Linker-Cyt b_5	C	Active FDH in soluble protein only
GlpF	N	No activity detected in membrane
UBC6	C	Active FDH detected in membrane; about 2.7-fold more activity in membrane than in soluble protein; chosen for further work
E'	N	No activity detected in membrane
L'	C	Activity detected in membrane; 33-fold higher activity in soluble protein
E'/L'	N/C	Hardly detectable activity in membrane and in soluble protein

Analysis and comparison of all anchoring motifs showed that anchoring using the C-terminal Cyt b_5 anchor resulted in inclusion body formation only, visible in SDS-PAGE (data not shown). Moreover, no active membrane-bound enzyme was detected. Insertion of linker sequences can prevent inclusion body formation (Sührer et al. 2014). Thus, a serine-glycine linker (sequence: SGSSSSGSSSSGS) sequence was inserted between the FDH and the Cyt b_5 anchor. However, the FDH-SG-Cyt b_5 could only be detected in the soluble protein and not in the membrane fraction after expression. Similarly, membrane anchoring with the N-terminal E' and GlpF membrane anchors resulted in non-immobilised protein only. Anchoring with combined N-and C-terminal anchors E' and L' resulted in low expression levels with hardly detectable activity in both membrane fraction and soluble protein. Notably, expression levels of the different FDH constructs were generally low and detection via SDS-PAGE was not possible. Due to a lack of commercially available antibodies, all comparisons were based on the activity detected in membranes from a defined amount of cells and no quantification and no distinct determination of specific activity was possible from membrane preparations.

Contrary to this, C-terminal anchoring with the L' and UBC6 anchors was successful. The FDH-L' showed activity in both soluble protein and cytoplasmic membranes. However, the observed activities were about 33-fold higher in the soluble protein and the activities within the membrane fraction were again hardly detectable. In expression of the FDH-UBC6 fusion protein 2.7-fold higher activities were detected in the membrane, which indicated sufficient

insertion for cellular envelope production. Since both, the C-terminal UBC6 and the L' anchor, offered FDH immobilisation, enzyme activities were compared in order to identify the best anchoring for the FDH. All comparisons were performed regarding the initial reaction rates of membrane with bound FDH gained under the same expression conditions. Thereby, 17-fold higher activity was detected in the membranes obtained from FDH-UBC6. The FDH-UBC6 was therefore chosen for further work.

5.2 Anchoring of the 3-ketoacyl-[acyl-carrier-protein]-reductase

This section describes different approaches on the membrane anchoring of the KR. Similarly to the FDH, the KR was cloned to the anchoring motifs summarised in Table 5-1 and it was possible to produce fusion constructs with the C-terminal membrane anchors Cyt b_b and UBC6 as well as the N-terminal GlpF anchor. The KR was expressed using vectors for high expression levels of the pET series at 37 °C for 3 h, which is the optimal expression condition for the KR. The KR membrane anchor fusion proteins were expressed and the membranes were purified and analysed for membrane insertion of the KR. Notably, the native KR associates to membranes, without containing a membrane anchor (Hölsch 2009). To confirm that membrane-associated activity was due to the membrane anchor and not only due to the KR-own membrane association, all results were compared to respective expressions of the native KR. The results on all membrane anchors analysed for the KR are summarised in Table 5-3.

Table 5-3 Summary results of KR membrane anchoring
The anchor motif chosen for further work is highlighted.

Anchor	N-/C-Terminal	Result
Cyt b_5	C	About 39% immobilised, chosen for further work
GlpF	N	Active KR in soluble protein only
UBC6	C	Active KR in soluble protein only

Membrane immobilisation with both the short C-terminal UBC6 anchor and the N-terminal GlpF anchor was not possible and active KR was only detected in the soluble protein. Contrary to this, membrane insertion with the C-terminal Cyt b_5 anchor was possible. Expression levels were sufficient for detection of the KR in SDS-PAGE, and densitometry was performed to quantify the amount of membrane-bound KR-Cyt b_5 and wild type KR, respectively.

Exemplary results are shown in Figure 5-2.

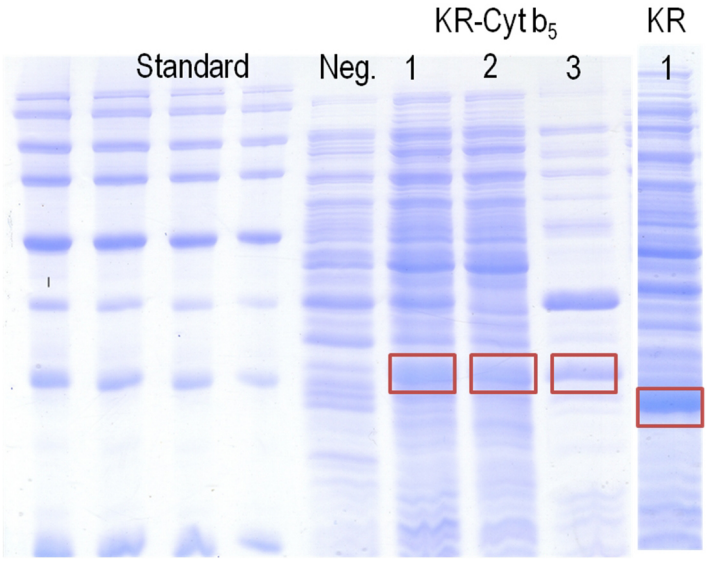

Figure 5-2 Exemplary densitometric analysis of KR-Cyt b5 expression.
The SDS-PAGE shows a standard using Perfect Protein marker, a negative control (neg.), and the total soluble protein (1) of KR- Cyt b_5 and KR, respectively. For KR-Cyt b_5 the soluble protein after ultracentrifugation (2), and the membrane fraction (3) of KR-Cyt b_5 are displayed. The bands for KR-Cyt b_5 and KR are highlighted. Notably, the native KR has no membrane anchor and is consequently smaller. The amount of immobilised enzyme was calculated as a ration of membrane-bound enzyme to the total enzyme in the soluble protein prior to membrane preparation.

The overall analysis of several expressions and multiple SDS-PAGE analysis showed that 38 ± 8% of the total KR-Cyt b_5 molecules could be immobilised in the membrane. Contrarily, 11 ± 4% of the native KR was immobilised. Thus, about 27% more enzyme molecules were immobilised if the membrane anchor Cyt b_5 was used. Consequently, immobilisation using the membrane anchor was more effective than the natural membrane association of the KR, and the KR-Cyt b_5 was chosen for further work.

The addition of the membrane anchor and the attachment to the membrane may have effects of the enzyme properties. So, membranes with immobilised KR-Cyt b_5 and native KR were analysed in asymmetric reductions of ECAA. Membrane preparations containing each were compared to the soluble protein after membrane removal. The results are summarised in Table 5-4.

Table 5-4 Summary of activity assays with KR-Cyt b_5 and native KR
Asymmetric reductions of ECAA were conducted in 300 mL total volume with 5 mM NADPH and 20 mM ECAA for 5 h at 30 °C. 60 µL membrane preparation or the respective amount of soluble protein after membrane removal were used. The membrane preparation and soluble protein were gained from 50 mL cell culture adjusted to OD_{600} = 2.0.

KR	Yield (*S*)-ECHB, %	ee (*S*)-ECHB, %
Cyt b_5 membrane-bound	3.7 ± 1.6	99 ± 1
Cyt b_5 soluble protein	6.0 ± 3.0	73 ± 18
Native membrane-bound	2.8 ± 1.0	96 ± 5
Native soluble protein	21 ± 4.3	99 ± 1

Alterations such as the addition of the membrane anchor and the immobilisation may have effects on the stereo-selectivity of the enzyme. The ee_s was compared for the asymmetric reductions of ECAA to (*S*)-ECHB (see Table 5-4). Native, membrane-attached KR had an ee_s of 96 ± 5% and membrane-immobilised KR-Cyt b_5 had an ee_s of 99 ± 1%. Contrarily, soluble native KR had an ee_s of 99 ± 1% and soluble KR-Cyt b_5 had an ee_s of 73±18%. Notably, the ratio in obtained yield of (*S*)-ECHB from soluble and membrane-bound enzyme coincide with the amounts of immobilised enzyme according to densitometry. As summarised in Table 5-4, membrane-bound KR-Cyt b_5 produced about 1/3 and membrane-bound native KR about 1/10 of the total yield, respectively, which indicated that the kinetic constants are not severely altered due to the immobilisation.

The specific activity of membrane-anchored KR-Cyt b_5 could not be determined, as the isolated hydrophobic membranes create a suspension in aqueous buffers, due to which the amount of membrane particles varies within each reaction batch. Flow cytometry was insufficient for quantification due to a high variability in particle size distribution. For the KR no commercially available antibodies exist, so quantification via immunological detection in ELISA or Western Blot was not possible.

5.3 Coupled enzyme catalysis with membrane-bound enzymes

For the application in cellular envelope production a working multi-enzyme system was required. The KR-Cyt b_5 was therefore co-expressed with the FDH-UBC6 for a first proof of principle. As high levels of protein expression were required, a high copy number vector was designed, which comprised two promotor binding sites from pCOLADuet and the ori and

backbone of the pET vector series, the pET28aDuet (see appendix Figure 12-1). Both enzymes were cloned into the vector. The FDH-UBC6 was inserted behind the first promotor binding site and the KR-Cyt b_5 behind the second one. Subsequently, both enzymes were co-expressed using the expression conditions used for the FDH (1 mM IPTG, 18 h, 20 °C). The soluble protein and membrane preparations were used for asymmetric reductions of ECAA. The results are summarised in Figure 5-3.

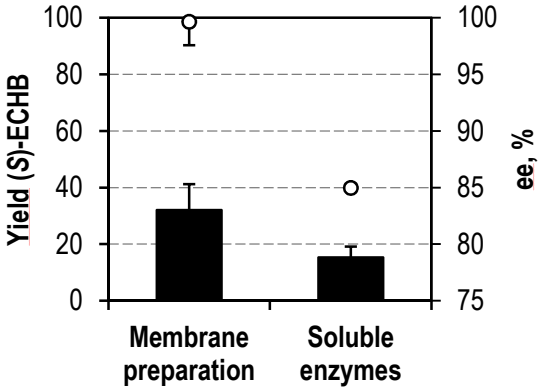

Figure 5-3 Results for asymmetric reduction of ECAA with membrane preparations containing KR-Cyt b_5
The yield in (*S*)-ECHB (black) and ee_s (white) are displayed for the membrane preparation and soluble enzyme. Reactions were performed in 300 µL at 30 °C with 15 mM ECAA, 5 mM $NADP^+$ and 0.5 M sodium formate for 24 h. 60 µL membrane preparation or volume of soluble protein with membrane anchor were used. The membranes were obtained from 50 mL cells with an OD_{600} of 2.0.

(*S*)-ECHB was detected for reaction with both soluble protein and membrane preparation, which showed that both enzymes could be co-expressed and co-immobilised successfully. The ee_s of reactions with the membrane-bound enzymes was 99 ±2%, and the ee_s for reactions with the soluble protein was 85 ± 0.3%, respectively. This coincided with experiments on the KR-Cyt b_5, where the ee_s of the soluble enzyme was also reduced. The membrane preparation yielded about 2-fold higher amounts of (*S*)-ECHB. It was not possible to quantify the FDH-UBC6 or KR-Cyt b_5 using SDS-PAGE, as the protein bands could not be distinguished from the host cell protein. Summarising the results, it was possible to perform a co-immobilisation of a working multi-enzyme system, thus a first proof of principle was successful.

5.4 Anchoring of a formate dehydrogenase-3-ketoreductase fusion protein

The space on the cytosolic membrane might be a limiting factor for the immobilisation of large quantities of enzymes. Fusion proteins comprise different catalytic properties within one polypeptide chain. By immobilising a fusion protein, it would be possible to immobilise two

catalytic moieties using just one anchor. So, additionally to the separate enzymes, the FDH-SG-KR fusion protein was analysed for membrane immobilisation (see section 3.2.5). The FDH-SG-KR comprised the mutant FDH similar to chapter 5.1 and the wild type KR connected by a serine-glycine-linker sequence (SGSSSSGSSSSGS).

The FDH-SG-KR was cloned to the different anchoring motifs described in Table 5-1. It was possible to obtain constructs for the C-terminal Cyt b_5 and UBC6 as well as the N-terminal GlpF membrane anchors. The FDH-SG-KR expresses best in low to medium copy vectors (Sührer et al. 2014), therefore the pCOLADuet™ vector was chosen for expression at 20 °C for 18 h. The different fusion protein membrane anchor constructs were expressed and analysed for membrane insertion, the results are summarised in Table 5-5.

Table 5-5 Summary of FDH-SG-KR membrane anchoring

Anchor	N-/C-Terminal	FDH-SG-KR
Cyt b_5	C	Inclusion body formation only
Linker-Cyt b_5	C	Inclusion body formation only
GlpF	N	Membrane-bound enzyme, only KR subunit active
UBC6	C	Membrane-bound enzyme, only FDH subunit active

It was not possible to immobilise the FDH-SG-KR to the cytoplasmic membrane with both subunits catalytically active. Membrane anchoring with the C-terminal Cyt b_5 caused inclusion body formation only. Insertion of a serine-glycine linker sequence similar to the FDH (see chapter 5.1) to prevent inclusion body formation was not successful. Anchoring with the C-terminal UBC6 and the N-terminal GlpF anchor resulted in membrane-bound fusion protein. However, in N-terminal anchoring the FDH subunit and in C-terminal anchoring the KR subunit each lost their catalytic activity. Since both N- and C-terminal membrane anchoring was not promising, immobilisation of the FDH-SG-KR fusion protein was not further pursued.

5.5 Discussion

Different membrane anchors for N-and C-terminal membrane anchoring with and without involvement of the secretory path were analysed for the FDH, the KR and the FDH-SG-KR fusion protein.

Immobilisation of the FDH was attempted with different N-and C-terminal anchors. Notably, immobilisation with N-terminal membrane anchors was not successful. The N-terminal addition of tags or groups is described unfavourable for the FDH (Hölsch & Weuster-Botz 2010a), so the results are in good agreement with data from the literature. C-terminal anchoring with the L' and the UBC6 anchors resulted in membrane-bound and catalytically active FDH. In comparison, immobilisation with the UBC6 anchor was preferable, as it enabled a 17-fold higher membrane-bound activity, and was consequently chosen for further work. Even though C-terminal modifications do not render the FDH inactive, such alterations are nevertheless described to have effects on the enzyme activity (Sührer et al. 2014). The L' anchor is 54 aa and the UBC6 anchor is 17 aa long. Thus, the shorter anchoring motif was possibly advantageous, since it had fewer effects on the enzyme properties. This work describes the first immobilisation of a heterologous enzyme using the short C-terminal UBC6 anchoring motif to the cytoplasmic membrane of *E. coli*. A comparison with existing data are consequently not possible.

Membrane immobilisation of the KR was attempted using N- and C-terminal anchors. In contrast to the N-terminal GlpF and the short C-terminal UBC6 anchor, the C-terminal Cyt b_5 anchor provided membrane anchoring of the KR. Using densitometry, the amount of membrane-bound enzyme molecules was determined to be 38 ± 8%. So membrane insertion was incomplete and more than 50% of the overall expressed enzyme was not attached to the cytoplasmic membrane. In the literature, membrane anchoring of the β-galactosidase with Cyt b_5 anchor is described to amount to 80% of the total enzyme (George et al. 1989). Anchoring of the KR with the Cyt b_5 anchor was less efficient. Since, these are the only data on membrane immobilisation with the Cyt b_5 anchor, it is open whether the choice of enzyme or other factors contribute to the ratio of soluble and membrane-bound enzyme. The membrane-bound KR-Cyt b_5 was catalytically active and had an ee_s of 99 ± 1%, which is comparable to the native KR (Hölsch et al. 2008). Notably, soluble KR-Cyt b_5 had a reduced ee_s of 73 ± 18%. So, the membrane anchor altered the stereo-selectivity of the soluble, but not the membrane-immobilised KR-Cyt b_5, which is an indicator for successful membrane insertion of the anchor. The data presented in this work describe the first successful attempt to immobilise the KR to the cytoplasmic membrane. Soluble native KR associates to membranes even without a membrane anchor. Native, membrane-attached KR had an ee_s of 96 ± 5%, while the ee_s of soluble KR is >99% (Hölsch et al. 2008). The nature of native KR membrane attachment is so

far unknown, however these results indicated the membrane attachment itself to have an effect on the stereo-selectivity of the enzymes (Havel 2006; Hölsch 2009).

Initial experiments on co-expression were successful. For a functional multi-enzyme system the two separately immobilised enzymes FDH-UBC6 and the KR-Cyt b_5 were cloned into a newly created pET28Duet vector for co-expression. It was possible to obtain membrane preparations which contained both enzymes and allowed for the asymmetric reduction of ECAA. Comparison of membrane-bound and soluble enzymes showed more than 2-fold higher activity when the enzyme was bound to the membrane. Expression of the FDH-UBC6 resulted in 2.7 fold higher activity in the membrane, while about 39% of the KR-Cyt b_5 was bound to the membrane. The activity of the free wild type KR is about 5-fold higher than that of the best free FDH mutant (regarding measurements at 30 °C) (Hölsch et al. 2008; Hoelsch et al. 2013), which indicates that the coupled reaction system is limited by the KR. Still, the membrane-associated activity was higher than that of soluble protein, even though higher amounts of the KR can be expected in the soluble protein. Close association of enzymes, which function together in coupled catalysis or in catalytic cascades, is frequently described to be advantageous (Huang et al. 2001; Simmel 2012). The close spatial proximity of both enzymes is assumed to cause locally enhanced substrate concentrations. It is possible that membrane association of both FDH and KR caused such an effect and thereby increased yields in comparison to the soluble enzymes, which are diluted. The expression optima of FDH and KR differ greatly, consequently optimisation of the expression conditions was required in combination of expression and lysis.

Different anchoring methods were analysed for the fusion protein FDH-SG-KR. It was possible to immobilise the fusion protein to the cytosolic membrane using N-and C-terminal anchors. However, only one catalytic subunit remained active after the immobilisation. The KR was active with the N-terminal GlpF anchor. The FDH subunit remained active in C-terminal anchoring with the UBC6-anchor. Notably, only the subunit not attached directly to the membrane remained active in each case. The FDH is only active as a dimer (Tishkov & Popov 2004), whereas the KR forms at least dimeric structures (Hölsch & Weuster-Botz 2011). It is possible that immobilisation of the fusion protein prevented the formation of the tertiary structure . Since it was not possible to obtain membrane-bound fusion protein with both catalytic subunits being active, the immobilisation of the FDH-SG-KR was abandoned.

Since expression levels were low and there are no commercially available antibodies for FDH and KR, all comparisons between different membrane anchors are based on the comparison of the immobilised enzyme activity. Portions of the membranes are lost during the preparation along with the cellular debris. It is therefore not possible to obtain the total membranes of the disrupted cells. Contrary to this, the gross of the soluble protein can be obtained during cellular disruption. Consequently, the results are impaired in favour of the soluble enzyme. This effects all ratios and quantifications described in this chapter. The amounts of membrane-bound enzyme might be higher if all membrane-bound enzyme could be collected. Similar problems are also described in the literature on the quantification of membrane-bound proteins in surface display (Jose et al. 2012). Therefore, the data displayed in this chapter can be used as a guideline, but not for a quantification of the number of immobilised enzyme molecules.

For the first time it was possible to co-immobilise a heterologous working multi-enzyme system to the cytoplasmic membrane of *E. coli* using C-terminal membrane anchoring motifs. The results on the combination of membrane anchoring and production of biocatalyst preparations will be discussed in the following chapters.

6 Process development for enzyme immobilisation and protein E-mediated lysis

After immobilisation of the synthesis enzymes, the production of cellular envelopes was investigated. For establishing the new technology and corresponding analytical techniques, cellular envelopes were first produced without coupled expression of the synthesis enzymes. Subsequently, expression and lysis were combined and a production process for the new biocatalysts was developed in a laboratory scale stirred-tank bioreactor.

6.1 Establishing protein E-mediated lysis

Initial experiments were focused on establishing protein E-mediated lysis without additional enzyme expression. Lysis of *E. coli* so far focused on e.g. probiotic *E. coli* Nissel cells, which are not designed for recombinant protein expression. For the production of biocatalysts, large amounts of immobilised enzymes were required. Expression strains were therefore used, which contain respective genomic mutations to enable sufficient expression levels of recombinant protein and *E. coli* BL21 (DE3) was chosen. Overexpression of membrane proteins is often toxic to the cells. Special strains are commercially available, which are better suitable to sustain membrane protein. These strains are derived from BL21, are referred to as "*Walker-strains"* and comprise *E. coli* C41 (DE3) and C43 (DE3), respectively. All cells were transformed with the lysis plasmid containing the gene encoding for protein E controlled by the phage promotor λ p_R with the altered temperature sensitive repressor cI857 for activation at 42 °C. Lysis performance of all strains was evaluated prior to application in combined expression and lysis.

6.1.1 Analytics

Protein E-mediated lysis can be observed online and at-line using e.g. the optical density or the dissolved oxygen concentration (DO). In literature, the lysis yields are calculated using colony forming units (CFU). However, overexpression of synthesis enzymes can lead to low cellular vitality and cell death without protein E-mediated lysis. It was therefore necessary to introduce an analytical method, which allows for a distinction between cells that lost their ability for proliferation, and protein E-mediated lysis. A method based on flow cytometry for the

monitoring of protein E-mediated lysis is described in the literature, which was introduced for this work. Exemplary data are given in Figure 6-1 and Figure 6-2. Distinction of the sub populations of living, dead and lysed cells is achieved by staining with $DiBAC_{[4]}(3)$ (see Figure 6-1).

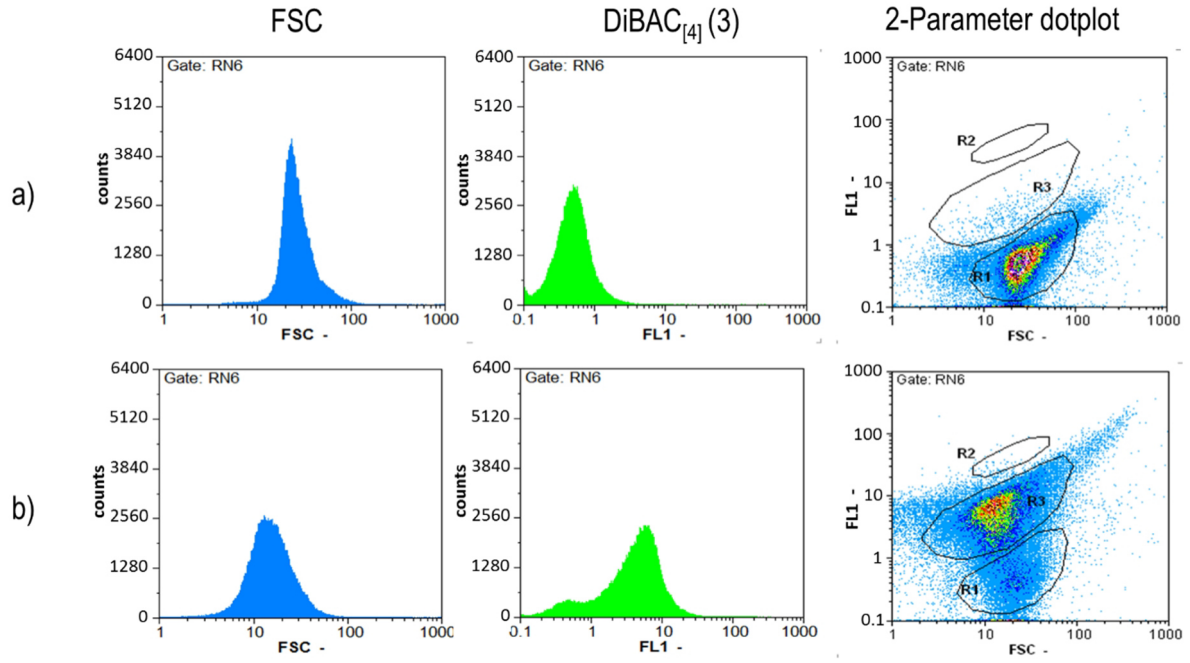

Figure 6-1 Distinction of *E. coli* populations in protein E-mediated lysis using flow cytometry
Exemplary flow cytometry data comparing cells prior to lysis (a) and after lysis (b): Histograms of the forward scatter (FSC) and the $DiBAC_{[4]}(3)$ staining signal (FL1) are displayed along with a 2-parameter dot plot of FSC and FL1. The sub populations are selected in polygons as: living cells (R1), dead/intact cells (R2) and cellular envelopes (R3). The same samples are depicted before and after protein E-mediated lysis. The gate RN6 incorporates all cellular particles according to positive RH414 staining.

$DiBAC_{[4]}(3)$ has a higher affinity to depolarised membranes than to polarised ones. Consequently, dead and lysed cells bind more dye molecules and exhibit higher fluorescence signals. Additional separation is possible using particle size. Due to the loss of the cytosol, cellular envelopes are smaller and cause a diminished forward scatter (FSC) signal. As displayed in Figure 6-1, using a 2-parameter dot plot of $DiBAC_{[4]}(3)$ fluorescence and FSC, the distinction of sub populations is possible. To remove background noise from other particles, samples were additionally stained with RH414, exemplary data are shown in Figure 6-2. RH414 binds to membranes and offers a distinction between background noise and cells.

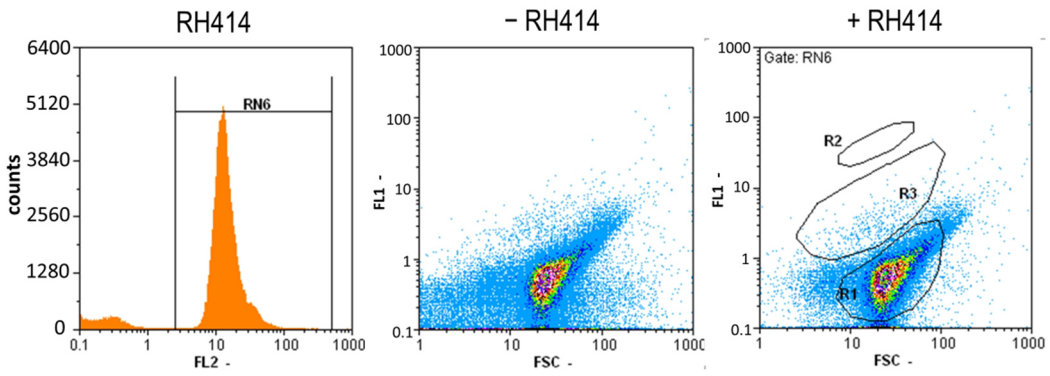

Figure 6-2 Exemplary data on RH414 staining for flow cytometry
RH414 staining is shown as histogram of fluorescence channel 2 (FL2) (a), the positive population is selected as RN6. 2-parameter dot plots of FSC and $DiBAC_{[4]}(3)$ staining are compared without (b) and with (c) selection of the respective population in RH414 staining (Gate RN6).

Flow cytometry was successfully established as an additional method for the analysis of protein E-mediated lysis. A mixed culture, containing cells which died from stress during expression instead of performing complete lysis, was used to determine the localisation of all sub populations (see Figure 6-3).

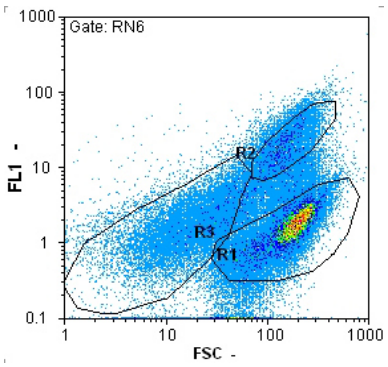

Figure 6-3 Exemplary flow cytometric data showing all populations
A 2-parameter dot plot of the forward scatter (FSC) and and the $DiBAC_{[4]}(3)$ staining signal (FL1). The sub populations are selected in polygons as: living cells (R1), dead/intact cells (R2) and cellular envelopes (R3). Gate RN6 comprises all particles with positive RH414 staining.

In mixed cultures it was possible to distinguish between living (R1), dead but intact (R2) and cellular envelopes (R3). Living and dead but intact cells were located at similar FSC signals, since the dead cells are intact and retain their shape, but at increased FL1 intensity, since the dead cells are depolarised and thus bind more $DiBAC_{[4]}(3)$ molecules. The transition between living and dead cells was thereby fluent and quantities of particles are visible between the polygons R1 and R2. Notably, the localisation of the R2 polygon of dead cells and R3 polygon containing cellular envelopes cannot be separated clearly. If cells were clearly dying because of protein E-mediated lysis (based on other parameters, e.g. OD_{600}), the R2 polygon was shifted

in order to include all signals belonging to the R3 polygon.

The applied staining methods for the separation of living cells and cellular envelopes do not allow for the populations to locate clearly in the different quadrants of the dot plot (see Figure 6-2). Rather, a polygon is applied to select the populations, which usually does not comprise all the events belonging to one population (exemplary see selected gate R3, Figure 6-2 c)). Using this method, the lysis yields are evaluated about 10 – 15% inferior to the actual result. CFU rather than flow cytometry was used for quantification of lysis yields, since it is the established method in the literature. Flow cytometric analysis was used for a qualitative analysis of protein E-mediated lysis in experiments in stirred-tank bioreactors and analysis of cellular envelope morphology. Exceptions were made in shaking flask experiments, because the large number of parallel experiments, experimental setup did not allow for CFU determination of each flask. Here, flow cytometry was also used for lysis yield calculation and was then calculated according to equation 4-11.

6.1.2 Shaking flasks

First experiments on protein E-mediated lysis were performed in shaking flasks in LB-medium. *E. coli* BL21 was compared with *E. coli* C41 and *E. coli* C43. Cells were grown until an OD_{600} of 0.6 to 0.8, then lysis was induced in mid exponential growth by a temperature shift to 42 °C. Lysis was observed using optical density and flow cytometry. For comparability with plasmid and antibiotic stress of subsequent experiments, cells carried an additional pET28a expression vector, which was not induced. Exemplary data are depicted in Figure 6-4.

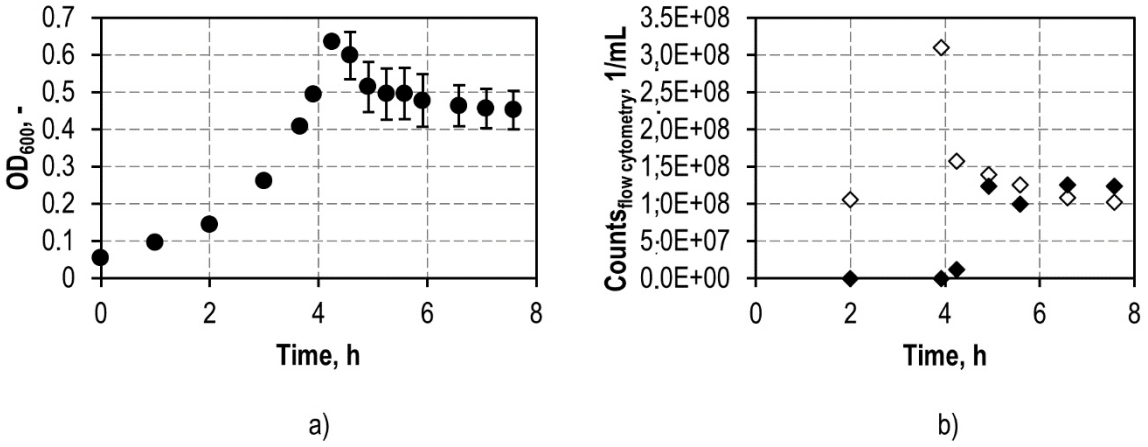

Figure 6-4 Exemplary data from protein E-mediated lysis in shaking flasks
Data from BL21 lysis in shaking flask is shown. The OD_{600} is depicted in the course of time (a). Counts from flow cytometry are shown for living cells (◊) and cellular envelopes (♦) in the course of time (b).

Lysis was induced after 4 h cultivation.

As displayed in Figure 6-4, the OD_{600} declines detectably after induction of protein E-mediated lysis. Correspondingly, the population of living cells decreases and the population of cellular envelopes increase respectively, as lysis progresses (see Figure 6-4 b)). The lysis yields are displayed in Figure 6-5.

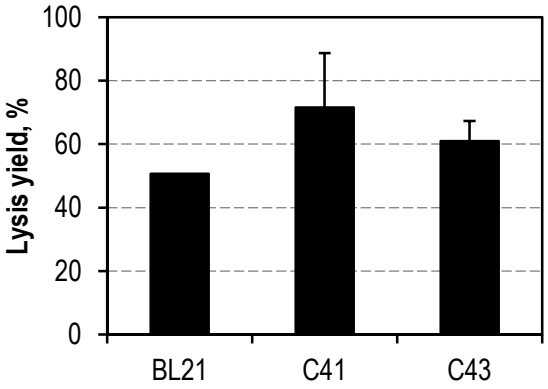

Figure 6-5 Lysis yields in shaking flask experiments
The lysis yields of *E. coli* BL21, *E. coli* C41 and *E. coli* C43 are compared. The yields were obtained using flow cytometry and calculated according to equation 4-11.

Generally, it was possible to achieve protein E-mediated lysis with all cell strains. The lysis yield of BL21 was 50.7%, that of C41 was 71.6 ± 17.0% and that of C43 was 60.9 ± 6.40, respectively. Lysis duration was between about 2 to 4 h. Cellular vitality is described to have effects on lysis. As lysis was induced in mid-exponential growth, incomplete lysis due to substrate limitation is unlikely. It can probably be referred to insufficient supply with dissolved oxygen, since unbaffled shaking flasks and 20% nominal culture volume were used. Therefore, subsequent comparisons were performed in stirred-tank bioreactors, which offer better supply with dissolved oxygen.

6.1.3 Batch process in a stirred-tank bioreactor

A thorough comparison of the different cell strains could be obtained using batch processes in a stirred-tank bioreactor. Cells were grown in a 7.5 L stirred-tank bioreactor in in 4.0 L defined medium with 20 g/L glucose as substrate. Lysis was induced in mid-exponential growth after ~50% of the glucose was consumed. It was possible to establish a batch process for cellular envelopes production in a stirred-tank bioreactor and typical process data are shown in Figure 6-6.

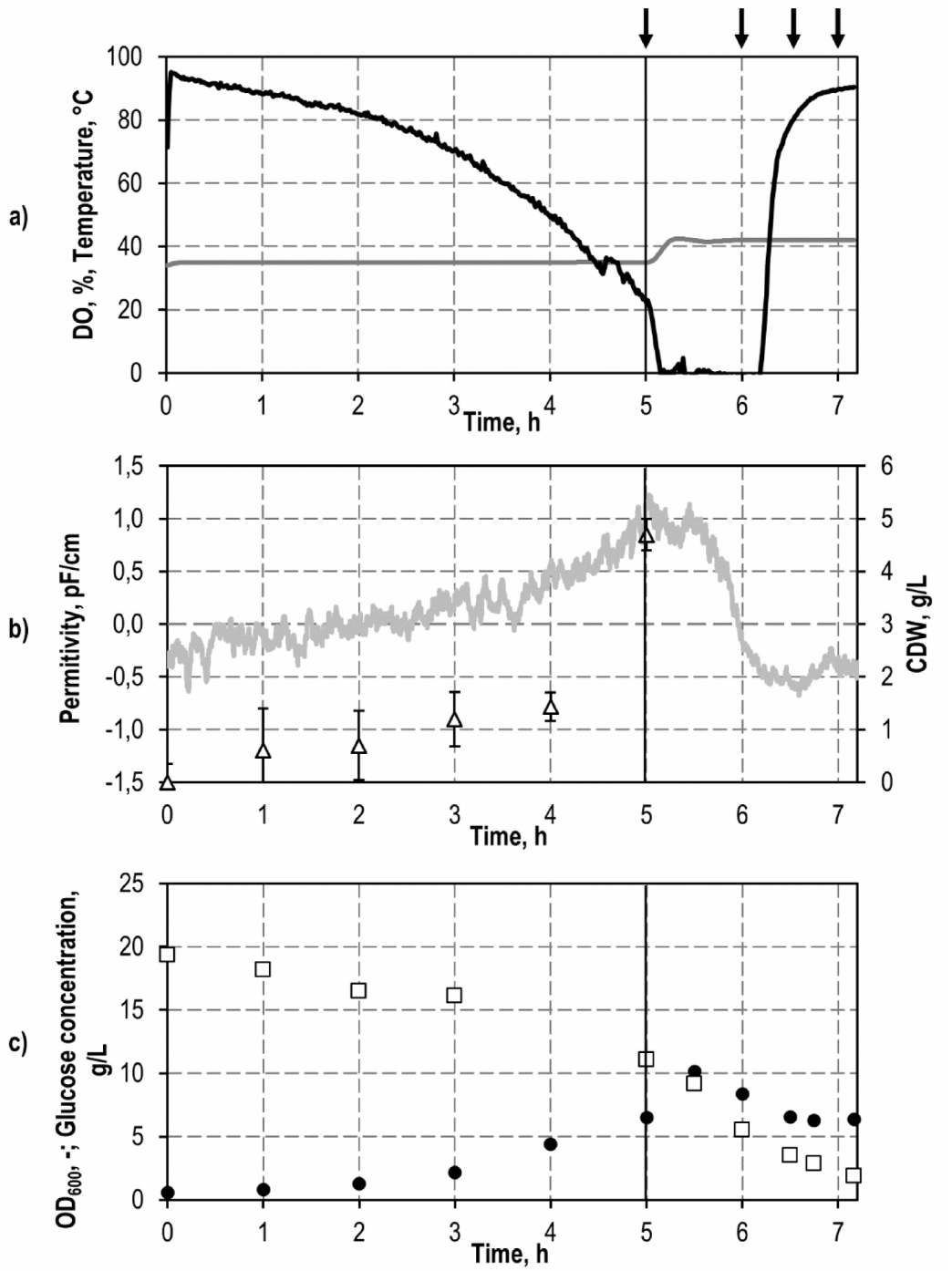

Figure 6-6 Exemplary process data from cellular envelope production with *E. coli* C41 in a batch process

a) The dissolved oxygen concentration (DO, black line), the temperature (dark gray line), b) the permittivity (light gray line), the cell dry weight concentration (CDW, Δ), c) the optical density (●) and the glucose concentration from enzyme kit measurement (□) are displayed in the course of time. The process conditions were: total volume = 4.0 L, maximum air flow = 8 L/min, stirring speed = 1000 rpm, pH = 7.2. The induction of lysis by a temperature shift to 42 °C is highlighted with a vertical line, samples from flow cytometric analysis displayed in Figure 6-7 are highlighted with black arrows. Standard deviations were calculated and are highlighted, but may be small and thus not visible.

During biomass formation prior to lysis, the temperature was adjusted to 35 °C, upon lysis the

temperature was shifted from 35 °C to 42 °C within 15 to 20 min at a process time of 5 h (see Figure 6-6 a)).

The dissolved oxygen concentration (DO) declined in correspondence with exponential growth of the cells during cultivation before lysis (see Figure 6-6 a)). After lysis induction the DO decreased to 0%. Although, stirring was at the maximum possible of 1000 rpm during the whole process, and the air flow was increased to the maximum, the DO could not be raised above 0%. At about 6.2 h process time the DO started to increase up to 90% at 7.2 h. The decrease of the DO at the start of lysis can be explained by reduced oxygen solubility in the medium at higher temperatures. The increase of the DO at 6.2 h process time was an indicator for protein E-mediated lysis. Due to the loss of the cytoplasm the oxygen is no longer required and the DO consequently increases. Notably, the maximum DO after lysis was not 100%, since the DO probe was calibrated at 35 °C. At the end of the process the temperature of the medium was 42 °C and consequently had a reduced maximum oxygen solubility.

The cell dry weight concentration (CDW) increases according to exponential cellular growth to a maximum of 4.7 g/L at 6.2 h (see Figure 6-6 b)). During lysis the release of the cytoplasm did not enable a clear separation of cells/cellular envelopes and medium by centrifugation, thus the CDW was only determined until lysis induction. Similarly, to data from shaking flask experiments, the OD_{600} increases during cellular growth and continues to increase after lysis induction until 5.5 h process time, after which the optical density starts do decrease. As described in section 6.1.2, decrease of the OD_{600} is an indicator of protein E-mediated lysis. Upon increasing cellular lysis, the reduced light scattering of cellular envelopes causes a decline in the optical density.

The glucose concentration was determined using an AccuCheck™ device during the experiment and afterwards in an additional detection with an enzyme kit. Starting from an initial concentration of about 20 g/L, the glucose concentration declines according to exponential cellular growth (see Figure 6-6 c)). After about 50% of the initial glucose was consumed, the lysis was induced during which the glucose concentration declined further and at the end of the process at 7.2 h, 1.9 g/L residual glucose was detected.

In addition to the dissolved oxygen concentration and the optical density, permittivity measurements with a biomass probe were used for the observation of protein E-mediated lysis during the process. Biomass probes detect the polarizability of cells generated by an electric field: the higher the permittivity, the higher the cell concentration (Davey et al. 1993). As depicted in Figure 6-6 b), the permittivity increases with cellular proliferation and in accordance

with the CDW. During lysis a sudden decrease can be observed, caused by the disruption of the cells and loss of the cytosol. The data also coincide with the amount of dissolved oxygen, which increases as lysed cells no longer require oxygen.

The increase in dissolved oxygen along with a decrease of the optical density are an indicator for protein E-mediated lysis. Notably, the amount of dissolved oxygen also increases if cells die due to low cellular vitality, but not as abrupt as it does with protein E-mediated lysis. Similarly, the permittivity decreases due to damages to the cell wall of dead but unlysed cells, but again the decline is not as abrupt and reduced compared to protein-E mediated lysis (data not shown). So, the observation of permittivity offers a new tool for the observation of protein E-mediated lysis on production scale.

Adjustment of the pH to 7.2 required titration with acid and base during the process. An increase of the pH was observed during lysis, which required the addition of acid and can likely be referred to a change of the pH by the release of the cytoplasm during protein E-mediated lysis.

Generally, protein E-mediated lysis was possible with all analysed *E. coli* strains. In several experiments, *E. coli* BL21, *E. coli* C41 and C43 were compared regarding their performance in protein E-mediated lysis in a stirred tank bio reactor. A summary of the main process parameters is given in Table 6-1.

Table 6-1 Summary of process parameters of different *E. coli* strains in cellular envelope production.

Cells were grown in 4.0 L defined medium with 20 g/L glucose at 25 °C. Lysis was induced when ~50% glucose was consumed. The final CDW and corresponding $Y_{XS\mu}$ were determined from the last sample taken before induction of lysis. Lysis duration was determined from the beginning of temperature increase until the end of the process at linear dissolved oxygen concentration. Each cultivation was performed as a duplicate.

Cell strain	Final CDW, g/L	$Y_{XS\mu}$, $g_{CDW}/g_{glucose}$	μ_{max}, 1/h	Duration of lysis, h	Lysis yield, %
E. coli BL21	5.7 ± 0.70	0.44 ± 0.01	0.33 ± 0.01	2.53 ± 0.04	> 99%
E. coli C41	4.4 ± 0.38	0.42 ± 0.03	0.31 ± 0.002	1.84 ± 0.47	> 99%
E. coli C43	3.5 ± 0.07	0.32 ± 0.04	0.47 ± 0.01	1.90 ± 0.98	> 99%

As described in Table 6-1, the lysis yield in all experiments was > 99%, so improved oxygen supply with stirring and aeration enabled complete lysis. Additionally, a correlation between final CDW and lysis duration could be observed. *E. coli* BL21 cells had the highest final CDW and the highest yield, but also the longest lysis duration. This observation is in agreement with shaking flask experiments. Thus, supply with dissolved oxygen is a limiting factor during lysis,

and cultivations with higher cell densities consequently need more time for lysis. Notably, in all experiments glucose was detected after lysis with an average of 24 ± 17% of the initial concentration

Additionally, flow cytometry was performed for a qualitative observation of protein E mediated lysis, data from flow cytometry is shown in Figure 6-7 and

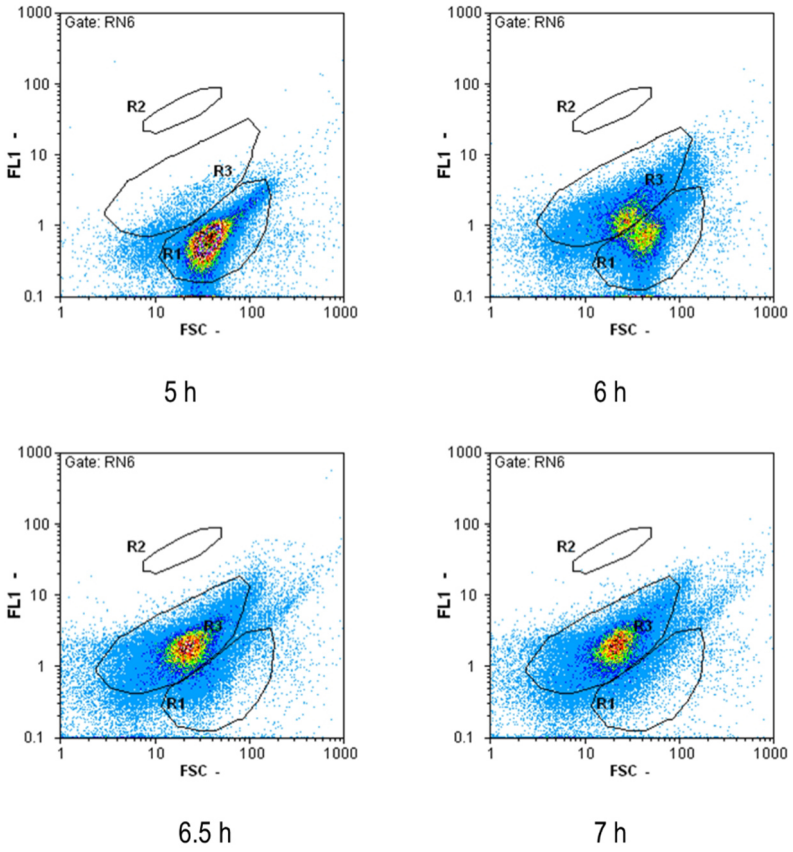

Figure 6-7 Exemplary data from analysis in flow cytometry
The 2-parameter dot plot of FSC and $DiBAC_{[4]}(3)$ staining (FL1) is shown for samples highlighted with a black arrow during lysis of C41 in batch cultivation in Figure 6-7. All dot plots contain particles with positive RH414 staining only (Gate RN6). Polygons are used to highlight the distinct populations of living cells (R1), dead but unlysed cells (R2) and cellular envelopes (R3).

Directly before lysis, only one population for whole, unlysed cells is visible (see R1 in Figure 6-7). In the course of time, the population is gradually shifted to cellular envelopes (see R3 in Figure 6-7). After about 1.5 to 2 h, no further change can be observed in flow cytometry.

Extended cultivation after lysis revealed that renewed cellular growth can be observed after lysis. This was confirmed with CFU and flow cytometry as well as another decline in dissolved oxygen, due to recommencing cellular growth (data not shown). The analysis of CFU on agar plates with and without antibiotics revealed these cells to have lost the lysis plasmid. The

growing cells are so called "*escape mutants"*, which have lost the ability to perform protein E-mediated lysis. Probably due to the release of the cytosol from large cell quantities, the resistance factors towards the antibiotics are released and the antibiotic concentration thus reduced. This probably protects cells which have lost the lysis plasmid and enables their cellular growth. Langemann et al. (2010) describe a down-stream protocol, which uses β-propiolactone to kill unlysed cells, which is added after concentration and washing of the cells. β-Propiolactone is highly toxic, and direct addition to the stirred-tank bioreactor was not attempted for safety reasons. Therefore, an antibiotic impulse with ampicillin was introduced, which is not used as a selective marker in cultivations. This successfully prevented the growth of *escape mutants* (data not shown). In all subsequent experiments ampicillin was added when the dissolved oxygen had reached approx. 50% after lysis.

6.1.4 Discussion

Protein E-mediated lysis was successfully established in single batch processes in a stirred-tank bioreactor along with the corresponding analytics. Flow cytometry was established for observation of protein E-mediated lysis according to Haidinger (2003) and Langemann (2010). Notably, staining intensity with $DiBAC_{[4]}(3)$ is highly dependent on the size and volume of the cells (Nebe-Von-Caron & Badley 1994; Nebe-Von-Caron et al. 2000). Thus, polygons for the selection of populations had to be adjusted individually for each experiment. In addition, there was a transition between the populations of living and dead but intact cells which incorporated a number of particles. Cells such as *E. coli* can exist in different "states of depolarisation", depending on whether the cells sustained small damages to the cell wall, making it more permeable, or whether the cells were completely permeabilised and depolarised. Depending on the amount of depolarisation, the amount of $DiBAC_{[4]}(3)$ molecules varies which can bind to the cell (Suller & Lloyd 1999).

Lysis performance was compared for *E. coli* BL21, *E. coli* C41 and *E. coli* C43 cells without additional expression of synthesis enzymes. First experiments were conducted in shaking flasks. It was possible to produce cellular envelopes in shaking flasks, however lysis was incomplete and lysis yields were not exceeding 80% in all experiments. Contrarily, literature data describe experiments with > 99% lysis yields in shaking flasks (Liu et al. 2012). However, these experiments used different *E. coli* strains, different flask systems and shakers in a water bath. These differences in e.g. oxygen supply can probably explain incomplete lysis in shaking flask experiments in this work.

Production of cellular envelopes in a stirred-tank bioreactor was introduced as a batch process according to Langemann et al. (2010). It was possible to lyse all *E. coli* strains with lysis yields > 99%; compared to unbaffled shaking flaks with filling of 20% nominal volume, the oxygen supply is improved in stirred-tank bioreactors. Successful lysis was possible for all cell strains, and the respective differences in the genomes of *E. coli* BL21, *E. coli* C41 and *E. coli* C43 had no effect on lysis efficiency. Notably, the final CDW and $Y_{XS\mu}$ in both *E. coli* C41 and *E. coli* C43 was lower than *E. coli* BL21 (see Table 6-1). The nature of mutations introduced to *E. coli* C41 and *E. coli* C43 has not been elucidated completely so far. Walker (1996) describe mutations in the promotor binding site of the T7 polymerase in *E. coli* C41 and *E. coli* C43 to cause lower expression levels of proteins, and consequently higher resistance to membrane protein overexpression. However, the exact mutations as well as possible side effects on the cellular performance are unknown (Miroux & Walker 1996; Wagner et al. 2008).

Protein E-mediated lysis in a stirred-tank bioreactor lasted up to about 2.5 h after the induction via temperature shift, which was longer than the 0.5 h described in Langemann (2010). Experiments in this work defined lysis duration from the onset of temperature increase to the final linear DO after lysis. Contrarily, data from Langemann (2010) comprise solely the time between reaching of 42 °C and the first increase of DO at the beginning of the lysis into consideration. Even if only the time span defined by Langemann et al. is used, lysis duration with *E. coli* BL21, *E. coli* C41 and *E. coli* C43 cells is prolonged compared to the probiotic *E. coli* Nissel described by Langemann et al. (2010). Differences in lysis duration even between related *E. coli* strains are described in the literature and seem to depend on the genetic background of the cells (Szostak et al. 1996). Moreover, in Langemann et al. (2010) a steel tank reactor was used, in which heating is provided by steam within about 10 min, in contrast to a glass vessel stirred-tank bioreactor employed in this work, which uses water for heating, which takes about 15 to 20 min for the shift from 35 °C to 42 °C. Heating with steam provides a faster temperature shift and thus possibly earlier induction of protein E expression, which consequently leads to an earlier lysis.

Establishing stirred-tank bioreactor processes was successful along with required analytics. Next, experiments were to focus on the combination of protein E-mediated lysis and expression, as described in the following section.

6.2 Combined expression and lysis of the multi-enzyme system

After successful establishment of protein E-mediated lysis in a simple batch process and the corresponding analytics, combined expression and lysis was performed. FDH was expressed and immobilised using the UBC6 anchor, KR was expressed and immobilised using the Cyt b_5 anchor as described before. Since, the KR has an about 6-fold higher v_{max} than the mutant FDH with 3 mutations for improved stability and activity towards NADPH, a defined ratio of membrane bound enzymes would be required to balance out these differences. Since immobilisation efficiencies, as well as the influence of the vector construction and the influence of the membrane anchor on the respective enzyme properties are unknown, such an aim challenging for a first study. Additionally, FDH and KR require different expression temperatures. KR is expressed best at 37 °C for 3 h, while FDH is not expressed in active form at such conditions (data not shown) and renders high yields if expressed at 20 °C overnight, conditions at which expression levels of the KR are low. Consequently, this first study of the new biocatalyst system was focused on a prove of principle incorporating a study of expression conditions, thus expression at 30 °C, 25 °C and 20 °C was compared.

6.2.1 Batch process

For combined membrane immobilization of the synthesis enzymes and subsequent lysis, *E. coli* BL21, *E. coli* C41 and *E. coli* C43 cells were co-transformed with the lysis plasmid and the expression plasmid pET28aDuet containing both enzymes with respective membrane anchors. Initial experiments for the comparison of different expression conditions were performed in shaking flasks before transfer to stirred-tank bioreactors, because this approach enabled a parallel analysis of different cultivation conditions in a short time. Cells were grown at 35 °C and expression was induced using 1 mM IPTG in mid-exponential growth. Expression for 18 h at 20 °C, 25 °C and 30 °C was analysed. The lysis yields in these experiments were between 20 and 50% and consequently incomplete. However, the standard deviations in multiple parallel experiments were high and the difference between results consequently not significant.

Since, comparison in shaking flasks was unsuccessful, the experimental setup was changed to a batch process in a stirred-tank bioreactor to provide complete lysis by improved oxygen supply, and to obtain a simple large scale production. In previous experiments on protein E lysis in a stirred-tank bioreactor, the dissolved oxygen was an important factor for lysis duration (see 6.1.3). Thus, the cultivation volume was reduced to obtain a better ratio of air flow to

reaction volume. 1.5 L medium was used and 20 g/L glucose was provided. Expression at 20 °C and 25 °C was analysed, as they proved advantageous in shaking flask experiments. Cells were grown at 35 °C until OD_{600} was ~3.5, then expression was induced using 1 mM IPTG and the temperature was lowered. After 18 h, a temperature increase was to induce lysis. However, the cells only died without E-mediated lysis as indicated by the combined data from batch processes (Figure 6-8).

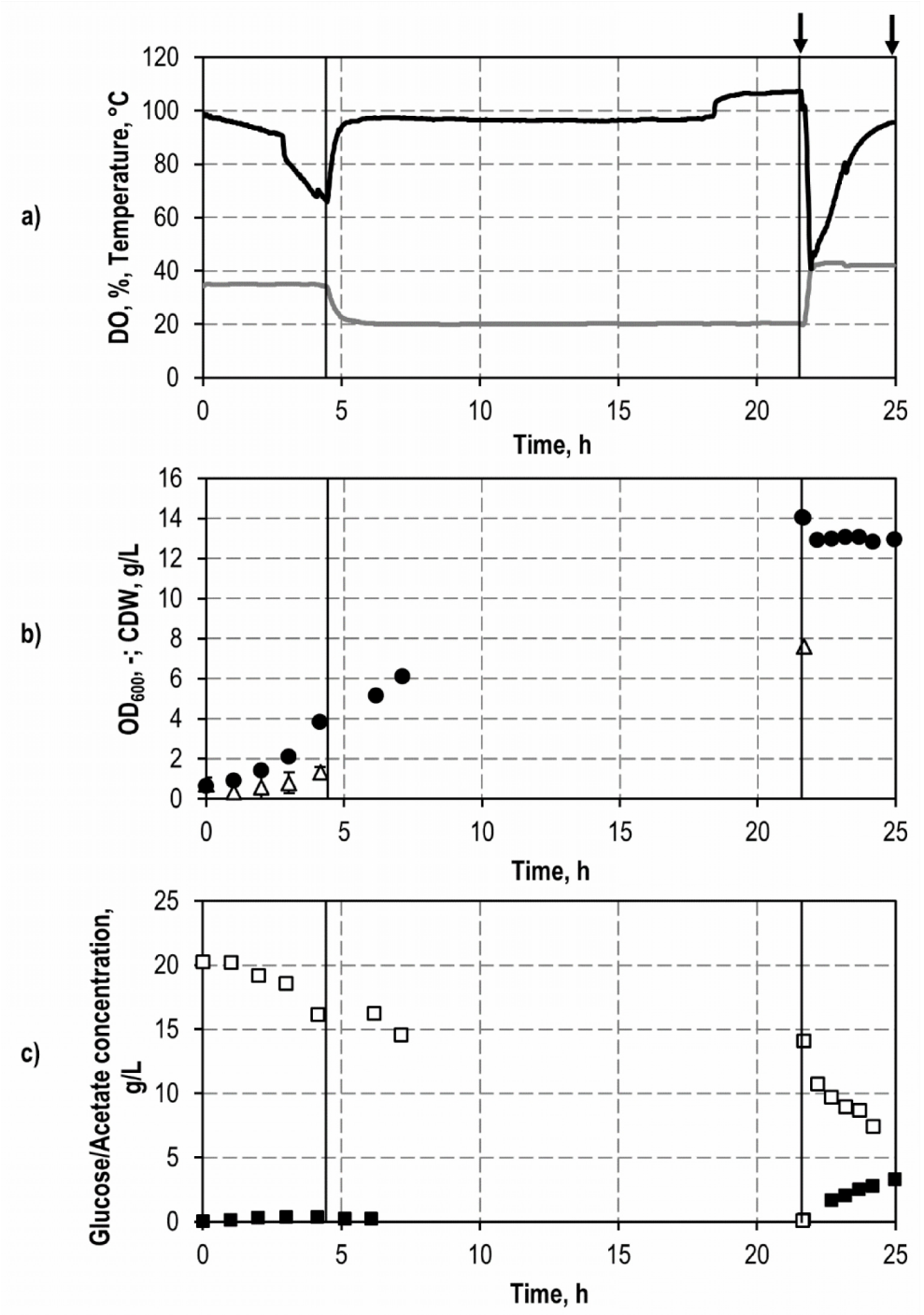

Figure 6-8 Exemplary data from batch process in a stirred-tank bioreactor for combined expression and lysis

a) Dissolved oxygen concentration (DO, black line), temperature (dark gray line), b) CDW (Δ), optical density (●), c) glucose (□) and acetate (■) concentration (enzyme kit measurement) are displayed in the course of time. The process conditions were: total volume 1.5 L, maximum air flow = 8 L/min, stirring speed = 1000 rpm, pH = 7.2. Induction of enzyme expression (by 1 mM IPTG addition) and a temperature shift to 42 °C are highlighted with a vertical line, samples for flow cytometric analysis shown in Figure 6-9 are highlighted with black arrows. *E. coli* BL21 were used for the cultivation. Standard deviations were calculated and are highlighted, but may be small and thus not visible.

The DO progressed according to exponential growth before induction of enzyme expression (see Figure 6-8, a)). Upon induction of enzyme expression at about 4.5 h and reduction of the temperature to 20 °C, the DO increased due to an improved oxygen solubility at reduced temperatures. During expression, the DO remains constant until about 18 h process time, at which the DO increases up to about 110%. Notably, the DO probe was calibrated at 35 °C, which explains DO values > 100% at reduced temperatures. After the temperature shift to 42 °C for lysis induction, the DO decreased rapidly to about 40% due to reduced solubility of oxygen at higher temperatures. Later, a gradual increase of the DO imply reduced ongoing metabolism and little or no cellular growth, however no continued phase of unlimited growth was observed compared to data displayed in section 6.1.3.

The optical density and CDW (see Figure 6-8 b)) progressed according to exponential growth upon expression induction, the cells continued to grow to a final CDW of 7.6 g/L. Notably, the OD_{600} remained constant after lysis induction, which indicated no further cellular growth. Moreover, no decline of the optical density was observed after lysis induction, which would be an indicator for successful protein E-mediated lysis.

The initial glucose concentration (see Figure 6-8 c)) was about 20 g/L, which declined according to exponential growth of the cells during biomass formation. After induction of expression the cells continued to metabolise the glucose and after 18 h expression (see 21.7 h process time) no residual glucose was left. In order to enable cellular growth during lysis, a glucose impulse of 15 g/L glucose was added at lysis induction. Notably, the glucose concentration declined after the glucose impulse to 7.4 g/L at 24.2 h process time.

Acetate concentrations <0.2 g/L were detected before and after expression (see Figure 6-8 c)). After addition of the glucose impulse and induction of lysis, the acetate concentration increased up to 3.3 g/L at the end of the experiment (24.2 h process time). Decrease of glucose and increase of acetate concentration indicate ongoing cellular metabolism, even though no further cellular proliferation was observed.

Flow cytometry was performed for a qualitative analysis of cell populations before and after lysis induction, the data are shown in Figure 6-9.

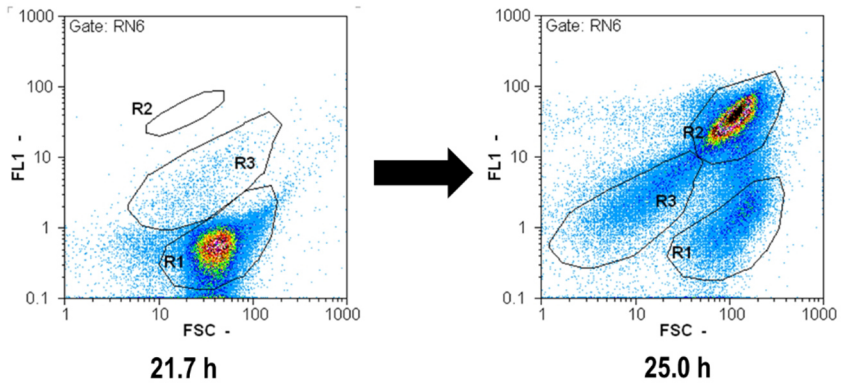

Figure 6-9 Exemplary data from flow cytometry analysis of batch cultivations with combined expression and lysis
2-parameter dot plots are shown for FSC and $DiBAC_{[4]}(3)$ staining (FL1) in cultivation of *E. coli* BL21. Data are shown for samples after overnight expression before lysis (21.7 h) and after attempted lysis at 42 °C at 25 h process time. Only signals with positive RH414 staining are shown (gate RN6) with (R1) living cells, (R2) dead cells and (R3) cellular envelopes. The samples displayed in this figure are highlighted in Figure 6-8 with black arrows

Contrary to typical vital cells before lysis (see Figure 6-7, 21.7 h), a part of the population was visible as depolarised cells in transition to dead cells (see R2 in Figure 6-9). After lysis induction the depolarisation was increased, the population of dead but intact cells was formed and little protein E-mediated lysis was observed. The shift from partly to complete depolarisation of whole cells can be explained by increased binding of dye molecules due to increased depolarisation, as discussed in section 6.1.4.

Low cellular vitality after expression can likely be referred to glucose depletion during expression, which is indicated by an increase of the DO at 18 h process time. Starving cells in combination with stress due to the temperature increase during lysis are likely factors which were responsible for cell death instead of protein E-mediated lysis. Vital and proliferating cells lyse best, as protein E requires the lipid structure of cell division in the membrane for insertion (see section 3.5.1). It was consequently attempted to revitalize the cells after the overnight expression prior to lysis. Therefore, several methods were analysed. Different amounts of glucose were added as an impulse prior to lysis to promote cellular growth. Additionally, the temperature was increased stepwise before heating to 42 °C, in order to reduce the heat shock for the cells. Cellular vitality was lost during expression overnight, and yeast extract was added to the defined medium to provide additional nutrients during expression. However, none of these attempts was successful. Glucose was consumed during overnight expression (as displayed using the DO in see Figure 6-8 a)), and low cellular vitality could likely be referred

to prolonged substrate limitation. Therefore, fed batch fermentations were analysed, the results will be discussed in the following section.

6.2.2 Fed-batch process in a stirred-tank bioreactor

To maintain cellular vitality during expression, fed-batch processes were analysed. Similar to the batch processes, a standard 1.5 L initial volume in a 3.6 L stirred-tank bioreactor was chosen. During expression, the cells were to grow exponentially under substrate-limiting conditions, to ensure sufficient supply with nutrients and to avoid acetate accumulation. Growth rates were adjusted accordingly to be below the maximum possible growth rate at the respective temperatures (see appendix Table 12-14). For first experiments, low final CDW were aimed for, to ensure comparability with batch-experiments.

A three step-production process was introduced for the production of biocatalysis. Exemplary process data are given in Figure 6-10. First, cells were grown for biomass production in a batch phase. Regarding the required glucose concentration of the feeding medium and the additional volume added to the stirred-tank bioreactor, feeding at low pump frequencies was aimed for to minimize the added volume. To ensure sufficient biomass for the subsequent feeding, the CDW needed to be high enough to avoid glucose accumulation in feeding at lowest pump frequencies (see equation 4-1). Therefore, about 2.5 g/L CDW were required regarding this set-up and 5 g/L glucose was chosen as the initial substrate concentration during the batch-phase. Expression of KR-Cyt b_5 and FDH-UBC6 was induced using IPTG upon glucose depletion, and expression lasted for 18 h at 20 °C, 25 °C or 30 °C. In batch processes without enzyme expression, the final CDW was up to 5.7 ± 0.7 g/L (regarding BL21). The growth rate during expression was chosen to be μ_{set} = 0.075 1/h to yield according amounts of biocatalysts in first experiments. Lysis was induced by the temperature shift to 42 °C and the growth rate was increased to 0.3 1/h at the induction of lysis. It was possible to obtain protein E-mediated lysis using this three-step protocol with fed-batch mode during expression and lysis. The process was terminated after DO was >50% air saturation using an ampicillin pulse to prevent "*escape mutant*" formation (see section 6.1.3). Exemplary process data are displayed in Figure 6-9.

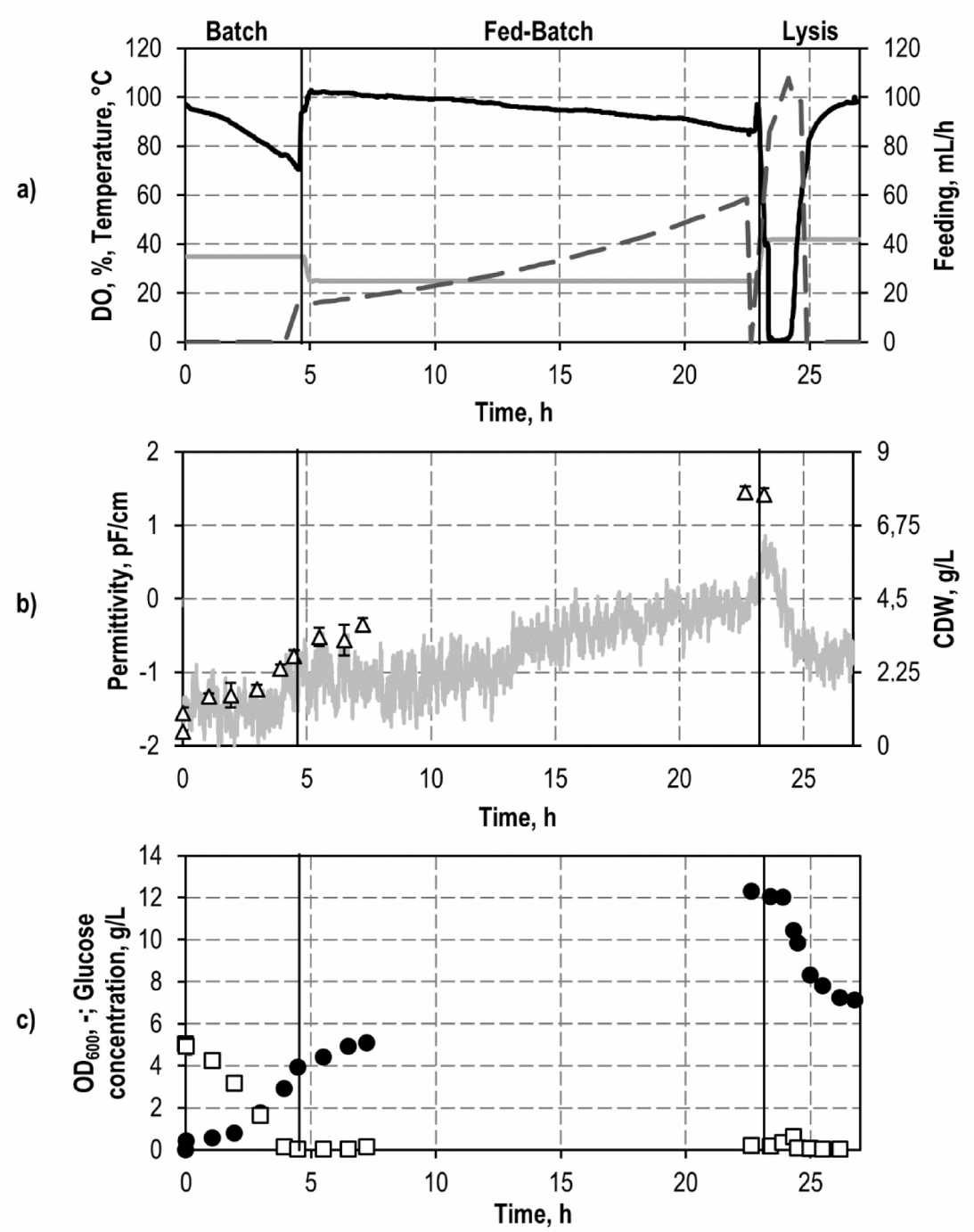

Figure 6-10 Exemplary process data of fed-batch production of cellular envelopes with immobilised oxidoreductases

a)The dissolved oxygen concentration (DO, black line), the temperature (dark gray line), the feed medium inflow (gray dashed line), b) the permittivity (light gray line), the CDW (Δ), c) the optical density (●), the glucose (□) concentration from enzyme kit measurement are displayed in the course of time. The process conditions were: initial volume = 1.5 L, maximum air flow = 8 L/min, stirring speed = 1000 rpm, pH = 7.2, $\mu_{set\ Expression}$ = 0.075 1/h (50 g/L glucose in feed medium) and $\mu_{set\ Lysis}$ = 0.3 1/h (100 g/L glucose in feed medium). The induction of enzyme expression (by 0.1 mM IPTG addition) and lysis by a temperature shift to 42 °C are highlighted with a vertical line, *E. coli* C41 were used for the cultivation. Standard deviations were calculated and are highlighted, but may be small and thus not visible.

Cellular envelope production can be observed using different parameters. In Figure 6-10 the exemplary process data are displayed in the course of a fed-batch process for combined expression and lysis in a stirred-tank bioreactor. The process is divided into three steps: a batch phase and two fed-batch phases for expression and lysis indicated by media inflow (see Figure 6-10 a)). During the process the DO declined according to the exponential growth during the batch phase for biomass formation (see Figure 6-10 a)). At induction of enzyme expression at 4.5 h, the DO increased from 70 to 102%, due to glucose depletion at the end of the batch-phase and the reduction of the temperature (to 25 °C), which caused improved oxygen solubility in the medium. During expression, the DO declined gradually to 86% within 18h, which was decelerated compared to unlimited growth, due to the reduced cellular growth at substrate limited feeding. Upon lysis induction at 23.4 h process time by increase of the temperature to 42 °C and enhanced cellular growth by increased feeding, the DO dropped to 0%. Similarly to data displayed in section 6.1.3, increase of the air flow to the maximum was insufficient to raise the DO. Finally, lysis was indicated by an increase of the DO at 24.9 h up to 98% after 27 h process time.

The CDW increased exponentially during the batch-phase to 2.8 g/L (see Figure 6-10 b)). After expression induction the CDW increased according to the reduced growth rate under substrate limiting conditions during the first fed-batch step, the final CDW before after expression was 7.7 ± 0.2 g/L at 23.4 h process time. As described in section 6.1.3, no further samples were taken for CDW determination after lysis induction due to insufficient separation of cells and supernatant after lysis of the cells.

The permittivity progressed similarly to the CDW with an exponential increase during batch production and a reduced increase during substrate-limited feeding (see Figure 6-10 b)). After induction of lysis at 23.4 h process time, the permittivity followed according to exponential growth due to the increased growth rate until about 24.7 h process time, after which the permittivity declined. As described in section 6.1.3, the decline in permittivity is caused by the release of the cytoplasm from the cells and their corresponding depolarization.

The optical density increased according to exponential growth during the batch-phase to OD_{600} = 4.5, upon induction of enzyme expression the OD_{600} increased with a reduced rate to 12.3 after 18 h (see Figure 6-10 c)). After lysis induction, the optical density remained constant until about 24.7 h process time, after which the OD_{600} decreased. The progress of the optical density was in agreement with the data from CDW, permittivity and DO. As described in section 6.1.2 and 6.1.3, the decline in optical density during lysis is caused by the release of the

cytoplasm and the corresponding reduced light scatter of the cellular envelopes.

The initial glucose concentration during batch phase was about 5 g/L, during biomass formation in the batch-phase, the glucose concentration decreased according to cellular growth (see Figure 6-10 c)). Upon glucose depletion a substrate limited fed-batch was initiated and no glucose was detected during or after expression, which indicated sufficient cellular metabolism for the consumption of the carbon source. Upon lysis induction, the growth rate and correspondingly the feed medium inflow was increased but no glucose was detected until 24.3 h process time, at which the feeding was terminated. Accumulation of glucose during lysis can very likely be referred to the increasing number of lysed cells, which do not longer require a carbon source. During the process, an accumulation of glucose during lysis could therefore be considered another indicator for protein E-mediated lysis.

The data from DO, $OD_{600,}$ flow cytometry (data not shown) and permittivity indicated a successful lysis. Notably, the accumulation of glucose was observed after the first decline of the optical density, while the increase of the DO was the last indicator for lysis. This observation is in accordance with flow cytometry data from section 6.1.3, which show a gradual increase of the population of cellular envelopes. Thus, the glucose only begins to accumulate once it is no longer metabolised by the remaining cells.

All combined data, including CFU and flow cytometry (data not shown) proved successful lysis.

Using CFU, lysis yields were calculated to be > 99% in all experiments. Lysis was successful with IPTG concentrations of 0.1 mM, higher concentrations led to decreased cellular vitality and consequently unsuccessful E-mediated lysis; expression at 30 °C too was unsuccessful. It was possible to establish fed-batch processes for the production of cellular envelopes with over-expressed KR-Cyt b_5 and FDH-UBC6. Prior to characterisation of the cellular envelopes, a work-up method was established, the results are discussed in the following section.

6.2.3 Downstream processing of cellular envelopes

After successful lysis, downstream processing of the cellular envelopes was required to remove host cell protein and soluble enzymes from the surrounding medium. Especially, the removal of soluble catalytic enzymes was of interest, as these would otherwise falsify the results in the characterisation of the cellular envelopes.

Centrifugation of cellular envelopes is possible, as they can be treated basically like whole cells. However, successive centrifugation only offers the treatment of small sample amounts and can

cause agglomeration of the cellular envelopes, which is highly undesirable. Langemann et al. (2010) described cross-flow filtration in a bypass, which can prevent agglomeration and was thus applied in this work. A 4.2 m^2 hollow fibre filter module was used with 0.22 µm pore size. Directly after lysis, cellular envelopes were concentrated in a bypass to about 1/3 of the initial volume. Concentration was initiated when the DO was > 90% after lysis. The concentrated cellular envelopes were frozen at −20 °C to perforate remaining whole cells by a disruption of the cell wall during freezing. After the freezing step, host cell protein and soluble enzymes were removed using cross-flow filtration. Using buffer, five successive washing steps with 2-fold or 5-fold of the culture volume in each step were analysed. The decrease in soluble protein was quantified using a BCA assay. Results are given in Figure 6-11.

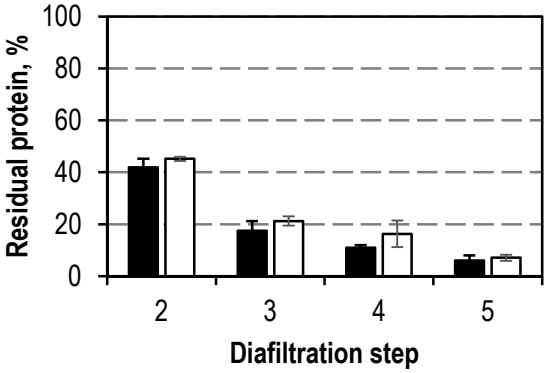

Figure 6-11 Decrease of soluble protein during downstream processing of cellular envelopes using cross-flow filtration
Residual amount of soluble protein during cross-flow filtration is compared for washing with 5-fold (black) and 2-fold (white) volume of the culture during 5 successive diafiltration steps. The initial protein concentration was equivalent to 100%.

Within successive washing steps, the protein concentration declined exponentially. The average residual amount of soluble protein 3 washing steps was 11 ± 1% of the initial concentration using 5-fold volume and 16 ± 5% in using 2-fold volume of the culture, respectively. Due to the duration of the process and the constant mixing of culture broth by pump circulation, the system can be considered ideally mixed. Thus, the observed exponential decline of the residual protein concentration was as expected.

Each washing step is time consuming. After three washing steps the decline of soluble protein in each step is reduced greatly. The main reason for washing was the reduction of soluble catalytic enzymes. Permeate collected after three washing steps did not exhibit catalytic activity regardless of the dilution used (data not shown) and were thus applied in all further experiments.

6.2.4 Comparison of cellular envelopes from different *E. coli* strains

A fed-batch process for the production of biocatalysts with immobilised KR-Cyt b_5 and FDH-UBC6 was established along with a corresponding downstream processing. Now, identification of the best cell strain and expression temperature was aimed for. Therefore, cellular envelopes were produced from *E. coli* BL21, *E. coli* C41 and *E. coli* C43 at both 20 °C and 25 °C expression temperature, each. Subsequently, the main process parameters and catalytic activity of the cellular envelopes were compared. A comparison of parameters from the batch phase is given in the appendix Table 12-15. All parameters depending on the expression temperature are summarised in Table 6-2.

Table 6-2 Comparison of process data from fed-batch production of cellular envelopes with immobilised oxidoreductases
All processes were performed using 0.1 mM IPTG for induction and a μ_{set} = 0.075 1/h adjusted using a $Y_{XS,\mu}$ = 0.4 $g_{CDW}/g_{glucose}$ during expression. The corresponding measured μ during expression and the CDW prior to the induction of lysis are summarised for processes with all cell strains using an expression temperature of 20 °C and 25 °C, respectively. Due to missing CDW data from the process, numbers marked with an asterisk (*) were calculated from the OD_{600} using a CDW to OD_{600} correlation factor of 0.55. Up to triplicate experiments were performed of each cultivation.

E. coli cell line	Expression temperature, °C	$\mu_{expression}$ measured, 1/h	CDW prior to lysis, g/L
BL21	20	0.08 ± 0.01	13.9 ± 1.7
C41	20	0.06	8.2 ± 0.2
C43	20	n.d.	7.1 ± 0.1*
BL21	25	0.09 ± 0.04	11.6 ± 3.9
C41	25	0.10 ± 0.06	8.0 ± 0.8
C43	25	0.05	7.6 ± 0.5

Regarding the final CDW prior to lysis, yields of *E. coli* C41 and *E. coli* C43 are about 7.7 g/L in average, and not significantly different regardless of the expression temperature used. Final CDW of *E. coli* BL21 are also not significantly different at different expression temperatures. However, BL21 cells yielded about 40% more CDW than *E. coli* C41 and *E. coli* C43 cells. This observation is in agreement with results from batch processes for establishing protein E-mediated lysis. Notably, the detected $\mu_{expression}$ vary from the μ_{set} = 0.075 1/h. The growth rates of *E. coli* BL21 were up to 0.09 ± 0.04 1/h. For adjusting μ_{set} a yield of $Y_{XS.\mu}$ = 0.4 $g_{CDW}/g_{glucose}$ was used, however the measured yield of *E. coli* BL21 was 0.44 ± 0.1 $g_{CDW}/g_{glucose}$. Thus, higher growth rates and final CDW can be explained by improved glucose utilisation of the cells. Similarly, *E. coli* C43 exhibited a $\mu_{expression}$ of 0.05, which is lower than $\mu_{set.}$ *E. coli* C43 has a measured $Y_{XS,\mu}$ of 0.32 ± 0.04 $g_{CDW}/g_{glucose,}$ which is below μ_{set} and thus explains reduced cellular growth and final CDW due to impaired glucose utilization of this cell strain.

The main parameter for the selection of the best expression conditions was the catalytic activity of the cellular envelopes in asymmetric reduction of ECAA to the corresponding (*S*)-alcohol (*S*)-ECHB. For the comparison of cellular envelopes from different *E. coli* strains and different expression conditions, incomplete conversion was required to be able to detect differences in activity. 20 mM ECAA were converted in the presence of 5 mM $NADP^+$ and 0.5 M sodium formate using $1x10^9$ cellular envelopes which equals 2.38 $g_{dry\ weight}$ /L for 18 h at 30 °C. The cellular envelope concentration was determined using positive RH414 staining in flow cytometry. A count to weight correlation was established using lyophilised cellular envelopes and flow cytometry (see appendix Figure 12-2). The correlation was used to calculate the corresponding cellular envelope dry weight concentrations in the batch reaction (see appendix, equation 12-1). A comparison of the catalytic activity of the cellular envelopes is displayed in Figure 6-12.

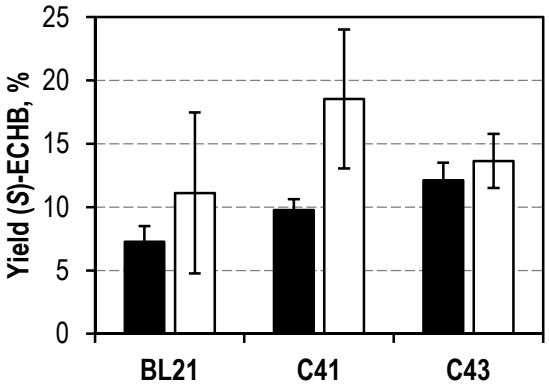

Figure 6-12 Comparison of catalytic activity of cellular envelopes gained at different expression conditions
The yield of (*S*)-ECHB in asymmetric reductions of ECAA is compared for cellular envelopes from *E. coli* BL21, C41 and C43 for expression at 20 °C (black) and 25 °C (white), each. 20 mM ECAA were converted in the presence of 5 mM $NADP^+$ and 0.5 M sodium formate using $1x10^9$ cellular envelopes, which equals 2.38 $g/L_{dry\ weight}$ for 18 h at 30 °C. Experiments were performed at least as triplicates and are average values from different cultivations.

The conversion of ECAA to the corresponding (*S*)-alcohol was incomplete, as required for the comparison and most results were not significantly different. The highest average yields were obtained using cellular envelopes from C41 at 25 °C expression temperature with 18.5 ± 5.5%, which indicated an advantage of the "*Walker*" cells in the expression of enzymes with C-terminal membrane anchors. Contrary to the activity of the cellular envelopes, *E. coli* BL21 cells yielded about 40% higher final CDW (see Table 6-2).The activity in *E. coli* C41 cellular envelopes was about 43% higher, thus the total activity obtained in the processes was about the same. Since the activity of the cellular envelopes was of highest interest, all further experiments

employed cellular envelopes that were produced from *E. coli* C41 cells at 25 °C expression temperature. Notably, the ee_s was not determined in these conversions because the product concentrations were too low to allow for a valid detection and conclusion. Analysis of the ee_s was therefore postponed to the characterisation of the cellular envelopes.

Increase of biocatalyst yield

First experiments for fed-batch production of biocatalysts were performed using low μ_{set} during expression to provide comparability with batch processes. Subsequently, an increase in biocatalyst yield was of interest. The growth rate during expression was therefore increased to $\mu_{set} = 0.09$ 1/h. Experiments were performed using *E. coli* C41 and *E. coli* C43 cells, and it was possible to perform combined expression and lysis with yields > 99% successfully. The final CDW was 12.1 ± 1.7 g/L for *E. coli* C41 and 14.0 ± 0.4 g/L for *E. coli* C43 cells, respectively and the yield in CDW was increased by 70% due to the increased growth rate compared to data shown in Table 6-2. Subsequently, the activity of cellular envelopes was compared from different growth rates during expression and no significant difference was observed from cellular envelopes gained at different growth rates during expression (data not shown).

The growth rate during expression was further increased to 0.12 1/h in combined expression and lysis of C41 cells. Successfully combined expression at 25 °C and subsequent lysis was possible with lysis yields >99% and a final CDW of 20.4 ± 0.7 g/l. Process data are shown in Figure 6-13.

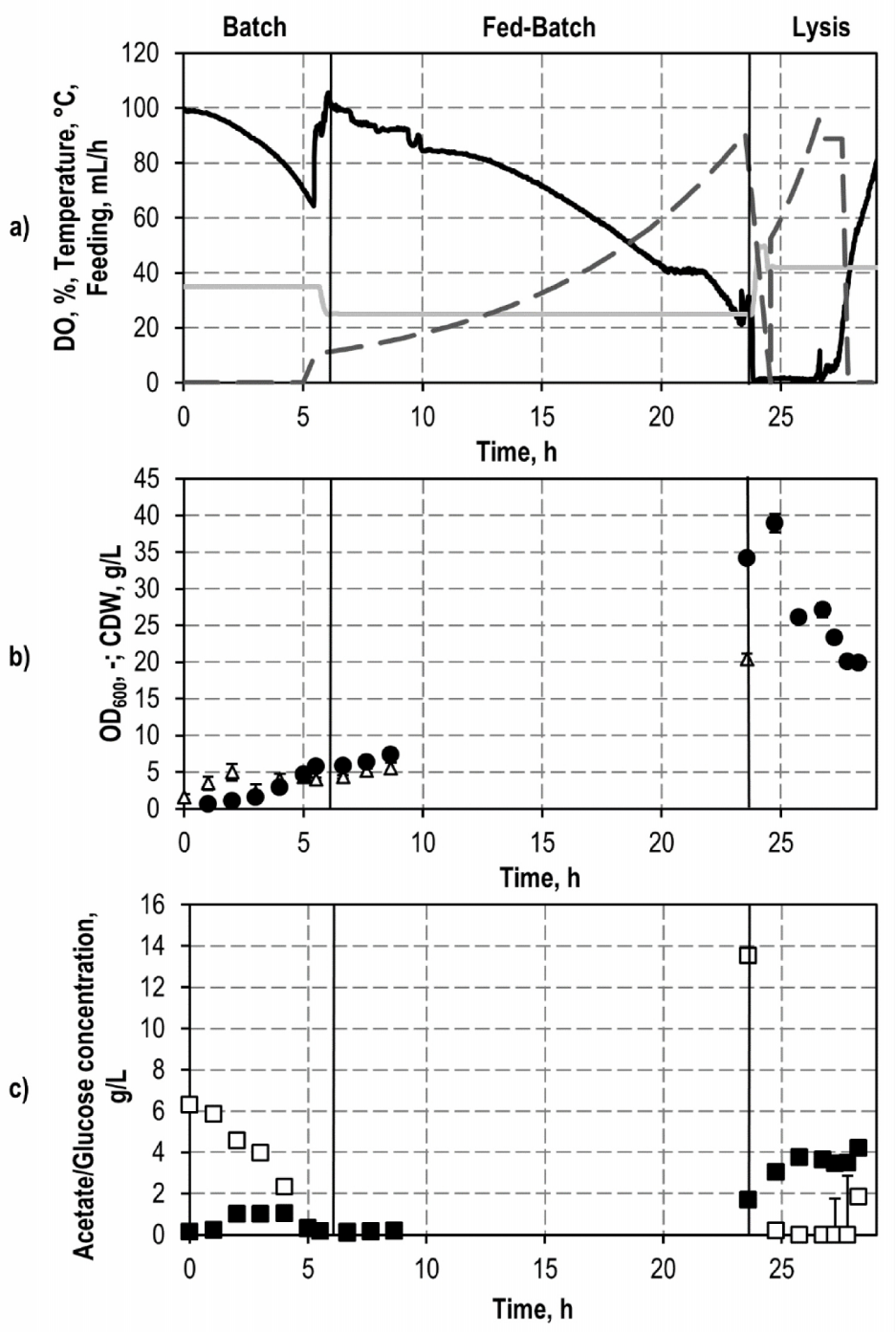

Figure 6-13 Process data from fed-batch cultivation for the production of cellular envelopes of *E. coli* C41 with increased μ_{set} = 0.12 1/h during expression

a) Dissolved oxygen concentration (DO, black line), temperature (dark gray line), feed medium inflow (gray dashed line), b) CDW (Δ), optical density (●), c) glucose (□) and acetate (■) concentration (enzyme kit measurement) are displayed in the course of time. The process conditions were: initial volume = 1.5 L, maximum air flow = 8 L/min, stirring speed = 1000 rpm, pH = 7.2, $\mu_{set\ Expression}$ = 0.12 1/h (200 g/L glucose concentration in feed medium) and $\mu_{set\ Lysis}$ = 0.3 1/h (400 g/L glucose concentration in feed medium) during lysis. Induction of enzyme expression (by 0.1 mM IPTG addition) and lysis by temperature shift to 42 °C are highlighted with a vertical line, *E. coli* C41 cells were used for the cultivation. Standard deviations were calculated and are highlighted, but may be small and thus not visible.

Process data from fed-batch production at increased growth rate during expression are generally comparable to data displayed in section 6.2.2, and the progress of the optical density and the CDW are in good agreement (see Figure 6-13 b)). The progress of the DO is also similar to expression at reduced growth rates with the exception of a stronger decrease during expression (see Figure 6-13 a)). It was caused by the increased growth rate leading to a DO of 22% at 23.6 h process time and occurred despite a maximum air flow of 8.0 L/min. Upon lysis induction and related temperature increase, the DO dropped to 0% and increased again starting at 26.6 h process time, the increase of the DO again being the indicator for protein E-mediated lysis (see sections 6.1.3 and 6.2.2).

Glucose was consumed according to exponential growth during batch-phase and after induction of enzyme expression and initiation of substrate limited feeding (at about 6 h process time) no glucose was detected within the first 3 h of expression (see Figure 6-13 c)). However, an accumulation of 14 g/L glucose was observed at 23.6 h process time after 18 h enzyme expression. Medium inflow was used for feeding during expression and lysis (see Figure 6-13 a)). Notably, no feed medium inflow was initiated at the beginning of lysis due to the accumulated glucose. The accumulated glucose was consumed at 24.8 h process time, after which the feed medium inflow was restarted with an increased glucose concentration in the feed medium. Afterwards, glucose amounts of <0.5 g/L were detected using the AccuCheck™ device, which indicated incomplete metabolising of glucose by the cells. At 28.3 h process time accumulation of 1.8 g/L glucose was detected and the feed medium inflow was terminated. Probably, the air saturation at the end of the expression-phase, being < 40%, was insufficient to provide for all cells and the glucose was consequently not metabolised completely. Similar to data displayed in section 6.1.3, accumulation of glucose during lysis was an indicator of cytoplasm release of the cells at the end of process. The cells no longer required the carbon source after cytoplasm release, which consequently accumulated.

The cells produced about 1 g/L acetate during biomass formation in the batch-phase, which was subsequently consumed within the first h of feeding under substrate limited conditions (see Figure 6-13 c)). After expression at 23.6 h process time, 1.6 g/L acetate was accumulated and the acetate concentration increased to 4.2 g/L at the end of the process. Acetate accumulation at the end of expression and during lysis can likely be referred to the accumulation of glucose in the medium, due to which the growth was not substrate limited.

The cellular envelopes gained in cultivation with μ_{set} = 0.12 1/h were analysed in asymmetric reductions. The results were compared to cellular envelopes from *E. coli* gained at lower growth

rates and no significant difference could be observed (data not shown).

The duration of lysis was compared for processes at with increased growth rates during expression. The general duration between induction of lysis and addition of ampicillin (at DO > 50%) was 1.9 ± 0.5 h in experiments with μ_{set} = 0.075 1/h, 3.8 ± 0.9 h with μ_{set} =0.09 1/h and 4.7 h with μ_{set} = 0.12 1/h (all results on lysis duration are summarised in the appendix Table 12-16). An increased duration of lysis was observed for higher cell densities.

6.2.5 Discussion

In this chapter, combined expression of KR-Cyt b_5 and the FDH-UBC6 with subsequent lysis were established. Both enzymes feature different expression optima, therefore expression at 20 °C, 25 °C and 30 °C was compared. Additionally, the cell strain *E. coli* BL21 was compared to *E. coli* C41 and *E. coli* C43.

Initial experiments were performed in shaking flasks, and subsequently the process was transferred to production in the stirred-tank bioreactor. Lysis in shaking flasks was incomplete, comparable to previous experiments without enzyme expression. Batch processes in a stirred-tank bioreactor for combined expression and lysis were not successful. Using exponential feeding under substrate-limiting conditions, cellular vitality was successfully maintained during expression, and combined expression and lysis was achieved in a stirred-tank bioreactor. In Bläsi et al. (1985), cellular vitality is described to be an important factor for protein E lysis and results obtained in this work are supporting this observation. Combined expression and lysis was possible using IPTG concentrations of 0.1 mM for the expression of oxidoreductases and temperatures of 20 °C or 25 °C, respectively. Higher IPTG concentrations for induction or expression at 30 °C rendered the cells unfit for protein E-mediated lysis. The KR expresses better at higher temperatures, but KR expression is described to be damaging to *E. coli* (Hölsch 2009). Higher expression temperatures probably caused increased expression of the KR. Reduced cellular growth at higher expression temperatures may therefore be related to increased KR expression.

E. coli BL21 cells yielded about 40% more CDW than *E. coli* C41 and *E. coli* C43 cells. This observation is in agreement with results from batch processes for establishing protein E lysis. As discussed in section 6.2.1 the difference in yield of BL21 and the "*Walker*" cells is not caused by the expression, but can be related to be an effect of the mutations introduced to *E. coli*

C41 and *E. coli* C43. The nature of these alterations in the genome is not fully elucidated (Miroux & Walker 1996; Wagner et al. 2008). Therefore, the exact reason for the impaired growth of *E. coli* C41 and *E. coli* C43 is unknown.

Fed-batch production was modified to increase yield of the biocatalyst by using higher growth rates during expression, and the yield of biocatalysts was successfully increased up to 20 g/L prior to lysis. In a batch process described by Langemann et al. (2010), lysis is induced at cell densities of 1-2 x 10^9 cells/mL. In Ra et al. (2010), intermitted feeding is used to produce vaccines from cellular envelopes with up to 22 g/L CDW in semi-defined medium (defined medium with yeast extract as an added component). Thus, results of this work were comparable to results from intermitted feeding in vaccine production. The activity of the biocatalysts was not affected by the growth rate during expression. Notably, growth during lysis was reduced at cell densities of 20 g/L. Probably, at higher densities the cells were suffering from oxygen limitation during lysis. Using improved oxygen supply during lysis by increase of pressure or gassing with oxygen was not tried, as it was still possible to achieve complete lysis. However, such measures could be of interest for future experiments if higher cell densities are aimed for, and it is likely that yields could be increased further by improving oxygen supply.

It was possible to establish a production process for cellular envelopes with a co-immobilised oxidoreductase system featuring FDH and KR. These biocatalytic cellular envelopes were successfully employed in asymmetric reduction, and the best production conditions were discovered by comparing different cell lines, expression temperatures and IPTG concentration using highest biocatalyst activity as the criterion. Subsequently, the biocatalysts were to be characterised thoroughly, the results are described in the following chapter.

7 Characterisation of cellular envelopes with immobilised multi-enzyme system

Subsequently to establishing the combined expression and lysis for the production of biocatalysts with co-immobilised FDH and KR, a characterisation of the obtained biocatalysts was aimed for. The highest biocatalyst activities were achieved using *E. coli* C41 cells and expression at 25 °C. High catalyst activities were of interest, thus all characterisations featured cellular envelopes gained under respective conditions. The characterisation focused on the individual enzymes as well as the biocatalyst in combined asymmetric synthesis, and all related results are described in this chapter.

7.1 Characterisation of immobilised FDH

7.1.1 Quantification of immobilised enzyme molecules

A quantification of the number of immobilised FDH-UBC6 molecules was of interest. Cellular envelopes containing both FDH-UBC6 and KR-Cyt b_5 were compared to cellular envelopes containing FDH-UBC6 only, which also were gained in fed-batch processes in stirred-tank bioreactor from *E. coli* C41 at 25 °C expression temperature.

As described in results on membrane anchoring in chapter 5.1, no thorough characterisation has been possible, since no distinct expression bands were visible in SDS-PAGE. Similarly, SDS-PAGE of cellular envelopes with immobilised enzymes featured no distinct expression bands. Expression amounts again were too low to be distinct from background protein (see appendix Figure 12-3). Immunological detection of FDH was not possible, as there are no commercially available antibodies for the FDH from *M. vaccae* N10 or closely related enzymes. Therefore, quantification using activity assays was aimed for, in which the activity of FDH-UBC6 bound to the cellular envelopes was to be determined under unlimited conditions. The activity of the free enzyme without a membrane anchor was then used to calculate the corresponding amount of enzyme molecules per cellular envelopes. Notably, all data obtained from activity assays is based on the assumption that there is no influence on enzyme activity due to the addition of the membrane anchor and the subsequent attachment to the cytosolic membrane.

For the characterisation the cellular envelope concentrations were adjusted using flow

cytometry (see section 4.7.4) to ensure measurement of linear initial reaction rates. The reference activity at 30 °C of free FDH with 7 mutations and no His_6-tag was determined. Non-linear regression was used to calculate the kinetic properties of free FDH to be a k_{cat} = 4.62 1/s with a corresponding K_m of 1.3 ± 0.1 mM for $NADP^+$ and a K_m of 99 ± 5 mM for sodium formate, respectively. The catalytic properties of FDH-UBC6 were assumed to be comparable. So, for characterisation of FDH-UBC6, 5 mM $NADP^+$ and 0.5 M sodium formate were used at 30 °C to ensure unlimited conditions. Cellular envelopes from multiple experiments on co-immobilisation of FDH and KR were analysed and compared to cellular envelopes, which contained the FDH-UBC6 only and were gained under identical process conditions. The obtained activity data was used to calculate the activity per defined number of cellular envelopes using equation 4-5. Then, the corresponding amount of enzyme molecules per cellular envelope was estimated using the reference activity and equation 4-6. The results are displayed in Figure 7-1.

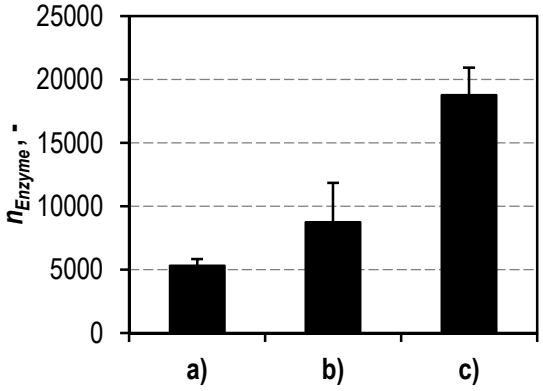

Figure 7-1 Quantification of immobilised FDH-UBC6 molecules in cellular envelopes using activity assays
The estimated numbers of immobilised FDH-UBC6 molecules (n_{Enzyme}) per cellular envelope or cell are summarised for a) co-immobilisation with the KR, b) immobilisation of FDH-UBC6 only and c) whole cells prior to lysis from immobilisation of FDH-UBC6 only. All quantifications were calculated using equation 4-6 and a reference k_{cat} of 4.62 1/s of free FDH.

Quantification of membrane-bound FDH-UBC6 in cellular envelopes was possible. The number of immobilised FDH-UBC6 molecules was 5,297 ± 536, if the KR was co-immobilised, and 8,732 ± 3,106, if only the FDH-UBC6 was immobilised. Notably, the number of immobilised FDH-UBC6 molecules was 65% higher, if only the FDH-UBC6 was immobilised. The corresponding FDH activity per dry weight of the cellular envelopes was calculated using the count to weight correlation (see appendix, equation 12-1), giving 4.07 ± 0.03 U/$g_{dry\ weight}$, if both enzymes were co-immobilised, and 10.11 ± 4.73 U/$g_{dry\ weight}$, if only FDH-UBC6 was immobilised, respectively. The observed effect can likely be referred to

an improved expression of the FDH-UBC6. FDH-UBC6 and KR-Cyt b_5 are co-expressed in a vector with two promotor binding sites. The expression levels are consequently reduced for each of the encoded enzymes. Expression of FDH-UBC6 only was performed using a vector with similar copy number, but just one promotor binding site. Higher expression levels and thus higher amounts of immobilised enzymes are therefore a likely explanation for the observed differences. The number of FDH-UBC6 molecules prior to lysis was 18,779 ± 2,155. Consequently the amount of immobilised enzyme was 46%.

7.1.2 Characterisation of enzyme stability

Biocatalytic preparations gained in this study are used for the asymmetric reduction of ECAA, which is a α-haloketone. Such substances can be damaging to the enzyme activity of the FDH, even though it is not directly involved in the conversion of the ketone. Alterations to the FDH, such as the addition of membrane anchors and membrane immobilisation, can possibly have effects on the enzyme properties. The enzyme stability of membrane-bound FDH-UBC6 in the presence of the α-haloketone ECAA was of interest and therefore determined using activity assays and equation 3-6. The results are summarised in Figure 7-2 and a comparison of all results with data from free FDH is given in Table 7-1.

.

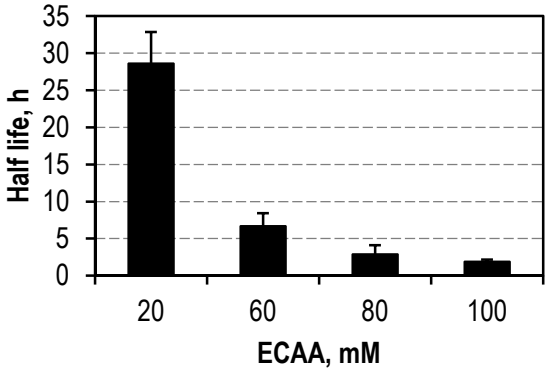

Figure 7-2 Summary of half lives of membrane-bound FDH-UBC6 in the presence of ECAA
The half lives of membrane-bound FDH-UBC6 are compared for ECAA concentrations ≥ 20 mM, determined at 30 °C.

Table 7-1 Comparison of the half lives of membrane-bound FDH-UBC6 with free FDH at different ECAA concentrations
The half life of membrane-bound FDH-UBC6 and free FDH are compared at different ECAA concentrations, determined at 30 °C. The result for 0 mM exceeded the acquisition time of the data, which was 5 d and is therefore only given as > 120 h.

Concentration of ECAA, mM	Half life of membrane-bound FDH-UBC6, h	Half life of free FDH, h
0	> 120	-
1	119 ± 56	-
6	78 ± 35	-
10	47 ± 13	-
20	29 ± 4	74 ± 13
60	6.6 ± 1.8	-
80	2.9 ± 1.3	-
100	1.8 ± 0.3	-
150	-	7.7 ± 2.8

The half life of the membrane-bound FDH-UBC6 was reduced by about 52% by addition of the membrane anchor and subsequent membrane immobilisation, regarding data at 20 mM ECAA (Figure 7-2). So, the impact on the enzyme stability compared to the free enzyme with no membrane anchor was drastic.

7.1.3 Discussion

This chapter describes the results on quantification and characterisation of membrane-bound FDH-UBC6. Quantification was performed using activity assays, since detection using SDS-PAGE or immunological assays was not possible. The number of membrane-bound molecules was approximated using a reference activity of free FDH with the same mutations as FDH-UBC6, but lacking the membrane anchor. The number of FDH-UBC6 molecules in cellular envelopes was determined to be 5,297 ± 536. If only FDH-UBC6 was expressed, the amount of membrane-bound enzymes was increased by 65%. Surface display using autotransporters also offers one step expression and immobilisation with 15,000 to 180,000 immobilised enzyme molecules per cell, depending on the enzyme used (Jose & Meyer 2007; Jose et al. 2012). Regarding the FDH-UBC6, the number of immobilised molecules is lower. However, activity assays were used for the quantification, based on the assumption that the enzyme activity is not altered by addition of the membrane anchor and immobilisation. The mutant FDH employed in this work has seven mutations compared to the wild type FDH from *M. vaccae* N10 and consequently altered catalytic properties (Sührer et al. 2014). The

C-terminus of the FDH is adjacent, but not in in close proximity to the catalytic center (Tishkov & Popov 2004), and C-terminal modifications on FDH have been described to reduce the enzyme activity (Tishkov & Popov 2004; Sührer et al. 2014). The UBC6 membrane anchor has a length of 17 amino acids (leading to 21 additional amino acids at the C-terminus including restriction site). The respective mutant FDH has been characterised with and without a His_6-tag. Addition of the His_6-tag led to 20 additional amino acids at the C-terminus of the enzyme in comparison to the FDH without His_6-tag. The added number of amino acids is therefore comparable to addition of the His_6-tag. FDH with His_6-tag has a k_{cat} of 4.03 1/s (unpublished data), so removal of the His_6-tag increased the catalytic activity by 14.6%. Attachment of the UBC6 membrane anchor is therefore likely to have effects on the enzyme properties of the FDH as well. As described above, additions to the C-terminus reduced the catalytic properties. Consequently, the calculations shown in Figure 7-1 can be assumed to result in too low amounts of immobilised FDH-UBC6 molecules.

46% of the total amount of FDH-UBC6 expression in *E. coli* cells was immobilised to the membrane of the cellular envelopes. Contrarily, 2.7-fold higher FDH-UBC6 activities were detected in the membrane compared to unbound enzyme in the cytoplasm in experiments of membrane immobilisation of the FDH (see section 5.1). The differences can possibly be explained by the differences in expression conditions. Experiments on membrane immobilisation were performed in shaking flasks using different media, at different expression durations, temperatures and IPTG concentrations without the presence of the lysis plasmid within the cell.

This work describes the first application of the C-terminal sequence of UBC6 for the membrane immobilisation of large quantities of heterologous enzymes to the cytoplasmic membrane of *E. coli*. Whether the amount and percentage of membrane-bound FDH-UBC6 molecules can be increased by improved expression conditions or is limited due to the membrane anchor is not known. It is likely that the amount of immobilised enzyme molecules is very specifically depending on the enzyme itself and the membrane anchor used with multiple interlinked effects, which are difficult to distinguish. Furthermore, the maximum amount of protein molecules which can be immobilised to the cytoplasmic membrane is not known, but it is very likely to depend on the protein and membrane anchor used as well.

Since the FDH is to be used for asymmetric reductions featuring the α-haloketone ECAA, the stability of the membrane-bound FDH-UBC6 was determined and compared to the free enzyme. The stability of the FDH was reduced after addition of the anchor and immobilisation to the cytoplasmic membrane (e.g. about 52% regarding the presence of 20 mM ECAA). Either factor, the anchor or the membrane immobilisation, could be responsible for the change. If a fusion enzyme is added C-terminally to the mutant FDH, the half life at 20 mM ECAA is 9.2 h, which is comparable to the half life of membrane-bound FDH-UBC6 (unpublished data). So it is likely, that attachment of C-terminal sequences decreases enzyme stability towards ECAA. Notably, the half life of wild type FDH at 20 mM is < 1 h (Hoelsch et al. 2013), so compared to the initial enzyme, membrane-bound FDH-UBC6 still had a prolonged half life, and application in asymmetric reductions was still possible.

7.2 Characterisation of immobilised KR

7.2.1 Quantification of immobilised KR

Similar to the FDH, the membrane-bound KR-Cyt b_5 was characterised. Comparable to the FDH-UBC6, expression bands in SDS-PAGE were insufficient for quantification using densitometry (see appendix Figure 12-3). Immunological detection too was not possible, as there are no commercial antibodies available. Consequently, quantification using activity assays and a reference activity of the free KR were aimed for the membrane-bound KR-Cyt b_5. Similar to the FDH, the activity of a defined number of cellular envelopes in reductions of ECAA was determined for the KR. The immobilised number of enzyme molecules was calculated using equation 4-6. The reference activity of the free KR without a membrane anchor is 38.29 ± 2.15 U/mg and the K_m is 8.31 ± 1.20 mM for ECAA and 0.40 ± 0.03 mM for NADPH, respectively (Hölsch et al. 2008).

During activity assays for detection of KR activity with ECAA and NADPH as substrates, The (*R*)-alcohol was detected alongside (*S*)-ECHB. The ee_s of membrane-bound and free KR is > 99%, consequently undesired by-product formation was assumed. Asymmetric reductions were performed with cellular envelopes containing KR and FDH, and with cellular envelopes containing FDH only, to verify the assumption. Exemplary data are displayed in Figure 7-3.

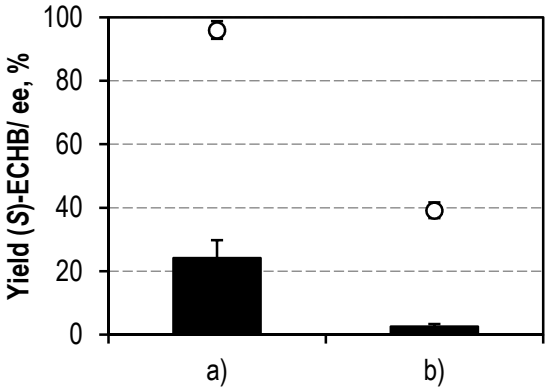

Figure 7-3 Exemplary data on comparison of asymmetric reduction of ECAA in cellular envelopes with and without KR-Cyt b_5
The yield of (*S*)-ECHB (black) in asymmetric reductions of ECAA and the corresponding ee_s % (white) are compared for a) cellular envelopes with FDH-UBC6 and KR-Cyt b_5 and b) cellular envelopes with FDH-UBC6 only. Asymmetric batch reductions were performed at 30 °C for 24 h using 40 g/L cellular envelopes, 5 mM $NADP^+$ and 50 mM ECAA.

Using cellular envelopes without membrane-bound KR it was possible to convert ECAA. Cellular envelopes containing KR-Cyt b_5 yielded about 9-fold more (*S*)-ECHB with an ee_s of 96.0 ± 2.7%, which is below the ee_s of membrane-bound KR-Cyt b_5 as described in chapter 5.2. Cellular envelopes containing no KR had an ee_s of 39.2 ± 2.5%. Thus, by-product formation was detected in cellular envelopes, which do not contain membrane-bound KR.

7.2.2 Discussion

The *E. coli* host genome encodes for several oxidoreductases, of which a number are membrane-associated (Keseler et al. 2013). Cellular envelopes contain membrane-bound enzymes found in the cytoplasmic membrane, the periplasm, and the outer membrane. Due to the modified expression and removal of the cytoplasm, it is likely that one or more enzymes were co-purified and concentrated along with the FDH-UBC6 and KR-Cyt b_5 in the biocatalyst preparation. It can be assumed that these unknown oxidoreductase(s) and the KR-Cyt b_5 compete for substrate and the cofactor NADPH. The observed reduction in the ee_s is thereby caused by the background enzyme(s). The activity of cellular envelopes containing the KR-Cyt b_5 is more than 9-fold higher, which indicates that the KR is superior to the background enzyme(s) under the given conditions and the majority of product is yielded by the KR. Since the nature and catalytic constants K_m and v_{max} of the background enzyme(s) are unknown, it cannot be exactly quantified how much product is yielded by each of the enzymes. The number of membrane-bound KR-Cyt b_5 molecules could therefore not be approximated using activity assays. Reduction of ECAA with whole cell biocatalysts in *E. coli* so far also resulted in ee_s

≥ 99% (Bräutigam 2008), however expression levels of the catalytic enzymes in such experiments were higher compared to cellular envelope biocatalysts.

Notably, no background activity was detected in initial experiments for membrane immobilisation of the KR. In these experiments, different expression conditions (temperature and medium) were used. Moreover, the cell membranes are disrupted during preparation and the periplasm is removed, whereas it remains intact in cellular envelopes. Consequently, background enzyme(s) are likely to have reduced expression levels at lower expression temperatures, and/or are present in the periplasm and were consequently removed during membrane preparation.

One major reason for the use of cellular envelopes as biocatalysts is the removal of the host cell metabolism to prevent undesired by-product formation. The fact that an undesired background enzyme was co-purified in cellular envelopes is unfortunate and unforeseen, as whole cell biocatalysts do not exhibit such background activity in similar applications (Bräutigam 2008). A knockout of the undesired enzyme activity was not performed. The oxidoreductase system immobilised is therefore unfit for these biocatalytic preparations. Since the general properties (regarding e.g. comparison to whole cells and storage properties) of the new biocatalyst were of interest, further experiments in asymmetric reductions were performed and the results are described in the following section.

7.3 Comparison to whole cells

Whole cell biocatalysts are state of the art in biotranformations. Consequently, comparison of cellular envelope biocatalysts to whole cells was aimed for after characterisation of the immobilised enzymes. Notably, quantification of membrane-bound KR-Cyt b_5 was not possible due to undesired by-product formation caused by unidentified host cell enzyme(s) of *E. coli*. To access the general properties of the new biocatalysts, characterisation and comparison to whole cell biocatalysts was performed, even though the present system was unfit for general application, since no knock-out of the undesired oxidoreductase activity was performed. Cellular envelopes were compared to whole cells sampled from the process prior to lysis. Thereby, the amount of background enzyme and consequently of undesired background activity

could be assumed identical in both cellular envelopes and whole cells, and comparison was therefore possible. Experiments were performed to elucidate the best conversion conditions in monophasic aqueous reactions. The performance of cellular envelopes and whole cells was compared in biphasic reactions with ionic liquids. Additionally, the storage properties were compared.

7.3.1 Asymmetric reductions in aqueous phase

Comparison of the new cellular envelope biocatalyst to whole cell biocatalysts was performed in simple one-phase reactions. Different reaction conditions were analysed, and whole cells and cellular envelopes were compared in asymmetric reductions of ECAA.

Determination of reaction conditions

Elucidation of distinct enzyme properties of membrane-bound KR and FDH was not possible (see section 7.1 and section 7.2). Additionally, it was unknown whether higher amounts of KR or FDH were immobilised, as membrane-bound KR could not be quantified. The activity of free KR at 30 °C is 38 U/mg, and that of the free mutant FDH was determined to be 6.3 ± 0.1 U/mg. Which enzyme was the limiting factor, either by activity or abundance, was of interest for the variation of substrate concentrations. Activity assays were used to determine the activity per dry weight of the cellular envelopes in coupled enzymatic reduction of ECAA. The slope was used to calculate the corresponding activity according to equation 4-5. 20 mM ECAA, 5 mM $NADP^+$, 0.5 M sodium formate were used to determine the activity of cellular envelopes containing FDH-UBC6 and KR-Cyt b_5 at 30 °C. Exemplary data are shown in Figure 7-4.

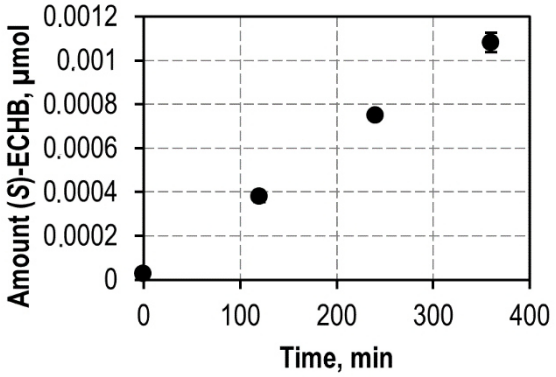

Figure 7-4 Exemplary data for activity determination in cellular envelopes
The average amount of (*S*)-ECHB (●) is summarised in the course of time. Reductions were performed at 30 °C in 200 µL total volume with 10g/L cellular envelopes, using 5 mM $NADP^+$, 0.5 M sodium formate and 20 mM ECAA. The activity per dry weight was calculated from the linear slope according to equation 4-4.

The activity of cellular envelope biocatalysts was determined to be 0.34 ± 0.23 $U/g_{dry\ weight}$. As

described in 7.1.1, the FDH activity in cellular envelopes was 4.07 ± 0.03 $U/g_{dry\ weight}$, which is about one order of magnitude higher. Consequently, the KR and not the FDH activity is limiting in coupled asymmetric reductions of ECAA. The activity of the free KR is about 6-fold higher than that of free FDH, however the FDH activity per dry weight of cellular envelopes was about 10-fold higher. Consequently, the KR was the limiting factor in asymmetric reductions with cellular envelopes, and most $NADP^+$ molecules can be assumed in reduced state within the reaction batch.

Comparisons were therefore performed regarding the amount of $NADP^+$ used. The K_m for NADPH of free KR is 0.40 ± 0.03 mM. Whether the K_m is altered in the membrane-bound KR-Cyt b_5 is not known. 2.5 mM $NADP^+$ would ensure unlimited conditions for free KR due to an at least 5-fold K_m. Different initial $NADP^+$ concentrations were analysed for the determination of best reaction conditions. The results are summarised in Figure 7-5.

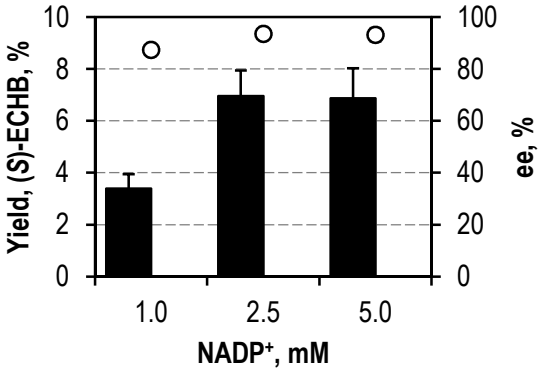

Figure 7-5 Comparison of different initial $NADP^+$ concentrations
The yield of (*S*)-ECHB (black) and corresponding ee_s (white) are summarised for asymmetric reductions of ECAA with cellular envelopes at different $NADP^+$ concentrations. Bath experiments were performed at 30 °C for 24 h with 50 mM ECAA, 0.5 M sodium formate and 10 g/L cellular envelopes.

Increase of the $NADP^+$ concentration from 1 mM to 2.5 mM $NADP^+$ increased the yield by 104%. The use of even higher concentration of $NADP^+$ did not alter the yield significantly. Notably, the ee_s was 87.3 ± 1.7% in reductions with 1 mM $NADP^+$ and 93.6 ± 1.0% in reductions with 2.5 mM $NADP^+$, respectively. So, the overall ee_e is below the ee_s of free KR, which is 99.8 ± 0.4%. This observation can be related to the undesired by-product formation described in 7.2. The host cell enzyme(s) are assumed to have a lower ee_s in reductions of ECAA and produce higher (*R*)-ECHB amounts, which lowers the ee_s of the product. As described above, most $NADP^+$ molecules can be assumed to be reduced to NADPH. The lower ee_s at lower NADPH concentrations indicates a higher activity of the respective enzyme(s) compared to higher NADPH concentrations. Possibly, the background enzyme(s) suffer either

from substrate or product inhibition at high NADPH concentrations or have a lower K_m for NADPH. The kinetic constants of the background enzyme and the membrane-bound KR-Cyt b_5 are unknown, consequently these explanations are based on assumptions only. Generally, reductions at $NADP^+$ concentrations ≥ 2.5 mM were favourable and consequently applied in future experiments.

Subsequently, the amount of ECAA used and the concentration of cellular envelopes were analysed. The amount of ECAA used is limited in aqueous one phase reactions by its solubility, which is 150 mM in 0.1 M sodium phosphate buffer at 30 °C (unpublished data). Moreover, ECAA is prone to hydrolysis and the half life was determined to be 17.6 ± 3.0 h in the reaction buffer, whereas the product alcohol has a half life of > 120 h (data not shown). Little to no substrate was left and no further conversion was observed after 24 h (see appendix Figure 12-4). Concentrations from 20 to 50 mM ECAA were compared to find the best reaction conditions. The amount of cellular envelopes used is limited by the high viscosity of the suspension at high cellular envelope concentrations. It was not possible to work with concentrations > 40 g/L, so cellular envelope concentrations of 10 g/L and 40 g/L were compared in asymmetric reductions. The results on different ECAA and cellular envelope concentrations are summarised in Figure 7-6.

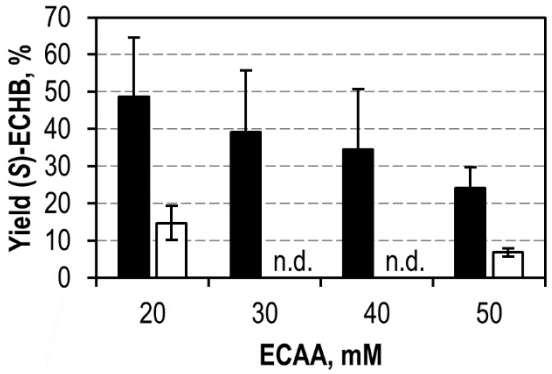

Figure 7-6 Comparison of different ECAA and cellular envelope concentrations
The yield of (*S*)-ECHB is compared for 40 g/L (black) and 10 g/L(white) cellular envelopes at different ECAA concentrations. The batch conversions were performed using 5 mM $NADP^+$ and 0.5 M sodium formate for 24 h at 30 °C.

The use of higher cellular envelope concentrations was favourable and the yield increased with decreasing substrate concentrations, which was as expected. Reduction of initial substrate concentration from 50 mM ECAA to 20 mM ECAA increased the yield by factor 2. The absolute amount of (*S*)-alcohol gained was equal in conversions with 20 mM and 50 mM ECAA, respectively. So, 40 g/L cellular envelopes were required to produce about 14 mM product.

There are several interlinked reasons for this observation. The first is the activity of the cellular envelopes, which was 0.34 ± 0.23 U/$g_{dry\ weight}$. So 40 g/L cellular envelope, equalling 1.52×10^{-2} U were used in one reaction batch of 1.12 mL, containing a total amount of 56 µmol (with 50 mM ECAA) substrate. The theoretically estimated time for the conversion of the total amount of substrate at unlimited conditions would therefore be 61.3 h for 50 mM ECAA and 24.5 h for 20 mM ECAA, respectively. Thereby, the calculations are based on the simplified assumption that the reduction of substrate (by conversion or hydrolysis) does not reduce the activity of the biocatalysts. Thus, the actual time for complete conversion can be assumed even longer. The substrate ECAA is affected by rapid hydrolysis, which decreases the substrate concentration during the reaction. The half life of ECAA is 17.6 ± 3.0 h, so complete conversion is not possible regarding the limited activity of the cellular envelopes. In addition to the substrate degradation, both enzymes are inactivated by the α-haloketone. The half life of the membrane-bound FDH was determined to be 6.6 ± 1.8 h at 50 mM ECAA and 29 ± 4 h at 20 mM ECAA, respectively (see Figure 7-2 b)). The free KR has a half life of 1.3 h in the presence of 20 mM and of 0.2 h in the presence of 150 mM ECAA, respectively (data not shown). Both values were obtained with isolated enzymes. Notably, if the half life of the KR was determined in cell lysate, it was 15.1 h regarding 20 mM ECAA (data not shown). Probably the presence of cellular protein lowered the resulting ECAA concentration, as they reacted with the α-haloketone. Whether such an effect also occurs within cellular envelopes is not clear (data not shown).

Comparison to whole cells

Comparison of whole cells and cellular envelopes was performed at various reaction conditions. Whole cells were sampled from the stirred-tank bioreactor after expression, directly before lysis was induced. For comparability, whole cells too were washed using cross-flow filtration and subsequently stored at 4 °C, as freezing can damage the cell wall (Calcott & MacLeod 1975). Regarding the results above, high catalyst concentrations were favourable. Consequently, all reactions were conducted using 40 g/L cellular envelopes. For comparison, the activity per cell or cellular envelope and not the activity per $g_{dry\ weight}$ was of interest. Whole cells were therefore applied in equal numbers of particles and not in mass. A summary of all data are given in Table 7-2.

Table 7-2 Comparison of whole cells and cellular envelopes in one-phase reactions in aqueous buffer

Comparison of 40 g/L cellular envelopes and whole cells in asymmetric reductions of different amounts of ECAA using different amounts of $NADP^+$. Experiments were performed at 30 °C with 0.5 M sodium formate for 24 h.

		Cellular envelope		**Whole cell**	
$NADP^+$, mM	ECAA, mM	Yield, %	ee_s, %	Yield, %	ee_s, %
5	20	48.6 ± 15.9	96.3 ± 2.4	52.6 ± 14.0	94.7 ± 1.6
5	30	39.1 ± 16.6	95.8 ± 2.9	56.9 ± 0.3	95.2 ± 1.1
5	50	24.1 ± 5.6	96.0 ± 2.7	26.7 ± 4.6	92.6 ± 0.2
1	50	17.3 ± 2.6	80.5 ± 1.5	34.7 ± 2.3	85.7 ± 1.6
1	80	18.0 ± 2.8	80.5 ± 1.5	36.2 ± 2.4	85.7 ± 1.6

The yield in asymmetric reductions was increased by about 2 to 18 percentage points, if whole cells were used instead of cellular envelopes. Depending on the reaction setup, cellular envelopes were thus equal or about 50% inferior to the whole cell biocatalyst, while the ee_s is not significantly different between both biocatalysts. However, the ee_s is generally reduced in reactions with 1 mM compared to 5 mM $NADP^+$, which is in agreement with data from the comparison of different $NADP^+$ concentrations. Notably, the standard deviation of yields is very high due to high standard deviations in reactions. For the calculation of the results multiple experiments using cells and cellular envelopes from different production charges were performed. Statistic deviations due to differences in the production process, flow cytometric analysis and handling are accumulated in these results, making them highly error prone. Whole cell biocatalysts yielded up to 2-fold higher amounts of product. As described above, the amount of KR within the cellular envelopes is the limiting factor in biotransformations, with about 10-fold higher amounts of FDH activity in the cellular envelopes. Contrary to cellular envelopes, whole cells retain their cytoplasm, which contains soluble KR-Cyt b_5 and FDH-UBC6 in addition to the membrane-bound enzymes. As described in section 5.2, 38 ± 8% of all KR-Cyt b_5 molecules are membrane-bound. So, a difference in activity of whole cells and cellular envelopes of about 62% can be expected, if it is assumed that membrane immobilisation does not alter the enzyme activity. Regarding the high standard deviations, the difference of activity is within that range. The biocatalyst concentrations in the reaction were adjusted according to the total particle number and not the mass. Whole cells contain a cytoplasm, and their mass can be expected higher. In the employment of equal masses of biocatalysts, cellular envelopes could be expected even less disadvantageous compared to whole cells.

Analysis of mass transfer

Mass transfer of the substrate is one factor, which influences the performance of whole cell biocatalysts. Diffusion of substrates to immobilised enzymes is limited, thus activities of enzymes can be impaired, which is a problem frequently faced in enzyme immobilisation. Thus it was of interest, if the formation of the lysis pore in cellular envelopes reduces the mass transfer limitation, or is even sufficient to overcome mass transfer limitation completely. Whole cell biocatalyst and cellular envelopes were compared, and to overcome mass transfer completely, biocatalysts were disrupted. Disruption of cells (mechanical or chemical) can have an impact on the enzyme properties. Consequently, several disruption methods were compared. The results are summarised in Figure 7-7.

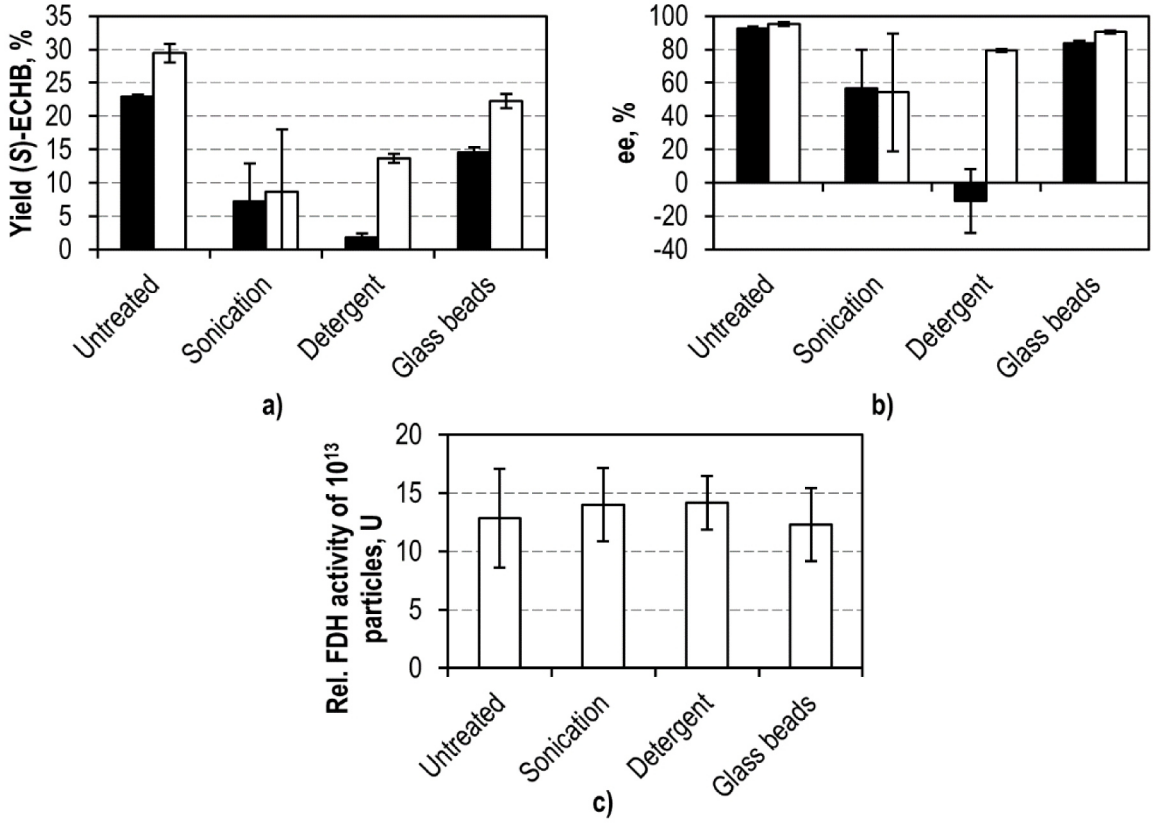

Figure 7-7 Analysis of mass transfer in biocatalysts with immobilised KR-Cyt b_5 and FDH-UBC6
The yield of (*S*)-ECHB (a) and the corresponding ee_s (b) are summarised for asymmetric reductions of ECAA using whole cells (black) and cellular envelopes (white). Batch reductions were performed for 24 h at 30 °C with 4 x 10^9 cellular envelopes or whole cells using 20 mM ECAA, 0.5 M sodium formate and 5 M $NADP^+$. Untreated biocatalysts are compared to those treated with sonication, detergent Popculture® and mechanical disruption using glass beads. The corresponding FDH activities in equivalently treated cellular envelopes are compared in (c).

As displayed in Figure 7-7 a), the activity of whole cells and cellular envelopes was decreased by disruption of the biocatalysts. The decrease of activity was different for each method used for the disruption, which indicates an impact on enzyme activity. Notably, the ee_s too is reduced

in all experiments, the diminution thereby also depending on the method used for the disruption. Low ee_s indicated lower KR activity and product production by the host cell enzyme(s). Consequently, all disruption methods had an effect on KR activity, and it was not possible to analyse mass transfer in biocatalysts with immobilised KR. Additionally, equally treated cellular envelopes were analysed for FDH activity (see Figure 7-7 c)). Contrary to the KR, FDH activity was not significantly changed by disruption of the cellular envelopes regardless of the methods used for the disruption. Effects on enzyme properties by the disruption can therefore be considered a specific effect of the KR. Notably, the FDH activity in disrupted cellular envelopes was not increased, which would be an indicator for mass transfer limitation. Consequently, membrane-bound FDH-UBC6 is not mass transfer limited in cellular envelopes.

Recycling of cellular envelopes

Depending on the biocatalyst, production can be expensive, thus recycling may be required to obtain a profitable process. Therefore, recycling of the cellular envelope biocatalysts was analysed. Successive asymmetric reductions of ECAA were performed using cellular envelopes with membrane-bound oxidoreductases. Batch conversions lasted for 24 h, after which the cellular envelopes were washed and reused. Four successive recycling steps were analysed at different ECAA concentrations. The results are summarised in Figure 7-8.

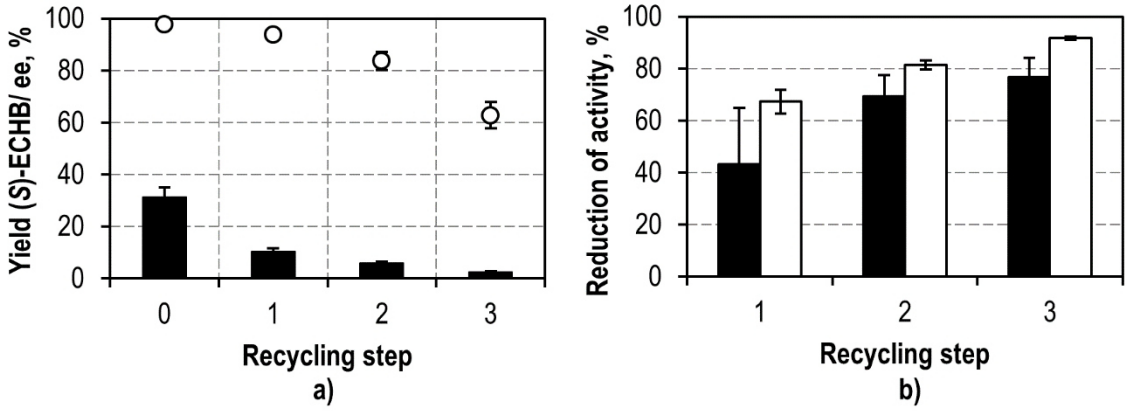

Figure 7-8 Summary of data from recycling experiments
a) The yield of (*S*)-ECHB (●) and corresponding ee_s (○) in asymmetric reductions of 60 mM ECAA after subsequent recycling steps are displayed. Batch reductions were performed with 40 g/L cellular envelopes, 5 mM $NADP^+$ and 0.5 M sodium formate. b) The reduction of activity is compared after successive recycling steps for reductions of 20 mM ECAA (black) and 60 mM ECAA (white), respectively.

Figure 7-8 a) shows exemplary data from a recycling experiment with 60 mM ECAA. The yield of (*S*)-ECHB as well as the corresponding ee_s are summarised. Notably, the yield is more than bisected after the first recycling step. Each successive recycling step causes about 50% reduction of yield. Correspondingly, the ee_s decreases from 97 ± 0.4% after the first use to

62.7 ± 5.0% after the fourth reaction with the same cellular envelopes. Figure 7-8 b) shows a comparison of inactivation at different ECAA concentrations. The higher the ECAA concentration, the higher the inactivation in each step. Notably, even though the 3-fold amount of ECAA is used, the inactivation is not threefold as high. As described above, the KR and FDH are prone to inactivation by the α-haloketone, which explains reduced yields in successive recycling steps. The decrease of the ee_s can be explained by by-product formation from host cell enzyme(s) (see chapter 7.2). Notably, the ee_s decreases with each recycling step. This indicates an increasing ratio of product from the background enzyme(s), which can therefore be assumed more stable towards the α-haloketone than the KR.

To avoid inactivation of enzymes by the α-haloketone ECAA and obtain high yields per reaction batch, reductions in biphasic systems were analysed and the results are displayed in the following section.

7.3.2 Asymmetric reductions in biphasic system using non-water miscible ionic liquids

In the previous section, comparison of whole cells and cellular envelopes in single aqueous phase reactions was performed. One problem in these experiments was strong inactivation of the enzymes by the α-haloketone ECAA. Best yields were obtained at low substrate concentrations, where enzyme inactivation is decreased. Additionally, the substrate suffers from strong hydrolysis and has limited solubility in aqueous buffers. However, maximizing the yield per reaction batch is of interest for application in biotransformations. Biphasic batch reaction systems, in which the substrate is provided from a reservoir in a second liquid phase with improved solubility, offer a solution to this problem. Frequently, organic solvents are used, in which many substrates have improved solubility compared to aqueous buffers. As discussed in section 3.2.6, organic solvents can be disadvantageous and ionic liquids (IL) offer an alternative. For reduction of ECAA, the IL [HMPL][NTF] proved advantageous. It was analysed for asymmetric reductions using cellular envelopes containing membrane-bound KR-Cyt b_5 and FDH-UBC6. Cellular envelopes were compared to the corresponding whole cell biocatalysts. Different substrate concentrations were compared; for handling reasons, only catalyst concentrations of 10 g/L were analysed. Whole cells were used in equivalent particle concentrations to cellular envelopes. The results are summarised in Figure 7-9.

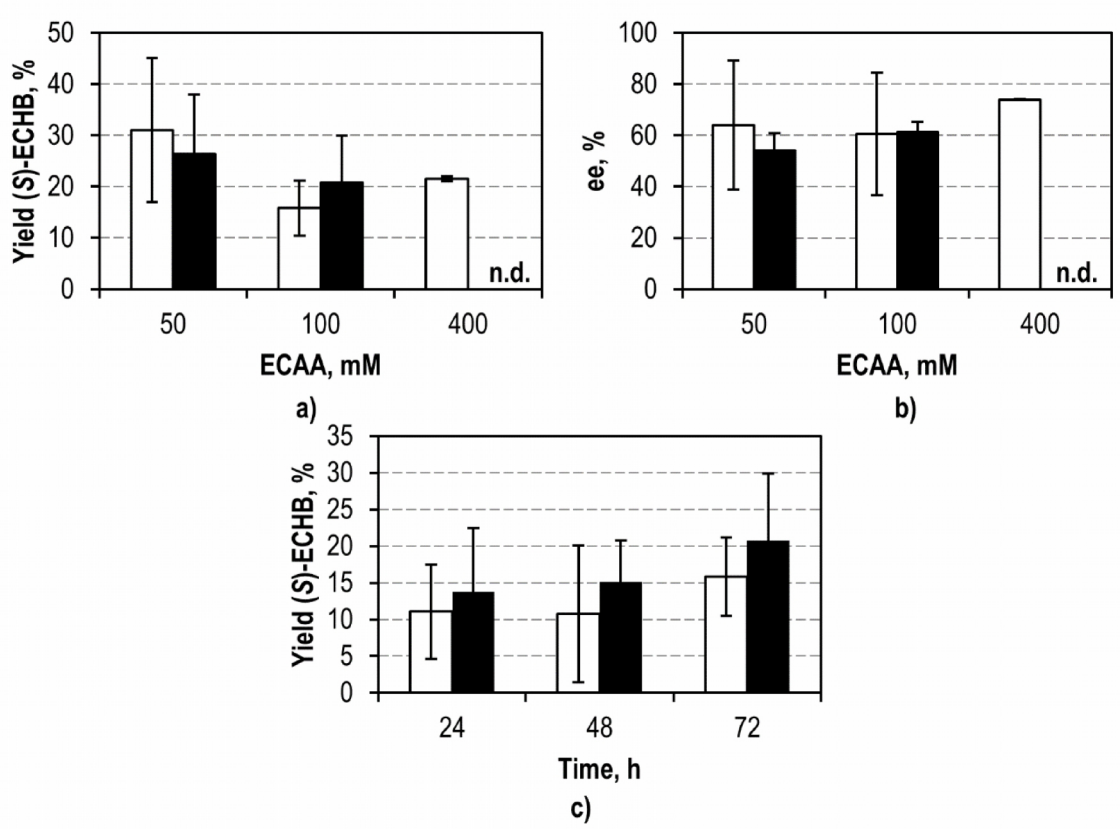

Figure 7-9 Summary of results from asymmetric reduction in biphasic systems
The yield of (*S*)-ECHB (a) and corresponding ee_s (b) in asymmetric reductions in two-phase systems are compared for whole cells (white) and cellular envelopes (black) after 72 h. Reactions were performed at 30 °C using 20% (v/v) [HMPL][NTF], 0.5 M sodium formate, 5 mM $NADP^+$ and 10 g/L cellular envelopes or corresponding particle concentration of whole cells. The yield of (*S*)-ECHB is displayed in the course of time (c) for whole cells (white) and cellular envelopes (black). Reactions were performed similar to a/b using 100 mM ECAA. The displayed ECAA concentration corresponds to the IL phase.

The display of yield in ECAA conversion (see Figure 7-9c)) shows ongoing conversion for 72 h. Afterwards, no further conversion was observed even though substrate was still present (data not shown). Notably, the standard deviation of all data are high due to high standard deviations in yields in reactions. Cells and cellular envelopes from different production charges were used for the calculation of the results in multiple experiments. Statistic deviations due to differences in the production process, flow cytometric analysis and handling are accumulated in these results, making them highly error prone. By using an IL as reservoir of the substrate hydrolysis was successfully prevented, which was one major issue in reductions in aqueous phase. However, it was not possible to obtain complete conversion of the substrate. Inactivation of the enzymes is a likely reason. The log $D_{buffer/IL}$ for the employed system is 1.88 for ECAA and 1.25 for the corresponding alcohols. So, at a concentration of 100 mM ECAA in the IL, 1.3 mM ECAA are in the corresponding aqueous phase. The half life of membrane-bound

FDH-UBC6 in the presence of 1 mM ECAA is 119 ± 56 h, which exceeds the process time of 72 h. The half life of membrane-bound KR-Cyt b_5 could not be determined. Free KR has a half live of 1.3 h in the presence of 20 mM ECAA (data not shown). It is therefore likely that KR inactivation is the reason for inactivation of cellular envelopes and whole cells. Regarding the yield after 72 h (see Figure 7-9a)) and in the course of time (see Figure 7-9 c)), cellular envelopes and whole cells displayed no significant difference in yield of (*S*)-ECHB. So, contrary to monophasic experiments, whole cell biocatalysts were not advantageous. As described above, the concentration of ECAA in the aqueous phase is 1.3 mM if 100 mM ECAA and 0.7 mM if 50 mM ECAA are dissolved in the IL phase, respectively. Substrate concentrations are low in comparison to monophasic reactions. Whole cell biocatalysts are prone to mass transfer limitation due to the cell wall and contain non-immobilised enzymes in their cytoplasm. As already discussed in section 7.3.1 it is possible that this counterbalances reduced enzyme activity due to mass transfer limitation at high substrate concentrations. At lower substrate concentration higher amounts of catalysts were probably insufficient to counterbalance reduced activity of the enzymes due to mass transfer limitation, thus rendering whole cell biocatalyst performance equal to cellular envelopes. These results would therefore indicate an improved mass transfer of substrates in cellular envelopes due to the lysis pore. Analysis of mass transfer limitation of the KR was not possible due to inactivation of the enzyme by disruption of the cells (see section 7.3.1). The FDH in cellular envelopes was demonstrated not to be limited by mass transfer (see section 7.3.1).

The ee_s was decreased in all conversions compared to the ee_s of free KR (see Figure 7-9 b)), and no significant difference between whole cell and cellular envelope biocatalysts was observed. As outlined in chapter 7.2, decreased ee_s can be explained by undesired by-product formation by enzyme(s) from the host cell metabolism. The more product is formed by the host cell enzyme, the lower the ee_s (see chapter 7.2). Generally, the ee_s was lower compared to reactions in monophasic systems. These results indicate that the background enzyme(s) have a higher activity at lower ECAA concentrations and are inhibited either by the substrate or the products, respectively. Additionally, it is likely that the host cell enzyme(s) are more stable in the presence of the α-haloketone than the KR, because the amount of (*R*)-alcohol increases with time.

Summarising the results, it was possible to perform reductions in biphasic systems using a non-water miscible IL with cellular envelopes containing membrane-bound FDH-UBC6 and KR-Cyt b_5. It was not possible to obtain complete conversion due to enzyme inactivation.

Additionally, the ee_s of the products was reduced compared to the free KR, probably due to increased by-product formation from host cell enzyme(s) at lower substrate concentrations. The yield and ee_s of cellular envelopes and whole cells was not significantly different, thus cellular envelopes performed equal to whole cells. Generally, application of cellular envelope biocatalysts in biphasic systems is not fit for application due to low ee_s and incomplete conversion of substrate.

In addition to performance of the biocatalysts, the morphological stability of the biocatalysts towards mechanical stress during the stirred reaction was of interest. The results are discussed in the following paragraph.

Stability of whole cells and cellular envelopes

In addition to the comparison of the catalytic properties of cellular envelopes and whole cells the morphological stability was of interest. During reductions with biocatalysts, the substrate ECAA as well as mechanical stress could be damaging to the cells and cellular structure. Changes in particle size due to disruption and cellular vitality can be monitored using flow cytometry as described in section 4.7.4 and section 6.1.1. The morphological stability of whole cells and cellular envelopes was compared in the course of asymmetric batch reductions for two-phase and single-phase reactions. Exemplary data are shown in Figure 7-10.

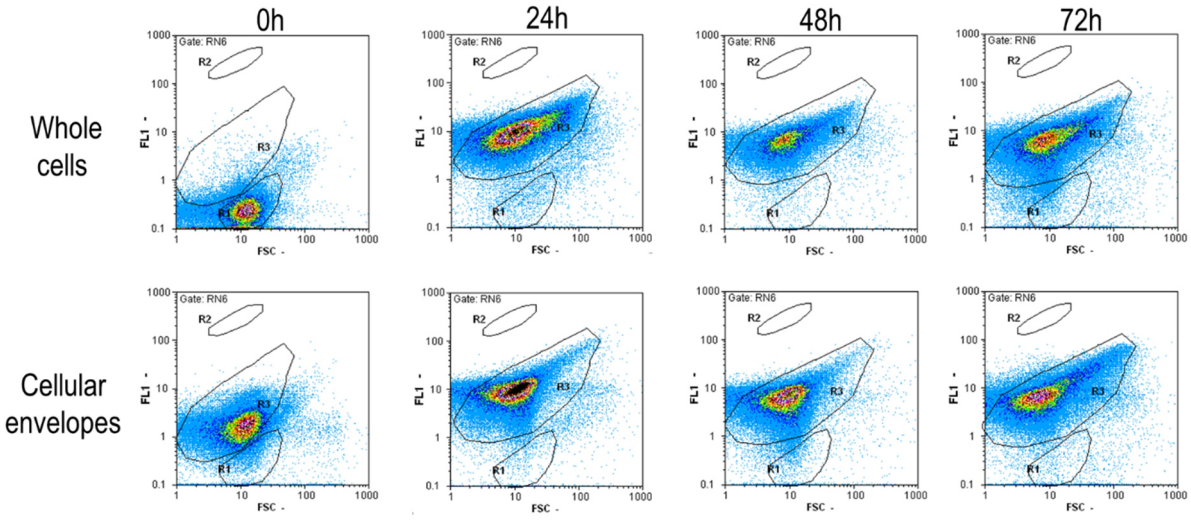

Figure 7-10 Comparison of morphology of whole cells and cellular envelopes in two-phase reactions using flow cytometry

2-Parameter dot plots are shown for FSC and $DiBAC_{[4]}(3)$ staining (FL1). Whole cells and cellular envelopes are compared at intervals in asymmetric batch reductions in two-phase systems. Only signals with positive RH414 staining are shown (gate RN6) with (R1) living cells, (R2) dead cells and (R3) cellular envelopes.

Flow cytometric data of cellular envelopes and whole cells were compared. Cellular envelopes largely maintain their morphological stability for 72 h. After 72 h increased scattering outside

the R3 polygon can be observed, which indicated beginning disruption of cellular envelopes. Contrary to cellular envelopes, the population of whole cells (see Figure 7-10, gate R1 at 0 h) shifts to the position of the R3 cellular envelope gate within the first 24 h. This is a mark for high depolarisation of the whole cells. Prior to application whole cells were stored at 4 °C to prevent depolarisation by the formation of ice crystals during freezing. Depolarisation is therefore caused by the reaction and is an indicator for damages to the cell wall during the reaction. Whether these damages impair the performance of whole cells in asymmetric reductions in two-phase systems is highly speculative and was not further analysed. After depolarisation of the cells, the population is maintained intact. Whole cells too are morphologically stable towards stirring in asymmetric reductions for 72 h. Subsequently, first disruption is indicated by increased scattering of signals outside the polygon similar to cellular envelopes. Notably, the imaging was only for qualitative not quantitative analysis, and the amount of disrupted cellular envelopes or whole cells in the scatter around the polygonal gates cannot be quantified using flow cytometry. So, morphological stability of cellular envelopes during stirred reactions was comparable to whole cell biocatalysts.

As described above, whole cell biocatalysts were stored at 4 °C to prevent disruption of the cell wall by ice crystals. The different storage properties of whole cells and cellular envelopes were therefore of interest and are discussed in the following section.

7.3.3 Storage properties

Storage properties are an important factor for the evaluation of biocatalysts. Whole cell biocatalysts can be stored at 4 °C and −20 °C in aqueous buffers or lyophilised and thus stored as a dried formulation. The activity of the enzymes as well as the morphology of the biocatalyst can be affected by prolonged storage or different formulation. Thus, the storage properties of whole cell biocatalysts and cellular envelopes were compared regarding storage in aqueous buffers at 4 °C and −20 °C. Samples stored at −20 °C were successively frozen and unfrozen to take samples. The activity of the biocatalysts in asymmetric reductions of ECAA was compared successively. Data from activity assays is shown in the appendix. Product yields after different time intervals were used to calculate the corresponding half lives of the biocatalysts. The half life of whole cells was 15.8 ± 4.5 d for storage at 4 °C and 17.8 ± 5.8 d for storage at −20 °C, respectively. The half life of cellular envelopes was 12.5 ± 2.5 d for storage at 4 °C and 12.3 ± 2.3 d for storage at −20 °C, respectively. Regarding the data, the decrease in activity was independent of the mode of storage. Additionally, the stability of whole cell biocatalysts and cellular envelopes was not significantly different. Along with the yield and activity of the

biocatalysts, the ee_s in asymmetric reductions was compared. The results are displayed in Figure 7-11.

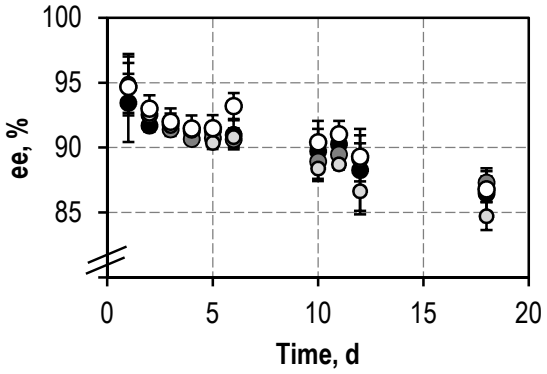

Figure 7-11 Comparison of ee_s of biocatalysts at different storage modes
The ee_s in asymmetric reductions is compared for whole cells stored at 4 °C (black) and −20 °C (dark grey) and cellular envelopes stored at 4 °C (light grey) and −20 °C (white). Batch reductions were performed at 30 °C for 24 h using 4×10^9 whole cells or cellular envelopes in 500 µL with 20 mM ECAA, 5 mM $NADP^+$ and 0.5 M sodium formate.

The ee_s between whole cell and cellular envelope biocatalysts was not significantly different. Additionally, the ee_s decreased during storage from 94.5 ± 2.3% to 86.3 ± 1.8%. Decline in ee_s is an indicator for KR inactivation within the biocatalyst. As described in 7.2, (*R*)-ECHB is assumed to be produced by unidentified host cell enzyme(s). A decreasing ee_s therefore indicated higher ratios of activity from the background enzyme. Consequently, inactivation of the KR is likely to cause inactivation of the biocatalysts. Whether the FDH within the biocatalysts is affected could not be determined.

In addition to the comparison of activity during storage, the morphology of the biocatalysts was compared using flow cytometry after different storage times. The data are summarised in Figure 7-12.

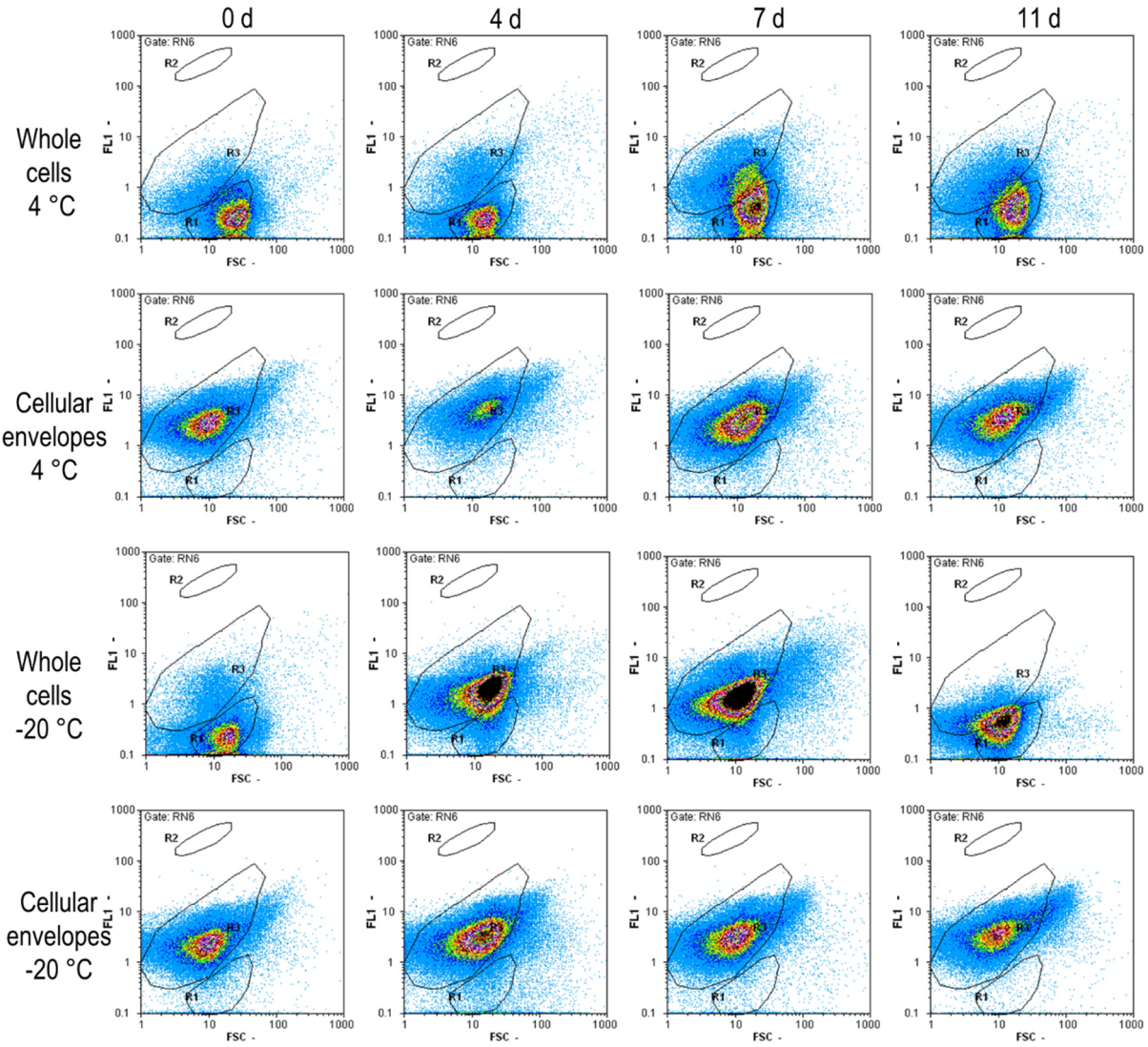

Figure 7-12 Comparison of morphology during storage at different conditions using flow cytometry

2-Parameter dot plots are shown for FSC and $DiBAC_{[4]}(3)$ staining (FL1). Whole cells and cellular envelopes stored at different conditions are compared. Only signals with positive RH414 staining are shown (gate RN6) with (R1) living cells, (R2) dead cells and (R3) cellular envelopes.

The morphology of whole cells and cellular envelopes stored each at 4 °C and −20 °C was compared. The populations of cellular envelopes are located in the R3 gate (see Figure 7-12). Cellular envelopes show no change in position and no increased scattering of populations regardless of the storage method used. The population of whole cells is located in gate R1 (see Figure 7-12). Whole cells stored at 4 °C show increasing amount of scattering and depolarisation of the cells. The population of whole cells stored at −20 °C shifts to the position of cellular envelopes in gate R3. Additionally, the population shows increased scattering of signals within storage time. As discussed in section 7.3.2, depolarisation of the whole cells is an indicator for damages to the cell wall. Strong depolarisation of whole cells stored at –20 °C

is probably caused by the formation of ice crystals during successive freezing, which damage the cell wall. Notably, the decrease in activity and correspondingly the half life as well as the ee_s of whole cells biocatalyst in asymmetric reductions was not affected by the damages to the cell wall (see Figure 7-12).

In addition to storage in aqueous buffers, lyophilisation was attempted for cellular envelopes with immobilised FDH-UBC6 and KR-Cyt b_5. It was possible to lyophilise cellular envelopes and perform asymmetric reductions with cellular envelopes which were lyophilised. Generally, lyophilisation and storage was possible while the structure of the biocatalysts was maintained. However, lyophilised cellular envelopes were prone to agglomeration. After solubilisation, quantification in flow cytometry was difficult due to agglomeration, which caused high standard deviations in asymmetric reductions. So, comparison to cellular envelopes stored in aqueous buffers was not possible (data not shown).

7.3.4 Discussion

In this chapter results on comparison of new cellular envelopes biocatalysts with immobilised FDH-UBC6 and KR-Cyt b_5 to whole cell biocatalysts are described. During characterisation of the distinct enzymes within the cellular envelope, by-product formation of the undesired enantiomer by host cell enzyme(s) was observed. To have the same background activity in both biocatalysts, whole cells sampled from the process directly before lysis were used for the comparison.

The activity of cellular envelopes containing membrane-bound KR and FDH in asymmetric reductions of ECAA was 0.34 ± 0.23 U/$g_{dry\ weight}$ in asymmetric reductions, whereas the same cellular envelopes have an FDH activity of 4.07 ± 0.03 U/$g_{dry\ weight}$. So activity of the FDH is about one order of magnitude higher, and the KR activity was consequently the limiting factor in asymmetric reductions. The activity of the free KR is 38 U/mg for ECAA, which is the highest known activity of this enzyme for any substrate. The activities for other substrates, which have highly reduced solubility in aqueous buffers, are considerably lower (e.g. 8.57 ± 0.49 U/mg for pentafluoroacetophenone (Hölsch et al. 2008)), consequently no other substrates were analysed. Comparison in single, aqueous phase using the different reaction conditions for cellular envelopes revealed equal or better performance of whole cell biocatalysts. However, standard deviations in reactions were high. The synthesis enzymes were immobilised using C-terminal membrane anchors, which is described to be incomplete (Kutay

et al. 1993; George et al. 1989). Whole cells contain non-immobilised enzymes in their cytoplasm. Better performance of whole cells is therefore probably due to higher catalyst numbers. Generally, ECAA was not completely converted to the product with yields < 49%. Substrate hydrolysis and inactivation of the KR by the α-haloketone are likely the cause for low yields. Recycling of cellular envelopes was also not successful due to enzyme inactivation. Such inactivation is also described for other enzymes used in asymmetric reduction of ECAA and is a frequently faced problem (Shimizu 1999; Kizaki et al. 2001).

Reactions in biphasic systems with non-water miscible IL were analysed and compared for cellular envelopes and whole cell biocatalysts. Conversion was incomplete, probably due to inactivation of the KR, also at low substrate concentrations, regardless whether cellular envelopes or whole cells were used. Yields of up to about 30% using 50 mM substrate were achieved (with a corresponding ee_s of about 74%), which is low compared to data from the literature. Reduction of ECAA with recombinant whole cell biocatalysts from *E. coli* is a frequently studied topic. Using the IL [HMPL][NTF] > 90% product yield was obtained from 600 mM substrate by Bräutigam (2008) with *E. coli* whole cell biocatalysts with co-expressed alcohol dehydrogenase from *Lactobacillus brevis*. Other publications use biphasic reaction systems with organic solvents, e.g. *n*-butyl acetate, in which up to 2.5 M substrate were converted in 34 h with a yield of 85% and an ee_s of 99% using *E. coli* whole cell biocatalysts containing a recombinant carbonyl reductase from *Candida magnoliae* and a glucose dehydrogenase (GDH) for cofactor regeneration (Kizaki et al. 2001; Ye et al. 2011).

In analysis of mass transfer limitation of the KR, inactivation of the KR by different disruption methods did not enable a characterisation of the KR regarding mass transfer limitation. The use of detergents as well as sonication can have negative effects on enzyme activity (Villamiel & De Jong 2000; Kirk et al. 2002; Iyer & Ananthanarayan 2008). The disruption in a rocker bar mill using glass beads can cause heat inactivation of enzymes by mechanical friction (Ahern & Klibanov 1985). It is very likely that the KR sustained inactivation by all disruption methods. Notably, membrane-bound FDH in cellular envelopes was not limited in mass transfer. So, neither immobilisation to a surface nor the cell wall caused limitation of the FDH-UBC6. Notably, the cell wall of *E. coli* contains the FocA transporter for formate import into the cells without ATP requirement (Wang et al. 2009). This channel probably mediates sufficient formate import to eliminate mass transfer limitation regardless of the existence of the lysis pore.

It is demonstrated in the literature that cellular envelopes maintain structural and morphological components of the cell surface of their living counterpart (Langemann et al. 2010). Analysis of morphology showed that cellular envelopes maintain their morphology during stirred reactions. Stability of cellular envelopes during stirred reactions and storage at different conditions was equal to or better than whole cells. Notably, whole cell biocatalysts depolarised during conversions in biphasic reaction systems with the IL [HMPL][NTF]. Significant depolarisation of whole cell biocatalysts due to the IL is also described in Fu (2013) and Weuster-Botz (2007) and can probably relate to decreased membrane integrity, which is described to be reduced to ~30% after 5 h incubation time at 20% (v/v) IL (Weuster-Botz 2007).

The general performance of cellular envelopes makes them an interesting platform technology which can be applied for multiple enzyme systems. Performance in stability and mass transfer of substrates was equal or better compared to whole cells. Cellular envelopes containing membrane bound KR and FDH can be regarded a model system, but are not suitable for industrial application. Low activity, instability and undesired competing host cell enzymes within the cellular envelopes makes this special system undesirable. Knock-out of host cell enzymes, or the use of a different oxidoreductase to replace the KR could be a solution to the issue.

This is the first successful attempt for the production of cellular envelopes, which contain a working multi-enzyme system and were extensively studied. These studies gave insight to the potential as well as obstacles and issues of the new biocatalyst system. Since, these are the first results on the new biocatalyst preparation, comparison to existing data are not possible and problems were consequently unpredicted.

8 Production and characterization of cellular envelopes with β-galactosidase[1]

The effects of membrane immobilisation could not be characterised thoroughly in cellular envelopes containing the multi-enzyme system. Due to a lack of commercially available specific antibodies for FDH and KR, a quantification using immunological detection methods was not possible. Therefore, immobilisation of the β-galactosidase (β-gal) from *E. coli* was chosen for which a variety of antibodies can be purchased. This was the first transfer of insights gained during the development of cellular envelope production with membrane bound oxidoreductases to be applied for a different enzyme. Cellular envelopes were produced containing β-galactosidase immobilised with the Cyt b_5-anchor. Subsequently, the amount of membrane-bound enzyme molecules per cellular envelope was quantified, and the effects of immobilisation on enzyme properties were characterised.

8.1 Membrane anchoring of β-galactosidase

Membrane immobilisation of the β-galactosidase was achieved using the Cyt b_5-anchor. The anchor was cloned C-terminally to the β-gal gene, creating the β-gal-Cyt b_5 fusion protein. Membrane immobilisation was validated by expression of the β-gal-Cyt b_5 and subsequent membrane preparation. SDS-PAGE were analysed, exemplary data are shown in Figure 8-1. 24 ± 16% β-gal-Cyt b_5 of the total amount of molecules were detected in the membrane preparation using SDS-PAGE and densitometry. β-gal-Cyt b_5 activity was determined by the detection of *o*NPG hydrolysis to *o*NP at 436 nm. It was possible to detect β-gal activity in both membranes and soluble protein. 24 ± 13% of the total activity were membrane-bound, which is in agreement with densitometry data. As discussed in chapter 5.5, the loss of membranes during preparation impairs the results in favour of soluble protein. A thorough quantification from membrane preparations was therefore not possible. The next step was combined expression and protein E-mediated lysis for the production of cellular envelopes with immobilised β-gal-Cyt b_5.

[1] Part of results described in this chapter were published in Sührer et al. 2015

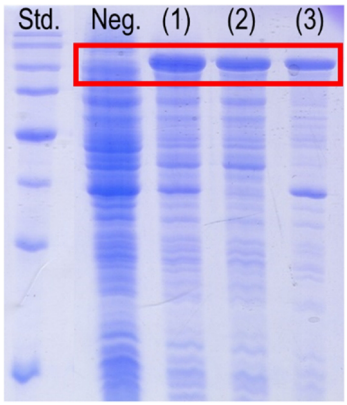

Figure 8-1 Exemplary SDS-PAGE from membrane purifications with β-gal-Cyt b_5
SDS-PAGE from membrane purifications with immobilised β-gal-Cyt b_5: (1) total cleared lysate, (2) soluble protein after membrane removal with ultracentrifugation and (3) membrane-bound enzyme. The β-gal-Cyt b_5 has a size of about 119 kDa, the distinct expression signals are highlighted

8.2 Production of cellular envelopes with immobilised β-galactosidase

Cellular envelope biocatalysts with high numbers of β-gal-Cyt b_5 molecules were aimed for, to provide sufficient catalytic activity. As described for the immobilisation of the multi-enzyme system, high expression levels of membrane proteins can be damaging to the cells. In previously described experiments, cellular vitality was highly crucial for protein E-mediated lysis after expression. For the comparison of different expression levels, the low to medium copy number plasmid pCOLADuet™ and the high copy number plasmid pET28a were compared. Similar to the immobilisation of the multi-enzyme system, cultivation in a stirred-tank bioreactor was used to validate industrial applicability and to ensure cellular vitality by supply with sufficient amounts of dissolved oxygen and nutrients. The general procedure in stirred-tank bioreactor experiments was also adapted from chapter 6.2. The β-galactosidase is best expressed at 37 °C for 3 h, but it may also be expressed over night at reduced temperatures. So, batch processes at 35 °C and fed-batch processes at 25 °C expression temperature were compared to find the best expression conditions. Process steps and expression conditions for the fed-batch process were similar to experiments described in 6.2.2 with a $\mu_{set} = 0.075$ 1/h. In batch processes, cells were grown to $OD_{600} \sim 0.5$ and subsequently induced. Expression lasted for 3 h until lysis was induced. *E. coli* C41 cells were used, as they proved superior in previous experiments (see section 6.2.4). IPTG was used for induction of β-gal-Cyt b_5 expression. After protein E-mediated lysis, cellular envelopes were washed using cross-flow filtration and analysed for biocatalytic activity. It was possible to obtain successful overexpression and lysis in all

experimental setups with IPTG concentrations of 0.1 mM, regardless whether batch or fed-batch mode was used. Similar to immobilisation of the multi-enzyme system, higher IPTG concentrations rendered the cells unfit for protein E-mediated lysis. All processes with respective conditions offered lysis yields of >99.0%. Process data from fed-batch production was in accordance to data displayed in section 6.2.2 (see appendix Figure 12-6). Exemplary data from a batch process is displayed in Figure 8-2

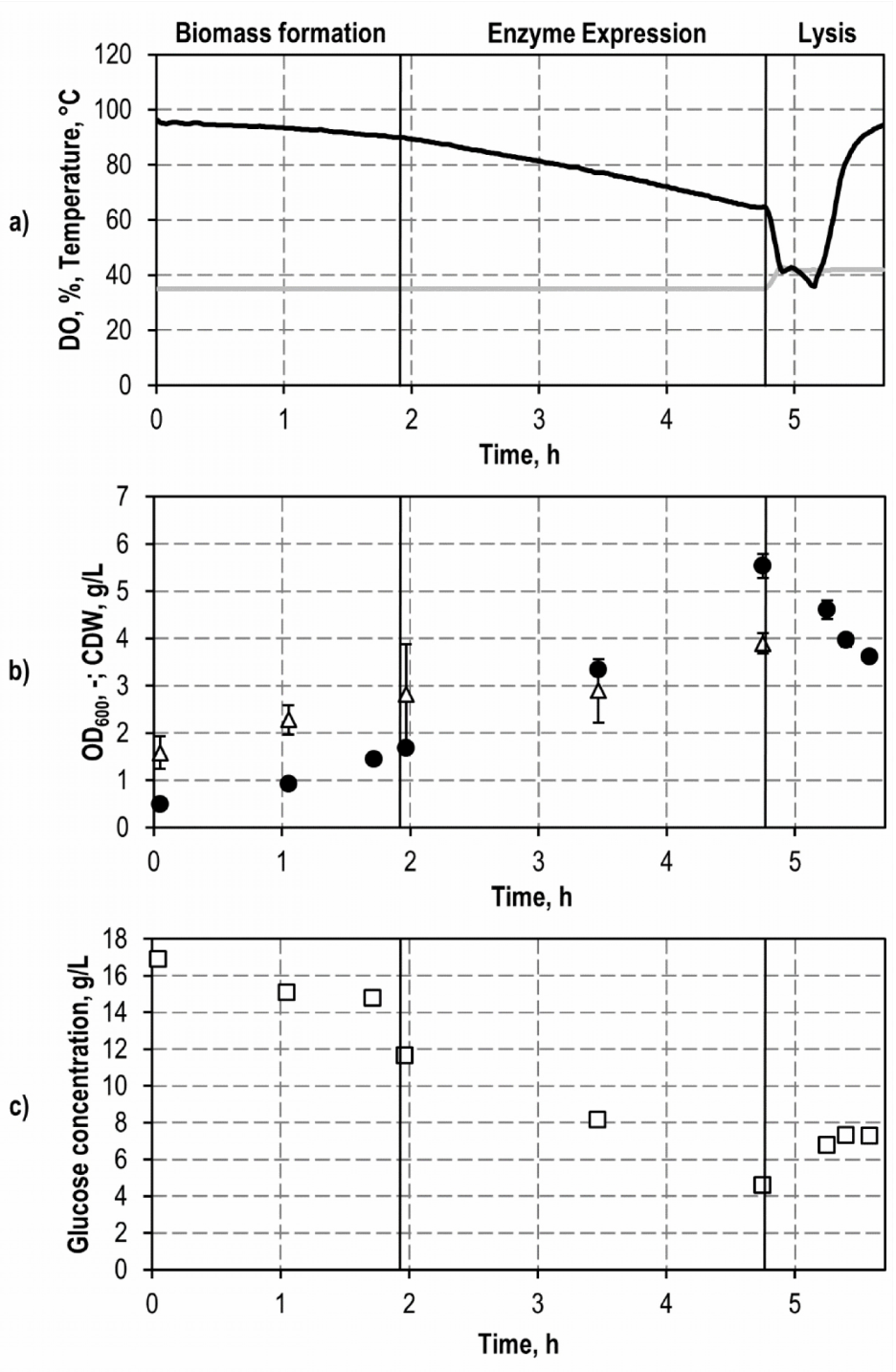

Figure 8-2 Exemplary process data from batch production of cellular envelopes with immobilised

β-gal-Cyt b_5 in a stirred-tank bioreactor
a) The dissolved oxygen concentration (DO, black line), the temperature (dark gray line), b) the CDW (Δ), the optical density (●) and c) the glucose concentration from (enzyme kit)are dis played in the course of time. The process conditions were: total volume = 1.5.0 L, maximum air flow = 8 L/min, stirring speed = 1000 rpm, pH = 7.2. The induction of enzyme expression (by 0.1 mM IPTG addition) and lysis by a temperature shift to 42 °C are highlighted with a vertical line, *E. coli* C41 cells were used for the cultivation. Standard deviations were calculated and are highlighted, but may be small and thus not visible.

Similar to fed-batch processed described in chapter 6.2, batch processes for combined expression and protein E-mediated lysis in stirred-tank bioreactors were divided into three steps. The temperature was 35 °C during biomass formation and expression of the β-gal-Cyt b_5, and 42 °C during lysis (see Figure 8-2 a)). The DO declined according to exponential growth during biomass formation and enzyme expression (induction at 1.9 h). Upon induction of lysis at 4.7 h process time, the DO decreased to 40% and declined further during lysis according to exponential growth until 5.2 h process time, after which the DO increased to 93% at 5.6 h (see Figure 8-2 a)). Notably the maximum DO after lysis was not 100%, since the DO probe was calibrated at 35 °C. At the end of the process the temperature of the medium was 42 °C, and consequently had a reduced maximum oxygen solubility. Increase of the DO at the end of lysis again was an indicator for successful protein E-mediated lysis.

The CDW increased according to exponential growth during biomass formation and enzyme expression up to 3.9 g/L after 5.2 h process time (see Figure 8-2 b)). As described in sections 6.1.3 and 6.2.2, no further CDW was determined after lysis induction due to insufficient separation of cells and medium by centrifugation after lysis and release of the cytoplasm.

The optical density progressed according to exponential growth during the first two process steps up to a value of 5.5 (see Figure 8-2 b)). After lysis induction at 5.2 h process time, the optical density declined, which was an indicator for protein E-mediated lysis as described in section 6.1.2.

The glucose concentration was about 17 g/L at the beginning of the process and it declined in accordance with exponential growth to about 7 g/L directly before lysis. After lysis induction no further glucose consumption can be observed. The $Y_{XS,\mu}$ during exponential growth was 0.23, which is below the value for *E. coli* C41 described in section 6.1.3. The lower yield can probably be referred to the expression of the β-gal-Cyt b_5 and the related metabolic stress of the cells.

The lysis duration between induction and addition of ampicillin (DO ≥50% after lysis induction) was 0.8 h, which is less than half the time needed in fed-batch processes described in section 6.2.4. The final CDW in batch process production of cellular envelopes with

immobilised β-gal-Cyt b_5 was 3.9 ± 0.2 g/L, which is below the yields obtained in batch and fed-batch processes in previous chapters. Thus, the observation is in accordance with data described in section 6.2.4, where it was noted that the higher the CDW, the longer was the lysis duration.

Cellular envelopes from all processes exhibited catalytic activity. So, it was possible to generate cellular envelopes with membrane-bound β-gal-Cyt b_5 using cultivation in a stirred-tank bioreactor. The cellular envelopes gained under different conditions (batch and fed-batch process) containing the immobilised β-gal-Cyt b_5 were analysed for enzyme activity. According to the dry weight to particle concentration correlation (see appendix, equation 12-1), the amount of activity per dry weight of cellular envelopes was estimated. The results for all different experimental setups are compared in Table 8-1.

Table 8-1 Summary of process parameters and results.
Expression was chemically induced in all experiments with 0.1 mM IPTG after biomass formation in a batch phase at 35 °C.

	Plasmid	**Expression duration, h**	**Expression temperature, °C**	**CDW concentration prior to lysis, g/L**	**Activity per dry weight cellular envelopes, $U/g_{dry\ weight}$**
Fed-batch	pCOLA Duet™	18	25	8.5 ± 0.3	312 ± 29
Batch	pCOLA Duet™	3	35	4.3 ± 0.3	632 ± 250
Batch	pET28a	3	35	3.9 ± 0.2	753 ± 190

Both batch processes yielded more than 2-fold higher activities per dry weight than those obtained in fed-batch cultivation with up to 753 ± 190 $U/g_{dry\ weight}$, however the final CDW was bisected. Thus, the total activity obtained in all processes was roughly the same. As discussed for the multi-enzyme system and demonstrated in section 6.2.4, increase of final CDW concentrations prior to lysis is possible, therefore higher amounts of cellular envelopes with membrane bound β-gal-Cyt b_5 could be produced. Since the maximum amount of enzymes per cellular envelope was of interest, all further experiments employed cellular envelopes that were produced in batch mode with the pET28a vector. The characterisation of cellular envelopes with immobilised β-gal-Cyt b_5 is described in the following sections.

8.3 Characterisation of cellular envelopes with immobilised β-galactosidase

The new cellular envelope biocatalysts with membrane bound β-gal-Cyt b_5 were characterised regarding the amount of immobilised enzyme molecules per cellular envelope, the effect of the immobilisation on the enzyme activity and alterations in mass transfer limitation.

8.3.1 Quantification of immobilised β-galactosidase molecules

First, the number of immobilised enzyme molecules was determined. Therefore, a sandwich enzyme linked immunosorbent assay (ELISA) was established. Purified β-galactosidase was used to calculate the corresponding amount of β-gal-Cyt b_5 molecules within one cellular envelope. The cellular envelopes were disrupted using sonication and detergent prior to the application to the assay in order to solubilize the immobilised enzymes. However, the applied method did not enable a complete solubilization of all membrane-bound enzymes. Therefore, the result was corrected according to the residual activity detected in the debris after disruption. Notably, the application of the detergent did not have an effect on enzyme activity (see appendix Figure 12-7). Multiple batch processes with pET28a vector were analysed. Using sandwich ELISA quantification, the amount of membrane-bound β-gal-Cyt b_5 molecules was determined to be 27,200 ± 10,460 per *E. coli* cell envelope.

8.3.2 Characterisation of immobilisation effect on enzyme properties

For a thorough characterisation, the effect of membrane immobilisation was determined. The solubilization of β-gal-Cyt b_5 from cellular envelopes was incomplete, and for a characterisation of the β-gal-Cyt b_5, a complete solubilization would have been required. β-gal-Cyt b_5 is known to insert spontaneously to artificial and cellular membranes. Therefore, β-gal-Cyt b_5 was immobilised to artificial liposomes, which could be easily degraded by detergents. Liposomes were generated as small unilamellar vesicles (SUV). The cleared lysate of *E. coli* BL21 cells overexpressing β-gal-Cyt b_5 was applied to the liposomes. It contained soluble β-gal-Cyt b_5 molecules that were not inserted into the plasma membrane. It was possible to immobilise β-gal-Cyt b_5 to artificial SUV from crude protein extracts. Notably, as only crude extract was used, other *E. coli* host cell proteins also immobilised to the artificial liposomes (see Figure 8-3).

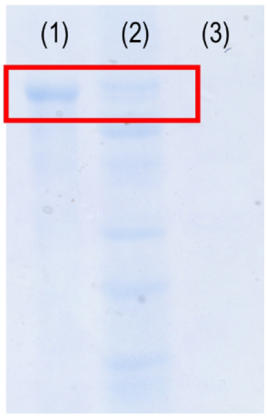

Figure 8-3 SDS-PAGE from SUV with immobilised β-gal-Cyt b_5
Comparison of (1) purified β-galactosidase with (2) SUV with immobilised β-gal-Cyt b_5 and (3) background from supernatant after liposome preparation. Immobilised β-gal-Cyt b_5 and β-galactosidase reference are highlighted. Notably, the reference has no membrane anchor and is consequently smaller.

The obtained liposomes contained sufficient activity for a characterisation of the immobilised β-gal-Cyt b_5. The artificial liposomes were analysed in activity assays and subsequently disrupted by detergent. Sandwich ELISA was used to quantify the number of enzyme molecules bound to the liposomes. Using the activity prior to disruption and the amount of β-gal-Cyt b_5 detected using ELISA, the activity of the membrane-bound molecules was estimated. The estimated activity of membrane-bound and soluble β-gal-Cyt b_5 were compared to a reference activity gained from purified β-gal with N-terminal His_6-tag using the same conditions. The results are summarised in Figure 8-4.

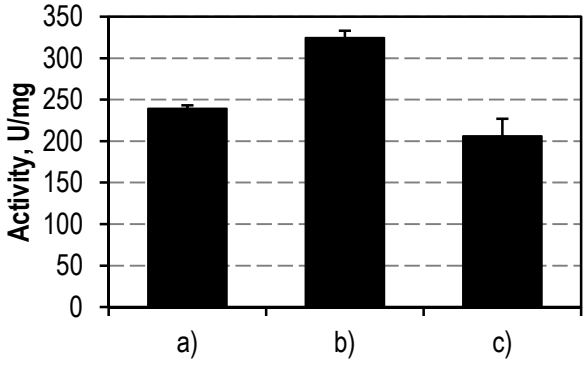

Figure 8-4 Comparison of activities of free and membrane-bound β-gal-Cyt b_5
The activity of β-gal-Cyt b_5 immobilised to liposomes (a) and the activity of the same samples after solubilisation of β-gal-Cyt b_5 by detergent treatment (b) are compared. The reference activity (c) was obtained from purified β-galactosidase with N-terminal His_6-tag.

The activity of membrane-bound β-gal-Cyt b_5 was 324 ± 9 U/mg, whereas the free β-gal-Cyt b_5 had an activity of 239 ± 4 U/mg. So, the activity was increased by 35.5 ± 7.8% due to the immobilisation on the membrane. Notably, the reference activity determined using purified

β-galactosidase with N-terminal His_6-tag was 206 ± 20 U/mg, and consequently lower than the activity of soluble β-gal-Cyt b_5. However, taking the standard deviation into account, it was only marginally smaller. Generally, the activity was enhanced by immobilisation rather than decreased.

One issue frequently faced when using immobilised enzymes and whole cell biocatalysts is mass transfer limitation of substrates or cofactors. Therefore, mass transfer was analysed in cellular envelopes with membrane-bound β-gal-Cyt b_5 compared to whole cells. Activity assays were used to compare cellular envelopes and whole cells sampled after expression but prior to lysis. Additionally, whole cells taken prior to lysis were treated with detergent in order to overcome mass transfer limitation. Exemplary data are given in Figure 8-5.

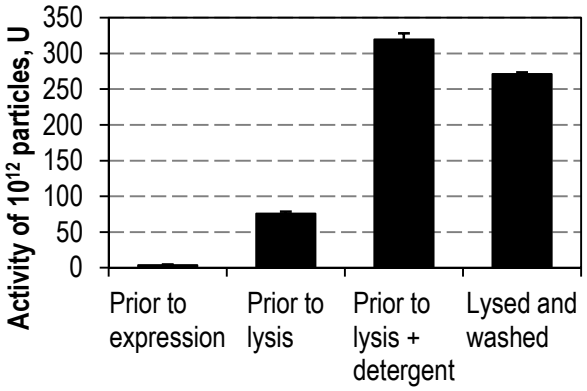

Figure 8-5 Comparison of β-gal-Cyt b_5 activity in whole cells and cellular envelopes for the analysis of mass transfer limitation.
The β-gal-Cyt b_5 activity was compared in whole cells prior to expression, whole cells prior to lysis, whole cells treated with detergent and cellular envelopes after work-up. All samples were adjusted to equivalent particle concentrations using RH414 staining in flow cytometry.

As demonstrated, cells prior to lysis had a reduced activity compared to cellular envelopes. So, due to the formation of the pore, mass transfer limitation was reduced. If the activity of cells treated with detergent was assumed 100%, cellular envelopes contained 78 ± 13% activity and cells prior to lysis 26 ± 10%, respectively. Notably, not all activity is retained in cellular envelopes after lysis. As described in section 3.4.2, C-terminal membrane immobilisation is assumed to occur posttranslationally and is also incomplete. So, the difference in activity of cellular envelopes can be explained by the loss of soluble enzyme due to loss of the cytosol during lysis.

8.4 Discussion

A thorough characterisation of the cellular envelopes with immobilised β-gal-Cyt b_5 was achieved. Batch and fed-batch cultivation of *E. coli* in a stirred-tank bioreactor were used to produce cellular envelopes by protein E-mediated lysis, which contain afore immobilised fusion protein β-gal-Cyt b_5 attached to the inner surface of the cytosolic membrane. A sandwich ELISA was established for quantification of the immobilised β-galactosidase. It was possible to obtain cellular envelopes which contain up to 27,200 ± 10,460 β-gal-Cyt b_5 molecules with an activity of 753 ± 190 U/$g_{dry\ weight}$. The highest amount of immobilised enzyme molecules on the outer membrane was achieved using autodisplay of a P450 enzyme with up to 180,000 molecules per *E. coli* cell (Jose & Meyer 2007; Jose et al. 2012). Generally, the reported number of immobilised molecules using surface display ranges between 15,000 and 180,0000 (Jose & Meyer 2007; Jose et al. 2012). So, the amount of membrane-bound β-gal-Cyt b_5 is within the order of magnitude of autodisplay. It was possible to immobilise higher numbers and amounts of activity of β-gal-Cyt b_5, than achieved for FDH and KR. Comparing these results on immobilisation of all enzymes, it becomes apparent that the resulting cellular envelope catalyst is greatly depending on the kind of enzyme which is immobilised. Consequently, the new biocatalyst technology needs to be evaluated anew for each enzyme.

Comparison of membrane-bound and free β-gal-Cyt b_5 showed an activity increase of 35.5 ± 7.8% due to the immobilisation. The data concurs with data from George et al. (1989), who also describe an increased activity of the membrane-bound fusion compared to the soluble enzyme. Immobilisation of enzymes can have multiple effects which result in altered enzyme properties (Mateo et al. 2007; Fernandez-Lafuente 2009). As the β-galactosidase is a tetramer, one possible explanation could be the stabilization of the tetramer in membrane-bound multimers. If the monomers of multimeric proteins are not connected by covalent bonds such as disulfides, they can be prone to dissociation. The rate constants of association and dissociation then reduce the catalytic activity of the multimer (Mateo et al. 2007). It has been demonstrated that attachment of multimers to surfaces can prevent dissociation of the subunits. Consequently, the multimer is stabilised and enzyme performance enhanced compared to the unbound enzymes (Mateo et al. 2007; Fernandez-Lafuente 2009). A respective stabilization can be assumed a possible explanation for the increased activities of membrane-bound β-gal-Cyt b_5 compared to the free enzyme. The crystal structure of the β-galactosidase shows it as a tetramer

consisting of two dimers, with their C-termini facing in opposite directions (Jacobson et al. 1994). It is therefore likely that only two or one of the anchors are inserted at a time.

Analysis of mass transfer revealed more than 2-fold increased activity in cellular envelopes compared to whole cell due to the pore formation. The cellular envelopes with immobilised β-gal-Cyt b_5 thus proved better catalysts than whole cells prior to lysis regarding this application. The amount of membrane-bound activity thereby concurs with data described by George et al. (1989), who reported up to 80% of immobilised enzyme activity of a similar β-gal-Cyt b_5 enzyme. Notably, only about 24% of the β-gal-Cyt b_5 were detected membrane-bound in initial experiments in shaking flasks. First experiments were conducted using different media, cultivation systems and IPTG amounts, which could explain the observed differences. Another explanation could be losses of membranes and consequently membrane bound enzymes along with the debris in membrane preparations, which impair the results in favour of soluble protein.

Using the β-galactosidase, it was possible to produce biocatalysts with membrane-bound enzymes and to perform a thorough characterisation of the new technology. Therefore, future application of the biocatalyst preparation for other enzymes and enzyme systems will be facilitated by experiences gained in this study.

9 Summary and outlook

Whole cell biocatalysts and isolated enzymes are considered as state of the art in biocatalytic preparations for industrial applications (Schoemaker et al. 2003; Bommarius & Paye 2013). Whole cells as biocatalysts are disadvantageous if substrate or products are toxic to the cells or undesired by-products are formed due to the cellular metabolism (Schrewe et al. 2013). The use of isolated enzymes, in comparison, is more expensive due to the required downstream processing (Schmid et al. 2001). Immobilisation of enzymes after purification increases preparation costs for biocatalysts significantly, but allows for the efficient reuse of the enzymes in the biocatalytic process (DiCosimo et al. 2013; Cantone et al. 2013). For a more rapid processing one-step expression and immobilisation is desirable, which would greatly facilitate the production of biocatalyst preparations with immobilized synthesis enzymes.

In this work, a new tool for the production of biocatalytic preparations with immobilised enzymes was successfully established. To achieve one-step expression and immobilisation, synthesis enzymes were equipped with membrane anchors to ensure immobilisation to the cytoplasmic membrane. Subsequently, the cytoplasm was removed by protein E-mediated lysis, thus creating cellular envelopes which contain afore-immobilised enzymes. The new technique offers one-step expression and immobilisation of synthesis enzymes and can be performed in one production process in stirred-tank bioreactors. Cellular envelopes containing different enzyme systems were produced. A multi-enzyme system of a mutant formate dehydrogenase (FDH) from *M. vaccae* N10 (Sührer et al. 2014) and 3-ketoacyl-[acyl-carrier-protein]-reductase (KR) from *Synechococcus sp.* PCC7942 (Hölsch et al. 2008) was immobilised for coupled asymmetric reduction of the α-haloketone ethyl 4-chloroacetoacetate (ECAA) to the corresponding (*S*)-alcohol ethyl (*S*)-4-chloro-3-hydroxybutyrate ((*S*)-ECHB) with internal cofactor regeneration. Additionally, cellular envelopes containing membrane-bound β-galactosidase were produced. Production processes for cellular envelopes with immobilised enzymes were established and the new biocatalysts were characterised. The properties of cellular envelopes and membrane-bound enzyme as well as the number of immobilised molecules per cellular envelope were determined. A schematic description of the new one-step expression and immobilisation is displayed in Figure 9-1.

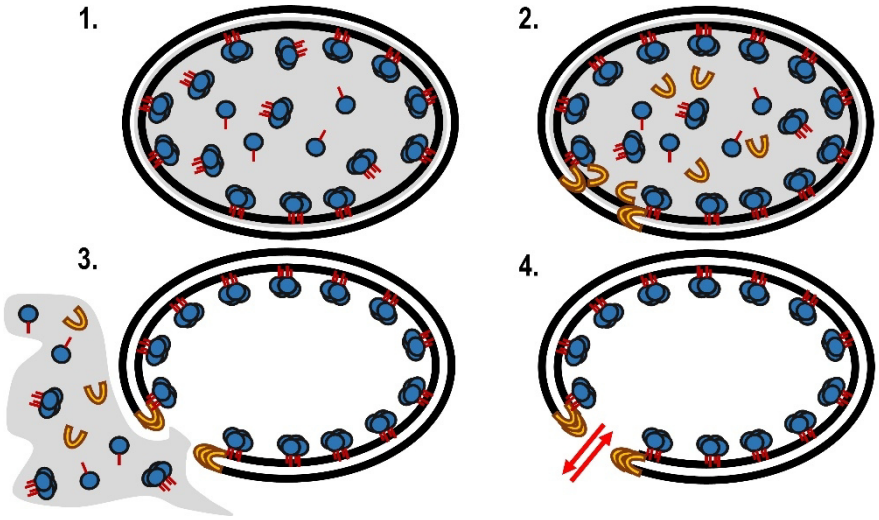

Figure 9-1 Schematic display of the new one-step expression and immobilisation technique applied using *Escherichia coli*
1) Expression of synthesis enzyme with C-terminal membrane anchor, possible multimer formation and inner membrane insertion. 2) Expression of lytic phage protein E and insertion into the cell membranes. 3) Pore formation by protein E and lysis with release of the cytosol. 4) Cellular envelope with immobilised enzymes and lysis pore.

For membrane immobilisation, several anchors were analysed for the FDH and the KR. C-terminal membrane anchoring was preferable, as it is independent from secretory pathway. Anchoring of high amounts of enzyme activity was aimed for. The KR was immobilised best with the C-terminal, hydrophobic sequence from cytochrome b_5 from rabbit liver with 38 ± 8% of the total enzyme bound to the membrane. The highest amounts of FDH were immobilised using the C-terminal sequence from ubiquitin-conjugating enzyme 6 from *S. cerevisiae*. This was the first application of the UBC6 membrane anchor for immobilisation of soluble enzymes to membranes.

Production of the new cellular envelope biocatalysts in stirred-tank bioreactors was established. A process for the production of cellular envelopes by removal of the cytoplasm is described by Langemann et al. (2010). A respective batch process was established along with the required analytics such as flow cytometry. In addition to the established methods, permittivity measurements were introduced for the on-line detection of protein E-mediated lysis.

To allow for combined expression and lysis of *E. coli*, the existing process was modified. Cellular vitality was crucial for successful protein E-mediated lysis, and expression of enzymes such as the KR were damaging to the cells. Usually, batch production is used in cellular envelope production in stirred-tank bioreactors. Batch processes to produce cellular envelopes

with immobilised KR and FDH were not possible as the cells were unfit for protein lysis after expression. Consequently, a fed-batch process using exponential feeding was successfully established, which ensured supply with nutrients during expression and sufficient cellular activity of *E. coli* for lysis yields > 99%. Final CDW prior to lysis was up to 20 g/L and activity of cellular envelopes was independent from cell density after expression. Subsequent to the production process, downstream processing of the cellular envelopes was introduced according to Langemann et al. (2010). Cross-flow filtration in a bypass to the stirred-tank bioreactor was used to concentrate the cellular envelope biocatalysts and to remove host cell protein and non-immobilised enzymes from the surrounding medium. A schematic description of the production process is given in Figure 9-2.

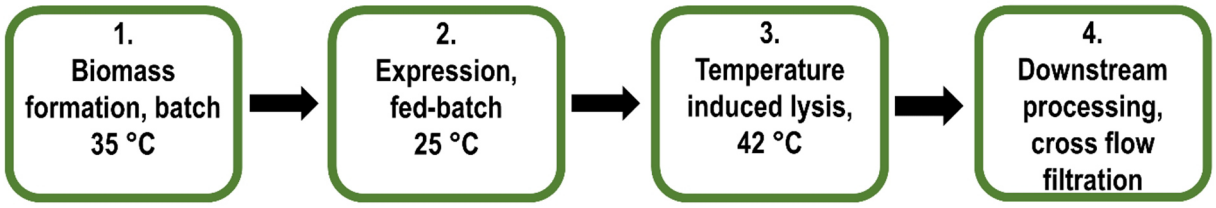

Figure 9-2 Schematic description of the established production process for the production of cellular envelopes with membrane-bound FDH and KR using *E. coli*

FDH and KR feature different expression optima. Different expression temperatures were compared to find conditions which rendered a high catalytic activity of the produced cellular envelopes. In addition, different *E. coli* strains were compared. *E. coli* BL21 was compared to the derivate cell strains *E. coli* C41 and *E. coli* C43, which are more robust towards over expression of membrane proteins (Miroux & Walker 1996; Wagner et al. 2008). Cellular envelopes with immobilised FDH-UBC6 and KR-Cyt b_5 from *E. coli* C41 cells gained at 25 °C expression temperature exhibited the highest activity in asymmetric reduction of the substrate ECAA. Production of cellular envelopes with co-immobilised FDU-UBC6 and KR-Cyt b_5 was possible and the biocatalysts were catalytically active in coupled asymmetric reductions of ECAA. A schematic description of the new cellular envelope biocatalyst is given in Figure 9-3.

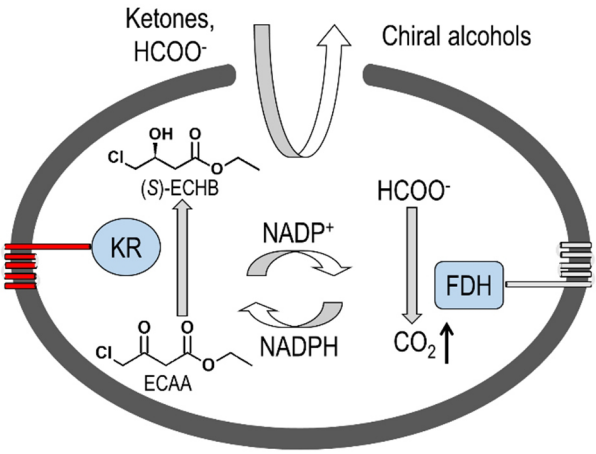

Figure 9-3 Schematic display of cellular envelopes with membrane-bound oxidoreductase system
Asymmetric reduction of ECAA to the corresponding (*S*)-alcohol by the KR with internal cofactor regeneration of NADPH by the FDH. Both enzymes are membrane-anchored to cellular envelopes and substrates and products diffuse through the lysis pore.

The immobilised enzymes in cellular envelopes were characterised. Immunological detection of FDH and KR was not possible due to a lack of commercially available antibodies. Characterisation was therefore performed using activity assays and a reference activity from free enzyme without a membrane anchor.

Using activity assays, the number of FDH-UBC6 was determined to be 5297 ± 536 if the KR was co-immobilised, and 8732 ± 3106 if only the FDH-UBC6 was immobilised, respectively. 46% of all enzyme was membrane-bound. This was the first application of the UBC6 membrane anchor for the immobilisation of a heterologous enzyme to the cytoplasmic membrane of *E. coli*, consequently there is no existing reference data on the immobilisation properties.

The enzyme stability of membrane-bound FDH-UBC6 was analysed. The half life in the presence of the α-haloketone ECAA was reduced more than 50% compared to the free enzyme without the membrane anchor. Reduction of enzyme properties are likely due to the addition of the membrane anchor.

The membrane-bound KR-Cyt b_5 was characterised too using activity assays in the reduction of ECAA to the corresponding (*S*)-alcohol. Notably, increased production of (*R*)-ECHB was observed. The ee_s of membrane-bound KR-Cyt b_5 was 99 ± 1% and thus comparable to the wild type KR. Analysis revealed by-product formation by host cell enzyme(s) from *E. coli*. In data described in the literature on ECAA reduction with whole cell biocatalysts, such a by-product formation was not observed (Bräutigam 2008). One major reason for the use of cellular envelopes as biocatalysts is the removal of the host cell metabolism to prevent undesired by-product formation. The fact that an undesired background enzyme was co-purified in cellular

envelopes is unfortunate and unforeseen.

To access the main properties of the new biocatalysts, a characterisation and comparison to whole cell biocatalysts was performed. Performance in asymmetric reductions was compared to whole cells sampled from the process prior to lysis. Thus, background activity could be assumed the same. The activity of cellular envelopes in asymmetric reductions of ECAA was 0.34 ± 0.23 U/$g_{dry\ weight}$ and therefore one order of magnitude lower than the activity of the same cellular envelopes in FDH assays (4.07 ± 0.03 U/$g_{dry\ weight}$). KR activity was consequently the limiting factor. The stability of cellular envelopes in storage and in asymmetric reductions was found to be comparable to whole cell biocatalysts. The morphology of cellular envelopes is maintained for at least 120 h during stirred reactions and for at least 14 d during storage at different conditions. Recycling of cellular envelopes was possible too. The recycling was limited by the stability of the enzymes in the cellular envelopes and not by the morphological stability of the cellular envelope biocatalyst.

A thorough characterisation of the new biocatalyst preparation regarding a comparison to whole cell biocatalysts, the number of immobilised enzyme molecules, and the effects of the immobilisation on enzyme properties was aimed for. Immobilisation of the β-galactosidase was analysed as a model system and a first transfer to a different enzyme of the new cellular envelope biocatalyst. Contrary to the oxidoreductases, there are commercially available antibodies for immunological detection and quantification. Membrane immobilisation of the β-galactosidase with the C-terminal hydrophobic sequence of cytochrome b_5 from rabbit liver is described in the literature, which was fused to the β-galactosidase, resulting in the β-gal-Cyt b_5.

Production of biocatalysts with membrane-bound β-gal-Cyt b_5 were developed as batch and fed-batch processes. Biocatalysts with membrane-bound β-gal-Cyt b_5 were successfully produced and a sandwich ELISA was developed for the quantification of membrane-bound β-gal-Cyt b_5. The number of immobilised enzyme molecules was determined to be $27{,}200 \pm 10{,}460$ (equalling 758 ± 190 U/$g_{dry\ weight}$) in cellular envelopes from batch processes. The number of FDH-UBC6 molecules determined by activity assays was 8732 ± 3106 if only the FDH-UBC6 was immobilised. So, immobilisation depended on the enzyme and anchor combination applied. 15,000 to 180,000 enzyme molecules can be immobilised using Surface display, which is an alternative method for one-step expression and immobilisation (Jose & Meyer 2007; Jose et al. 2012). Thus, the amount of enzyme molecules within cellular envelopes

was within the order of magnitude of the surface display.

The properties of free and membrane-bound β-gal-Cyt b_5 were compared. Interestingly, the activity of membrane-bound β-gal-Cyt b_5 was increased by 35.5 ± 7.8% compared to the soluble enzyme. Increase of activity of the membrane-bound enzyme can possibly be referred to the stabilization of the enzyme tetramer by immobilisation to the membrane. Mass transfer in whole cells and cellular envelopes was analysed. Cellular envelopes had a more than 2-fold increased activity, which could be related to an improved mass transfer of the substrate due to the formation of the lysis pore.

In conclusion, establishing a new one-step expression and immobilisation method for the production of biocatalyst preparations was successful. Cellular envelopes are generally used in vaccine development. In this work, the technology was transferred to biocatalysts by immobilising large quantities of synthesis enzymes prior to lysis. The general performance of cellular envelopes makes them an interesting platform technology, which can be applied for multiple enzyme systems. Performance in stability and mass transfer of substrates was equal or better compared to whole cells. Cellular envelopes containing β-gal-Cyt b_5 were superior to whole cells, as they featured a more than 200% higher activity due to an improved mass transfer. Cellular envelopes containing membrane-bound FDH-UBC6 and KR-Cyt b_5 had equal storage stability but lower catalytic activity compared to whole cells. Thus, the performance of the cellular envelope biocatalyst greatly depends on the enzyme system used for the immobilisation. Factors such as the immobilisation ratio and the amount of membrane bound enzymes influence the performance of cellular envelopes in comparison to whole cells. Notably, cellular envelopes containing FDH-UBC6 and KR-Cyt b_5 will not be suitable for industrial application. Low KR activity and an undesired competing host cell enzyme within the cellular envelopes makes this special system undesirable. This is the first attempt of producing biocatalyst from cellular envelopes by immobilising the synthesis enzymes to the membrane, so comparison to existing data is not possible.

Results of this work describe the first application of cellular envelopes containing large quantities of synthesis enzymes immobilised to the cytoplasmic membrane as biocatalysts, and gained insights will help in future studies. Whereas the so far applied oxidoreductase system was not suitable for application, cellular envelopes with immobilised β-galactosidase were superior to whole cells and the immobilisation of new enzymes and multi-enzyme systems

should be the topic of future studies. Cellular envelopes with membrane bound enzymes are of special interest as an alternative for whole cell biotransformations which suffer from strong mass transfer limitation.

The number of enzyme molecules attached to the cellular envelope determines its final performance. Increasing the number of enzyme molecules bound to the cellular envelope biocatalyst is of interest for future studies. So far, only the inner surface of the cytoplasmic membrane was used. As a 2-dimensional surface, the space for immobilisation of enzymes can expected to be limited. Combination of the cellular envelope technology and surface display was demonstrated in vaccine development (Jechlinger et al. 2005; Hjelm et al. 2015) and could be a method to increase the number of enzyme molecules per cellular envelope. Further increase of enzyme molecules per particle could be achieved by filling the interior of the cellular envelope as well as its surface areas. S-layer proteins, which incorporate the desired synthesis enzymes, can form crystalline structures within cells. The formation of S-layer structures prior to lysis was demonstrated in vaccine development and could be analysed in future studies (Lubitz et al. 1999; Eko et al. 1999).

Results of this work demonstrated that the choice of the enzyme as well as the membrane anchor have influence on immobilisation properties and numbers of immobilised enzyme molecules. Future studies should therefore also focus on the choice of the membrane anchor and other anchors described in the literature should be analysed. Thereby, differences in activities of the different enzymes could be balanced out by immobilising respective ratios of the enzymes. Immobilisation of the oxidoreductases as one multifunctional fusion protein was not possible. However, fusion enzymes should be tried again in the immobilisation of new enzyme systems.

10 References

Ahern, T.J. & Klibanov, a M., 1985. The mechanisms of irreversible enzyme inactivation at 100C. *Science (New York, N.Y.)*, 228(4705), pp.1280–1284.

Ahuja, S., Jahr, N., Im, S.C., Vivekanandan, S., et al., 2013. A model of the membrane-bound cytochrome b5-cytochrome P450 complex from NMR and mutagenesis data. *Journal of Biological Chemistry*, 288(30), pp.22080–22095.

Bali, S., Hare, H.M.O. & Weissman, K.J., 2006. Broad Substrate Specificity of Ketoreductases Derived from Modular Polyketide Synthases. *ChemBioChem*, (7), pp.478–484.

Baneyx, F., 1999. Recombinant protein expression in *Escherichia coli*. *Current Opinion in Biotechnology*, (10), pp.411–421.

Bisswanger, H., 2008. *Enzymkinetik Theorie und Methoden*, Weinheim, Germany: Wiley-VCH Verlag GmbH & Co. KGaA.

Bläsi, U., Henrich, B. & Lubitz, W., 1985. Lysis of *Escherichia coli* by cloned phi X174 gene E depends on its expression. *Journal of General Microbiology*, 131, pp.1107–1114.

Bläsi, U., Linke, R.P. & Lubitz, W., 1989. Evidence for membrane-bound oligomerization of bacteriophage PhiX174 lysis protein-E. *Journal of Biological Chemistry*, 264(8), pp.4552–4558.

Van Bloois, E., Winter, R.T., Kolmar, H. & Fraaije, M.W., 2011. Decorating microbes: Surface display of proteins on *Escherichia coli*. *Trends in Biotechnology*, 29(2), pp.79–86.

Bommarius, A.S. & Paye, M.F., 2013. Stabilizing biocatalysts. *Chemical Society Reviews*, 42, pp.6534–65.

Bräutigam, S., 2008. *Ganzzell-Biokatalyse in Gegenwart ionischer Flüssigkeiten mit rekombinanten Escherichia coli*. Technische Universität München.

Bräutigam, S., Dennewald, D., Schürmann, M., Lutje-spelberg, J., et al., 2009. Whole-cell

biocatalysis : Evaluation of new hydrophobic ionic liquids for efficient asymmetric reduction of prochiral ketones. *Enzyme and Microbial Technology*, 45, pp.310–316.

Bülow, L., 1987. Characterization of an artificial bifunctional enzyme, beta-galactosidase/galactokinase, prepared by gene fusion. *European Journal of Biochemistry / FEBS*, 163(3), pp.443–448.

Calcott, P.H. & MacLeod, R. a, 1975. The survival of *Escherichia coli* from freeze-thaw damage: the relative importance of wall and membrane damage. *Canadian Journal of Microbiology*, 21(12), pp.1960–1968.

Caner, H., Groner, E. & Levy, L., 2004. Trends in the Development of Chiral Drugs. *Drug Discovery Today*, 9(3), pp.105–110.

Cantone, S., Ferrario, V., Corici, L., Ebert, C., et al., 2013. Efficient immobilisation of industrial biocatalysts: criteria and constraints for the selection of organic polymeric carriers and immobilisation methods. *Chemical Society Reviews*, 42(15), pp.6262–76.

Chartrain, M., Greasham, R., Moore, J., Reider, P., et al., 2001. Asymmetric bioreductions: application to the synthesis of pharmaceuticals. *Journal of Molecular Catalysis B: Enzymatic B Enzymatic*, 11(4-6), pp.503–512.

Chenault, H.K. & Whitesides, G.M., 2007. Regeneration of Nicotinamide Cofactors for use in Organic Synthesis. *Applied Biochemistry and Biotechnology*, 14(11), pp.147–197.

Clayden, J., Greeves, N., Warren, S. & Wothers, P., 2001. *Organic Chemistry* 1st ed., Oxford: Oxford University Press.

Conrado, R.J., Varner, J.D. & DeLisa, M.P., 2008. Engineering the spatial organization of metabolic enzymes: mimicking nature's synergy. *Current Opinion in Biotechnology*, 19, pp.492–499.

Cornelis, P., 2000. Expressing genes in different *Escherichia coli* compartments. *Current Opinion in Biotechnology*, (11), pp.450–454.

Cornish-Bowden, A., 2012. *Fundamentals of Enzyme Kinetics* 4th ed., Wiley-Blackwell.

Cupples, C.G., Miller, J.H. & Huber, R.E., 1990. Determination of the roles of Glu-461 in beta-galactosidase (*Escherichia coli*) using site-specific mutagenesis. *The Journal of biological chemistry*, 265(10), pp.5512–5518.

Davey, C.L., Davey, H.M., Kell, D.B. & Todd, R.W., 1993. Introduction to the dielectric estimation of cellular biomass in real time, with special emphasis on measurements at high volume fractions. *Analytica Chimica Acta*, 279, pp.155–161.

DeLisa, M.P., Li, J., Rao, G., Weigand, W. a, et al., 1999. Monitoring GFP-operon fusion protein expression during high cell density cultivation of *Escherichia coli* using an on-line optical sensor. *Biotechnology and bioengineering*, 65, pp.54–64.

Dennewald, D., 2011. *Biphasic whole-cell synthesis of R -2-octanol with recycling of the ionic liquid*. Technische Universität München.

DiCosimo, R., McAuliffe, J., Poulose, A.J. & Bohlmann, G., 2013. Industrial use of immobilized enzymes. *Chemical Society Reviews*, 42(15), pp.6437–74.

Drauz, K., Gröger, H. & May, O., 2012. *Enzyme Catalysis in Organic Synthesis* Third. K. Drauz, H. Gröger, & O. May, eds., Weinheim, Germany: Wiley-VCH Verlag GmbH & Co. KGaA.

Ebensen, T., Paukner, S., Link, C., Kudela, P., et al., 2004. Bacterial ghosts are an efficient delivery system for DNA vaccines. *Journal of Immunology*, 172(11), pp.6858–6865.

Eko, F.O., Witte, a., Huter, V., Kuen, B., et al., 1999. New strategies for combination vaccines based on the extended recombinant bacterial ghost system. *Vaccine*, 17, pp.1643–1649.

Etayo, P. & Vidal-Ferran, A., 2013. Rhodium-catalysed asymmetric hydrogenation as a valuable synthetic tool for the preparation of chiral drugs. *Chemical Society Reviews*, 42(2), pp.728–54.

Faber, K., 2011. *Biotransformations in Organic Chemistry* 6th ed., Heidelberg: Springer Verlag.

Fairbanks, G., Steck, T.L. & Wallachl, D.F.H., 1968. Electrophoretic Analysis. *Biochemistry*, 10(13), pp.2606–2617.

Fernandez-Lafuente, R., 2009. Stabilization of multimeric enzymes: Strategies to prevent subunit dissociation. *Enzyme and Microbial Technology*, 45, pp.405–418.

Fowler, a V & Zabin, I., 1977. The amino acid sequence of beta-galactosidase of *Escherichia coli*. *Proceedings of the National Academy of Sciences of the United States of America*, 74(4), pp.1507–1510.

Fu, Y., 2013. *Asymmetric reductions using novel ene-reductases from cyanobacteria*. Technische Universität München.

Galkin, a., Kulakova, L., Tishkov, V., Esaki, N., et al., 1995. Cloning of formate dehydrogenase gene from a methanol-utilizing bacterium *Mycobacterium vaccae* N10. *Applied Microbiology and Biotechnology*, 44, pp.479–483.

Garcia-Urdiales, E., Lavandera, I. & Gotoor, V., 2012. Concepts in Biocatalysis. In K. Drauz, H. Gröger, & O. May, eds. *Enzyme Catalysis in Organic Synthesis*. Weinheim, Germany: Wiley-VCH Verlag GmbH & Co. KGaA.

George, S.K., Najera, L., Sandoval, R.P., Countryman, C., et al., 1989. The hydrophobic domain of cytochrome b5 is capable of anchoring beta-galactosidase in *Escherichia coli* membranes. *Journal of Bacteriology*, 171(9), pp.4569–4576.

Goldberg, K., Edegger, K., Kroutil, W. & Liese, A., 2006. Overcoming the Thermodynamic Limitation in Asymmetric Hydrogen Transfer Reactions Catalyzed by Whole Cells.

Gray, C.J., Weissenborn, M.J., Eyers, C.E. & Flitsch, S.L., 2013. Enzymatic reactions on immobilised substrates. *Chemical Society Reviews*, 42(15), pp.6378–405.

Gröger, H. & Asano, Y., 2012. Introduction - principles and historical landmarks of enzyme catalysis in organic synthesis. In K. Drauz, H. Gröger, & O. May, eds. *Enzyme Catalysis in Organic Synthesis*. Weinheim, Germany: Wiley-VCH Verlag GmbH & Co. KGaA.

Hanefeld, U., Cao, L. & Magner, E., 2013. Enzyme immobilisation: fundamentals and application. *Chemical Society Reviews*, 42, pp.6211–6212.

Hannig, G. & Makrides, S.C., 1998. Strategies for optimizing heterologous protein expression in *Escherichia coli*. *Trends in Biotechnology*, 16(2), pp.54–60.

Hatrongjit, R. & Packdibamrung, K., 2010. A novel NADP+-dependent formate dehydrogenase from *Burkholderia stabilis* 15516: Screening, purification and characterization. *Enzyme and Microbial Technology*, 46(7), pp.557–561.

Hatti-Kaul, R., Törnvall, U., Gustafsson, L. & Börjesson, P., 2007. Industrial biotechnology for the production of bio-based chemicals - a cradle-to-grave perspective. *Trends in Biotechnology*, 25(3), pp.119–124.

Havel, J., 2006. *Asymmetrische Synthesen mit phototrophen Mikroorganismen*. Technische Universität München.

Hjelm, A., Söderström, B., Vikström, D., Jong, W.S.P., et al., 2015. Autotransporter-Based Antigen Display in Bacterial Ghosts. *Applied and Environmental Microbiology*, 18(2), pp.726–735.

Hoelsch, K., Sührer, I., Heusel, M. & Weuster-Botz, D., 2013. Engineering of formate dehydrogenase: Synergistic effect of mutations affecting cofactor specificity and chemical stability. *Applied Microbiology and Biotechnology*, 97(6), pp.2473–2481.

Hollmann, F., Arends, I.W.C.E. & Holtmann, D., 2011. Enzymatic reductions for the chemist. *Green Chemistry*, 13(9), p.2285.

Hölsch, K., 2009. *Asymmetrische Synthese mit neuen Oxidureductasen aus Cyanobakterien*. Technische Universität München.

Hölsch, K., Havel, J., Haslbeck, M. & Weuster-Botz, D., 2008. Identification, cloning, and characterization of a novel ketoreductase from the cyanobacterium *Synechococcus sp.* strain PCC 7942. *Applied and Environmental Microbiology*, 74(21), pp.6697–6702.

Hölsch, K. & Weuster-Botz, D., 2010a. Enantioselective reduction of prochiral ketones by engineered bifunctional fusion proteins. *Biotechnology and Applied Biochemistry*, 56(4), pp.131–140.

Hölsch, K. & Weuster-Botz, D., 2011. Kinetic mechanism of 3-ketoacyl-(acyl-carrier-protein) reductase from *Synechococcus sp.* strain PCC 7942: A useful enzyme for the production of chiral alcohols. *Journal of Molecular Catalysis B: Enzymatic*, 69, pp.89–94.

Hölsch, K. & Weuster-Botz, D., 2010b. New oxidoreductases from cyanobacteria: Exploring nature's diversity. *Enzyme and Microbial Technology*, 47, pp.228–235.

Huang, X., Holden, H.M. & Raushel, F.M., 2001. Channeling of Substrates and Reactions. *Annual Review of Biochemistry*, pp.149–180.

Hutchison, C. a & Sinsheimer, R.L., 1966. The process of infection with bacteriophage phi-X174. X. Mutations in a phi-X Lysis gene. *Journal of molecular biology*, 18(3), pp.429–447.

Iyer, P. V. & Ananthanarayan, L., 2008. Enzyme stability and stabilization-Aqueous and non-aqueous environment. *Process Biochemistry*, 43(10), pp.1019–1032.

Jacobson, R.H., Zhang, X.J., DuBose, R.F. & Matthews, B.W., 1994. Three-dimensional structure of beta-galactosidase from *E. coli*. *Nature*, 369, pp.761–766.

Jalava, K., Hensel, A., Szostak, M., Resch, S., et al., 2002. Bacterial ghosts as vaccine candidates for veterinary applications. *Journal of Controlled Release*, 85(1-3), pp.17–25.

Jechlinger, W., Haller, C., Resch, S., Hofmann, A., et al., 2005. Comparative immunogenicity of the Hepatitis B virus core 149 antigen displayed on the inner and outer membrane of bacterial ghosts. *Vaccine*, 23, pp.3609–3617.

Jechlinger, W., Szostak, M.P., Witte, A. & Lubitz, W., 1999. Altered temperature induction sensitivity of the lambda p(R)/cI857 system for controlled gene E expression in *Escherichia coli*. *FEMS Microbiology Letters*, 173, pp.347–352.

Jenzsch, M., Gnoth, S., Beck, M., Kleinschmidt, M., et al., 2006. Open-loop control of the biomass concentration within the growth phase of recombinant protein production processes. *Journal of Biotechnology*, 127, pp.84–94.

Jia, F., Narasimhan, B. & Mallapragada, S., 2014. Materials-based strategies for multi-enzyme immobilization and co-localization: A review. *Biotechnology and Bioengineering*, 111(2), pp.209–222.

Jose, J., 2006. Autodisplay: Efficient bacterial surface display of recombinant proteins. *Applied Microbiology and Biotechnology*, 69, pp.607–614.

Jose, J., Maas, R.M. & Teese, M.G., 2012. Autodisplay of enzymes-Molecular basis and perspectives. *Journal of Biotechnology*, 161(2), pp.92–103.

Jose, J. & Meyer, T.F., 2007. The autodisplay story, from discovery to biotechnical and biomedical applications. *Microbiology and molecular biology reviews : MMBR*, 71(4), pp.600–619.

Juers, D.H., Hakda, S., Matthews, B.W. & Huber, R.E., 2003. Structural Basis for the Altered Activity of Gly794 Variants of *Escherichia coli* beta-Galactosidase. *Biochemistry*, 42(46), pp.13505–13511.

Juers, D.H., Heightman, T.D., Vasella, A., McCarter, J.D., et al., 2001. A structural view of the action of *Escherichia coli* (lacZ) beta-galactosidase. *Biochemistry*, 40(49), pp.14781–14794.

Juers, D.H., Matthews, B.W. & Huber, R.E., 2012. LacZ beta-galactosidase : Structure and function of an enzyme of historical and molecular biological importance. *Protein Science*, 21, pp.1792–1807.

Karzanov, V. V., Correa, C.M., Bogatsky, Y.G. & Netrusov, A.I., 1991. Alternative NAD+-dependent formate dehydrogenases in the facultative methylotroph *Mycobacterium vaccae* N10. *FEMS Microbiology Letters*, 65(1), pp.95–9.

Kataoka, M., Kita, K., Wada, M., Yasohara, Y., et al., 2003. Novel bioreduction system for the production of chiral alcohols. *Applied Microbiology and Biotechnology*, 62, pp.437–445.

Katchalski-Katzir, E., 1993. Immobilized enzymes — learning from past successes and failures. *Trends in Biotechnology*, 11(November), pp.471–478.

Keseler, I.M., Mackie, A., Peralta-Gil, M., Santos-Zavaleta, A., et al., 2013. EcoCyc: Fusing model organism databases with systems biology. *Nucleic Acids Research*, 41(D1), pp.605–612.

Kirk, O., Borchert, T.V. & Fuglsang, C.C., 2002. Industrial enzyme applications. *Current Opinion in Biotechnology*, 13(4), pp.345–351.

Kizaki, N., Yasohara, Y., Hasegawa, J., Wada, M., et al., 2001. Synthesis of optically pure ethyl

(S)-4-chloro-3-hydroxybutanoate by *Escherichia coli* transformant cells coexpressing the carbonyl reductase and glucose dehydrogenase genes. *Applied Microbiology and Biotechnology*, 55(5), pp.590–595.

Kutay, U., Hartmann, E. & Rapoport, T. a, 1993. A class of membrane proteins with a C-terminal anchor. *Trends in Cell Biology*, 3(March), pp.72–75.

Lamzin, V.S., Dauter, Z., Popov, V.O., Harutyunyan, E.H., et al., 1994. High resolution structures of holo and apo formate dehydrogenase. *Journal of Molecular Biology*, 236(3), pp.759–785.

Langemann, T., Koller, V.J., Muhammad, A., Kudela, P., et al., 2010. The bacterial ghost platform system: Production and applications. *Bioengineered Bugs*, 1(5), pp.326–336.

Langley, K.E., Villarejo, M.R., Fowler, a V, Zamenhof, P.J., et al., 1975. Molecular basis of beta-galactosidase alpha-complementation. *Proceedings of the National Academy of Sciences of the United States of America*, 72(4), pp.1254–1257.

Lee, S.Y., Choi, J.H. & Xu, Z., 2003. Microbial cell-surface display. *Trends in Biotechnology*, 21(1), pp.45–52.

León, R., Fernandes, P., Pinheiro, H.M. & Cabral, J.M.S., 1998. Whole-cell biocatalysis in organic media. *Enzyme and Microbial Technology*, 23(98), pp.483–500.

Liese, A. & Hilterhaus, L., 2013. Evaluation of immobilized enzymes for industrial applications. *Chemical Society Reviews*, 42, pp.6236–49.

Liu, J., Wang, W.D., Liu, Y.J., Liu, S., et al., 2012. Mice vaccinated with enteropathogenic *Escherichia coli* ghosts show significant protection against lethal challenges. *Letters in Applied Microbiology*, 54(3), pp.255–262.

Lo, S., Dugdale, M.L., Jeerh, N., Ku, T., et al., 2010. Studies of Glu-416 variants of beta-galactosidase (E. coli) Show that the active site Mg2+ is not important for structure and indicate that the main role of Mg2+ is to mediate optimization of active site chemistry. *Protein Journal*, 29, pp.26–31.

Lottspeich, F. & Zorbas, H., 1998. *Bioanalytik* 1st ed., Heidelberg: Spektrum Akademischer

Verlag GmbH.

Lubitz, W., Harkness, R.E. & Ishiguro, E.E., 1984. Requirement for a functional host cell autolytic enzyme system for lysis of *Escherichia coli* by bacteriophage PhiX174. *Journal of Bacteriology*, 159(1), pp.385–387.

Lubitz, W., Witte, a., Eko, F.O., Kamal, M., et al., 1999. Extended recombinant bacterial ghost system. *Journal of Biotechnology*, 73, pp.261–273.

Magnuson, K., Jackowski, S., Rock, C.O. & Cronan, J.E., 1993. Regulation of fatty acid biosynthesis in *Escherichia coli*. *Microbiological Reviews*, 57(3), pp.522–542.

Margolin, a. L., 1993. Enzymes in the synthesis of chiral drugs. *Enzyme and Microbial Technology*, 15(4), pp.266–280.

De Maria, P.D., 2012. *Ionic Liquids in Biotransformations and Organocatalysis*, Hoboken: John Wiley & Sons, Ltd.

Mateo, C., Palomo, J.M., Fernandez-Lorente, G., Guisan, J.M., et al., 2007. Improvement of enzyme activity, stability and selectivity via immobilization techniques. *Enzyme and Microbial Technology*, 40, pp.1451–1463.

Matsuda, T., Yamanaka, R. & Nakamura, K., 2009. Recent progress in biocatalysis for asymmetric oxidation and reduction. *Tetrahedron Asymmetry*, 20(5), pp.513–557.

Mayr, U.B., Walcher, P., Azimpour, C., Riedmann, E., et al., 2005. Bacterial ghosts as antigen delivery vehicles. *Advanced Drug Delivery Reviews*, 57(9), pp.1381–1391.

Miroux, B. & Walker, J.E., 1996. Over-production of proteins in *Escherichia coli*: mutant hosts that allow synthesis of some membrane proteins and globular proteins at high levels. *Journal of molecular biology*, 260, pp.289–298.

Nebe-Von-Caron, G. & Badley, R. a., 1994. Viability assessment of bacteria in mixed populations using flow cytometry. *Journal of Microscopy*, 179(1), pp.55–66.

Nebe-Von-Caron, G., Stephens, P.J., Hewitt, C.J., Powell, J.R., et al., 2000. Analysis of bacterial function by multi-colour fluorescence flow cytometry and single cell sorting.

Journal of Microbiological Methods, 42(1), pp.97–114.

Neophytou, I., Harvey, R., Lawrence, J., Marsh, P., et al., 2007. Eukaryotic integral membrane protein expression utilizing the *Escherichia coli* glycerol-conducting channel protein (GlpF). *Applied Microbiology and Biotechnology*, 77, pp.375–381.

Noyori, R., 2001. Asymmetric Catalysis in Science and Opportunities. Nobel Price Lecture.

Noyori, R. & Ohkuma, T., 2001. Asymmetric catalysis by architectural and functional molecular engineering: Practical chemo- and stereoselective hydrogenation of ketones. *Angewandte Chemie - International Edition*, 40(1), pp.40–73.

Noyori, R., Yamakawa, M. & Hashiguchi, S., 2001. Metal-ligand bifunctional catalysis: A nonclassical mechanism for asymmetric hydrogen transfer between alcohols and carbonyl compounds. *Journal of Organic Chemistry*, 66(24), pp.7931–7944.

Panke, S., Held, M. & Wubbolts, M., 2004. Trends and innovations in industrial biocatalysis for the production of fine chemicals. *Current Opinion in Biotechnology*, 15(4), pp.272–279.

Panke, S. & Wubbolts, M., 2005. Advances in biocatalytic synthesis of pharmaceutical intermediates. *Current Opinion in Chemical Biology*, 9(2), pp.188–194.

Pettersson, H. & Pettersson, G., 2001. Kinetics of the coupled reaction catalysed by a fusion protein of β-galactosidase and galactose dehydrogenase. *Biochimica et Biophysica Acta - Protein Structure and Molecular Enzymology*, 1549, pp.155–160.

Pfizer Worldwide, 2015. *Worldwide revenue of Pfizers Lipitor from 2003 to 2014*,

Pfruender, H., Jones, R. & Weuster-Botz, D., 2006. Water immiscible ionic liquids as solvents for whole cell biocatalysis. *Journal of Biotechnology*, 124(1), pp.182–190.

Pollard, D.J. & Woodley, J.M., 2007. Biocatalysis for pharmaceutical intermediates: the future is now. *Trends in Biotechnology*, 25(2), pp.66–73.

Popov, V. & Lamzin, V., 1994. NAD+ dependent formate dehydrogenase. *Biochemical Journal*, 301(1994), pp.625–643.

Ra, C.H., Kim, Y.J., Park, S.J., Jeong, C.W., et al., 2009. Evaluation of optimal culture conditions for recombinant ghost bacteria vaccine production with the antigen of *Streptococcus iniae* GAPDH. *Journal of Microbiology and Biotechnology*, 19(April), pp.982–986.

Ra, C.H., Park, S.J., Kim, K.H. & Kim, S.K., 2010. Production of recombinant ghost bacterial vaccine against streptococcal disease of olive flounder. *Process Biochemistry*, 45, pp.317–322.

Rippka, R., Deruelles, J., Waterbury, J.B., Herdman, M., et al., 1979. Generic Assignments , Strain Histories and Properties of Pure Cultures of Cyanobacteria. *Journal of General Microbiology*, 110(2), pp.1–61.

Rock, C.O. & Jackowski, S., 2002. Forty Years of Bacterial Fatty Acid Synthesis. *Biochemical and Biophysical Research Communications*, 1166, pp.1155–1166.

Rodrigues, R.C., Ortiz, C., Berenguer-Murcia, Á., Torres, R., et al., 2013. Modifying enzyme activity and selectivity by immobilization. *Chemical Society Reviews*, pp.6290–6307.

Rogers, R.D. & Seddon, K.R., 2003. Chemistry. Ionic liquids--solvents of the future? *Science*, 302(5646), pp.792–793.

Roosild, T.P., Greenwald, J., Vega, M., Castronovo, S., et al., 2005. NMR structure of Mistic, a membrane-integrating protein for membrane protein expression. *Science*, 307(5713), pp.1317–1321.

Roosild, T.P., Vega, M., Castronovo, S. & Choe, S., 2006. Characterization of the family of Mistic homologues. *BMC Structural Biology*, 6, p.10.

Rozzell, J.D., 1999. Commercial scale biocatalysis: Myths and realities. *Bioorganic and Medicinal Chemistry*, 7(10), pp.2253–2261.

Rupp, S., 2013. Next-generation bioproduction systems: Cell-free conversion concepts for industrial biotechnology. *Engineering in Life Sciences*, 13(1), pp.19–25.

Schmid, A., Dordick, J.S., Hauer, B., Kiener, A., et al., 2001. Industrial biocatalysis today and tomorrow. *Nature*, 409(January), pp.258–268.

Schoemaker, H.E., Mink, D. & Wubbolts, M.G., 2003. Dispelling the myths--biocatalysis in industrial synthesis. *Science (New York, N.Y.)*, 299(5613), pp.1694–1697.

Schön, P., Schrot, G., Wanner, G., Lubitz, W., et al., 1995. Two-stage model for integration of the lysis protein E of phi X174 into the cell envelope of *Escherichia coli*. *FEMS Microbiology Reviews*, 17, pp.207–212.

Schrewe, M., Julsing, M.K., Bühler, B. & Schmid, A., 2013. Whole-cell biocatalysis for selective and productive C-O functional group introduction and modification. *Chemical Society Reviews*, 42(15), pp.6346–77.

Schüürmann, J., Quehl, P., Festel, G. & Jose, J., 2014. Bacterial whole-cell biocatalysts by surface display of enzymes: toward industrial application. *Applied Microbiology and Biotechnology*, pp.8031–8046.

Secundo, F., 2013. Conformational changes of enzymes upon immobilisation. *Chemical Society Reviews*, 42, pp.6250–61.

Segel, I.H., 1993. *Enzyme Kinetics- Behavior and Analysis of Rapid Equilibrium and Steady-State Enzyme Systems* 1st ed., Toronto: John Wiley & Sons, Ltd.

Sharma, S.K., 1990. Key issues in the purification and characterization of recombinant proteins for therapeutic use. *Advanced Drug Delivery Reviews*, 4, pp.87–111.

Sheldon, R. a & van Pelt, S., 2013. Enzyme immobilisation in biocatalysis: why, what and how. *Chemical Society reviews*, 42, pp.6223–35.

Shimizu, S., 1999. Diversity of 4-Chloroacetoacetate Ethyl Ester-Reducing Enzymes in Yeasts and Their Application to Chiral Alcohol Synthesis. *Journal of Bioscience and Bioengineering*, 88(6), pp.591–598.

Simmel, F.C., 2012. DNA-based assembly lines and nanofactories. *Current Opinion in Biotechnology*, 23(4), pp.516–521.

Smith, M.R., Khera, E. & Wen, F., 2015. Engineering Novel and Improved Biocatalysts by Cell Surface Display. *Industrial & Engineering Chemistry Research*, p.150202122506008.

Stewart, J.D., 2001. Dehydrogenases and transaminases in asymmetric synthesis. *Current Opinion in Chemical Biology*, pp.120–129.

Stoops, J.K., Arslanian, M.J., Oh, Y.H., Aune, K.C., et al., 1975. Presence of two polypeptide chains comprising fatty acid synthetase. *Proceedings of the National Academy of Sciences of the United States of America*, 72(5), pp.1940–1944.

Sührer, I., Haslbeck, M. & Castiglione, K., 2014. Asymmetric synthesis of a fluoxetine precursor with an artificial fusion protein of a ketoreductase and a formate dehydrogenase. *Process Biochemistry*, 49(9), pp.1527–1532.

Sührer, I., Langemann, T., Lubitz, W., Weuster-Botz, D., et al., 2015. A novel one-step expression and immobilization method for the production of biocatalytic preparations. *Microbial Cell Factories*, 14:180.

Suller, M.T.E. & Lloyd, D., 1999. Fluorescence monitoring of antibiotic-induced bacterial damage using flow cytometry. *Cytometry*, 35(3), pp.235–241.

Sun, B., Kantzow, C., Bresch, S., Castiglione, K., et al., 2013. Multi-enzymatic one-pot reduction of dehydrocholic acid to 12-keto-ursodeoxycholic acid with whole-cell biocatalysts. *Biotechnology and Bioengineering*, 110(1), pp.68–77.

Sutton, P.W., Adams, Joseph, P., Archer, I., Auriol, D., et al., 2012. Biocatalysis in the Fine Chemical and Pharmaceutical Industries. In J. Whittall & P. W. Sutton, eds. *Biocatalysis and Biotransformations 2*. Chinchester: John Wiley & Sons, Ltd.

Szostak, M.P., Hensel, A., Eko, F.O., Klein, R., et al., 1996. Bacterial ghosts: Non-living candidate vaccines. *Journal of Biotechnology*, 44(95), pp.161–170.

Tabrizi, C.A., Walcher, P., Mayr, U.B., Stiedl, T., et al., 2004. Bacterial ghosts - Biological particles as delivery systems for antigens, nucleic acids and drugs. *Current Opinion in Biotechnology*, 15(6), pp.530–537.

Tishkov, V.I., Galkin, a G., Marchenko, G.N., Egorova, O. a, et al., 1993. Catalytic properties and stability of a *Pseudomonas sp.*101 formate dehydrogenase mutants containing Cys-255-Ser and Cys-255-Met replacements. *Biochemical and biophysical research*

communications, 192(2), pp.976–981.

Tishkov, V.I. & Popov, V.O., 2004. Catalytic mechanism and application of formate dehydrogenase. *Biochemistry (Moscow)*, 69(11), pp.1252–1267.

Tishkov, V.I. & Popov, V.O., 2006. Protein engineering of formate dehydrogenase. *Biomolecular Engineering*, 23, pp.89–110.

Villamiel, M. & De Jong, P., 2000. Influence of high-intensity ultrasound and heat treatment in continuous flow on fat, proteins, and native enzymes of milk. *Journal of Agricultural and Food Chemistry*, 48(2), pp.472–478.

Wagner, S., Bader, M.L., Drew, D. & de Gier, J.-W., 2006. Rationalizing membrane protein overexpression. *Trends in biotechnology*, 24(8), pp.364–371.

Wagner, S., Klepsch, M.M., Schlegel, S., Appel, A., et al., 2008. Tuning *Escherichia coli* for membrane protein overexpression. *Proceedings of the National Academy of Sciences of the United States of America*, 105(38), pp.14371–14376.

Wakil, S.J., 1989. Fatty acid synthase, a proficient multifunctional enzyme. *Biochemistry*, 28(1), pp.4523–4530.

Wang, Y., Huang, Y., Wang, J., Cheng, C., et al., 2009. Structure of the formate transporter FocA reveals a pentameric aquaporin-like channel. *Nature*, 462(7272), pp.467–472.

Wang, Y., San, K.Y. & Bennett, G.N., 2013. Cofactor engineering for advancing chemical biotechnology. *Current Opinion in Biotechnology*, 24, pp.994–999.

Weickert, M.J., Doherty, D.H., Best, E.A. & Olinst, P.O., 1996. Optimization of heterologous protein production in *Escherichia coli*. *Current Opinion in Biotechnology*, 7, pp.494–499.

Weuster-Botz, D., 2007. Process intensification of whole-cell biocatalysis with ionic liquids. *Chemical Record*, 7(6), pp.334–340.

Wichmann, R., Wandrey, C., Buckmann, A.F. & Kula, M.-R., 1981. Continuous Enzymatic Transformation in an Enzyme Membrane Reactor with Simultaneous NAD(H) Regeneration. *Biotechnology and Bioengineering*, 23, pp.2789–2802.

Witte, A., Reisinger, G.R., Säckl, W., Wanner, G., et al., 1998. Characterization of *Escherichia coli* lysis using a family of chimeric E- L genes. *FEMS Microbiology Letters*, 164(1), pp.159–167.

Wolf, K.-H., 1991. *Kinetik in der Bioverfahrenstechnik* 1st ed., Hamburg: Behr.

Wolfenden, R. & Snider, M.J., 2001. The depth of chemical time and the power of enzymes as catalysts. *Accounts of Chemical Research*, 34(12), pp.938–945.

Yamamoto, H., Mitsuhashi, K., Kimoto, N., Kobayashi, Y., et al., 2005. Robust NADH-regenerator: Improved α-haloketone-resistant formate dehydrogenase. *Applied Microbiology and Biotechnology*, 67, pp.33–39.

Yang, M., Ellenberg, J., Bonifacino, J.S. & Weissman, A.M., 1997. The transmembrane domain of a carboxyl-terminal anchored protein determines localization to the endoplasmic reticulum. *Journal of Biological Chemistry*, 272(3), pp.1970–1976.

Yasohara, Y., Kizaki, N., Hasegawa, J. & Wada, M., 2001. Stereoselective reduction of alkyl 3-oxobutanoate by carbonyl reductase from *Candida magnoliae*. , 12, pp.1713–1718.

Ye, Q., Ouyang, P. & Ying, H., 2011. A review-biosynthesis of optically pure ethyl (S)-4-chloro-3-hydroxybutanoate ester: recent advances and future perspectives. *Applied Microbiology and Biotechnology*, 89(3), pp.513–522.

Zhao, H., 2005. Effect of ions and other compatible solutes on enzyme activity, and its implication for biocatalysis using ionic liquids. *Journal of Molecular Catalysis B: Enzymatic*, 37(1-6), pp.16–25.

Zhao, H. & Van Der Donk, W. a., 2003. Regeneration of cofactors for use in biocatalysis. *Current Opinion in Biotechnology*, 14, pp.583–589.

11 Abbreviations

His_6	Hexahistidine
$[HMPL]^+$	1-Hexyl-1-methylpyrrolidinium
$[NTF]^-$	Bis-trifluormethylsulfonylimide
µ	Micro
Aa	Amino acid
APS	Ammoniumpersulfate
BCA	Bicinchoninic acid
bp	Base pairs
BSA	Bovine serum albumine
CDW	Cell dry weight concentration
Cyt b_5	Cytochrome b_5 from rabbit liver
$DiBAC_{[4]}(3)$	Bis-(1,3-dibutylbarbituric acid)trimethine oxonol
DNA	Desoxyribonucleic acid
dNTP	Desoxynucleotide triphosphate
DO	Dissolved oxygen
DTT	Dithiothreitol
EC	Enzyme commission
ECAA	Ethyl-4-chloroacetoacetate
EDTA	Ethylenediaminetetraacetic acid
ee	Enantiomeric excess
ELISA	Enzyme linked immunosorbent assay
EtBr	Ethidium bromide
EtOAc	Ethyl acetate
EtOH	Ethanol
FACS	Fluorescence aided cell sorting
FDH	Formate dehydrogenase
FID	Flame ionization detector
FPLC	Fast protein liquid chromatography
g	Gram
GC	Gas chromatography
GlpF	Glycerol conducting channel from *E. coli*

h	Hour
IL	Ionic liquid
IPTG	Isopropyl β-D-1-thiogalactopyranoside
kb	Kilobasepair
KR	3-Ketoacyl-(acyl-carrier-protein)-reductase
L	Litre
LB	Lurian broth
$logD_{IL/buffer}$	Decadic logarithm of the distribution coefficient between ionic liquid and buffer
m	Metre
M	Molarity
MALDI	Matrix assisted laser desorption ionization
min	Minute
mL	Millilitre
mm	Millimetre
mol	Mole
MOPS	3-(*N*-morpholino)propanesulfonic acid
MS	Mass spectrometry
MW	Molecular weight
MWCO	Molecular weight cut off
NAD^+	Nicotinamide adenine dinucleotide oxidized
NADH	Nicotinamide adenine dinucleotide reduced
$NADP^+$	Nicotinamide adenine dinucleotide phosphate oxidized
NADPH	Nicotinamide adenine dinucleotide phosphate reduced
OD	Optical density
PBS	Phosphate buffered saline
PMSF	Phenylmethylsulfonyl fluoride
PTV	Programmable temperature vaporizing
RH414	*N*-(3-Triethylammoniumpropyl)-4-(4-(4-(diethylamino)phenyl)butadienyl)pyridinium dibromide
rpm	Rotations per minute
RT	Room temperature
s	Second
SDS	Sodium dodecylsulfate
SDS PAGE	Sodium dodecylsulfate polyacrylamide gelelectrophorese

SNARE	Soluble *N*-ethylmaleimide-sensitive-factor attachment receptor
t	Time
TAE	Tris-acetate-EDTA
TEMED	Tetramethylethylenediamine
TFF	Cross-flow filtration
TMB	3,3',5,5'-Tetramethylbenzidine
Tris/HCl	Tris-(hydroxymethyl)-aminomethane hydrochloride
U	Enzyme unit, 1 U = 1 µmol/min
UBC6	Ubiquitin-conjugating enzyme 6 from *S. cerevisiae*
UV-Vis	Ultraviolet-visible
v/v	Volume fraction
w/v	Mass concentration
x g	Multiples of the standard gravity (9.80665 m/s²)
β-gal	β-galactosidase from *E. coli* K12

12 Appendix

12.1 Materials and consumables

Table 12-1 General equipment

Equipment	Manufacturer
AccuCheck®	Roche, Penzberg, Germany
Analytic scale Explorer E1M213	Ohaus, Gießen, Germany
Analytic scale Extend ED124S	Satorius, Göttingen, Germany
Autoclave Varioklav	E H+P Labortechnik, Oberschleißheim, Germany
Bench-top centrifuge Biofuge	Stratos Kendro-Heraeus, Langenselbold, Germany
Centrifuge Rotixa 50 RS	Hettich, Tuttlingen, Germany
Electroporator, Gene Pulser X cell	BioRad, München, Germany
Gel iX, Imager INTAS	Science imaging Instruments, Göttingen, Germany
Incubator IPP500	Memmert, Schwabach, Germany
Micropipette 20 µL, 200 µL, 1000 µL	Brand, Wertheim, Germany
Micropitette Eletric Transferpette 10 µL, 200 µL, 1000 µL	Brand, Wertheim, Germany
MTP-photometer, Infinite M200	Tecan, Männedorf, Germany
MTP-photometer, Multiscan	Thermo Fischer Scientific, Rockford, USA
Multiple magnetic stirring plate	Variomag H+P Labortechnik, Oberschleißheim, Germany
Multiple Transferpette 200 µL, 300 µL	Brand, Wertheim, Germany
pH-electrode BlueLine 24 pH	Schott, Mainz, Germany
pH-meter CG	Schott, Mainz, Germany
Photometer Genesys 20	Thermo Spectronic, Neuss, Germany
Rocker-bar mill MM200	Retsch, Haan, Germany
Rotary evaporator LABOROTA 4003 and vacuum pump ROTAVAC vario control	Heidolph, Schwabach, Germany
SDS-gel electrophorese chamber	Peqlab Biotechnologie GmbH, Erlangen, Germany
Shaking incubator, Multitron	Infors, Bottmingen, Switzerland
Shaking incubator, Wise cube	Witeg Labortechnik GmbH Wertheim, Germany
Table-top Ultra-centrifuge Beckman Optima max with TLA-5 Rotor	Beckmann-Coulter, Pasadena, USA

Thermal shaker, RiO	QUANTOFOIL Instruments, Jena, Germany
Thermo cycler, Mastercycler gradient	Eppendorf, Hamburg, Germany
Thermo cycler, MJMini	BioRad, München, Germany
Tip Sonicator Sonoplus DH 2070	Bandelin Electronic, Berlin, Germany

Table 12-2 Special consumables

Equipment	Manufacturer
96-multiwell plates	Nunc, Roskilde, Denmark
96-multiwell plates Maxisorp®	Nunc, Roskilde, Denmark
Cuvettes for electroporation 1 mm	Peqlab, Darmstadt, Germany
Filter 0.22 µm	Roth, Karlsruhe, Germany
Glass beads 0.5-0.25 mm	Roth, Karlsruhe, Germany
Spin column Viva Spin 20 mL, MWCO 3 kDa	GE Healthcare, Freiburg, Germany
Stericup® & Steritop filter, 0.22 µm	Merck Millipore, Darmstadt, Germany
Microfuge®Tube Polyallomer utracentrifuge tube 1.5 mL	Beckmann-Coulter, Pasadena, USA

Table 12-3 Flow cytometry

Equipment	Manufacturer
Flow cytometer CyFlow®SL	Partec, Münster, Germany
Software FlowMax®	Partec, Munich, Germany
Sample tubes 3.5 mL, 55 x 12 mm, PS	Sarsted, Nümbrecht, Germany

Table 12-4 Gas chromatography

Equipment	Manufacturer
Gas chromatograph CP-3800	Varian, Darmstadt, Germany
Injector 1079 PTV, temperature programmable	Varian, Darmstadt, Germany
Lipodex E column	Macherey Nagel, Düren, Germany
Flame ionization detector	Fuel gas: hydrogen/air, helium: carrier gas
Software Star version 5.51	Varian, Darmstadt, Germany
Autosampler CombiPal	CTC Analytics Zwingen, Switzerland
Helium 99.999% (v/v)	Air Liquide, Krefeld, Germany
Hydrogen 99.999% (v/v)	Air Liquide, Krefeld, Germany
Synthetic air	House internal gas supply

Table 12-5 Stirred-tank bioreactor and cross-flow filtration

Equipment	Manufacturer/Type
Stirrer	2 – 3 six-bladed Rushton impellors
Drive top	Top, mechanical seal drive coupling
Aeration	Mass flow valve sparger
Control station	Infors HAT, Bottmingen-Basel, Switzerland
pH Electrode 405-DPAS-SC-K8S/225	Mettler Toledo, Gießen, Germany
pH Electrode 405-DPAS-SC-K8S/325	Mettler Toledo, Gießen, Germany
DO-probe InPro 6000	Mettler Toledo, Gießen, Germany
DO-probe InPro 6800	Mettler Toledo, Gießen, Germany
Massflow controller Advance SCC-F	ABB, Frankfurt, Germany
Permittivity biomass probe I biomass	Hamilton Bonaduz AG, Bonaduz, Swizerland
Pump ISM 444	Isamtec SA, Glattbrugg, Swizerland
Hollow fiber module 0.22 µm, 4.2 m^2 surface	GE Healthcare, Uppsala, Sweden
Labfors stirred-tank bioreactor 7.5 l	Infors HAT, Bottmingen-Basel, Switzerland
Labfors stirred-tank bioreactor 3.6 L	Infors HAT, Bottmingen-Basel, Switzerland
Sofware Iris-NT Pro Version 4.11	Infors HAT, Bottmingen-Basel, Switzerland

Table 12-6 FPLC

Equipment	Manufacturer
GradiFrac FPLC-Unit	GE-Healthcare, Uppsala, Sweden
HisTrap FF crude column, 1 mL	GE-Healthcare, Uppsala, Sweden
IV-7 valve	GE-Healthcare, Uppsala, Sweden
Pump P50	GE-Healthcare, Uppsala, Sweden
UV spectrophotomteter LKB Uvicord SII, 280 nm	GE-Healthcare, Uppsala, Sweden
LabVIEW 6.0	National Instruments, Munich, Germany

Table 12-7 Software and programs

Equipment	Manufacturer
Basic Local Alignment Tool (BLAST)	http://blast.ncbi.nlm.nih.gov/Blast.cgi
GENtle	http://gentle.magnusmanske.de/
PyMOL	www.pymol.org, Schrödinger, Tokyo, Japan
Serial Cloner	http://serialbasics.free.fr/Serial_Cloner.html
Sigma Plot 12.3	Systat Software, Chicago, USA
YASARA	www.yasara.org; Watching Nature @ Work™, Yasara Biosciences, Vienna Austria

12.2 Chemicals, antibodies and enzymes

Table 12-8 Chemicals

Chemical	Purity	Manufacturer/Provider
[HMPL][NTF]	-	Merck
1.4-Dithiothreitol (DTT)	≥ 99.0%	Merck
2-Heptanone	≥ 98%	Merck
2-Oleoyl phosphatidylcholine (POPC)	≥ 99%	Sigma-Aldrich
Acetic acid	≥ 99.5%	Roth
Acetophenone	> 98.0%	Merck
Acrylamide/bisacrylamide (19:1)	-	Roth
Agar-agar	-	Roth
Agarose NEEO	DNA-grade	Roth
Ammonia 25% (v/v)	25%	Roth
Ammonium persulfate (APS)	98.0%	Merck
Ampicillin	-	Applichem
Antifoam 204	-	Sigma-Aldrich
Boric acid	≥99.8%	Roth
Bromophenol blue	-	Merck
BSA (bovine serum albumine)	-	New England Biolabs'inc
Calcium chloride (x6 H_2O)	>99.5%	Merck
Citric acid	≥99.0%	Applichem
Cobalt chloride	>98.0%	Sigma-Aldrich
Coomassie Brilliant Blue R-250	-	Roth
Copper(II) chloride (x 2 H_2O)	≥99.0%	Merck
$DiBAC_{[4]}(3)$	98.0%	AAT Bioquest

Dipotassium hydrogen phosphate	≥99.0%	Roth
Disodium hydrogen phosphate	≥99.0%	Roth
Ethanol	≥99.5%	Merck
Ethyl acetate (EtOAc)	≥99.5%	Merck
Ethyl-(*R*)-4-chloro-3-hydroxybutyrate	≥96.0%	Sigma-Aldrich
Ethyl-(*S*)-4-chloro-3-hydroxybutyrate	≥96.0%	Sigma-Aldrich
Ethyl-4-chloroacetoacetate (ECAA)	≥98.0%	Merck
Ferric citrate (III)	-	Sigma-Aldrich
Gentamycin sulfate	-	Roth
Glucose monohydrate	≥99.5%	Roth
Glycerol	≥98.0%	Roth
Hydrochloric acid 32.0%	Pro analysis	Merck
Imidazole	≥99.0%	Alfa Aesar
Isopropyl alcohol	≥99.5%	Merck
Isopropyl-β-D-thiogalactopyranoside (IPTG)	≥98.0%	Roth
Magnesium sulfate (x7 H_2O)	≥98.0%	Merck
Magnesium(II) chloride	≥99.0%	Merck
Magnesium(II) sulfate	≥98.0%	Merck
Manganese(II) chloride (x4 H_2O)	≥99.0%	Merck
Milk powder	Blotting grade	Roth
Monopotassium phosphate	≥99.0%	Roth
Monosodium phosphate	≥99.0%	Merck
3-(*N*-morpholino)propanesulfonic acid (MOPS)	≥99.0%	Roth
N,*N*,*N*′,*N*′-tetramethyl-ethane-1,2-diamine (TEMED)	≥99.0%	Roth
Nicotinamide adenine dinucleotide phosphate (NADP) disodium salt	≥98.0%	Roth
Nicotinamide adenine dinucleotide phosphate reduced (NADPH) tetrasodium salt	≥98.0%	Roth
Nickel(II) sulfate	≥99.0%	Roth

Peptone from Caseine	-	Roth
Phenylmethylsulfonyl fluoride (PMSF)	≥99.0%	Roth
Phosphoric acid	85.0%	Roth
Plate count agar	-	Roth
Potassium acetate	≥99.0%	Merck
Potassium carbonate	≥99.5%	Merck
Potassium dihydrogen phosphate	≥99.0%	Roth
Potassium hydroxide	≥86.5%	Sigma-Aldrich
RH414 N-(3-Triethylammoniumpropyl)-4-(4-(4-(diethylamino)phenyl)butadienyl)pyridinium dibromide	95.0%	AAT Bioquest
Roti® Stain safe	-	Roth
Sodium carbonate	≥99.5%	Roth
Sodium chloride	≥99.0%	Roth
Sodium dihydrogen phosphate	≥99.0%	Roth
Sodium dodecylsulfate (SDS)	≥85.0%	Merck
Sodium formate	≥98.0%	Fluka
Sodium hydrogen carbonate	≥99.5%	Roth
Sodium hydroxide	≥99.0%	Roth
Sodium hypochlorite	12%	Roth
Sodium molybdate	≥99.5%	Merck
Thiamine hydrochloride	-	Sigma-Aldrich
Tris-hydroxymethyl-amino-methane (Tris/HCl)	≥99.0%	Roth
Yeast extract	-	Roth
Zinc acetate (x 2 H_2O)	≥99.5%	Merck
β-Mercaptoethanol	>99%	Merck

Table 12-9 Kits and standards

Kit and standard	Manufacturer
100 bp DNA-ladder extended	Roth, Karlsruhe, Germany

Acetic Assay Kit	Böhringer Mannheim/R-Biopharm, Mannheim, Germany
Bicinchoninic acid (BCA), Protein assay kit	Thermo Scientific, Schwerte, Germany
Cold Fusion Cloning Kit	BioCat, Heidelberg, Germany
D-Glucose Assay	Böhringer Mannheim/R-Biopharm, Mannheim, Germany
dNTP-Mix	New England Biolabs, Frankfurt am Main, Germany
GenElute™ Gel extraction Kit	Sigma-Aldrich, St. Louis, USA
GenElute™ HP Plasmid Miniprep Kit	Sigma-Aldrich, St. Louis, USA
GenElute™ PCR Clean-Up Kit	Sigma-Aldrich, St. Louis, USA
Just Blue Bluestar prestained protein marker	Nippon Geneteics GmbH Europe, Düren, Germany
Perfect Protein™ Marker, 10-225 kDa	Merck Millipore, Darmstadt, Germany
PopCulture® Reagent	Merck Millipore, Darmstadt, Germany
QuickChange® Lightnin Site-Directed Mutagenesis Kit	Agilent Technologies, Oberhaching, Germany
Roti®-Mark Standard	Roth, Karlsruhe, Germany
Roti®-Transform	Roth, Karlsruhe, Germany
TBM Substrate Solution	Thermo Scientific, Schwerte, Germany

Table 12-10 Enzymes and antibodies

Enzyme/Antibody	Manufacturer
Antibodies	
Capture antibody: Monoclonal anti β-galactosidase from mouse, MA1-152	Thermo Scientific, Schwerte, Germany
Detection antibody: Polyclonal anti β-galactosidase from rabbit, PA1-21477 antibody	Thermo Scientific, Schwerte, Germany
Secondary antibody: Goat Anti Rabbit IgG H&L antibody HRP	Biorbyt Limited, Cambridge, United Kingdom
Enzymes	
Antarctic phosphatase	New England Biolabs
Phusion® High-Fidelity DNA Polymerase	Finnzymes
Phusion® Hot Start High-Fidelity DNA-Polymerase	Finnzymes
Restriction Enzyme AscI	New England Biolabs
Restriction Enzyme AvrII	New England Biolabs
Restriction Enzyme BamHI	New England Biolabs
Restriction Enzyme BglII	New England Biolabs
Restriction Enzyme BlpI	New England Biolabs

Restriction Enzyme BnpI	New England Biolabs
Restriction Enzyme EcoRI	New England Biolabs
Restriction Enzyme FspI	New England Biolabs
Restriction Enzyme HindIII	New England Biolabs
Restriction Enzyme KpnI	New England Biolabs
Restriction Enzyme NcoI	New England Biolabs
Restriction Enzyme NdeI	New England Biolabs
Restriction Enzyme NheI	New England Biolabs
Restriction Enzyme NotI	New England Biolabs
Restriction Enzyme SalI	New England Biolabs
Restriction Enzyme XbaI	New England Biolabs
Restriction Enzyme XhoI	New England Biolabs
T4 DNA-Ligase	New England Biolabs
Taq DNA-Polymerase	New England Biolabs

12.3 Cell strains, plasmids and oligonucleotides

Table 12-11 *E. coli* strains

Strain	Genotype	Provider
E. coli BL21 (DE3)	B F^{-} *dcm ompT hsd*S(r_B^- m_B^-) *gal* λ(DE3)	Novagen, San Diego, USA
E. coli C41 (DE3)	F^{-} *ompT gal* dcm hsdSB(rB^- mB^-)(DE3)	OverExpress™, Lucigen, Middleton, USA
E. coli C43 (DE3)	F^{-} *ompT gal* dcm hsdSB(rB^- mB^-)(DE3)	OverExpress™, Lucigen, Middleton, USA
E. coli DH5α	F^- *end*A1 *gln*V44 *thi*-1 *rec*-A1 *rel*A1 *gyr*A96 *deo*R *nup*G	Novagen, San Diego, USA
	Φ80d*lacZ*ΔM15 Δ(*lac*ZYA-*arg*F)U169, hsdR17($r_K^-m_K^+$),λ-	
E. coli XL-10Gold	*gyr*A96 *rel*A1 *lac Hte* [F' *pro*AB *lacI*^{q}ZDM15	Agilent Technologies, Oberhaching, Germany
	*Tn*10(Tet^r)$AmyCam^r$	

Table 12-12 Primers and oligonucleotides

Forward (fw) and reverse (rw) primers of all cloning experiments are given. Oligonucleotides purchased with a phosphorylated 5'-end are marked with **P**. All reverse (rw) primers named FDH refer to the mutant M7 described in (Sührer et al. 2014). The abbreviations stand for: FDH = formate dehydrogenase, KR = 3-ketoreductase, MCS = multiple cloning site from pCOLADuet®, Cyt b_5 = C-terminal hydrophobic sequence cytochrome b_5 from rabbit liver, UBC6 = C-terminal hydrophobic sequence of the ubiquitin-conjugating enzyme 6 from *S. cerevisiae,* Eivb = lysis protein E from phage PhiX174.

Name	Sequence (5'→ 3') (for reverse primers the reverse complement ordered is given)
	Oligonucleotides for cloning of membrane anchors
Cyt b5 (FDH M7) ASCI and NotI fw	**P**-CGCGCCTGAGCAAACCGATGGAAACCCTGATTACCACCGTGGATA GCAATAGCAGCTGGTGGACCAATTGGGTGATTCCGGCGATTAGCGCG CTGATTGTGGCGCTGATGTATCGTCTGTATATGGCGGATGATTAGC
Cyt b5 (FDH M7) ASC I and NotI rw	**P**-GGCCGCTAATCATCCGCCATATACAGACGATACATCAGCGCCACA ATCAGCGCGCTAATCGCCGGAATCACCCAATTGGTCCACCAGCTGCT ATTGCTATCCACGGTGGTAATCAGGGTTTCCATCGGTTTGCTCAGG
Cyt b5 (KR) XhoI und AvrII fw	**P**-TCGAGCCTGAGCAAACCGATGGAAACCCTGATTACCACCGTGGAT AGCAATAGCAGCTGGTGGACCAATTGGGTGATTCCGGCGATTAGCGC GCTGATTGTGGCGCTGATGTATCGTCTGTATATGGCGGATGATTAGC
Cyt b5 (KR) XhoI und AvrII rw	**P**-CTAGGCTAATCATCCGCCATATACAGACGATACATCAGCGCCACA ATCAGCGCGCTAATCGCCGGAATCACCCAATTGGTCCACCAGCTGCT ATTGCTATCCACGGTGGTAATCAGGGTTTCCATCGGTTTGCTCAGGC
Cyt b5 fw (FDH und Fus) AscI/ NotI fw	**P**-CGCGCCTGAGCAAACCGATGGAAACCCTGATTACCACCGTGGATA GCAATAGCAGCTGGTGGACCAATTGGGTGATTCCGGCGATTAGCGCG CTGATTGTGGCGCTGATGTATCGTCTGTATATGGCGGATGATTAGC
Cyt b5 rw (FDH and Fusion protein) AscI/ NotI rw	**P**-GGCCGCTAATCATCCGCCATATACAGACGATACATCAGCGCCACA ATCAGCGCGCTAATCGCCGGAATCACCCAATTGGTCCACCAGCTGCT ATTGCTATCCACGGTGGTAATCAGGGTTTCCATCGGTTTGCTCAGG
UBC6 fw	GATACAGGCGCGCCAATGGTGTATATTGGCATTGCGATTTTTCTGTTT CTGGTGGGCCTGTTTATGAAATAGGCGGCCGCGATACA
UBC6 rw	TGT ATC GCG GCC GCC TAT TTC ATA AAC AGG CCC ACC AGA AAC AGA AAA ATC GCA ATG CCA ATA TAC ACC ATT GGC GCG CCT GTA TC
	Primers for amplification in cloning experiments
Cyt b5 KpnI Stop rw	CGTCTGTATATGGCGGATGATTAGGGTACCGATACA
Cytb5 KpnI fw	GATACAGGTACCCTGAGCAAACCGATGGAAAC
Cytb5 XhoI rw Stop	TGTATCCTCGAGCTAATCATCCGCCATATACAGAC
E' NcoI fw	GATACA CC ATGGTACGCTGGACTTTGTGG
FDH AscI fw	GATACAGGCGCGCCATGGCAAAGGTCCTGTGCGTTCT

FDH EcoRI Stop rw	TGTATC GAATTC CTA GACCGCGCTGCTGGACCC
FDH HindIII rw	TGTATC AAGCT T G GACCGCGCTGCTGGACCC
FDH HindIII Stop rw	TGTATC AAGCT T CTA GACCGCGCTGCTGGACCC
FDH KpnI fw	GATACA GGTACC G GCAAAGGTCCTGTGCGTTCT
FDH NcoI fw	CCATGGCAAAGGTCCTGTGCGTTCTTTACGA
FDH XbaI fw	GATACA T CTAGA G GCAAAGGTCCTGTGCGTTCT
FDH XbaI rw	TGTATC TCTAG GACCGCGCTGCTGGACCC
FDH(M7) AscI rw	TGTATCGGCGCGCCGCGACCGCGCTGCTGGACCC
FDH(M7) BamHI rw Stop	TGTATCGGATCC TTAGACCGCGCTGCTGGACCC
GlpF NcoI fw	GATACACCATGGCGATGAGTCAAACATCAACCTTGAAAGGC
GlpF- NdeI rw	CAGAACAAAAAGCTTCGCTG CATATG GATACA
GlpF-NdeI fw	GATACACATATGATGAGTCAAACATCAACCTTGAAAGGC
KR AscI rw	TGTATCGGCGCGCCGCGGCCATCACCAAGCCG
KR KpnI f	GATACA GGTACC G ACTGCTTTGCCCCTAACCGAT
KR NdeI fw	GATACACATATGACTGCTTTGCCCCTAACCGA
KR NdeI fw	GATACA CATATG ACTGCTTTGCCCCTAACCGAT
KR NotI Stop rw	TGTATC GCGGCCGC CTA GGCCATCACCAAGCCGCCAT
KR SalI rw	TGTATC GTCGA C GGCCATCACCAAGCCGCCAT
KR SalI Stop rw	TGTATC GTCGAC CTA GGCCATCACCAAGCCGCCAT
KR XbaI fw	GATACA T CTAGA G ACTGCTTTGCCCCTAACCGAT
KR XbaI rw	TGTATC TCTAG GGCCATCACCAAGCCGCCAT
KR XbaIStop rw	TGTATC TCTAGA CTA GGCCATCACCAAGCCGCCA
KR XhoI rw	TGTATCCTCGAGGCCATCACCAAGCCGCCAT
KR-NotI rw	TGTATC GCGGCCGC GGCCATCACCAAGCCGCCAT
L' EcoRI rw	TGT ATC GAA TTC TTA AGT AAG CAA TTG CTG TAA AGT CG
L' Not I rw Stop	TGTATCGCGGCCGCTTAAGTAAGCAATTGCTGTAAAGTCG
Linker SG fw	GATACAGGCGCGCCAGAGCGGATCCTCCTCCTC
Linker SG rw	TGTATCGGCGCGCCTGACTACCGCTGGAAGAGC
MSC pCOLA XbaI fw	CCGTCTAGAAATAATTTTGTTTAACTTTAAGAAGG
SeqCt1 MSC Duet rw	CAGCACCAGCAGAACTCGCGTA
UBC6 EcoRI rw stop	TGTATCGAATTCCTATTTCATAAACAGGCCCAC
UBC6 NotI rw	TGTATCGCGGCCGCCTATTTCATAAACAGGCCCACC

Stop	
UBC6 NotI fw	GATACA GCGGCCGCG ATGGTGTATATTGGCATTGCG
UBC6 XhoI rw Stop	TGTATC CTCGAG CTATTTCATAAACAGGCCC
β-Gal AscI rw	TGTATCGGCGCGCCGCTTTTTGACACCAGACCAACTGGT A
β-Gal AscI stop rw	TGTATCGGCGCGCCCTATTTTTGACACCAGACCAACTGGT
β-Gal NcoI fw	GATACACCATGGCGATGACCATGATTACGGATTCACTGG
	Sequencing primers
T7 promotor fw	TAATACGACTCACTATAGGG
T7 terminator rw	GCTAGTTATTGCTCAGCGG (also used as rw primer in amplification of MSC)
ACYCDuetUP1	GGATCTCGACGCTCTCCCT

Table 12-13 Vectors and genomic DNA

Vecors	Manufacturer/Specification
	Commercially available vectors
pET21a(+)	Novagen, San Diego, USA
pET28a(+)	Novagen, San Diego, USA
pCOLA-Duet-1®	Novagen, San Diego, USA
	Vectors and genomic DNA provided by the Institute of Biochemical Engineering (Technische Universität München)
pET21a (+)- PQTEV FDH M7	Vector containing His_6-TEV-FDH(M7), for the purification of free FDH(M7) without His_6-tag, kindly provided by K. Castiglione
pCOLA-Duet-1-FDH(M7)-SG-KR-His_6	Described in (Sührer et al. 2014), used as template for the amplification of FDH(M7), KR and the fusion protein FDH-SG-KR
Genomic DNA from *E. coli* K12	For the amplification of β-galactosidase, kindly provided by K. Castiglione
	Vector newly designed in this work (for detailed map see Figure 12-1)
pET28aDuet	pET28a with multiple coning site from pCOLADuet inserted between XbaI and BnpI
	Vectors kindly provided by the project partner Prof. Dr. Lubitz, company BIRD-C, Vienna
pGlysivb	Contains the lysis gene Eivb, which encodes for protein E controlled by the temperature sensitive repressor CI857 (Hutchison & Sinsheimer 1966; Jechlinger et al. 1999)
pKSEL5-2	Contains the membrane anchor sequences of E' and L' (Lubitz et al. 1999; Langemann et al. 2010)

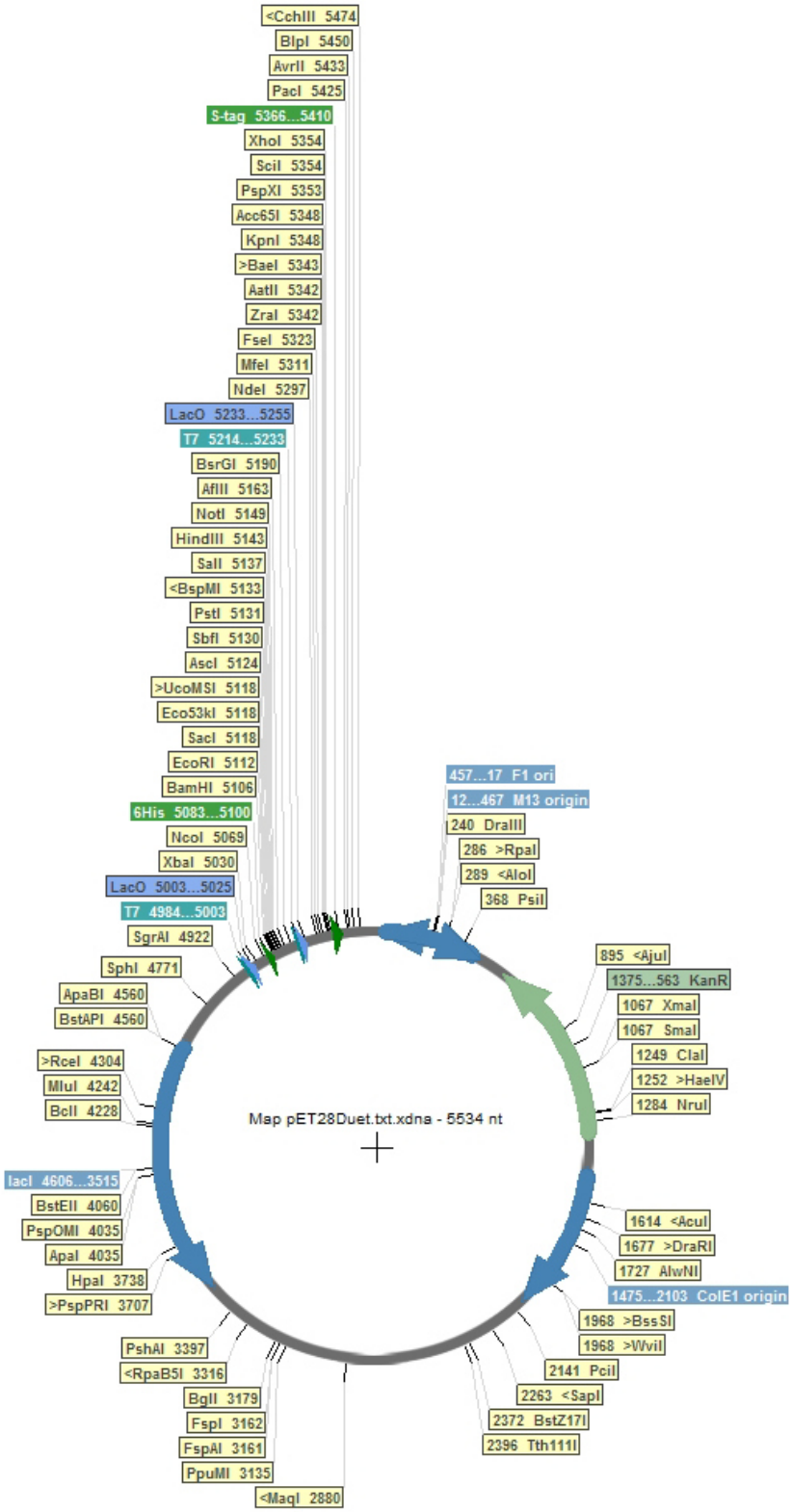

Figure 12-1 Map of pET28aDuet vector
All singular restriction sites are given, the ori, lacI promotor, antiobiotic resistance (KanR) and binding sites for sequencing primers are highlighted.

12.4 Supplementary data

Determination of growth rates for fed-batch set-up

Table 12-14 Maximum growth rates of BL21 at different temperatures
The growth rates were determined in shaking flasks (200 mL total volume) and defined medium with 8 g/L glucose at 35 °C. Since CDW are highly error prone at low cell concentrations, the OD_{600} was measured and the corresponding CDW was calculated using an OD_{600} to CDW correlation coefficient of 0.55 (data not shown). The corresponding growth rates were determined using equation 4-2.

Temperature, °C	20	25	30
μ_{max}, 1/h	0.174 ± 0.003	0.259 ± 0.002	0.341 ± 0.008

Data from batch-phase data from cellular envelope production

Table 12-15 Process data from batch phase in fed-batch production of biocatalysts

Cell line	μ_{max} batch phase, 1/h	$Y_{XS\mu}$, g/g
BL21	0.22 ± 0.1	0.29 ± 0.08
C41	0.30 ± 0.08	0 40 ± 0.07
C43	0.33 ± 0.14	0.35 ± 0.08

Cellular envelope count-to-weight correlation

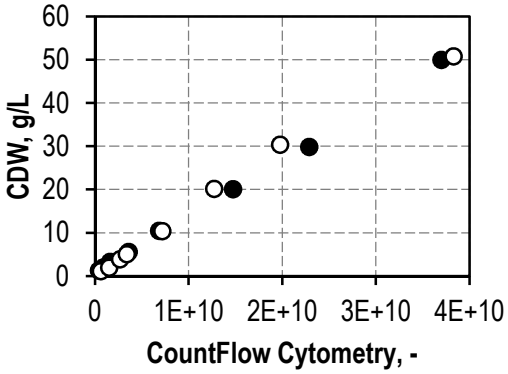

Figure 12-2 Cellular envelope count-to-weight correlation
Defined amounts of lyophilised cellular envelopes from *E. coli* BL21 (black) and *E. coli* C41 (white) batch process without immobilised enzymes were analysed using flow cytometry. The populations with positive signal for RH414 staining were used to calculate a correlation from the linear slope (see equation 12-1)

$$DW = 1{,}33 \cdot 10^{-9}\ g\ mL\ L^{-1} \cdot Count_{FACS} + 0{,}92\ g\ L^{-1} \qquad \textbf{12-1}$$

DW Dry weight concentration of cellular envelopes, g/L

$Count_{FACS}$ Count of positive fluorescence signals at 590 nm in flow cytometry using RH414 staining, 1/mL

Lysis duration in fed-batch processes

Table 12-16 Lysis duration in fed-batch processes
Lysis duration in fed-batch processes in compared for different cell strains and expression conditions (growth rate and expression temperature)

Cell line	Growth rate, 1/h	Lysis duration after expression at 25 °C, h	Lysis duration after expression at 20 °C, h
BL21	0.075	2.8 ± 0.2	3.5 ± 0.6
C41	0.075	1.9 ± 0.5	2.9
C43	0.075	2.1	2.0
C41	0.09	5.0 ± 2.2	-
C43	0.09	3.8	-
C41	0.12	4.7	-

Exemplary SDS-PAGE from fed-batch process

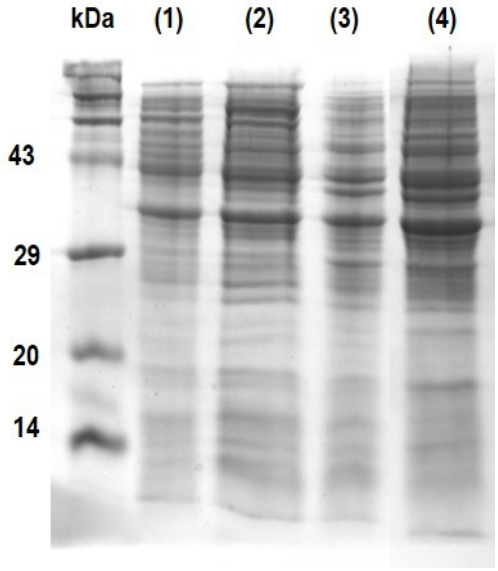

Figure 12-3 Exemplary SDS-PAGE from fed-batch process
SDS-PAGE showing: (1) negative control from BL21, (2) sample from prior to expression, (3) sample from prior to lysis and (4) sample after lysis. The samples from cultivation of BL21 with FDH-UBC6 and KR-Cyt b_5 expression at 25 °C are shown. All samples were adjusted to similar particle concentrations prior to application.

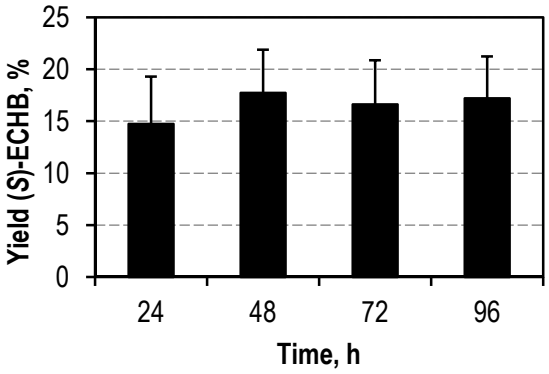

Figure 12-4 Exemplary data on ECAA conversion in the course of time
Conversion of ECAA in the course of time with cellular envelopes from C41 at 25 °C. 10 g/L cellular envelopes were used to convert 20 mM ECAA using 5 mM $NADP^+$ and 0.5 M sodium formate at 30 °C.

Long-term storage experiments

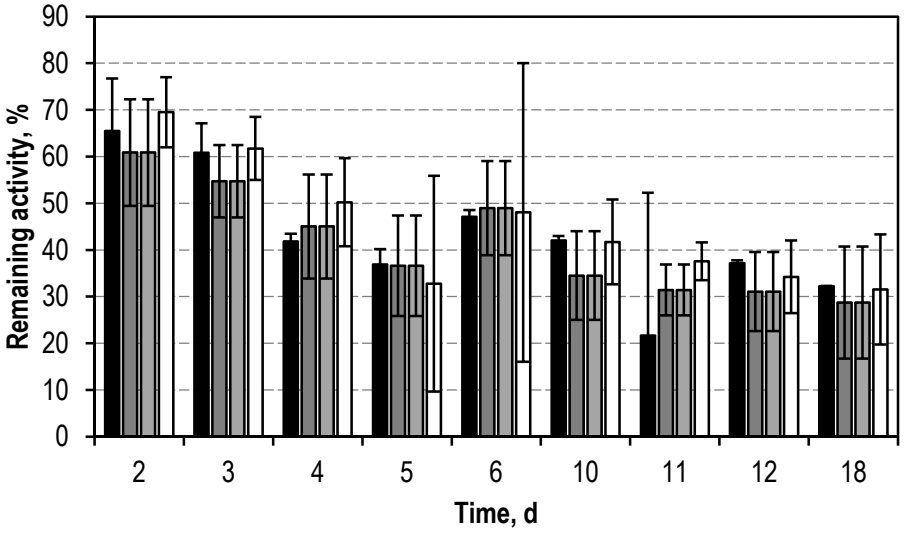

Figure 12-5 Activity of whole cells and cellular envelopes in long-term storage
The remaining activity after different storage durations is given for whole cell stored at 4 °C (black), whole cells stored at −20 °C (dark gray), cellular envelopes stored at 4 °C (light gray) and cellular envelopes stored at −20 °C (white). Reactions were performed using 4 x 10^9 cells or cellular envelopes to convert 20 mM ECAA in the presence of 5 mM $NADP^+$, 0.5 M sodium formate at 30 °C for 24 h. The activity determined after 1 d storage is assumed 100% and used to calculate the corresponding remaining activities.

Process data from fed-batch production of cellular envelopes with immobilised β-gal-Cyt b_5

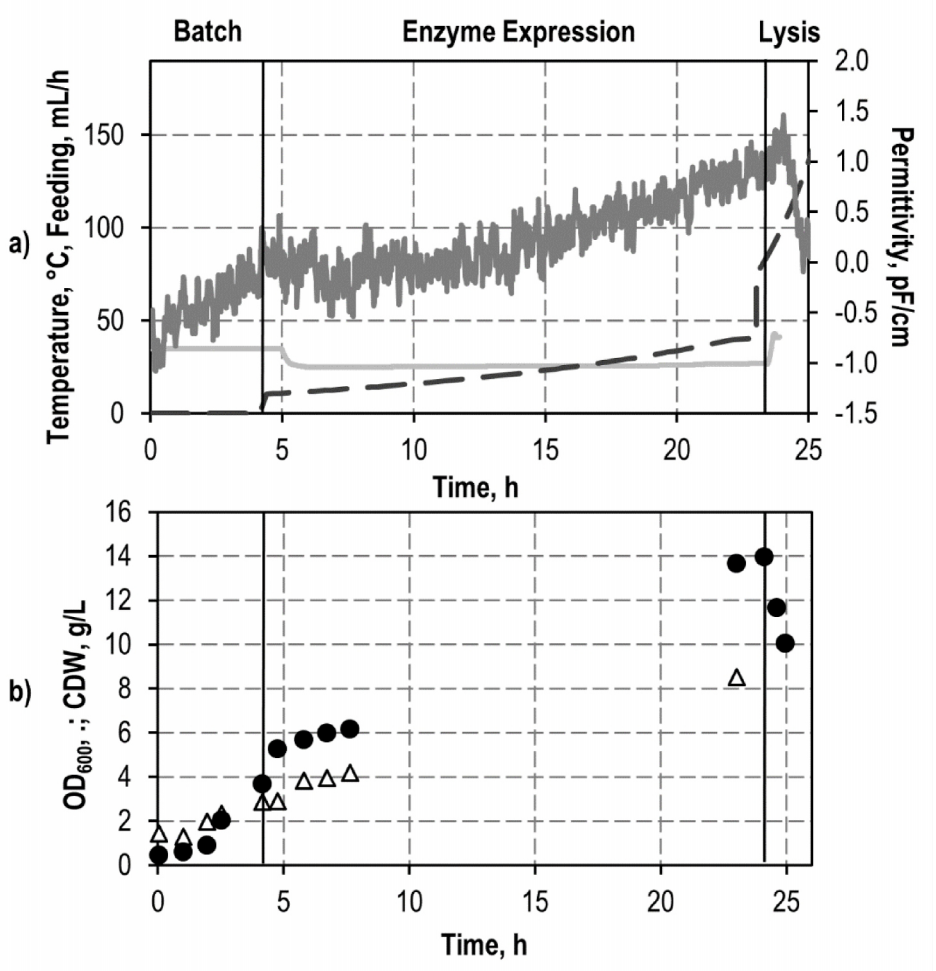

Figure 12-6 Exemplary process data from fed-batch production of cellular envelopes with immobilised β-gal-Cyt b_5 in a stirred-tank bioreactor
a) The temperature (gray line), the feed medium inflow (gray dashed line), the permittivity (dark gray line), b) the CDW (Δ) and the optical density (●) and are displayed in the course of time. The process conditions were: initial volume = 1.5 L, maximum air flow = 8 L/min, stirring speed = 1000 rpm, pH = 7.2, $\mu_{set\ Expression}$ = 0.075 1/h (50 g/L glucose in feed medium) and $\mu_{set\ Lysis}$ = 0.3 1/h (100 g/L glucose in feed medium). The induction of enzyme expression (by 0.1 mM IPTG addition) and lysis by a temperature shift to 42 °C are highlighted with a vertical line, *E. coli* C41 were used for the cultivation. Standard deviations were calculated and are highlighted, but may be small and thus not visible.

β-galactosidase activities with and without detergent

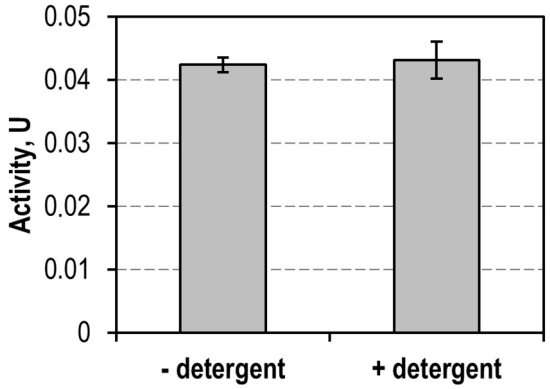

Figure 12-7 Comparison of β-galactosidase activities without detergent treatment
The activity of equal amounts of β-galactosidase before and after detergent treatment are compared. Protein preparations with soluble β-gal-Cyt b_5 (see section 4.5.7) were used and either treated with the detergent PopCulture® or the equivalent amount of PBS and subsequently analysed for enzyme activity. The slope was used to calculate the corresponding activity according to equation 4-4.